Arnold Schwarzenegger
Governor

AIR QUAILTY IMPACTS OF DISTRIBUTED GENERATION

DRAFT PIER CONSULTANT REPORT

Prepared For:
California Energy Commission
Public Interest Energy Research Program

Prepared By:
Professor Scott Samuelsen
Professor Donald Dabdub
Dr. Jacob Brouwer
University of California, Irvine

Prepared By:
University of California, Irvine
Professor Scott Samuelsen
Professor Donald Dabdub
Dr. Jacob Brouwer
Irvine, CA
Contract No. 500-00-033

Prepared For:
California Energy Commission
Public Interest Energy Research (PIER) Program

Marla Mueller,
Contract Manager

Kelly Birkinshaw,
Program Area Team Lead

Ron Kukulka,
Acting Deputy Director
**ENERGY RESEARCH AND DEVELOPMENT
DIVISION**

Scott W. Matthews
Acting Executive Director

Final Report

For:

Air Quality Impacts of Distributed Generation

California Energy Commission Contract # 500-00-033
Public Interest Energy Research (PIER) Program Area:
Energy-Related Environmental Research

Submitted to:

Ms. Marla Mueller, Contract Manager
Public Interest Energy Research Program
California Energy Commission
1516 Ninth Street
Sacramento, California   95814

Submitted by:

Professor Scott Samuelsen and Professor Donald Dabdub
University of California, Irvine
131 Engineering Laboratory Facility
Irvine, California 92679-3550
Tel: (949) 824-1999 x120
Fax: (949) 824-7423
gss@nfcrc.uci.edu
ddabdub@uci.edu

Co-Workers:

Dr. Jacob Brouwer, Associate Director
Tel: (949) 824-1999 x221
jb@nfcrc.uci.edu

Dr. Marc Medrano (mm@apep.uci.edu)
Dr. Marco Rodriguez (marcor@uci.edu)
Marc Carreras (mcarrera@uci.edu)

November 30, 2004

LEGAL NOTICE

This report was prepared as a result of work sponsored by the California Energy Commission (Commission, Energy Commission). It does not necessarily represent the views of the Commission, its employees, or the State of California. The Commission, the State of California, its employees, contractors, and subcontractors make no warranty, express or implied, and assume no legal liability for the information in this report; nor does any party represent that the use of this information will not infringe upon privately owned rights. This report has not been approved or disapproved by the Commission nor has the Commission passed upon the accuracy or adequacy of this information in this report.

ACKNOWLEDGEMENTS

TABLE OF CONTENTS

DRAFT

LIST OF FIGURES

LIST OF TABLES

1   PREFACE

The Public Interest Energy Research (PIER) Program supports public interest energy research and development that will help improve the quality of life in California by bringing environmentally safe, affordable, and reliable energy services and products to the marketplace.

The Pier Program, managed by the California Energy Commission (Commission), annually awards up to $62 million to conduct the most promising public interest energy research by partnering with Research, Development, and Demonstration (RD&D) organizations, including individuals, businesses, utilities, and public or private research institutions.

PIER funding efforts are focused on the following six RD&D program areas:

- Buildings End-Use Energy Efficiency
- Industrial/Agricultural/Water End-Use Energy Efficiency
- Renewable Energy
- Environmentally-Preferred Advanced Generation
- Energy-Related Environmental Research
- Strategic Energy Research

What follows is the final report of the Air Quality Impacts of Distributed Generation, 500-00-033, conducted by the University of California, Irvine. The report is entitled Draft Final Report for Air Quality Impacts of Distributed Generation. This project contributes to the Energy-Related Environmental Research program.

For more information on the PIER Program, please visit the Commission's Web site at: http://www.energy.ca.gov/research/index.html or contact the Commission's Publications Unit at 916-654-5200.

2   EXECUTIVE SUMMARY

Distributed generation of energy (DG) has the potential to meet the power demands of the near future. Deployment of DG technologies might provide additional benefits in electrical reliability and quality, besides reductions in electricity production costs. The use of Combined Heat and Power (CHP) could increase further energy consumption efficiency as well as reduce emissions from fuel usage. Furthermore, having power generation near the place of use minimizes electricity transmission losses. DG is characterized by a widely dispersed distribution of emission sources within an air basin. In contrast, conventional, centralized sources of emissions from large central power plants are concentrated and localized in remote areas. In addition, in some areas, such as the South Coast Air Basin of California (SoCAB), central power plants are mostly outside the air basin. Consequently, air quality impacts associated to changes from centralized power generation to DG still need to be estimated.

Undoubtedly, the presence of DG in urban air basins raises numerous concerns that must be examined. This study provides to regulatory agencies a scientific basis to design policies with respect to DG implementation. Namely, how will DG likely be implemented in the SoCAB? Will increased emissions from DG implementation affect the levels of ambient ozone with respect to ozone standards? Could any increase in NO_X emissions enhance secondary particulate matter formation?   What DG implementation scenarios could reduce overall environmental impacts?

Previous research has not determined through air quality modeling any impacts on air quality due to emissions from DG units. The results and conclusions of these studies were based purely on emissions assessments. Changes in emissions profiles affect the concentrations of primary and secondary atmospheric contaminants. These effects need to be evaluated with detailed air quality models that include chemical and physical processes that occur in the atmosphere.

The present effort aims to develop a set of realistic scenarios for DG application in the south coast air basin of southern California (SoCAB) and the assessment of their air quality impacts with a detailed three-dimensional Eulerian air quality model. The California Institute of Technology (CIT) model includes atmospheric processes such as homogeneous and heterogeneous chemistry; advective and turbulent transport; and the spatial and temporal variability of the emissions and meteorology. The model is under continuous revision and development at University of California, Irvine, in collaboration with researchers from other institutions. The primary objectives of this study are to:

1. construct a set of distributed generation implementation scenarios for the SoCAB of California;
2. determine the potential air quality impacts of DG in the SoCAB by application of these scenarios to a detailed air quality model for SoCAB.

To accomplish the first objective a systematic and general approach was delineated to develop realistic DG implementation scenarios in the SoCAB by the year 2010. This approach is novel in using land-use geographic information systems (GIS) data as a foundation for the DG scenarios. DG scenarios are classified in two categories according to the likelihood of its

occurrence. Some scenarios reflect an expected or realistic implementation of DG in the SoCAB, others are developed to consider an ample range of possibilities (spanning). Spanning scenarios are developed for scientific completeness, sensitivity analyses, and to determine the potential impacts of unexpected outcomes. A total of 5 realistic and 20 spanning DG scenarios were developed.

The sensitivity of the CIT model to input variables and to model components is evaluated for baseline year 2010 simulations and the parameters and elements that influence the most on air quality predictions were identified. In addition, simulation results are compared with predictions shown in the 2003 SoCAB Air Quality Management Plan using different air quality models. Furthermore, sensitivity of the CIT model to emissions changes due to weekday-weekend variation and to DG implementation is analyzed.

Prior to establishing any potential impacts of DG implementation in the SoCAB, a complete characterization of baseline results for year 2010 is presented. The baseline scenarios are based on emissions inventories that do not consider significant DG emissions, except for emissions from DG units already installed. All of the simulations that were developed to assess potential DG air quality impacts *add* the emissions from the DG scenario to this baseline case.

Results from this project lead to the following major findings and conclusions:
- CHP emissions displacements associated with most of the realistic scenarios lead to significant reductions in some criteria pollutant emissions and CO_2 emissions. For NOx, displaced boiler emissions are higher than NOx emissions directly produced by DG, resulting in net negative values for realistic scenarios with CHP.
- Realistic DG implementation scenarios introduce small basin-wide mass increases no larger than 0.43% with respect to baseline emissions. Mass increments for spanning DG scenarios are no larger than 1.35%.
- The spatial distribution of DG power based on GIS land-use data results in DG scenarios that concentrate large capacity DG technologies nearby industrial zones due to the relatively high adoption rate intensity factor estimated for the industrial sector.
- The calculation of basin-wide DG power distribution amongst the various sectors showed that 60% of total DG power is implemented in the industrial sector and nearly 32% is going to the commercial-institutional sector.
- Results of basin-wide relative contribution of each type of DG technology showed that 49% of the DG market is being met by gas turbines, whereas ICEs, MTGs, PV, FC, and GT-FC hybrids account for 17%, 15%, 5%, 10% and 4% of the total 2010 DG power market, respectively.
- The air quality model shows observable changes in ambient concentrations of ozone and PM2.5 due to DG installation
- In general, increases in NO_X emissions produced by DG scenarios reduce ozone concentrations in the central area of Los Angeles – typically VOC-limited – and increase ozone concentrations at downwind locations – typically NOX-limited. Increases in NO_X emissions also lead to an increase in 24-hour average PM2.5 concentrations over downwind locations near Riverside. Scenarios in which there is a net reduction of NO_X

due to emissions displacement by CHP produce small increments in ozone over the central area of Los Angeles and no significant changes elsewhere

- With representative characterizations of DG use in SoCAB for the year 2010 the air quality impacts of DG scenarios are:

Realistic DG scenarios:
  o Maximum basin-wide ozone concentrations do not change. Changes in maximum basin-wide 24-hour average $PM_{2.5}$ range from 0 to -3 $\mu g/m^3$
  o Maximum changes in ozone concentrations at any point throughout the basin range from $+5$ ppb to -9 ppb. Increases of up to 3 ppb in ozone concentration occur in areas where baseline values already exceed air quality standards.
  o Maximum changes in 24-hour average $PM_{2.5}$ concentrations range within ± 3 $\mu g/m^3$

Spanning DG scenarios:
  o Changes in basin-wide maximum ozone concentration ranges within ± 1 ppb. Maximum 24-hour average $PM_{2.5}$ changes from -2 $\mu g/m^3$ to $+2$ $\mu g/m^3$
  o Typically, maximum changes in ozone concentrations at any point throughout the basin are within ± 10 ppb, although there are specific cases in which changes in ozone concentration range from -26 ppb to $+34$ ppb. Maximum changes in 24-hour average $PM_{2.5}$ concentrations range from -4 $\mu g/m^3$ to $+6$ $\mu g/m^3$

- Various cases with different DG spatial distributions are explored. The level of emissions introduced by these spanning DG scenarios produce similar air quality impacts. However, additional scenarios that place a considerably higher concentration of DG show that air quality impacts due to DG are affected by the geographical location of DG units. In particular, results suggest that if DG is to be widely used in the basin, then it should net be concentrated in a small area
- Different temporal distributions of DG emissions are explored. Results show that an amount of DG emissions concentrated during a 6-hours period (peak duty cycle) produce a larger impact in air quality than the same amount emitted during 24 hours (base load duty cycle)
- Impacts on air quality estimated by this study are small, however, DG may increase localized exposure to pollutants, and higher levels of DG penetration in out years may lead to more significant air quality impacts than those presented in this study
- DG installations may impact basin wide compliance with air quality standards only if they are adopted at significantly higher levels and/or emit more pollution than those considered in this study

3   ABSTRACT

Distributed Energy Resources (DER) have the potential to supply a significant portion of increased power demands in California and the rest of the US. Distributed generation is characterized by a dispersion of many stationary power generators throughout an urban air basin. In contrast, central-generation sources are typically localized in remote areas, and occasionally outside the basin. As a result, distributed generation may lead to increased pollutant emissions within an urban air basin, which could adversely affect air quality. The present project develops a systematic approach based on land-use GIS data for characterizing the installation of DER in an urban air basin and simulates the potential air quality impacts using a state-of-the-art three-dimensional computer model. Model sensitivity and model uncertainty analyses are also developed in this project. The assessment of the air quality impacts associated with DER is made in the South Coast Air Basin (SoCAB) of California for the year 2010. Results suggest that DER characterization can be systematically applied to urban air basins, and that realistic DER implementation in SoCAB by the year 2010 only slightly affects concentrations of ozone and particulate matter in the basin. However, DG may increase localized exposure to pollutants, and higher levels of DG penetration in out years may lead to more significant air quality impacts than those presented in this study.

Keywords: Distributed generation (DG), distributed energy resources (DER), air quality, air quality impacts, scenarios, air quality model, land-use GIS data

4   INTRODUCTION

Distributed generation (DG) has the potential to meet the power demands of the near future. Deployment of DG technologies might provide additional benefits in electrical reliability and quality, besides reductions in electricity production costs. The use of Combined Heat and Power (CHP) could improve energy consumption efficiency as well as reduce emissions from fuel usage. Furthermore, having power generation near the place of use minimizes electricity transmission losses. DG is characterized by a widely dispersed distribution of emission sources within an air basin. In contrast, conventional, centralized sources of emissions from large central power plants are concentrated and localized in remote areas. In addition, in some areas, such as the case of the South Coast Air Basin of California (SoCAB), central power plants are mostly outside the air basin. Consequently, air quality impacts associated to changes from centralized power generation to DG still need to be estimated.

California, as one of the first regions in the US facing the renovation of its electric power industry, will likely be one of the first locations with widespread adoption of Distributed Energy Resources (DER). According to the strategic plan for DG developed by the California Energy Commission (Tomashefsky and Marks, 2002), more than 2,000 MW can be currently classified as DG in California. From January 2001 through May 2002, 192 DG projects were proposed throughout the state, representing more than 400 MW of new generation.

The implementation of a paradigm shift from central generation to distributed generation would result in significantly different emissions profiles with increased and widely dispersed stationary source emissions increases in several air basins (compared to central generation outside of the basin). One would like to determine whether increases in pollutant emissions in the air basin would lead to ambient ozone levels that exceed the proposed new 8-hour ozone standard. Also, increases in NOx emissions can trigger increases in secondary particulate formation that could impact compliance with proposed Federal $PM_{2.5}$ standard. The determination of these and other potential air quality impacts is of significant strategic importance to the advancement of DG technology. In addition, these impacts need to be assessed to provide a scientific basis for the design of policies related to DG implementation.

In a recent study Lents et al. (2000) determined the forms of DG that are most likely to improve environmental quality, and to reduce air pollution in California. The strategy they adopted was to comparatively analyze the level of pollutant emissions associated with a range of DG technologies and fuel types. They concluded that only the lowest emitting DG technologies (e.g., fuel cells) with significant waste heat recovery are even marginally competitive with the emissions performance of modern combined cycle power production from a criteria pollutant emissions perspective. However, in cases where waste fuel is being flared or directly emitted within the basin (e.g., in landfills), in-basin pollutant emissions can be reduced if this fuel is used to drive the DG units.

Ianucci et al. (2000) evaluated the net air emissions effects from the potential use of cost-effective distributed generation in California. First, the study used the available DG technologies and their costs to assess the economic market potential for DG for both utilities and

large commercial/industrial customers in years 2002 and 2010. Second, total emissions were calculated for the selected years, given the estimated market penetration levels for each type of DG, and compared with central-generation only scenario. The study concluded that the current California central generation mix is so clean that virtually no cost-effective distributed generation source could lower net emissions, even when transmission and distribution electric line losses are included. Fuel cells resulted in a marginal market penetration, due their high cost, but showed great promise because fuel cell air emissions are much lower than central station generation.

Significantly, this previous research did not model impacts on air quality due to emissions from DG units. The results and conclusions of these studies were based purely on emissions assessments. Changes in emissions profiles affect the concentrations of primary and secondary atmospheric contaminants. These effects need to be evaluated with detailed air quality models that include chemical and physical processes that occur in the atmosphere. The present effort, funded by the California Energy Commission under the Public Interest Energy Research (PIER) program, aims to develop a set of realistic scenarios for DG application in the south coast air basin of southern California (SoCAB) and the assessment of their air quality impacts with a detailed three-dimensional Eulerian air quality model. The California Institute of Technology (CIT) model includes atmospheric processes such as homogeneous and heterogeneous chemistry; advective and turbulent transport; and the spatial and temporal variability of the emissions and meteorology. The model is under continuous revision and development at University of California, Irvine, in collaboration with researchers from other institutions. The CIT Model has been used in previous applications: e.g., to study control measures of NOx and VOCs, and the effect on particulate matter formation (Nguyen and Dabdub, 2002); to assess the impact of chlorine chemistry in ozone formation over coastal urban environments (Knipping et al., 2003).

The primary objectives of this study are to: (1) construct a set of distributed generation implementation scenarios for the SoCAB of California; (2) improve and validate an existing air quality modeling system for use in distributed generation analyses; and (3) determine the potential air quality impacts of DG in the SoCAB by application of these scenarios to a detailed air quality model for SoCAB.

The first part of this report presents the project approach which includes three sections:
  (1) DG scenario development strategy that includes the methodology to define each DG scenario.
  (2) Air quality modeling approach, which describes the inputs required for air quality simulations to determine impacts of DG and presents a comparison of simulation results with measurements.
  (3) Methodology to determine the uncertainty and sensitivity of the chemical mechanism and the full three-dimensional air quality model

The second part of this report presents the project outcome that includes five sections:
  (1) Final DG scenarios, which include the parameters that define each scenario and the net emissions resulting from DG implementation
  (2) Baseline air quality simulation results for the year of study 2010

(3) Air quality modeling evaluation, which includes comparison of modeling results with simulations obtained by other models. In addition, this section presents improvements included in the air quality model to capture DG impacts and states the present understanding of model sensitivity to DG

(4) Air quality impacts of DG scenarios, which includes impacts on ozone, nitric oxide and particulate matter concentration

(5) Uncertainty and sensitivity analysis results for the chemical mechanism and the full air quality model

The final part of the report summarizes the conclusions extracted from this study. In addition, it includes final recommendations for the implementation of DG in the South Coast Air Basin and for future evaluations of DG implementation in other areas in California.

5   PROJECT APPROACH

5.1   Distributed Generation: Scenario Development

5.1.1   Characterization of DG Scenarios

To fully characterize how distributed generation (DG) resources may be implemented in the south coast air basin of California, one must describe in detail a significant set of parameters that define the operating characteristics of the DG units, their spatial and temporal distribution throughout the basin, and other characteristics of the particular instance of DG use in the basin. A compilation of the entire suite of information and characteristics that are required to fully describe all of the DG characteristics as installed in SoCAB is called a "DG Scenario."

The Advanced Power and Energy Program (APEP) team has determined that the space required to fully define a DG Scenario can be characterized by a set of seven parameters and various factors that are subsets of these parameters. The seven parameters have been identified to fully characterize a DG scenario are presented schematically in Figure 1. The seven parameters of Figure 1 include: (1) the total fraction of SoCAB energy needs that are met by DG in the scenario, (2) the allocation of DG resources to meet that need, (3) the emissions associated with each DG unit type, (4) the spatial distribution of the DG in SoCAB, (5) the operational duty cycle of each DG, (6) the accounting for any emissions that are displaced by installation of the DG, and (7) other estimates that are required to account for the DG and relate the emissions to requirements of the air quality model (AQM). Each of the parameters may have several factors that are varied within the parameter space.
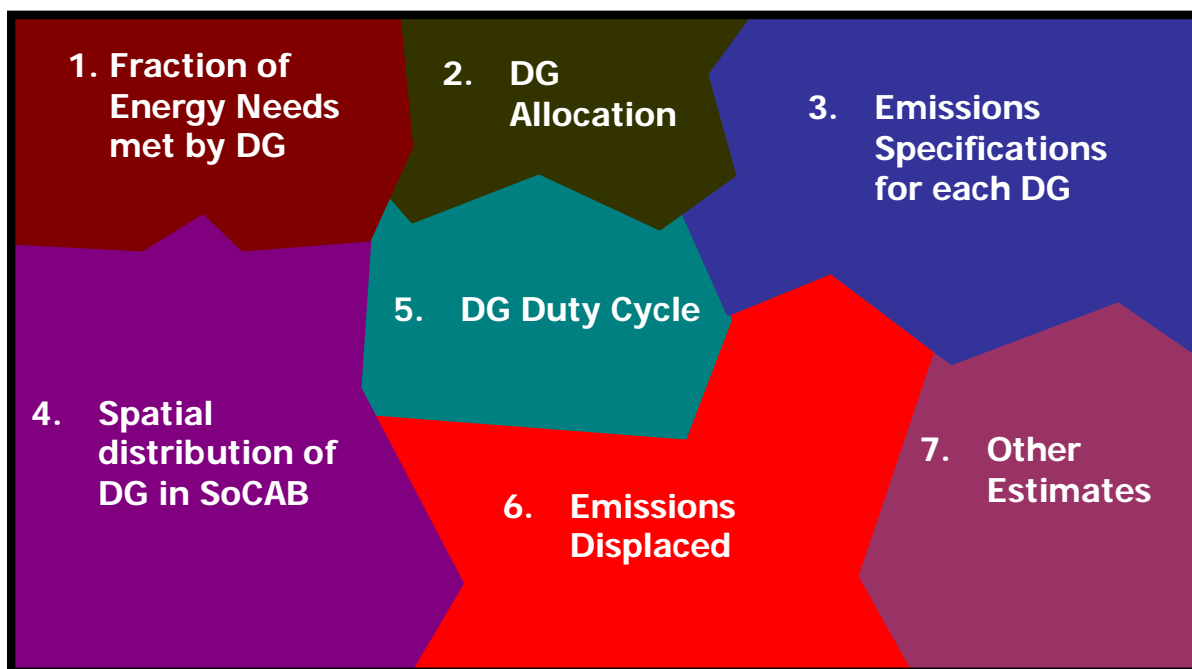
Figure 1: Schematic of the DG scenario parameter space.

Table 1 presents more details of the parameter space and all of the factors that are considered in the development of the DG scenarios. The overall outline of these parameters (highest level of characterization) and factors (lower level variables) is presented in Table 1 below. Note that we consider some of the parameters as fully characterized by variations in primary factors, whereas other parameters require characterizations and variation of primary and secondary factors in their definition.

Table 1. List of parameters and factors that are required to be characterized to represent a full distributed generation scenario for the South Coast Air Basin.

Main DG Parameter	Primary Factors	Secondary Factors
1. Fraction of energy needs met by DG	1.1. Limited (5% of increase)	
	1.2. Medium (10% of increase)	
	1.3. High (15-20% of increase)	
2. DG allocation	2.1. Types of DG units	2.1.1. All NG large GT-DG (50 MW)
		2.1.2. Fuel Cell Only
		2.1.3. MTG only
		2.1.4. Renewables – yes, no
		2.1.5. Mix of DG (MTG, FC, NG-ICE, Stirling, hybrid, …)
		2.1.6. Mix of DG and large GT-DG (50 MW)
		2.1.7. Diesel included – yes or no
	2.2. Number of DG units of each type	2.2.1. Large DG unit size vs. small DG unit size

		2.2.2. Technology Mix Factors
		  - High penetration of low emissions technologies (strong regulation/policy drivers)
		  - Low penetration of low emissions technologies (either modest regulation or lack of technology advancement)
		  - Zoning or land-use
		  - Economic factors

3. Emissions specification for each DG	3.1. Current emissions factors	3.1.1. Known emissions factors – literature, data
		3.1.2. Estimated emissions factors
	3.2. Future advancements to meet regulatory requirements	3.2.1. Fraction that meets 2003 standards
		3.2.2. Fraction that meets 2007 standards
4. Spatial distribution of	4.1. Even	
	4.2. Population weighted	

DG in SoCAB	4.3. Population growth weighted	
	4.4. Land-use weighted	4.4.1.Classify Land-use
		4.4.2.Land-use energy adoption rate factors
		4.4.3.Land-use weighted technology adoption factors
	4.5. Electrical use weighted (need data from SCE/LADWP)	
	4.6. Freeway weighted	
5. DG duty cycle	5.1. Base-loaded	
	5.2. Peaking	
	5.3. Mix of base-loaded and peaking	
6. Emissions displaced	6.1. Port Emissions	NOTE: only if DG is installed in place of idling ships
	6.2. Landfill/digester/other flared or wasted gas use	NOTE: most of these sources have already implemented emissions mitigation technology
	6.3. CHP	6.3.1.Displace old boilers and equipment
		6.3.2.Displace new boilers and equipment
		6.3.3.Percentage of CHP value recovered
	6.4. In-Basin electricity emissions displaced	
7. Other estimates	7.1. Emissions assumptions	7.1.1.Speciation of total hydrocarbons into specific hydrocarbon compounds and particulate matter (PM) into 8 size classes and 19 species of PM
	7.2. Performance degradation (yes or no)	
	7.3. Geometrical features (elevated emissions – yes or no)	
	7.4. DG Commercial Adoption Rate	7.4.1.High Early Adoption (logarithmic increase of cumulative DG Power from 2003 to 2010)
		7.4.2.Low Early Adoption (exponential increase of cumulative DG power)
		7.4.3.Medium Early Adoption (linear increase of cumulative DG power)

Once all of the parameters and factors of Table 1 are specified, the DG scenario is fully characterized and the corresponding DG emissions inventory for each of the discrete cells in the computational model can be developed for each instance in time. The model calculates the transport, chemical reaction, diffusion, etc. of all the species within the basin on an hourly averaged basis. As a result, DG emissions rates must be specified for as listed in Table 1 for

each cell and for each of the 24 hours of each day of the simulation. This DG emissions inventory is then formatted as a model input file and added to the baseline emissions inventory for use in the model to assess the air quality impacts of the DG emissions. The baseline emissions inventory includes the emissions forecasted for 2010 by the California Air Resources Board (CARB) and South Coast Air Quality Management District (SCAQMD) (Allen, 2002).

Note that two types of DG Scenarios are developed in the current effort as follows:

- "Realistic" DG Implementation Scenarios, and
- "Spanning" DG Implementation Scenarios.

These two categories segregate the DG Scenarios on the basis of the "likelihood" of the scenario. "Realistic" implementation scenarios for DG in the South Coast Air Basin are assessed by the APEP team and stakeholders who participated in the September 19, 2002 and May 20, 2003 workshops to be likely instances of DG installation in the SoCAB. However, for scientific completeness, for sensitivity analyses, and for determination of potential impacts for unexpected outcomes "Spanning" scenarios are required. These spanning scenarios must not be considered realistic or probable. The spanning DG scenarios are not expected and are only used for purposes of garnering insights that may be useful.

5.1.1.1 Fraction of Energy Met by DG

The "Fraction of Energy Met by DG" parameter has a strong influence in the final air quality impact that a DG scenario exhibits. A high penetration scenario implies that DG units throughout the basin meet a considerable portion of the total energy needs of the SoCAB. In this case, DG emissions extensively contribute to the total SoCAB pollutant emissions. However, for the same level of emissions, air quality impacts might be very different depending on other DG scenario characterization parameters such as spatial distribution of the DG power or duty cycle. In addition, these impacts are not easy to predict without a detailed and comprehensive model due to the highly non-linear processes that govern the coupled transport and atmospheric chemistry of an air basin.

According to the California Energy Commission Strategic Plan for DG (Tomashefsky and Marks 2002), the forecasted adoption of DG in California for the year 2020 could be as high as 20% of the electricity load growth. The current DG scenarios are considered high penetration scenarios if the power demand met by DG is greater than 15% of the increased SoCAB power. Medium and low penetration are assigned to cases with about 10% and 5%, respectively, of the increased power demands met by DG.

Since the fraction of energy met by DG is quite uncertain, a wide variety of DG penetration levels is investigated in the DG scenarios to span the spectrum of possible air quality impacts.

5.1.1.2 DG Allocation

Based on input from the first industry stakeholders workshop held in September 2002 (See Appendix A for full details and results from this workshop), the current study includes distributed generators with power capacities that range from a few kilowatts (kW) up to 50

megawatts (MW). The 50 MW limit on DG is selected due to the permitting construct of the SoCAB. The DG technologies that are likely to be implemented in the SoCAB include commercial technologies (natural gas fired combustion turbines (up to 50 MW) and natural gas fired reciprocating internal combustion engines (ICE)), and emerging technologies (solar photovoltaics (PV), fuel cells (PEMFC, MCFC and SOFC), gas turbine fuel cell hybrids, natural gas fired micro-turbine generators (MTGs), and external combustion Stirling engines).

The specific mix of DG technologies that is likely to be installed in any one region of the SoCAB in 2010 is very difficult to forecast. The technology mix is dependent on the number and type of energy customers in that region as well as a host of other economic and regulatory variables (e.g. electricity prices, gas prices, DG incentives, transmission constraints, emissions standards) that exist in that particular zone.

Every market segment can be preferentially associated with specific DG technologies that are likely to be predominant, mainly because their capacity and features are best suited to the energy demands of that segment. For example, residential applications in the range 1-5 kW will likely favor fuel cells and photovoltaics; commercial and small industrial sectors, with capacities ranges of 25-500 kW are more suited for PV, MTGs, small ICEs and FCs; large commercial and institutional sectors, in the range of 500-2MW, will likely favor natural gas reciprocating engines and gas turbines; and finally the large institutional and industrial sectors with 2-50 MW capacity will be mainly served by gas turbines. This relationship between DG type and market sector, together with spatial distributions of such in SoCAB is used in some of the scenarios to estimate the distribution and duty cycle of technologies in each of the discretized cells of the model on the basis of land-use zoning classification data.

The DG scenarios developed in this effort are not based upon a detailed market penetration analysis for the various DG technologies in SoCAB, but rather upon studies that are currently available in the literature, APEP insights, and stakeholder feedback. The resources used include: (1) previous studies that determined a reasonable mix of technologies (e.g., Ianucci et al., 2000; Marnay et al., 2001), (2) input from the industry stakeholder workshops (see Appendix A and Appendix B), (3) current APEP understanding of technology features, (4) current penetration of certain technologies (e.g., MTGs), and (5) APEP intuition; engineering insight and/or brainstorming.

Diesel and petroleum distillate fueled units are not included in the current mix of DG technologies since the SCAQMD does not currently permit them to run on a continual basis as distributed generators. These types of units are only permitted to run as back-up generators.

5.1.1.3   Spatial distribution of DG in SoCAB

It is important to capture the spatial distribution of emissions in an air basin in order to accurately determine species concentrations that contribute to air quality. The location of the emissions, together with meteorology, mass transport, photochemical reaction times, and the mixture of chemical compounds (both gases and aerosols), radiation intensity, etc. all contribute to the eventual air quality prediction (e.g., ozone, NOx, PM_{10} concentrations). To accurately estimate the spatial distribution of DG adoption, a detailed market penetration study should be conducted at the scale of model resolution. However, this is beyond the scope of the current

study, so reasonable estimates of DG power in 2010 are developed based strictly upon demographic and economic parameters that can be correlated to power (e.g., population data, population growth data, electricity consumption data, land-use data). In most of the DG scenarios developed in this effort (spanning scenarios), the forecast of DG power in each cell is proportional to the number of inhabitants forecasted for 2010 in that cell, i.e., the DG spatial distribution is population weighted. The other spatial distributions that are applied in this study are:

- Even,
- Population growth weighted,
- Land-use weighted (used for all of the realistic scenarios),
- Electrical use weighted (based on available data from SCE and LADWP), and
- Freeway weighted.

5.1.1.4   DG Duty Cycle

The DG duty cycle parameter accounts for the temporal variation of DG power production that leads to the overall capacity factor (number of hours operating/total hours) for each of the individual DG devices. The actual duty cycle for an individual DG unit depends upon maintenance schedules, economics, power demand, and many other factors. For a specific scenario some DG technologies (e.g. high temperature fuel cells) will likely operate as base-loaded devices, i.e., they will operate essentially continuously. This is due to both economic (high efficiency and high capital cost portend continuous operation for reasonable payback) and operational factors (high temperature operation leads to long start-up, and high thermal stresses associated with transients). On the other hand, many other DG types are expected to operate primarily during peak hours. The combined DG duty cycle of all DG units operating in each cell results in a different set of pollutant emissions for each hour of the simulation. The air quality model can assess the air quality impacts of this duty cycle, which is capable of accepting DG emissions profiles that vary on an hourly basis.

5.1.1.5   Emissions Specifications

There is a wide range of emissions factors that are either available as measured data or estimated by various investigators for each of the DG technologies. Some DG technologies are environmentally friendly, with zero emissions (e.g., wind turbines, photovoltaics) or near zero emissions (e.g., fuel cell systems using on-site natural gas reformation), while others may emit more pollutants than central station power plants. For the some of the spanning DG scenarios the emissions factors proposed by Allison et al. (2002), which are best estimates from a compilation of sources, have been used directly. This data set, however, includes emissions factors that are higher than the current regulated limits for DG units permitted by SCAQMD (ICEs and GT) and the others certified by ARB (MG, FC, Stirling engines, and others with less than 1 MW capacity). Whenever this occurred, the values selected to characterize a specific DG unit were the applicable standards levels instead of the emissions factors of Allison et al. (2002). The emissions factors proposed by Allison et al. (2002) for a collection of gas-driven DG technologies are presented in Table 2.

Table 2: Emissions Factors and Efficiencies for some DG technologies (after Allison and Lents, 2002)

Generation Type	Efficiency	CO	VOC	NOx	SOx	PM2.5	CO$_2$
	Elec. Out / Energy In	Lbs/kWh	lbs/kWh	lbs/kWh	lbs/kWh	lbs/kWh	lbs/kWh
Gas Turbine Combined Cycle - central	0.52	1.70E-04	1.10E-04	1.30E-04	2.00E-05	2.00E-05	0.62
MTG	0.27	2.85E-03	5.00E-05	1.40E-03	2.00E-05	9.00E-05	1.25
Advanced Turbine	0.36	2.60E-03	3.00E-05	1.09E-03	2.00E-05	7.00E-05	0.95
Conventional Turbine	0.28	1.51E-03	4.00E-05	1.24E-03	3.00E-05	9.00E-05	1.2
Gas Powered ICE	0.35	8.00E-03	1.70E-03	3.20E-03	1.00E-05	4.75E-04	0.97
Diesel ICE	0.44	3.00E-02	2.00E-03	1.70E-02	3.00E-04	3.00E-03	1.7
PEM Fuel Cell	0.36	0.00E+00	9.00E-04	2.00E-05	1.00E-05	0.00E+00	0.95
Direct Fuel Cell	0.4	0.00E+00	0.00E+00	0.00E+00	0.00E+00	0.00E+00	0.68

For the realistic scenarios and to determine a more likely set of emissions for each of the DG technology types, the current study conducted an extensive literature search. This literature search, together with insights, reports, and feedback from agencies, industries, and colleagues has led the compilation of various emissions estimates as presented in Table 3. Six primary sources are presented in Table 3 with each of the DG technologies that are covered by each reference, and a listing of the pollutant species emissions rates that are available in each study.

Appendix C presents the details of emissions rates represented by the sources listed in Table 3. One should note that there is wide variability of emissions factors amongst the studies that are currently available. Also presented in Appendix C are the DG emissions standards for 2003 and 2007 and the current BACT requirements of SCAQMD for DG in the SoCAB.

Table 3: DG technologies and pollutant species available in 6 literature references for DG emissions factors.

Generation Type	NREL, 2003,	Nexus, 2002	Allison and Lents, UCR, 2002	Regulatory Assistant Project (RAP), 2001	Marnay et al., LBNL, 2001	Ianucci et al., DUA, 2000
Gas Turbine Combined Cycle – central	N/A	N/A	✓ CO, VOC, NO_x, SO_x, PM, CO_2	✓ CO, VOC, NO_x, SO_x, PM, CO_2	N/A	N/A
Microturbine Generator	✓ CO, NO_x, VOC, CO_2	✓ CO, NO_x, VOC	✓ CO, VOC, NO_x, SO_x, PM, CO_2	✓ CO, VOC, NO_x, SO_x, PM, CO_2	✓ CO, NO_x, PM	✓ CO, VOC, NO_x, SO_x, PM, CO_2
Advanced Turbine	N/A	✓ CO, NO_x, VOC	✓ CO, VOC, NO_x, SO_x, PM, CO_2	✓ CO, VOC, NO_x, SO_x, PM, CO_2	N/A	✓ CO, VOC, NO_x, SO_x, PM, CO_2
Conventional Turbine	N/A	✓ CO, NO_x, VOC	✓ CO, VOC, NO_x, SO_x, PM, CO_2	✓ CO, VOC, NO_x, SO_x, PM, CO_2	N/A	✓ CO, VOC, NO_x, SO_x, PM, CO_2
Uncontrolled Gas Powered Lean Burn ICE	N/A	N/A	✓ CO, VOC, NO_x, SO_x, PM, CO_2	✓ CO, VOC, NO_x, SO_x, PM, CO_2	✓ CO, NO_x, PM	✓ CO, VOC, NO_x, SO_x, PM, CO_2
Uncontrolled Diesel ICE	N/A	N/A	✓ CO, VOC, NO_x, SO_x, PM, CO_2	✓ CO, VOC, NO_x, SO_x, PM, CO_2	✓ CO, NO_x, PM	✓ CO, VOC, NO_x, SO_x, PM, CO_2
PEMFC	N/A	✓ CO, NO_x, VOC	✓ CO, VOC, NO_x, SO_x, PM, CO_2	N/A	N/A	✓ CO, VOC, NO_x, SO_x, PM, CO_2
DFC	N/A	✓ CO, NO_x, VOC	✓ CO, VOC, NO_x, SO_x, PM, CO_2	N/A	N/A	N/A
SOFC	N/A	✓ CO, NO_x, VOC	N/A	✓ NO_x, SO_x, PM, CO_2	N/A	N/A
3-way Catalyst Gas Powered Rich Burn ICE	N/A	✓ CO, NO_x, VOC	N/A	✓ CO, VOC, NO_x, SO_x, PM, CO_2	N/A	N/A
SCR Controlled Diesel ICE	N/A	✓ CO, NO_x, VOC	N/A	✓ CO, VOC, NO_x, SO_x, PM, CO_2	N/A	N/A

Appendix C presents plots for emissions rates of different DG technologies for the main 6 air pollutants (CO, NOx, VOC, SOx, PM, and CO_2). Minimum, maximum and average values of emissions estimates from all of the 6 literature sources presented in Table 3 are presented in Appendix C.

Table 4 and Table 5 present the recently approved California Air Resources Board emission standards (CO, VOC, NOx and PM limits) for type certification of DG. These standards apply to

DG units that do not fall under the jurisdiction of SCAQMD for control of stationary point sources. The capacity limit for SCAQMD rules to apply is 1MW, below which the regulatory requirements presented in Table 4 and Table 5 apply.

The SCAQMD best available control technology (BACT) permitted levels for DG emissions are presented in Table 6. The current project expended significant effort to study both the regulatory requirements of Table 4, Table 5, and Table 6 and all of the emissions estimates presented in Appendix C. This effort proved that significant disparities in the emissions rates and DG performance expectations exist, which adds uncertainty to the evaluation of DG environmental impacts. To address these disparities, the current project includes a sensitivity analyses effort that will determine model output sensitivities to emissions rates as well as search out measurements and verifiable performance data to include in the analyses. At the same time, the best possible estimates that are deemed reasonable and feasible and that do not violate current regulations are used in the scenario development of the current study.

In a couple of the spanning scenarios, DG emissions limits as currently set by ARB for 2003 and 2007, as well as SCAQMD best available control technology (BACT) standards for DG are used directly for all of the DG implemented. These spanning scenarios are presented as reference cases only.

Table 4: Approved ARB DG emissions standards for 2003 (Chin et al., 2001)

Pollutant / DG type	CO lbs/MWh	VOC lbs/MWh	NOx lbs/MWh	PM lbs/MWh
DG Unit not integrated with Combined Heat and Power	6.00	1.00	0.50	An emission limit corresponding to natural gas with sulfur content of no more than 1 grain 100 standard cubic feet (scf)
DG Unit integrated with Combined Heat and Power	6.00	1.00	0.70	An emission limit corresponding to natural gas with sulfur content of no more than 1 grain 100 standard cubic feet (scf)

Table 5: Approved ARB DG emissions standards for 2007 (Chin et al. 2001)

Pollutant / DG type	CO lbs/MWh	VOC lbs/MWh	NOx lbs/MWh	PM lbs/MWh
Emissions	0.100	0.020	0.070	An emission limit corresponding to natural gas with sulfur content of no more than 1 grain 100 standard cubic feet (scf)

Table 6: SCAQMD BACT guidelines for gas turbines and internal combustion engines (SCAQMD 2000)

Subcategory	VOC	NOx	SOx	CO	PM$_{10}$	Inorganic (NH$_3$)
NG GT, < 3 MWe						
ppm@15% O$_2$	**2**	**9**	--	**10**	--	**9**
lbs/MMBtu	0.0026	0.0332	**0.0008**	0.0224	**0.0066**	0.012
lbs/MW-hr	0.0358	0.4638	0.0112	0.3137	0.0923189	0.170
NG GT, ≥ 3 MWe and < 50 MWe						
ppm@15% O$_2$	**2**	**3.6**	--	**10**	--	**5**
lbs/MMBtu	0.0026	0.0133	**0.0008**	0.0224	**0.0066**	0.007
lbs/MW-hr	0.0243	0.1257	0.0076	0.2126	0.0626	0.064
Non-Emergency NG ICE, < 2064 bhp						
ppm@15% O$_2$	32.42	11.28	--	74.18	--	--
lbs/MMBtu	0.0415	0.0415	**0.0008**	0.1663	**0.0066**	--
grams/bhp-hr	**0.15**	**0.15**	0.003	**0.600**	0.024	--
lbs/MW-hr	0.4431	0.4431	0.0085	1.7723	0.0704	--

Using the compilation of literature emissions factor data and the ARB and SCAQMD limits presented in Table 4, Table 5, and Table 6 as an upper bound, we have constructed two tables with emissions factors for DG systems installed in the periods 2003-2006 and 2007-2010, respectively, as shown in Table 7 and Table 8. These sets of DG emission factors are the ones utilized in the development of DG implementation scenarios, both the spanning and the realistic scenarios, unless otherwise specified.

Table 7: Emissions factors used to develop DG Scenarios in the current study for DG units installed in the period 2003-2006.

Generation Type	Efficiency (based on HHV)	CO lbs/kWh	VOC lbs/kWh	NOx lbs/kWh	SOx lbs/kWh	PM lbs/kWh	CO$_2$ lbs/kWh	NH$_3$ lbs/kWh
MTG	0.27	2.85E-03	5.00E-05	7.00E-04	1.01E-05	8.35E-05	1.50	0E+00
GT (<3 MW)	0.244	3.12E-04	3.58E-05	4.62E-04	1.12E-05	9.23E-05	1.66	1.70E-04
GT (>3 MW)	0.36	2.12E-04	2.43E-05	1.26E-04	7.59E-06	6.26E-05	1.13	6.42E-05
Gas ICE	0.32	1.77E-03	4.43E-04	4.43E-04	8.54E-06	7.04E-05	1.27	0.E+00
LT FC	0.36	1.00E-04	9.00E-04	7.00E-05	7.59E-06	6.26E-05	1.13	0.E+00
HT FC	0.48	1.00E-04	2.00E-05	7.00E-05	5.69E-06	4.69E-05	0.85	0.E+00
Stirling	0.27	6.00E-03	1.00E-03	5.00E-04	1.01E-05	8.35E-05	1.50	0.E+00
Hybrid	0.7	6.00E-03	1.00E-03	5.00E-04	3.90E-06	3.22E-05	0.58	0.E+00

Table 8: Emissions factors used to develop DG Scenarios in the current study for DG units installed in the period 2007-2010.

Generation Type	Efficiency (based on HHV)	CO	VOC	NOx	SOx	PM	CO_2	NH_3
		lbs/kWh	lbs/kWh	lbs/kWh	lbs/kWh	lbs/kWh	lbs/kWh	lbs/kWh
MTG	0.27	1.00E-04	2.00E-05	7.00E-05	1.01E-05	8.35E-05	1.50	0.00E+00
GT (<3 MW)	0.244	3.12E-04	3.58E-05	4.62E-04	1.12E-05	9.23E-05	1.66	1.70E-04
GT (>3 MW)	0.36	2.12E-04	2.43E-05	1.26E-04	7.59E-06	6.26E-05	1.13	6.42E-05
Gas ICE	0.32	1.77E-03	4.43E-04	4.43E-04	8.54E-06	7.04E-05	1.16	0.00E+00
LT FC	0.36	1.00E-04	2.00E-05	7.00E-05	7.59E-06	6.26E-05	1.13	0.00E+00
HT FC	0.48	1.00E-04	2.00E-05	7.00E-05	5.69E-06	4.69E-05	0.85	0.00E+00
Stirling	0.27	1.00E-04	2.00E-05	7.00E-05	1.01E-05	8.35E-05	1.50	0.00E+00
Hybrid	0.7	1.00E-04	2.00E-05	7.00E-05	3.90E-06	3.22E-05	0.58	0.00E+00

The emissions factors presented in Table 7 and Table 8 indicate that the DG technologies that can be deployed in the SoCAB have relatively low criteria pollutant emissions rates (i.e., they are clean DG technologies). Nonetheless, if DG are widely adopted in the SoCAB, the contribution of DG emissions compared to total emissions estimates in the SoCAB for 2010 is important enough to be concerned about potential air quality impacts of DG deployment. For example, one of the spanning scenarios, characterized by an extra high penetration (20% of total power met by DG) and a mix of DG technologies, produces DG NOx emissions that account for 2% of total SoCAB NOx emissions inventory for 2010.

Figure 2 presents a comparison of DG criteria pollutant emissions (carbon monoxide, nitrogen oxides, reactive organic gases, and particulate matter) and the total basin emissions inventory for the SoCAB in 2010. The data of Figure 2 represent the attainment emissions inventory (i.e., one that scales emissions for population and vehicle miles traveled growth and assumes additional regulatory measures are adopted to meet attainment with ambient air quality standards (SCAQMD, 2003)) compared to the high DG penetration scenario described above

Even though the realistic DG scenarios typically contain lower DG penetration and result in much smaller contributions of DG emissions to the inventory, the air quality impacts of these DG emissions may still be significant. First, many particular locations in the SoCAB are "on the edge" between compliance and non-compliance. Even a 1 ppb change in ozone concentrations in one location, for example, could result in the basin not achieving attainment. In addition, since the coupled transport and atmospheric chemistry interactions are of a highly non-linear nature small changes in emissions fields could lead to substantial air quality impacts.
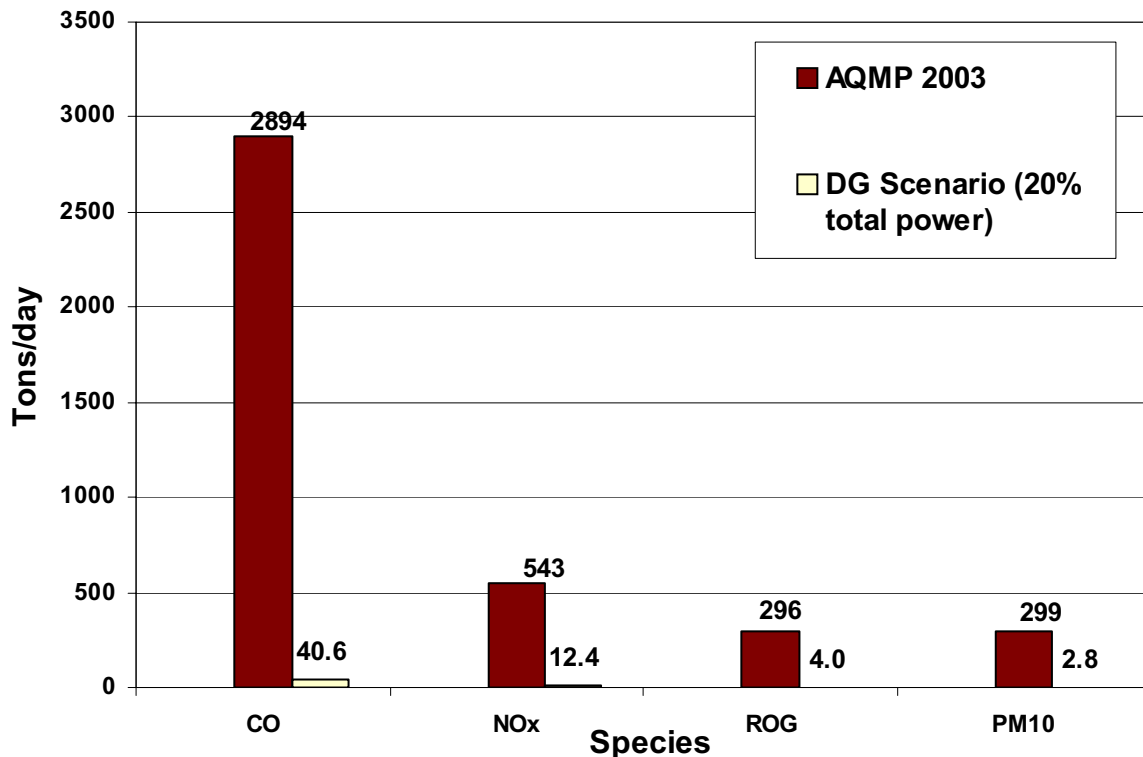
Figure 2: Comparison of total SoCAB emissions in 2010 and DG emissions from an extra high DG penetration scenario.

5.1.1.6 Emissions Displaced

Many of the DG technologies that are being and will be adopted in the SoCAB will be used in combined heating cooling and power (CHP) applications because the higher overall energy efficiency of CHP improves the economics of certain DG projects. Waste heat produced during electricity generation can be captured by a heat recovery system that provides useful heat to meet facility thermal loads, which can significantly decrease operating costs. As a result, DG/CHP can replace the heat produced by burning fuel in a boiler leading to a reduction (displacement) of boiler-associated emissions in the basin. For retrofit DG/CHP applications, old, more polluting boilers are likely to be displaced, whereas for new applications displacement of emissions from new equipment (i.e., more efficient and lower polluting boilers) should be considered.

Emissions into the SoCAB can also be displaced by application of DG to waste gases from solid landfills, oil fields, or biomass gas emissions (e.g., dairy farm gaseous emissions). In these cases the DG application displaces either direct hydrocarbon emissions or flared gas emissions depending upon the current status of the waste gas emission. According to Lents et al. (2002), all DG units in this type of application reduce ozone related emissions compared to a central station combined cycle power plant. Due to this fact and due to encouragement from the SCAQMD, most of the landfills in the SoCAB have already implemented DG (Lenssen, 2001) to substitute for flares and produce on-site power and heat.

Other DG applications in which emissions could be displaced include the replacing of old central power plants in the basin and the substitution of lower emitting DG technologies for the diesel generators that are extensively used in Los Angeles port and vicinity. All of the above potential displacements of emissions are taken into account in the development of realistic DG scenarios.

5.1.1.6.1 CHP emissions displacement

To assess the displaced boiler emissions and net DG emissions for each of the discretized model cells in scenarios in which CHP emissions displacement is considered, the following procedure is applied:

1. Estimate a reasonable share of DG implemented in the SoCAB that is installed with waste heat recovery equipment (e.g., $f_{CHP} = 60\%$ was suggested in the stakeholder workshop).

2. Assume an average heat recovery utilization factor or heat recovery capacity factor, which includes the lost waste heat due to supply and demand mismatch (e.g., $f_{HR} = 50\%$).

3. Evaluate the total amount of thermal heat recovered in each hour, Q_{HR}, taking into account the electric energy produced by the DGs, Q_{elec}, the electrical and total efficiencies of each fuel-driven DG technology, $\eta_{elec,i}$ and $\eta_{total,i,}$, respectively, and the particular mix of DG, $f_{DG,i}$, which can vary hour by hour due to possible differences in duty cycle for each technology.

$$Q_{HR} = Q_{elec} \sum_{i}^{n} \left(f_{DG_i} \frac{(\eta_{total\,i} - \eta_{elec\,i})}{\eta_{elec_i}} \right) \cdot f_{CHP} \cdot f_{HR} \qquad (1)$$

4. Assume a reasonable mix of old, inefficient, dirty boilers (associated with retrofit DG/CHP) and new, clean, more efficient boilers (associated with new DG/CHP projects). Example: $f_{old} = 30\% : f_{new} = 70\%$.

5. Evaluate the total amount of offset fuel that would otherwise be burnt in the boilers to produce the same quantity of thermal energy delivered by the DG/CHP units. Consider both old boilers and new boilers efficiencies (e.g.: $ef_{old} = 0.8$ and $ef_{new} = 0.9$).

$$Q_{fuel} = \frac{Q_{HR}}{(ef_{old} f_{old} + ef_{new} f_{new})} \qquad (2)$$

6. Use both emissions factors for old (em_{old}) and new boilers (em_{new}) and calculate the avoided emissions in each cell. As an example, the expression for displaced boiler CO emissions is presented below:

$$M_{CO,off} = Q_{fuel} \left(em_{old,CO} f_{old} + em_{new,CO} ef_{new} \right) \qquad (3)$$

7. Determine the net flux of emissions for each pollutant in a cell due to DG, subtracting the displaced boiler emissions from the total DG emissions contribution. In the case of CO, the net DG emissions can be written as follows:

$$M_{CO,net} = M_{CO,DG} - M_{CO,off} \qquad (4)$$

5.1.1.6.2 Emissions factors for boilers

New and old SCAQMD values for avoidable boiler air emissions are presented in Table 9. The avoided emissions per kWh of electric generation for a particular DG-CHP technology can be written as:

$$DGHeatRate(Btu_{in} / kwh_e) \cdot \frac{(ef_{tot} - ef_{elec})}{ef_{boiler}} \cdot f_{boiler} (lbs / Btu) \qquad (5)$$

Table 9: Typical boiler air emissions (Ianucci et al., 2000; Kay, 2003)

	CO lbs/MMBtu	**VOC** lbs/MMBtu	**NOx** lbs/MMBtu	**SOx** lbs/MMBtu	**PM$_{2.5}$** lbs/MMBtu	**CO$_2$** lbs/MMBtu
New	2.35E-02	5.39E-03	1.5E-02	5.90E-04	7.45E-03	118
Old	8.24E-02	5.39E-03	3.6E-02	5.90E-04	7.45E-03	118

5.1.1.6.3 Analysis of maximum potential emissions displacement for each DG technology

This section assesses the reduction in emissions for four representative DG technologies in the case when the heat recovery unit is running continuously, 24 hours a day and is fully utilized. This case represents the maximum theoretical emissions displacement, when both the share of CHP and the heat recovery capacity factor are equal to 100 %. Therefore, this exercise gives an upper bond of emissions offsets that DG implementation scenarios would be able to provide if all DG installations included CHP. Table 10 shows CO, VOC, NOx and CO$_2$ emissions reductions when CHP is applied to 4 DG types (fuel cells, natural gas ICEs, diesel ICEs and MTGs). Boiler emissions displacements both for new and retrofit applications are presented in Table 10.

Table 10: Maximum emission displacements for 4 types of CHP units

Type of DG	Type of application	CO			VOC			NOx			CO$_2$		
		DG (lbs/kWh)	Boiler (lbs/kWh)	% Red.	DG (lbs/kWh)	Boiler (lbs/kWh)	% Red.	DG (lbs/kWh)	Boiler (lbs/kWh)	% Red.	DG (lbs/kWh)	Boiler (lbs/kWh)	% Red.
Fuel cell (PEM)	Retrofit	0.0001	0.00048	**478.4%**	0.0009	3.1E-05	**3.5%**	7E-05	0.00021	**298.6%**	1.16	0.685	**59.1%**
	New	0.0001	0.00012	**121.2%**	0.0009	2.8E-05	**3.1%**	7E-05	7.7E-5	**110.6%**	1.16	0.609	**52.5%**
Natural gas ICE	Retrofit	0.0018	0.00058	**32.2%**	0.00044	3.8E-05	**8.6%**	0.00044	0.00025	**57.3%**	1.27	0.834	**65.6%**
	New	0.0018	0.000148	**8.3%**	0.00044	3.4E-05	**8.6%**	0.00044	9.4E-5	**21.2%**	1.27	0.741	**58.3%**
Diesel ICE	Retrofit	0.0077	0.00033	**4.3%**	0.0014	2.1E-05	**1.5%**	0.013	0.00014	**1.1%**	1.3	0.469	**63.9%**
	New	0.0077	8.3E-05	**1.1%**	0.0014	1.9E-05	**1.4%**	0.013	5.3E-5	**0.4%**	1.3	0.417	**32.1%**
MTG	Retrofit	0.00285	0.00076	**26.5%**	0.00005	4.9E-05	**98.8%**	0.0007	0.00033	**47.12%**	1.5	1.081	**72.1%**
	New	0.00285	0.00019	**6.7%**	0.00005	4.4E-05	**87.8%**	0.0007	0.00012	**17.45%**	1.5	0.961	**64.1%**

Note that for natural gas and diesel ICEs, with higher pollutant emission footprints (see Allison and Lents (2002) for ICE emissions and Table 7 for the other DG emissions), boiler emission displacements are not very high (0-32 %). The only exception is the 57.3% reduction in NOx emissions for a natural gas ICE displacing an old boiler. On the other hand, when cleaner fuel driven DG such as MTGs or fuel cells are considered, significant reductions are achieved, resulting in some cases in a negative net emissions flux (e.g. NOx emissions for fuel cells with CHP). Furthermore, all natural gas driven CHP technologies yield to significant displacement (52-72% reduction) of global warming CO_2 emissions.

All of the CHP technologies of Table 10 were considered in different shares with different heat recovery capacity factors that were all significantly less than 100% to account for losses, temporal non-coincidence, and end-use thermal requirements. In realistic DG scenarios, where diesel ICE CHP was not included, only small reductions in air pollutant emissions in the range 0-20% are expected. On the other hand, reductions in CO_2 emissions may be higher, in the range of 20-40%.

5.1.1.7   Other Estimates

As some of the DG technologies are just emerging in the marketplace, certain features of these technologies, including accurate pollutant emissions rates and emissions speciation, are not readily available. In addition, understanding of features such as continuous versus peak power applicability, size of equipment, availability of fuel, emissions stack height, etc. may need to be estimated for the current study. Currently our group is carrying out a detailed emissions measurement process for various DG types in a DG testing facility, which is being used to complete some of the missing data. When data are still not available, however, reasonable estimates or assumptions are applied only as required for compatibility with the simulation software.

One significant factor that must be estimated for the current study is the degradation rate for technologies installed in the earlier years between now and the study year of interest. All DG technologies experience some degradation in efficiency performance and many may also degrade in the pollutant emissions performance. However, measurements of DG performance degradation are still limited, and therefore, a degradation rate due to operation of DG must be estimated. The adoption cumulative curve of DG power in the following year is also uncertain and various curves (exponential, linear, etc.) are considered. Finally, some technologies are expected to substantially improve their emissions and efficiency performance over the next several years. This improvement in performance must also be estimated for accurate development of a DG scenario.

5.1.1.8   Speciation of criteria pollutants

Emissions from DG are estimated on a basis of a limited set of generic pollutants: NO_X, SO_X, VOC and PM. To make the emissions fluxes from any DG scenario compatible with the input required by the air quality model, one must provide emissions fluxes for all species that the model currently considers in its detailed chemical mechanism. Consequently, emissions of these

generic pollutants have to be speciated into a finer level of detail. Table 11 shows the speciation and weighting factors used for each of the species for which this procedure was required. The codes presented in Table 11 for the species in VOC and PM are the same as those used in CACM chemical mechanism. The chemical name associated with each code is listed in Table 12.

Table 11: Speciation used for criteria pollutants from DG scenarios

Criteria Pollutant	Species							Comments
NOx	**NO**			**NO$_2$**				APEP estimates
% Weight	95%			5%				
SOx	**SO$_2$**			**SO$_3$**				APEP estimates
% Weight	95%			5%				
VOC	**CH$_4$**	**HCHO**	**ALKL**	**AROH**		**AROL**		VOC Speciation from ARB data for gas external combustion boiler profile (http://www.arb.ca.gov/emisinv/speciate/speciate.htm)
% Weight	58%	8%	29%	4%		2%		
PM	**EC**	**OC**	**Cl**	**Sf**	**Nt**	**K**	**Ca**	PM Speciation from ARB data for gas ICE profile (http://www.arb.ca.gov/emisinv/speciate/speciate.htm)
% Weight	20%	26%	7%	45%	1%	1%	1%	

Table 12: Chemical names for species considered in VOC and PM CACM speciation

Species	Species ID in CACM	Chemical Name	Criteria Pollutant
HCHO	4	Formaldehyde	VOC
ALKL	10	C2-C6 Alkanes	VOC
AROH	19	High Yield Aromatics	VOC
AROL	20	Low Yield Aromatics	VOC
EC	29	Elemental Carbon	PM
OC	30	Unresolved Organic Carbon	PM
Cl	32	Chloride ion	PM
Sf	34	Sulfur (VI)	PM
Nt	35	Nitrate	PM
K	37	Potassium	PM
Ca	38	Calcium	PM

5.1.1.8.1   *Low early adoption of DG power*

In all spanning scenarios except #S5 HEAPW20%, a realistic low early adoption of DG power is assumed. This implies that the curve of the annual rate of DG power adoption over the period 2003-2010 increases each year (exponentially or parabolic) until the DG power estimated for 2010 is achieved. Quantitatively, this means that only about 2% of the total DG power adopted in the period 2003-2010 will be implemented before 2007. For the remaining 98% of DG power that will be installed after 2007, those small units under the

ARB certification program will have to meet the more stringent 2007 ARB emissions limits (see Table 5).

5.1.1.9   Performance degradation and geometrical features

Only one of the spanning scenarios accounts for performance degradation of the DG units. This spanning scenario includes a decrease of efficiency and an increase in emissions that occurs over the years with all of the DG units. The emissions degradation is allowed to proceed for all DG units up to the applicable regulatory requirement. The remainder of the spanning scenarios assumes no degradation. Moreover, all of the scenarios included in the present study consider DG emissions to occur at ground level (i.e., no elevated emissions). A small number of DG may be installed on rooftops of tall buildings, but, this fact is not included in the DG scenarios.

5.1.1.10 Scenarios that include Emissions Displacement from in-basin Power Plants

The approach used to develop DG emissions inventories for scenarios that include emissions displacement from in-basin power plants is as follows:

Randomly locate one or more power plants in the SoCAB with approximately the same amount of power as the estimated DG power implemented for 2010 (1060 GW when 20% of the increased demand is met by DG). The database consulted is the one available in the website of the California Energy Commission for power plants in California (ENERGY COMMISSION, 2001). Two combustion turbine/steam turbine power plants situated in Long Beach and Huntington Beach with a total aggregated online capacity of 1090 GW were selected for the 20% of increased demand case, for example. The main characteristics of these plants are presented below in Table 13.

Table 13: Main characteristics of selected power plants in the SoCAB

Name	Address	Primary fuel	Technology	Online capacity (MW)	Cogen	Date Online	Type
Long Beach	2665 SEASIDE BLVD., LONG BEACH, CA 91770	NATURAL GAS	COMBUSTION TURBINE, STEAM TURBINE	530	NO	1/1/1976	Base loaded
Huntington Beach	21730 NEWLAND ST., HUNTINGTON BEACH, CA 92646	NATURAL Gas, DISTILLATE	STEAM TURBINE, COMBUSTION TURBINE	563	NO	6/1/1958	Base loaded

1. Determine the most recent emissions flux rates for each of the selected power plants from ARB website (ARB, 2000). Continuing with the same example, the values for criteria pollutant emissions from the Long Beach and Huntington Beach power plants in 2000 are shown below in Table 14.

Table 14: Emissions from selected power plants in the SoCAB

Name	Year	CO (tons/year)	NOx (tons/year)	VOC (tons/year)	SOx (tons/year)	PM (tons/year)	NH$_3$ (tons/year)
Long Beach	2000	80.8	159	366.8	0.5	10.8	-
Huntington Beach	2000	56.5	290.7	39.7	2.8	9.2	0.18

2. Identify the model cells where the power plants are installed. For this purpose we used the web map tool developed in the first stages of this project (see Appendix D), which allows the user to click in any particular point in a SoCAB map and get the air quality model coordinates as well as the UTM coordinates of that point. In the case of the current example, the X and Y model coordinates for Huntington Beach and Long Beach power plants are (41,10) and (35,12), respectively.

3. Determine the power plants emissions in the suitable units of the model. To do that, we have assumed a capacity factor for both power plants of 80%, a reasonable value for base loaded power plants.

4. Evaluate the net emissions from the DG scenario in each cell of the computational domain. The only cells that have different emissions from the ones in Scenario #S1 are precisely those cells with displaced emissions from the power plants. For the current example, the 2 cells that represent Huntignton Beach and Long Beach power plants contain negative emissions fluxes in the DG scenario because emissions from the power plants is significantly higher than the emissions from the DG units implemented in those same cells. However total emissions of this scenario plus the baseline emissions are still positive.

5.1.1.11 Business As Usual DG Scenario Development

To develop a "business as usual" scenario, one can assume a linear extrapolation of DG power and DG mix from the current trends in the SoCAB area as documented in the years 2001 and 2002. Data for current trends of DG power in California under 1 MW were extracted from the Self-Generation Incentive Program Second Year report (CPUC, 2003). Table 15 shows the evolution of active programs in terms of kW for the different incentive levels of the program. The levels presented in Table 15 correspond to the following DG incentives:

Level 1: The lesser of 50% of project costs or $4.50/watt for photovoltaics, wind turbines, and fuel cells operating on renewable fuels;

Level 2: The lesser of 40% of project costs or $2.50/watt for fuel cells operating on non-renewable fuel and utilizing sufficient waste heat recovery,

Level 3-R: The lesser of 40% of projects costs or $1.50/watt for microturbines, internal combustion engines, and small gas turbines utilizing renewable fuel.

Level 3-N: The lesser of 30% of project costs or $1.00/watt for the above combustion technologies operating on non-renewable fuel, utilizing sufficient waste heat recovery and meeting certain reliability criteria.

Table 15: Active DG CPUC projects (in kW) in 2001 and 2002

Incentive Level	Total Active 2001 (kW)	Total Active 2002 (kW)
Level 1	2291	26875
Level 2	200	600
Level 3N	15452	57625
Level 3R	-	1585
Total	17943	86685

It was also roughly assumed that only the DG projects administered by Southern California Edison (SCE) and Southern California Gas Company (SoCal Gas) are to be implemented in the SoCAB, which accounts for 51% of the total DG power. For the other large electricity company in the SoCAB, the Los Angeles Department of Water and Power municipal utility (LADWP), no data on DG power installed under LADWP service territory is available. As a result, an assumption has been made that the total DG power installed in 2001 and 2002 in the LADWP service territory is 35% of that installed in SCE territory. This level of DG penetration directly corresponds to the ratio of LADWP to SCE power delivered in the SoCAB in 2002.

The distribution of power among the DG types under 1 MW is also based on the CPUC data for the business as usual cases. This leads to adoption of DG types as follows: 32% PV, 1.2% FC, 7.5% MTG, and 59.3% ICE. This DG mix is considered constant in the extrapolation of DG power up to 2010 for all business as usual cases. For the LAWDP DG power, we have estimated the same mix of DG types as that reported by SCE and SoCal Gas.
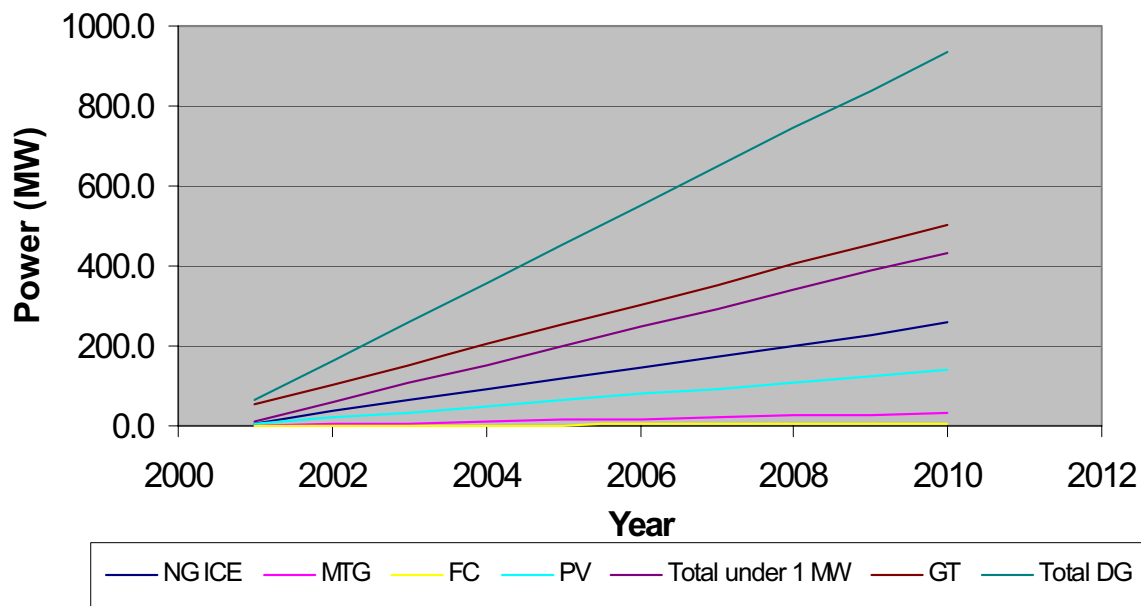
Figure 3: Projected DG power trends in the SoCAB according to CPUC Self-Generation Program DG data for 2001 and 2002 using a linear fit.

According to the installed peak power plants in the SoCAB in the last 2 years with less than 50 MW total capacity each (ENERGY COMMISSION, 2003), a constant increase of large gas turbines of 49 MW at a rate of 1 unit per year was assumed in this business as usual case. Entering this amount of DG power from large gas turbines into the DG mix mentioned above, and recalculated the distribution of DG types in 2010 thus leads to the following adoption rates, based on total power production, for the business as usual cases: 59% GT, 25% ICE 13% PV, 3% MTG, and 0.5% FC.

Figure 3 shows the projected linear trends for accumulated DG power in the period 2001-2010 based on real data in years 2001 and 2002. A total DG power capacity of 936 MW is projected for the year 2010, which requires a total installation of 680 MW additional DG capacity in the period 2003-2010.

Alternatively, one could apply an increasing parabolic extrapolation of the DG power data of 2001 and 2002 instead of a linear extrapolation by assuming zero DG power was installed in the year 2000. In this case, more DG power and more emissions from DG are expected. Projections of DG power for this case are shown in Figure 4. Note that this set of assumptions for DG adoption in the business as usual cases leads to a total installed capacity of DG that is almost 1800 MW in the year 2010.
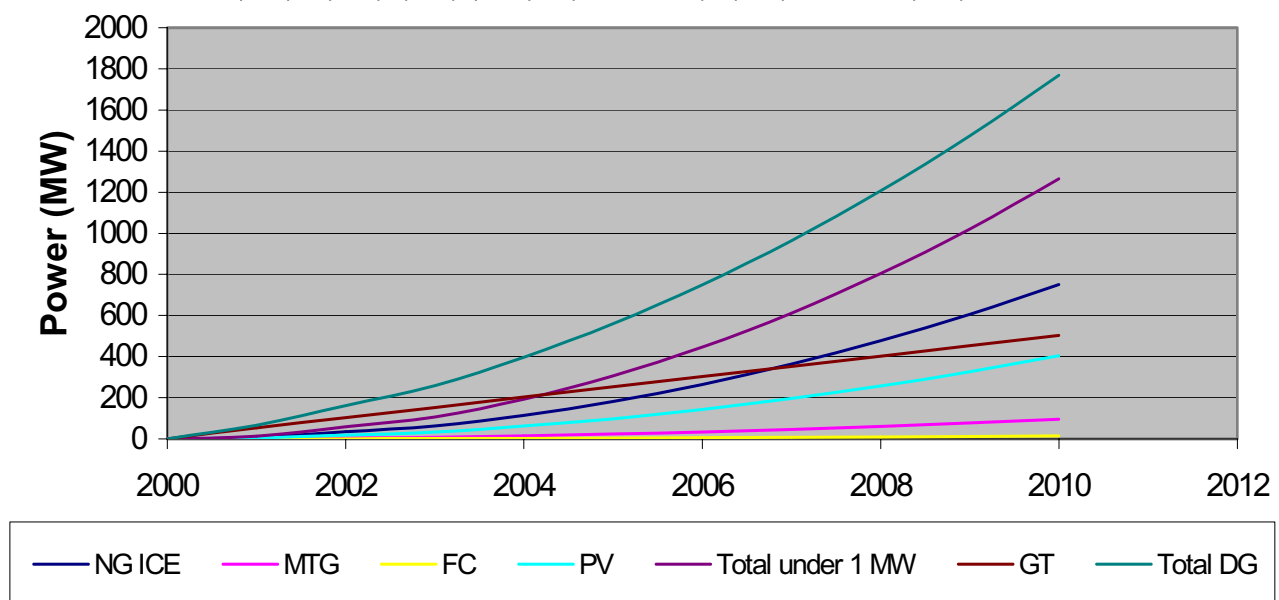
Figure 4: Projected DG power trends in the SoCAB according to CPUC Self-Generation Program DG data for 2001 and 2002 using a parabolic fit.

5.1.2   DG Scenario Screening criteria

If one decided to investigate all possible permutations of the parameters and factors identified above, one would need to simulate 2.04×10^{46} ($= 39!$) scenarios. To accomplish the simulation of air quality in SoCAB for such a large number of cases is not feasible. In addition, we desire to narrow the scope of the current investigations by focusing on the appropriate parameters and factors of concern. As a result, we propose an approach for systematically screening the number of scenarios to a much smaller number by using screening criteria.

By requirement of the contract with the California Energy Commission, the criteria used to screen the scenarios and select a more reasonable number of computations in this study must be presented in both draft and final form in deliverable documents to the Energy Commission. In order to meet this contractual obligation, APEP decided to develop the criteria, present the criteria to experts in the air quality modeling and DG communities (in both public workshops and in coordination meetings with the South Coast Air Quality Management District, Air Resources Board and California Energy Commission) and to subsequently submit these criteria in a draft screening criteria document. As a result of our initial criteria development, and modifications of such as suggested by the coordination group and experts in public workshops, APEP staff are able to present the final screening criteria used in this program as follows.

Table 16 presents the final screening criteria for selecting a limited number of DG Scenarios from the list of possible scenarios that could be comprised of variations in all of the parameters and factors identified in Table 1. Table 16 presents seven primary screening criteria and a description of each. Note that the description of each criterion is stated in the affirmative. Any set of parameter variations that positively meets any one of the screening criteria of Table 16, as a result, has been retained in the current study.

The criteria of Table 16 were applied to the parameter and factor space outlined above and their application resulted in the selection of about 100 DG Scenarios. This number of scenarios is still too large to reasonably accomplish in the current effort. As a result and with feedback and encouragement from the industry stakeholder workshop participants, APEP was able to develop two additional criteria that were further used to screen the scenarios. These two criteria were used to cast a deciding vote on whether or not a scenario is included in this study. These Criteria are presented in Table 17. Note that the criteria A and B are subjective, however, these criteria are applied and based upon all the literature reviewed to-date, all of the expertise of the APEP team, and insights garnered from ARB, AQMD, and industrial participants in the stakeholder workshops. This process is briefly described in the descriptions of each criterion in Table 17.

Table 16. Final Screening Criteria.

Criterion Number	Criterion	Description
1	Likelihood of implementation	Are the variations in the parameters and factors considered realistic or not realistic based upon team and stakeholder input? If they are realistic or possible, then the variation is included in the current study
2	Variety of implementation	Are the variations in the parameters and factors required to span the spectrum of possible implementations and/or technologies of interest? If yes, then the scenario should be included in the current study.
3	Potential for socio-political forcing	Is there a potential for social demand, regulatory requirements, energy crises or other socio-political forcing functions to support the variations in the parameters and factors considered for a specific DG Scenario? If yes, then the scenario should be included in the current study.
4	Fundamental understanding	Does inclusion of the DG Scenario provide insight into any specific aspect of the air quality results or model itself (e.g., atmospheric chemistry, mass transport, DG emissions, etc.)? If yes, then the scenario should be included in the current study.
5	Data acquisition or additional funding required	Is the inclusion of the scenario consistent with the contract, the funding level provided, and is sufficient information to characterize the scenario already available? If yes, then the scenario should be included in this study. If additional funding or data acquisition is required to develop or include the scenario then the scenario is rejected.
6	Availability of resources	Are sufficient resources such as published results, stakeholder insights, Energy Commission studies, or APEP measurements and expertise available to develop and support the validity of the variations in the parameters and factors considered for a specific DG Scenario? If yes, then the scenario should be included in the current study.
7	Required for determining specific sensitivity of the model	Is the specific DG Scenario required to conduct an appropriate sensitivity analysis or to provide insight regarding model sensitivity to simulation parameters? If yes, then the scenario should be included in the current study.

Table 17. Additional Screening Criteria.

Criterion Letter	Criterion	Description
A	*Is the DG scenario realistic?*	A subjective determination is made regarding whether or not a DG scenario is realistic. This determination is made on the basis of literature review, APEP expertise, and industry and other stakeholder insights. If the scenario is deemed to be realistic or probable, then the scenario is included in the current study.
B	*Does the investigation of the DG scenario contribute to increased understanding?*	An assessment is made of the value of including the DG scenario, even if Criterion A is not met. The assessment is based upon whether or not the team believes increased understanding of DG air quality impacts may be garnered by inclusion of the scenario. If the scenario is deemed to have merit in this regard, then it is included in the current study.

5.1.3   Extraction and processing of GIS land-use data

The use of a realistic means of defining the spatial distribution of DG in the SoCAB is critically important to the realistic prediction of air quality impact. In addition, the first industry stakeholder workshop strongly recommended spatial allocation of the DG technologies throughout the basin according the actual electrical and thermal demand anticipated for 2010 and the type of end-use for each spatial location. The sort of information required to accomplish this is only available from special sources. These sources include the local utilities, which have spatially resolved data on electricity consumption, and local governmental agencies that have global information systems (GIS) information for SoCAB.

The Southern California Area Governments (SCAG) generously donated GIS land-use data for the following counties: Los Angeles, Orange, San Bernardino, Riverside, Imperial and Ventura. The latest data in this GIS data set were collected in the year 2000. Figure 5 shows how the computational domain of the air quality model for the SoCAB includes partially or wholly the counties of Orange, Los Angeles, Riverside, San Bernardino and Ventura.
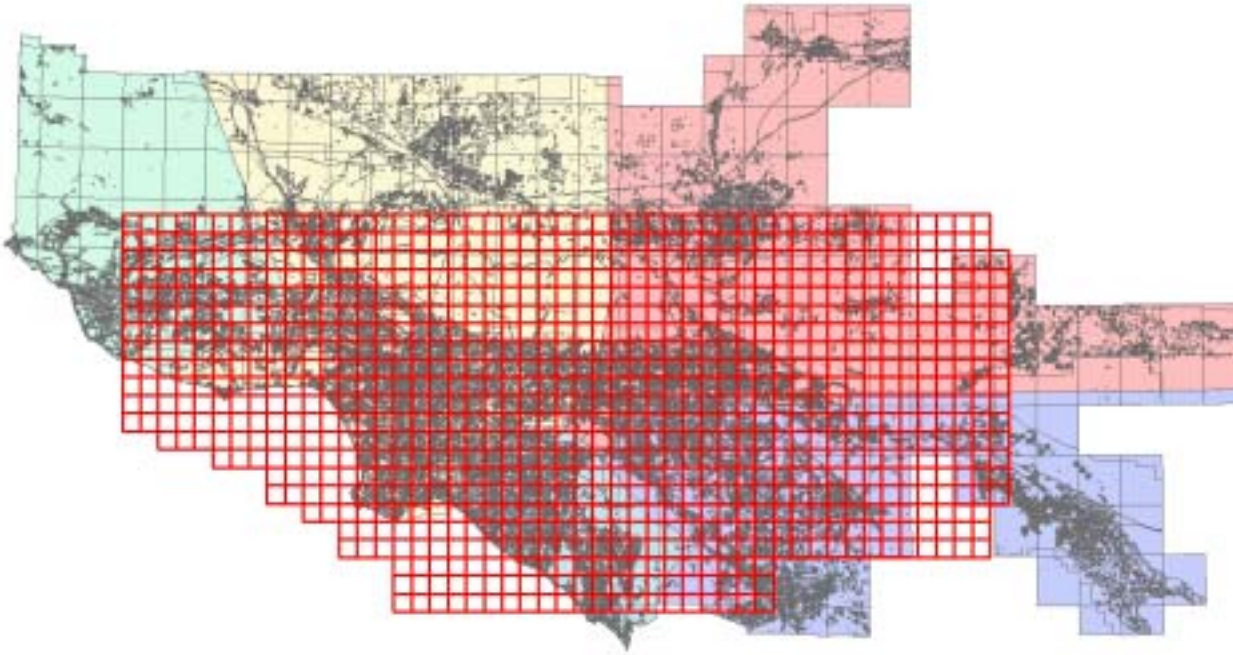
Figure 5: Southern California Counties with land-use GIS data and the computational grid of the air quality model (in red lines).

These data consist of each of the counties divided into land parcels (polygons) of different area and shape. The number of parcels per county is rather large. For example the total number of individual land parcels in LA County alone is more than 40,000. The land parcels have a resolution of 2 acres (0.0081 km^2). Each of the polygons has associated with it a database that contains an ID number, total area, and zone classification code. Figure 6 presents a picture of a small region near Long Beach to illustrate the typical number and resolution of the land parcel polygons. The location of the 5 km x 5 km model cells and corresponding resolution of the air quality model in this same region are represented by the red lines of Figure 6.
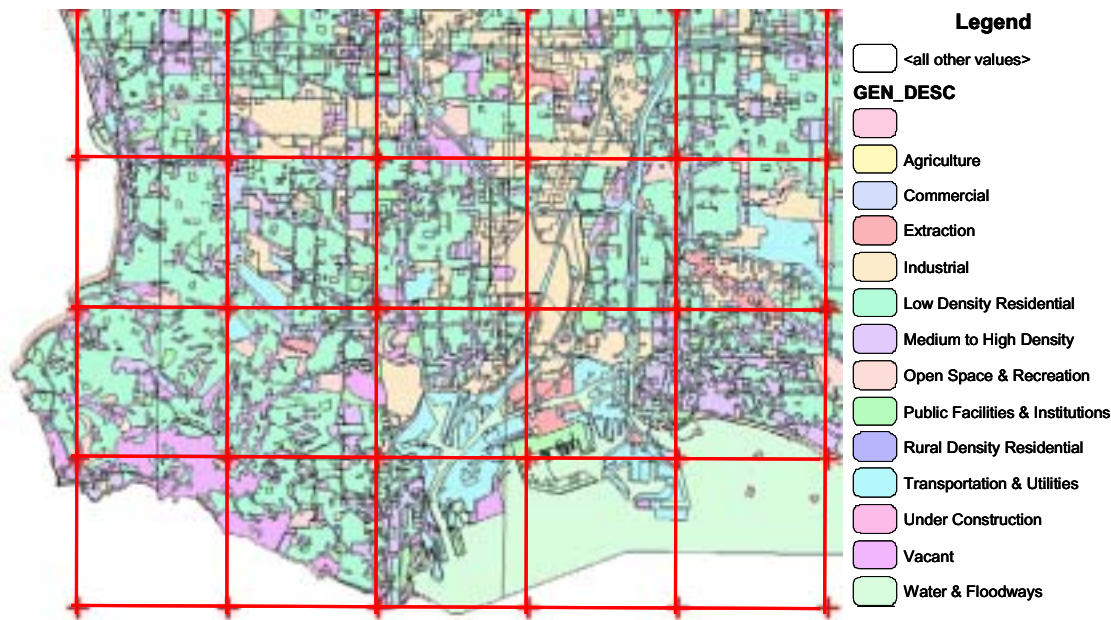
Figure 6: Example of generic land-uses in Long Beach area.

The GIS database contains 132 different specific land-use types that are aggregated into 13 generic land use types. The 13 generic land use types are the only types presented in Figure 6. Table 18, on the other hand, shows both the specific land-use types and the generic types that are contained in the GIS database.

Table 18: Land-use codes and descriptions

LU CODE	LAND USE DESCRIPTION	GENERIC LAND USE TYPE
1000	Urban or Built-Up	
1100	Residential	Low Density Residential
1110	Single Family Residential	Low Density Residential
1111	High Density Single Family Residential	Low Density Residential
1112	Low Density Single Family Residential	Low Density Residential
1120	Multi-Family Residential	Medium to High Density Residential
1121	Mixed Multi-Family Residential	Medium to High Density Residential
1122	Duplexes, Triplexes & 2 or 3 Unit Condos & Townhomes	Medium to High Density Residential
1123	Low-Rise Apartments Condominiums and Townhouses	Medium to High Density Residential
1124	Medium-Rise Apartments and Condominiums	Medium to High Density Residential
1125	High-Rise Apartments and Condominiums	Medium to High Density Residential
1130	Mobile Homes and Trailer Parks	Medium to High Density Residential
1131	Trailer Parks and Mobile Home Courts High Density	Medium to High Density Residential
1132	Mobile Home Courts and Subdivisions Low Density	Medium to High Density Residential
1140	Mixed Residential	Medium to High Density Residential
1150	Rural Residential	Low Density Residential
1151	Rural Residential High Density	Low Density Residential
1152	Rural Residential Low Density	Rural Density Residential
1200	Commercial and Services	Commercial
1210	General Office Use	Commercial

LU CODE	LAND USE DESCRIPTION	GENERIC LAND USE TYPE
1211	Low- and Medium-Rise Major Office Use	Commercial
1212	High-Rise Major Office Use	Commercial
1213	Skyscrapers	Commercial
1220	Retail Stores and Commercial Services	Commercial
1221	Regional Shopping Mall	Commercial
1222	Retail Centers, Non-Strip Contiguous Interconnected Off-Street	Commercial
1223	Modern Strip Development	Commercial
1224	Older Strip Development	Commercial
1230	Other Commercial	Commercial
1231	Commercial Storage	Commercial
1232	Commercial Recreation	Commercial
1233	Hotels and Motels	Commercial
1234	Attended Pay Public Parking Facilities	Commercial
1240	Public Facilities	Public Facilities & Institutions
1241	Government Offices	Public Facilities & Institutions
1242	Police and Sheriff Stations	Public Facilities & Institutions
1243	Fire Stations	Public Facilities & Institutions
1244	Major Medical Health Care Facilities	Public Facilities & Institutions
1245	Religious Facilities	Public Facilities & Institutions
1246	Other Public Facilities	Public Facilities & Institutions
1247	Non-Attended Public Parking Facilities	Public Facilities & Institutions
1250	Special Use Facilities	Public Facilities & Institutions
1251	Correctional Facilities	Public Facilities & Institutions
1252	Special Care Facilities	Public Facilities & Institutions
1253	Other Special Use Facilities	Public Facilities & Institutions
1260	Educational Institutions	Public Facilities & Institutions
1261	Pre-Schools Day Care Centers	Public Facilities & Institutions
1262	Elementary Schools	Public Facilities & Institutions
1263	Junior or Intermediate High Schools	Public Facilities & Institutions
1264	Senior High Schools	Public Facilities & Institutions
1265	Colleges and Universities	Public Facilities & Institutions
1266	Trade Schools	Public Facilities & Institutions
1270	Military Installations	Public Facilities & Institutions
1271	Base Built-up Area	Public Facilities & Institutions
1272	Vacant Area	Vacant
1273	Air Field	Public Facilities & Institutions
1300	Industrial	Industrial
1310	Light Industrial	Industrial
1311	Manufacturing Assembly and Industrial Services	Industrial
1312	Motion Picture and Television Studio Lots	Industrial
1313	Packing Houses and Grain Elevators	Industrial
1314	Research and Development	Industrial
1320	Heavy Industrial	Industrial
1321	Manufacturing	Industrial
1322	Petroleum Refining and Processing	Industrial
1323	Open Storage	Industrial
1324	Major Metal Processing	Industrial
1325	Chemical Processing	Industrial
1330	Extraction	Extraction
1331	Mineral Extraction - Other Than Oil and Gas	Extraction
1332	Mineral Extraction - Oil and Gas	Extraction

LU CODE	LAND USE DESCRIPTION	GENERIC LAND USE TYPE
1340	Wholesaling and Warehousing	Industrial
1400	Transportation Communications and Utilities	Transportation & Utilities
1410	Transportation	Transportation & Utilities
1411	Airports	Transportation & Utilities
1412	Railroads	Transportation & Utilities
1413	Freeways and Major Roads	Transportation & Utilities
1414	Park and Ride Lots	Transportation & Utilities
1415	Bus Terminals and Yards	Transportation & Utilities
1416	Truck Terminals	Transportation & Utilities
1417	Harbor Facilities	Transportation & Utilities
1418	Navigation Aids	Transportation & Utilities
1420	Communication Facilities	Transportation & Utilities
1430	Utility Facilities	Transportation & Utilities
1431	Electrical Power Facilities	Transportation & Utilities
1432	Solid Waste Disposal Facilities	Transportation & Utilities
1433	Liquid Waste Disposal Facilities	Transportation & Utilities
1434	Water Storage Facilities	Transportation & Utilities
1435	Natural Gas and Petroleum Facilities	Transportation & Utilities
1436	Water Transfer Facilities	Transportation & Utilities
1437	Improved Flood Waterways and Structures	Transportation & Utilities
1438	Mixed Wind Energy Generation and Percolation Basin	Transportation & Utilities
1440	Maintenance Yards	Transportation & Utilities
1450	Mixed Transportation	Transportation & Utilities
1460	Mixed Transportation and Utility	Transportation & Utilities
1500	Mixed Commercial and Industrial	Industrial
1600	Mixed Urban	Industrial
1700	Under Construction	Vacant
1800	Open Space and Recreation	Open Space & Recreation
1810	Golf Courses	Open Space & Recreation
1820	Local Parks and Recreation	Open Space & Recreation
1821	Local Park Developed	Open Space & Recreation
1822	Local Park Undeveloped	Open Space & Recreation
1830	Regional Parks and Recreation	Open Space & Recreation
1831	Regional Park Developed	Open Space & Recreation
1832	Regional Park Undeveloped	Open Space & Recreation
1840	Cemeteries	Open Space & Recreation
1850	Wildlife Preserves and Sanctuaries	Open Space & Recreation
1860	Specimen Gardens and Arboreta	Open Space & Recreation
1870	Beach Parks	Open Space & Recreation
1880	Other Open Space and Recreation	Open Space & Recreation
1900	Urban Vacant	Vacant
2000	Agriculture	Agriculture
2100	Cropland and Improved Pasture Land	Agriculture
2120	Non-Irrigated Cropland and Improved Pasture Land	Agriculture
2200	Orchards and Vineyards	Agriculture
2300	Nurseries	Agriculture
2400	Dairy and Intensive Livestock	Agriculture
2500	Poultry Operations	Agriculture
2600	Other Agriculture	Agriculture
2700	Horse Ranches	Agriculture
3000	Vacant	Vacant
3100	Vacant Undifferentiated	Vacant

LU CODE	LAND USE DESCRIPTION	GENERIC LAND USE TYPE
3200	Abandoned Orchards and Vineyards	Vacant
3300	Vacant With Limited Improvements	Vacant
3400	Beaches (Vacant)	Open Space & Recreation
4000	Water	Water & Floodways
4100	Water	Water & Floodways
4200	Harbor Water Facilities	Water & Floodways
4300	Marina Water Facilities	Water & Floodways
4400	Water Within a Military Installation	Water & Floodways
4500	Area of Inundation (High Water)	Water & Floodways

5.1.3.1 GIS data extraction

The first step required to make effective use of the land-use GIS data in our DG scenarios was to correlate (i.e., scale-up) the resolution of the GIS data with the 5 km x 5 km resolution of the air quality model grid. This task proved to be quite challenging, requiring the assistance of a skilled computer programmer with expertise in graphical data extraction. In this process, Tony Soeller, staff member of the Network and Academic Computing Services (NACS) at UCI, and an expert in GIS data management and manipulation, assisted APEP staff.

After some weeks of intensive work, the APEP team, working with Tony Soeller, came up with a 15-step procedure that uses the GIS software ArcMap to satisfactorily map the GIS data to the air quality model grid. This strategy for integrating GIS data with the AQM is described in this section of the report.

Table 19 presents a small cross-section of the model grid as a sample of the type of data we now have available to use for all of the cells in the model. The *X* and *Y* coordinates of the model are presented in Table 19, followed by the square kilometers (km^2) of area within each cell that correspond to Agriculture, Commercial, Extraction, Industrial, Low Density Residential, etc. land use types. Issues that had to be resolved in the process of extracting GIS data included:

- How does one define and create the 5 x 5 km cell layer in GIS?
- How does one identify the location of each polygon with respect to the cells?
- How can one determine if land-use polygons are entirely inside one cell or shared amongst cells?
- How can one account for land-use polygons that occupy more than one cell?
- How the GIS data be exported in a convenient way to use in the Excel scenario development files?

All of these issues have been resolved to the satisfaction of the APEP team.

Table 19: Detail of some cells with GIS land-use data extracted

Ymodel	Xmodel	Agriculture	Commercial	Extraction	Industrial	Low Density Residential
		A_{Agric} km^2	A_{Comm} km^2	A_{Ext} km^2	A_{Ind} km^2	A_{Lowres} km^2
26	19	1.335	0.000	0.549	0.000	0.031
26	20	0.012	0.000	0.503	0.000	0.000
26	21	0.175	0.000	0.000	0.000	0.000
26	22	5.147	0.000	0.000	0.000	0.000
26	23	0.043	0.000	0.026	0.000	0.000
26	24	0.040	0.000	0.137	0.000	0.000
26	25	1.453	0.000	0.136	0.000	0.000
26	26	0.044	0.000	1.310	0.000	0.000
26	27	0.545	0.000	1.116	0.000	0.586
26	28	2.896	0.868	1.498	1.128	0.685
26	29	3.212	0.151	0.000	1.520	4.766
26	30	0.650	0.125	0.000	0.120	5.810
26	31	0.180	0.319	0.000	0.173	1.779
26	32	0.123	0.008	0.932	0.037	2.120
26	33	0.028	0.000	0.388	0.000	0.000
26	34	0.090	0.000	0.000	0.018	0.000

In the process of extracting the GIS data, the APEP team isolated each of the 13 generic land-use categories. These generic land use categories are listed in Table 20. Reducing the total number of land use types to the 13 generic land use types allowed reasonable identification of the spatial distribution of land use types in the SoCAB. Maps with the locations of all the parcels belonging to each land-use types are presented in Appendix E.

Table 20. Generic Land Use Categories

LU CODES	GENERIC LAND USE TYPE
1000 – 1112, 1150 – 1151	Low Density Residential
1120 – 1140	Medium to High Density Residential
1152	Rural Density Residential
1200 – 1234	Commercial
1240 – 1273	Public Facilities & Institutions
1300 – 1325, 1340, 1500, 1600	Industrial
1330 – 1332	Extraction
1400 – 1460	Transportation & Utilities
1700, 1900, 3000, 3100, 3200, 3300	Vacant
1800 – 1880, 3400	Open Space & Recreation
2000 – 2700	Agriculture
4000 – 4500	Water & Floodways

PIER

Figure 7 presents a bar chart with the total areas for the 13 generic land-use categories. Note that the "Vacant" area is by far the largest land-use category with more area (greater than 12,000 km^2) associated with it than any other category. The vacant area is followed by the "Low Density Residential" land use category with about 3,000 km^2 in the SoCAB. The third and forth land-use categories with significant area in the SoCAB are "Agriculture" and "Transportation and Utilities", respectively. For perspective on the land-use categories with smaller total areas, Figure 8 presents the total areas for the 12 of the 13 generic land-use categories. All but the "Vacant" land-use categories are presented in Figure 8.
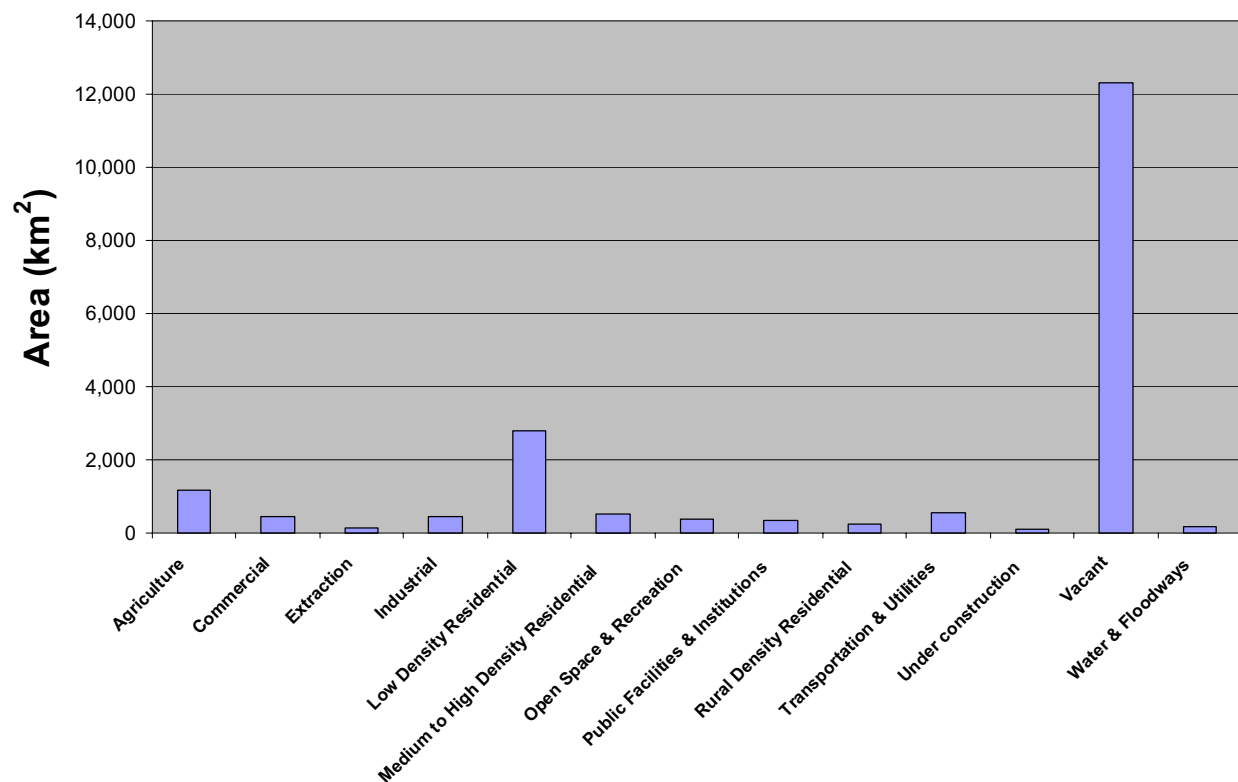
Figure 7: Total land-use areas in the 13 generic land use categories in SoCAB.
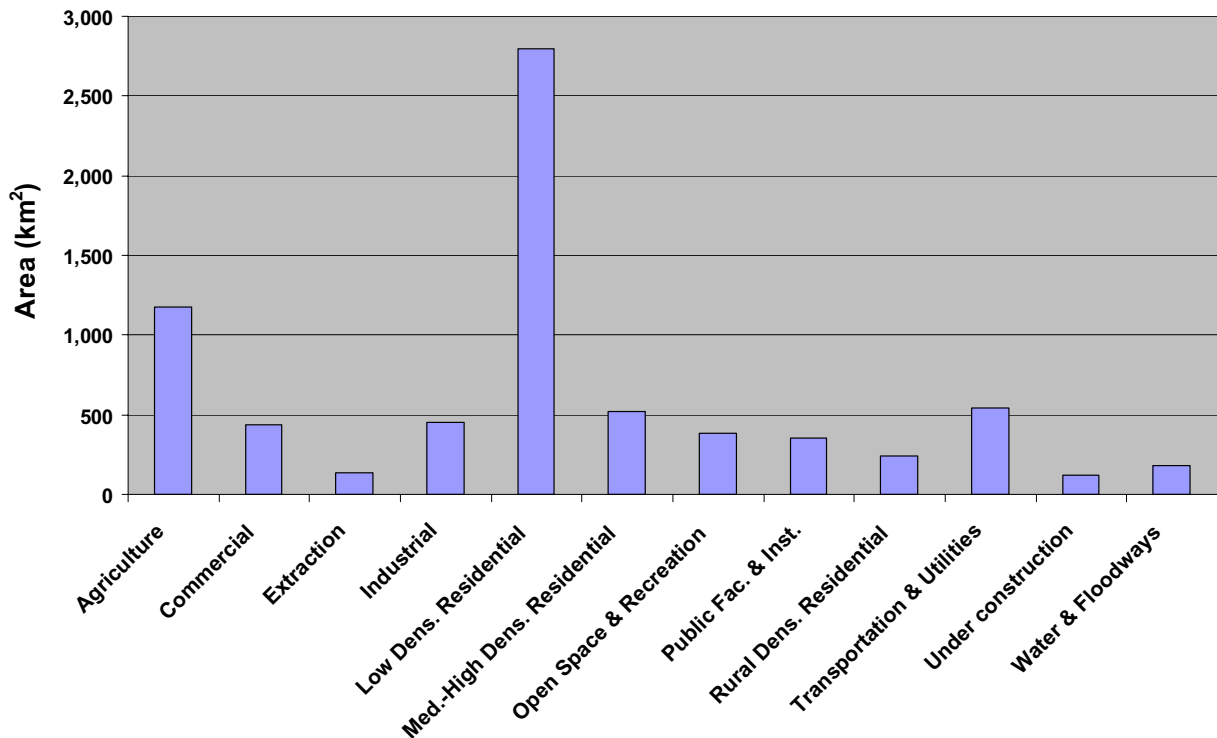
Figure 8. Total land-use areas in 12 of the 13 generic land use categories in SoCAB (Vacant category not plotted).

5.1.3.2   Approach to relate land-use data to DG power and DG mix

After extracting the areas in each cell for the 13 generic land-use categories, the next step was to design a strategy to relate land-use areas to the amount of DG power and to the mix of DG technologies assigned to each cell of the grid. Since the land-use categories generally refer to a sector of the economy that is expected to use DG (of various types and to varying degrees in various applications), the label used for groupings of land-use categories in this section is "sector."

A systematic approach to relate DG power and DG mix to land-use data has been developed that is well grounded in and fully based upon the most recent data and reports that are currently available. The approach presented herein was well received by the stakeholders in the second Workshop (May 21, 2003), organized specifically to discuss the scenario development tasks and to receive a critique and feedback from DG stakeholders.

The systematic approach consists of a 10-step procedure that is described in this section of the report. The nomenclature used in the equations that define the approach is presented in Table 21 together with definitions for each variable.

Table 21: Nomenclature used in the equations that define the systematic approach for developing realistic DG scenarios

$A_{i,k}$	Area of sector i in cell k
$S_{i,j}$	Relative area of sector i in size category j
$A_{i,j,k}$	Area of sector i in size category j in cell k
A_{SoCAB}	Total Area in the SoCAB
$D_{i,h}$	Duty cycle factor in sector i and hour of the day h
$R_{i,j}$	Adoption rate relative intensity (in terms of DG power/square foot) for sector i in size category j
$F_{power,k}$	Factor accounting for the total DG power in each cell
$P_{Tot,k}$	Total DG power (in MW) assigned to each cell
$P_{Tot,SoCAB}$	Total DG power (in MW) estimated for the SoCAB in 2010
$P_{i,j,k}$	DG power (in MW) of specific sector i in size category j in cell k
$W_{l,i,j}$	Relative weight for DG type l in sector i and size category j
$T_{l,k}$	Relative contribution to DG power of DG type l in cell k
$T_{l,k,h}$	Relative contribution to DG power of DG type l in cell k at hour h
$P_{l,k}$	DG power (in MW) of DG type l in cell k
$P_{l,k,h}$	DG power (in MW) of DG type l in cell k at hour h
$e_{l,X}$	Emission factor for species X of DG type l
$[X]_{emiss,k}$	Total DG emissions of species X in cell k

In reading this section of the report one should periodically refer back to Table 21. Note that the subscript i refers to the sector type (i.e., groupings of land-use categories), the subscript j refers to the DG size class, and the subscript k refers to the AQM model cell. The subscript h refers to the hour of the day and the subscript l refers to the type of DG technology. These subscripts are consistent throughout the derivation presented in this section. Note that to develop a realistic DG implementation scenario, one must consider a large number of factors as shown in Table 21.

The development of a realistic scenario based on land-use data, DG size, DG type, and other available data and insights is presented in this section as a ten (10) step procedure. This process has been derived, honed and developed by the APEP team through many internal iterations and brainstorming sessions. This process has been vetted by colleagues; the California Energy Commission; SCAQMD and ARB staff; and the DG stakeholders who participated in the workshops (see Appendix A and Appendix B). The ten-step procedure is defined as follows.

> **STEP 1.** The starting point for the DG scenario development is the extracted land-use data in 5x5 km resolution. These data consist of the areas (in square kilometers) of all 13 of the generic land use types for each of the 994 cells of the model grid. The 13 land use area types are aggregated into 6 different sectors (i.e., low density residential, medium-to-high density residential, commercial, industrial, agriculture, and others), as shown in Table 22. The amount of square kilometers of a sector type in any specific cell is represented by A_i. Figure 9 presents a representative picture of the aggregated GIS land-use categories as integrated into the six (6) economic sectors for the Central LA area.

Table 22: Integration of land-use types into energy sectors

Sector	Land use types considered in that sector *
Low Density Residential	*Low Density Residential*
	Rural Density Residential
Medium to High Density Residential	*Medium to High Density Residential*
Commercial	*Commercial*
Industrial	*Industrial*
Agriculture& Water Pumping	*Agriculture*
Other	*Extraction*
	Public Facilities & Institutions
	Transportation & Utilities
	Under Construction

* The rest of the land use categories (Vacant, Water and Flood Ways, and Open Space and Recreation) assumed to adopt zero DG power

☐ Low Density Res.   ☐ Medium to High Density Res.   ■ Industrial
☐ Commercial   ■ Agriculture   ☐ Others
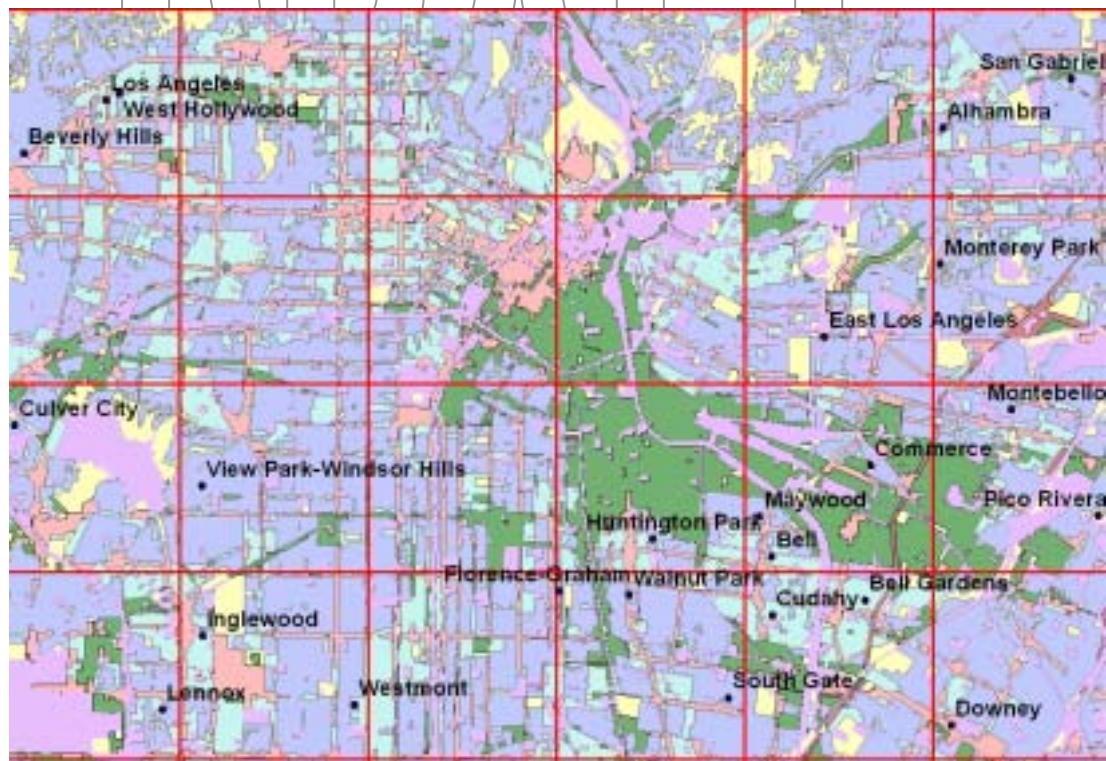
Figure 9: Land use parcels in central LA aggregated into 6 energy sector categories

STEP 2. The second step is to disaggregate each of the sector areas in each cell into six (6) sub-categories according to DG size capacity. The six DG size classes that are used are:

- <50 kW,
- 50-250 kW,
- 250-1,000 kW,
- 1-5 MW,
- 5-20 MW, and
- 20-50 MW.

The bases of this disaggregating process are several reports on energy consumption surveys in the commercial, residential and manufacturing sectors by the Energy Information Agency (1999; 1999; 2000). These reports relate total floor space of various establishment types in each sector to the annual electricity consumption. From these data the average power demand for each establishment is estimated and the potential for each sector to adopt DG in each of the six size classes is determined. The results of these analyses are normalized by dividing the area of each size-category by the total area in that sector to get a relative area per sector (i) and per size category (j), which is represented by $S_{i,j}$. Two of the sectors (Agriculture and Other) required the development of estimated S_{ij} since no data is currently available for these sectors. Reasonable estimates were made based on the S_{ij} of the other sectors and insights of the APEP team. The equation that relates total area to area per size category for each of the sectors considered is:

$$A_{i,j,k} = S_{i,j} \cdot A_{i,k} \qquad (6)$$

Table 23 shows the resulting normalized area factors that are applied to disaggregate (split) the sectors (groups of GIS land-use areas) into specific areas for each DG size category.

Table 23: Normalized area factors for each DG size category for the different sectors ($S_{i,j}$).

Size category	Low Density Residential	Medium and high density residential	Commercial	Industrial	Agriculture	Other
< 50 kW	99%	95%	55%	0%	80%	0%
50-250 kW	1%	5%	17%	5%	10%	5%
250-1,000 kW	0%	0%	20%	15%	10%	15%
1-5 MW	0%	0%	8%	22%	0%	22%
5-20 MW	0%	0%	0%	30%	0%	30%
20-50 MW	0%	0%	0%	28%	0%	28%
Total	100%	100%	100%	100%	100%	100%

STEP 3. The third step is to determine DG power in each of the disaggregated (DG size class dependent) areas in each cell of the model based on a third factor included in this approach. This third factor is called the "Adoption Rate Relative Intensity" factor and has the units of DG power per square kilometer. This relative adoption rate intensity is a function of both the sector and the DG power size category, and is represented by $R_{i,j}$ in the current approach. The adoption rate relative intensity factor, $R_{i,j}$, accounts for the fact that a certain amount of land that is occupied by a certain economic sector will adopt DG technology at a rate that differs from that of other sectors.

The adoption rate relative intensity factor, $R_{i,j}$, are determined in the current approach as a function of both size category and sector based on a report that describes CHP penetration in the commercial and industrial sectors in California (ENERGY COMMISSION, 1999). Note that this report only provides combined market penetration of DG with CHP and includes both the industrial and the commercial sectors. The relative adoption rates for DG in other sectors are estimated from comparison to these data, from other DG market penetration studies (see Table 3), and from APEP team insights. Table 24 presents the current estimates for these intensity factors normalized to the smallest non-zero entry of the table (other sector; < 50kW).

The factors should be interpreted as follows: if the DG power penetration in a square kilometer of the low density residential sector is 1.6 MW in the size category <50 kW, the corresponding DG power penetration in the same area for the industrial sector in the range capacity 20-50 MW is 567.2 MW. The adoption rate relative intensity factors of Table 24 are well grounded in the literature and APEP insights that are currently available. However, these factors can be refined and modified at any time as additional detailed market penetration studies are completed and as information becomes available for DG market penetration in California (especially in the SoCAB).

Table 24: Adoption Rate Relative Intensity ($R_{i,j}$) per size category and per sector

Size category	Low Density Residential	Medium and high density residential	Commercial	Industrial	Agriculture	Other
< 50 kW	1.6	16.4	7.9	7.9	3.2	1.0
50-250 kW	8.3	208.1	151.7	151.7	8.6	19.1
250-1,000 kW	0.0	0.0	141.5	141.5	8.6	17.9
1-5 MW	0.0	0.0	221.5	221.5	0.0	27.9
5-20 MW	0.0	0.0	0.0	376.9	0.0	47.6
20-50 MW	0.0	0.0	0.0	567.2	0.0	71.6

As a result of the above development of areas and factors, one can determine the total DG power in each cell as a sum of the areas per sector and per size category ($A_{i,j,k}$) multiplied by the adoption rate relative intensity. This factor F_{power} is determined for each individual cell of the air quality model as follows:

$$F_{power,k} = \sum_i \sum_j A_{i,j,k} R_{i,j} \tag{7}$$

The total DG power in real units (MW) assigned to each cell k of the model is then determined as a function of the assumed total implementation of DG power in the SoCAB (portion of increased power demand met by DG) and the normalized power factor as follows:

$$P_{Tot,k} = \frac{F_{power,k}}{\sum_k F_{power,k}} \cdot P_{Tot,SoCAB} \tag{8}$$

Once the total DG power in each cell is determined, DG power associated with each of the size categories in each sector can be described by the following equation:

$$P_{i,j,k} = \frac{A_{i,j,k} R_{i,j}}{F_{power}} P_{Tot,k} \tag{9}$$

Finally then, the total DG power per sector and per cell can be written as:

$$P_{i,k} = \frac{\sum_j A_{i,j} R_{i,j}}{F_{power}} P_{Tot,k} \tag{10}$$

STEP 4.   At this point one must consider the operational duty cycle of DG units. The temporal variation of the DG power due to the variety of duty cycles of the units is introduced into this procedure as a function of the particular sector that the DG units are serving. Average load profiles are calculated for each sector based on hourly electric data obtained from the Southern California Edison web page (refer to Appendix F for details). To apply the sector specific duty cycle one must determine a normalized vector factor, $D_{i,h}$, which describes the hour-by-hour duty expected in each sector. The total power for a particular sector in a cell is presented in equation 10 as $P_{i,k}$. This factor is considered the peak DG power output that can occur at any one hour of the day in a particular sector. Thus, multiplying the normalized duty cycle by the peak sector power in each cell produces the total power per sector and per cell as a function of the time of the day as:

$$P_{i,k,h} = P_{i,k} D_{i,h} \tag{11}$$

The next step consists of determining the relative contribution to total power in a cell by each of the DG types considered (namely, low temperature (LT) fuel cells, high

temperature (HT) fuel cells, MTGs, NG ICEs, PV, conventional gas turbine (CGT), advanced gas turbine (AGT), Stirling engines, and Hybrid fuel cell systems).   To accomplish this, 6 tables must be developed (one for each sector), in which the relative expected contribution of each DG type in each size category, $W_{i,l,j}$, is presented. And the total DG power in each cell supplied for each of the DG types considered is:

$$P_{l,k,h} = T_{l,k,h} \cdot P_{Tot,k,h} \tag{13}$$

STEP 5.   Table 25 below presents the relative contributions of DG technology types ($W_{i,l,j}$) for the industrial sector as an example. Tables presenting $W_{i,l,j}$ for all the sectors are included in Appendix G. The relative contribution factors all six (6) sectors are based on market penetration of DG technology types in the industrial sector (Little, 2000), utility sector (Ianucci et al., 2000), and building sector (Boedecker et al., 2000) and APEP team or other expert estimates on market distribution of DG technology types in each of the size categories.

As a result, the equation that determines the relative contribution of each DG technology in each cell for a particular hour of the day, $T_{l,k,h}$, is given by:

$$T_{l,k,h} = \frac{\sum_i \sum_j W_{i,l,j} \cdot P_{i,j,k,h}}{P_{Tot,k,h}} \tag{12}$$

And the total DG power in each cell supplied for each of the DG types considered is:

$$P_{l,k,h} = T_{l,k,h} \cdot P_{Tot,k,h} \tag{13}$$

Table 25: Estimated relative contributions of DG technology types ($W_{i,l,j}$) in the Industrial sector as a function of size class.

Size categories	% LT Fuel cells	% HT Fuel cells	% MTGs	% NG ICEs	% PV	% CCT	% AGT	Stirling	Hybrid
< 50 kW	0.0%	0.3%	0.7%	0.0%	0.0%	0.0%	0.0%	0.0%	0.0%
50-250 kW	0.0%	2.1%	13.6%	0.0%	0.0%	0.0%	0.0%	0.0%	0.0%
250-1,000 kW	0.0%	2.9%	0.0%	10.1%	0.0%	9.7%	0.0%	0.0%	2.5%
1-5 MW	0.0%	0.0%	0.0%	10.1%	0.0%	9.7%	0.0%	0.0%	2.5%
5-20 MW	0.0%	0.0%	0.0%	0.0%	0.0%	9.7%	13.0%	0.0%	0.0%
20-50 MW	0.0%	0.0%	0.0%	0.0%	0.0%	0.0%	13.0%	0.0%	0.0%
Total	0.0%	5.2%	14.4%	20.1%	0.0%	29.2%	26.0%	0.0%	5.0%

STEP 6.   At this point an estimate of the spatial distribution of DG power and the mix of DG technologies in each cell of the model and the power that each is producing at each hour of the day has been determined. The sixth step to consider is a weighting factor for relative DG adoption rates that is a function of the location within the basin that one is considering. The systematic procedure presented thus far, uses average DG adoption factors for all cells throughout the basin. No local information on forecasted DG penetration in certain zones of the SoCAB due to any potential driver (e.g., transmission or distribution constraints in utility grid, strong DG incentives in particular cities, anticipated larger DG installations) has been included in the approach thus far.
Since data was not available to suggest preferential DG adoption at any particular location or set of locations in the SoCAB, the APEP team decided to retain average adoption rates. However, if at any time preferential DG adoption rates that apply to the spatial distribution of DG in the SoCAB become available one should apply a normalized adoption rate factor in this step. So far no local data is available and, therefore, no modification to the first five steps of this systematic approach is applied in this analysis.

STEP 7.   The seventh step is to calculate pollutant emissions in each cell and each hour of the day based on the emissions factors for each of the DG types, e_l. As explained in Section 5.1.1.5 Emissions Specifications, the emissions factors, e_l, for each of the DG types are determined from literature sources (Ianucci et al. 2000; Marnay et al. 2001; 2001; Allison and Lents 2002; 2002; 2003) and APEP measurements of emissions from various DG technologies. Note that, based on current emission factors gathered from literature in Table 2, some DG technologies do not meet the applicable emission standards (summarized in Table 4, Table 5 and Table 6). However, in all cases the emissions from DG are never allowed to exceed the applicable ARB and SCAQMD emissions limits, since any DG unit must comply with the emission standards to be installed in the basin. In other words, if a certain DG technology is to be installed in the SoCAB, but has emission factors that exceed the standards, the applicable emission standards are assumed instead of its corresponding emission factor to calculate DG emissions. The emissions for all the DG pollutants considered in a given cell of the model can be determined through the following equations:

$$[CO]_{emiss,k,h} = \sum_{l} P_{l,k,h} \cdot e_{l,CO} \tag{14}$$

$$[NOx]_{emiss,k,h} = \sum_{l} P_{l,k,h} \cdot e_{l,NOx} \tag{15}$$

$$[VOC]_{emiss,k,h} = \sum_{l} P_{l,k,h} \cdot e_{l,VOC} \tag{16}$$

$$[SOx]_{emiss,k,h} = \sum_{l} P_{l,k,h} \cdot e_{l,SOx} \tag{17}$$

$$[PM]_{emiss,k,h} = \sum_{l} P_{l,k,h} \cdot e_{l,PM} \tag{18}$$

$$[CO_2]_{emiss,k,h} = \sum_l P_{l,k,h} \cdot e_{l,CO2} \tag{19}$$

Although CO_2 emissions do not contribute to the atmospheric chemistry, they are accounted in this step to ascertain the possible global warming impacts of DG implementation in the SoCAB.

STEP 8.   To fully characterize the emissions coming from potential DG operation in the SoCAB at the level required by the air quality model, a further speciation of the above criteria pollutants, i.e., NOx, CO, VOC, SOx, and PM, must be applied. This step requires that one directly correlate each of the pollutant emissions calculated in the first seven steps to the pollutant flux rates that are required by the particular chemical mechanism that the AQM is using. In this particular case, the species that are considered in the AQM are those associated with the CACM mechanism. Use of the CACM mechanism requires splitting of NOx emissions into NO and NO_2, SOx emissions into SO_2 and SO_3, characterization of the VOCs as 5 distinct hydrocarbon compounds, and supplying a distribution of particulate matter that is comprised of 19 species and 8 size classes. The process of accomplishing this is presented in more detail in section 5.1.1.8.

STEP 9.   The effects of any emissions displacement that may occur as a result of DG installations in the SoCAB are accounted for in step nine. Once the speciated emissions from the DG realistic scenario are known, the process described in section 5.1.1.10 to account for displaced emissions due to the operation of CHP DG units (or other emissions displacement) is applied. The resulting net emissions fluxes are calculated in this step by direct subtraction of emissions fluxes that account for displaced emissions.

STEP 10. The last step that is required to complete the development of a realistic scenario based upon land-use data is to take into account other realistic factors that can affect the final emissions levels for the particular date that one desires to simulate. The factors that can be included are first the date of the simulation (upon which all factors above must be scaled) together with an adoption rate curve, or any performance degradation that one wants to include for the installed DG systems.

With regard to the adoption rate, both a realistic exponential increase and a less realistic linear increase of the accumulated DG power installed in the period 2003-2010 have been implemented in the current study as shown in section 5.1.1.11 of this report. The performance degradation can include both an increase of criteria pollutant emissions and a decrease of electrical efficiency that will likely occur throughout the lifetime of any DG unit.   As practically no public data on DG performance degradation are currently available, the APEP team suggests a 10% annual increase in criteria pollutant emissions. According to the estimated adoption rate, 2 average years of installation for the DG units are determined, one for the DG fleet as adopted in the period 2003-2006, and the other for the one introduced in 2007-2010. The corrections of net emissions for both the 2003-2006 and the 2007-2010 DG fleets due to selected annual performance degradation are determined according to their average year of installation. See section 5.1.1.11 for more details of this procedure.

5.2   Air Quality Modeling: Approach and Results

5.2.1   Input considerations

Simulations of air quality episodes with a three-dimensional model require a series of input parameters used to compute the numerical solution of the atmospheric diffusion/advection equation (Equation 20).

$$\frac{\partial Q_m^k}{\partial t} + \nabla \cdot \left(u Q_m^k\right) = \nabla \cdot \left(K \nabla Q_m^k\right) + \left(\frac{Q_m^k}{\partial t}\right)_{sources/\sin ks} + \left(\frac{Q_m^k}{\partial t}\right)_{aerosol} + \left(\frac{Q_m^k}{\partial t}\right)_{chemistry} \tag{20}$$

Input data needed include the meteorological conditions and the emissions inventory. In particular, the following fields describe the meteorological data in the model: temperature, relative humidity, solar radiation, three-dimensional wind fields and inversion height. Gas-phase reactions and aerosol-phase conversion processes are included in the model through a state-of-the-art chemical mechanism and a comprehensive aerosol-phase formation module. Finally mixing and transport of pollutants are also considered.

5.2.1.1   Meteorological Conditions

The Southern California Air Quality Study (SCAQS) completed a comprehensive campaign of atmospheric observations in the South Coast Air Basin (SoCAB), during August 27-29th 1987. The campaign collected an extensive set of meteorological and air quality data that has been used widely to validate air quality models (Moya 2002 et al., Griffin et al. 2002b, Knipping et al. 2002, Meng et al. 1998). During SCAQS, temperature, humidity and winds vertical profiles were obtained along with the temporal and spatial distribution of these fields. Further analysis of these measurements has provided a complete set of gridded meteorological data readily available to be used in air quality simulations. Zeldin et al., (1990) found that August 28th, 1987 falls within a 'reasonable central met-class tendency', and makes it suitable for modeling. In addition, the August 27-29th 1987 episode was found statistically within the top 10% most severe ozone-forming meteorological conditions (SCAQMD 2003). Furthermore, this episode is also used by the AQMD to show that air pollution control strategies proposed in the 2003 Air Quality Management Plan (AQMP 2003) will lead to ozone attainment by 2010. Hence, this episode is selected in this study to evaluate the air quality impacts of DG during severe smog conditions.

During a typical day, the dominant direction followed by the winds in the SoCAB is from west to east. The San Gabriel and San Bernardino Mountains form a natural barrier that enhances accumulation of air pollutants, especially in downwind locations, such as Riverside and San Bernardino. In addition, warm and sunny conditions together with lack of natural scavenging processes, such as rain, promote the formation of photochemical smog and ozone.

The SCAQS episode in August 27-29th 1987 was characterized by a weak onshore pressure gradient and warming temperatures aloft. The wind flow was characterized by a sea breeze during the day and a weak land-mountain breeze at night. The presence of a well-defined diurnal inversion layer at the top of neutral and unstable layers near the surface, and a slightly stable

nocturnal boundary layer, facilitated the concentration of pollutants over the SoCAB and lead to an episode with high ozone concentrations.

5.2.1.2   Emissions Inventory

The South Coast Air Quality Management District (SCAQMD) and the California Air Resources Board (CARB) have prepared the gridded emission inventories used in this report. Back-casting of emissions has lead to emission inventories used for modeling purposes. Emission inventories for the years 1987 and 1997 are used to compare simulation results with measured data. Forecasting of emissions is used to generate emission inventories for the year 2010. Forecasted emissions are required by state agencies to evaluate emission control measures that might lead to attainment of ozone federal air quality. Two different emission inventories have been prepared: (1) a 2010 baseline emission inventory, which accounts for increase in population and does not consider any future emissions control measures (Figure 10 and Figure 12), and (2) a 2010 attainment scenario, which includes all the control measures proposed by state agencies to accomplish ozone federal air quality standards attainment by 2010 (Figure 11 and Figure 13).
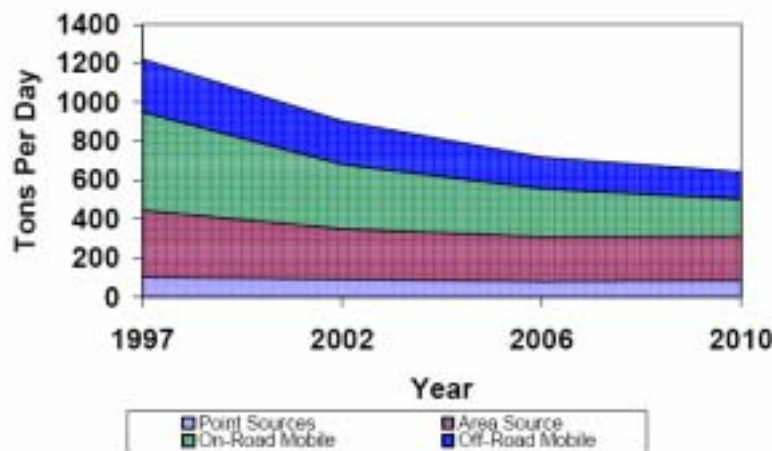
Figure 10. Baseline VOC emissions (AQMP, 2003)
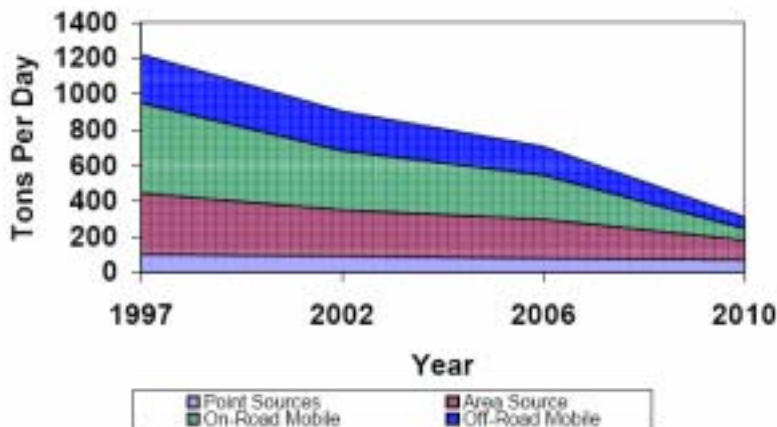
Figure 11. Attainment VOC emissions (AQMP, 2003)
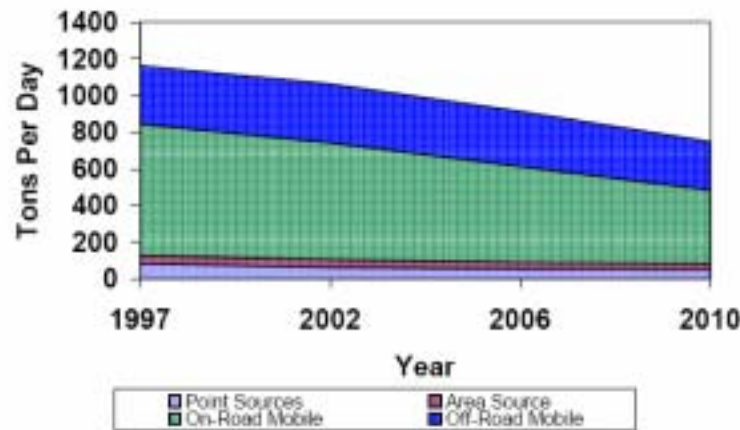
Figure 12. Baseline NOx emissions (AQMP, 2003)
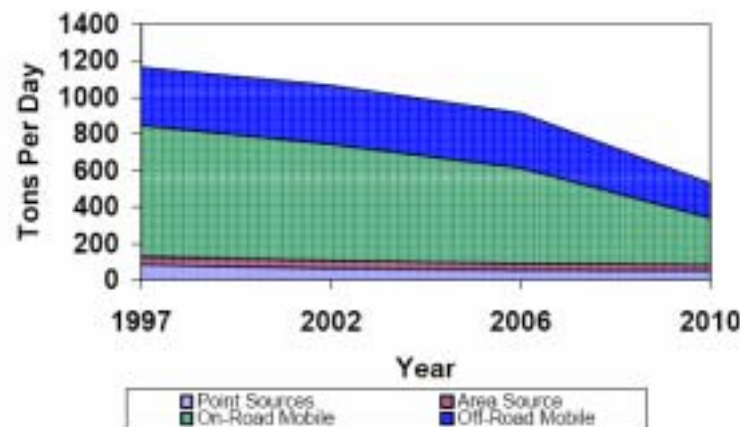
Figure 13. Attainment NOx emissions (AQMP, 2003)

Determination of DG air quality impacts depends on the emission inventory used for the simulations. VOCs and NO_X in the attainment emission inventory are lower than those of the baseline scenario by 40% and 27%, respectively. As a result, air quality impacts due to DG on the attainment scenario may be significantly greater than impacts on the baseline scenario. Results in this work, however, are based on the baseline emission inventory since the attainment emission inventory is under ongoing development. A section reporting air quality impacts of DG using the attainment emissions inventory is included in this study to discuss the effects of base emissions on DG air quality impacts.

5.2.1.3 Chemical Mechanism

The gas-phase chemical mechanism used in the present simulations is the Caltech Atmospheric Chemical Mechanism (CACM, see Griffin et al. 2002b). CACM is based on the work of Stockwell et al. (1997), Jenkin et al. (1997), SAPRC-97 and SAPRC-99 (available from W.P.L. Carter at http://pah.cert.ucr.edu/~carter/) and includes O_3 chemistry and a state-of-the-art mechanism of the gas phase precursors of secondary organic aerosol (SOA). The full mechanism

consists of 361 chemical reactions and 191 gas-phase species which describe a comprehensive treatment of VOCs oxidation.

5.2.1.4 Aerosol-phase Dynamics

Inorganic aerosol formation is calculated using the Simulating Composition of Atmospheric Particles at Equilibrium 2 model (SCAPE2, Meng et al., 1995). SCAPE2 has been modified to account for the interaction between organic ions present in the aqueous phase and the inorganic aerosol components.

The model used to determine the partitioning of secondary organic compounds is the Model to Predict the Multiphase Partitioning of Organics already built in the CIT Airshed model (MPMPO, Griffin et al., 2002b). MPMPO allows the simultaneous formation of SOA in a hydrophobic organic phase and a hydrophilic aqueous phase. The module consists of 37 size-resolved aerosol-phase species, in 8 different size bins ranging from 0.04 to 10 micrometers. The integrated module, allows particulate matter to undergo advection, turbulent diffusion, condensation/evaporation, nucleation, emissions and dry deposition processes.
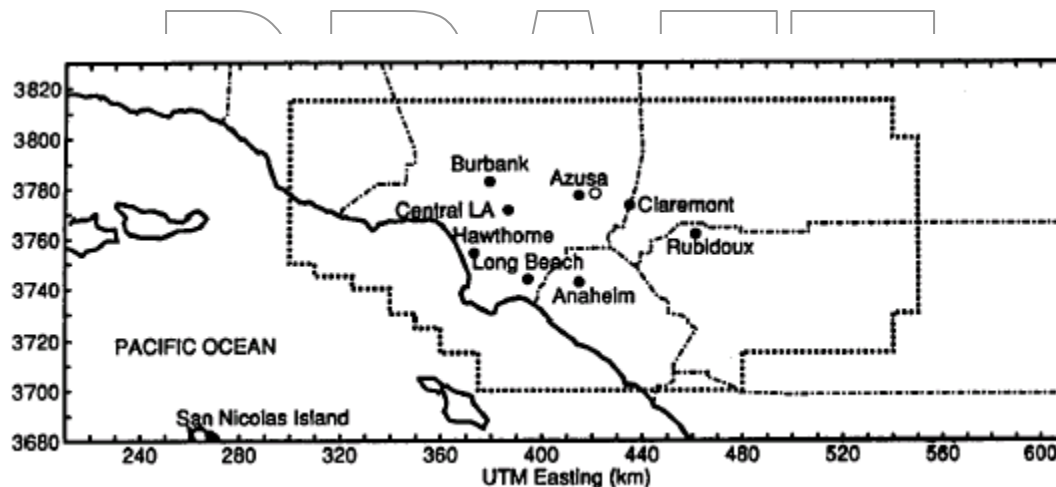
Figure 14. CIT Airshed domain (from Griffin et al., 2002a)

5.2.1.5 Mixing and Transport Mechanism

The California Institute of Technology (CIT) Airshed Model is used as the host model for the chemical and aerosol mechanisms (Harley et al., 1993, Griffin et al., 2002a and Meng et al., 1998). The grid used by the CIT model encompasses the Orange County and part of Los Angeles, Ventura, San Bernardino and Riverside counties (Figure 14). The grid consists of cells with an area of 5 km by 5 km, with a vertical resolution defined by 5 vertical layers of increasing thickness from ground level up to 1100 meters of altitude. The respective 5 layers thicknesses are 38.5, 115.5, 154, 363 and 429 meters, from the bottom to the top layer.

5.2.2   Comparison of simulation results with measured data

Model performance needs to be analyzed and compared with available observations since simulation of an air quality episode requires various input parameters, each one subject to different sources of uncertainty. Griffin et al. validated results obtained with the CIT model and the CACM chemical mechanism using the August 27-29th 1987 meteorology and emissions inventory (see Figure 15). Griffin et al. also reported comparisons between observed and simulated data at Pasadena and Riverside. In general, ozone concentrations in Pasadena are under-predicted each day, whereas NO concentrations at this location compare reasonably well with observation, except for the third day. In Riverside, ozone concentrations agree with observed data for the second and third day. However, NO concentrations are under-predicted during the daylight hours and over-predicted at nighttime. A statistical analysis was conducted to determine the overall performance of the model versus observed data (see Table 26). Results show a typical level of agreement for current three-dimensional air quality models.
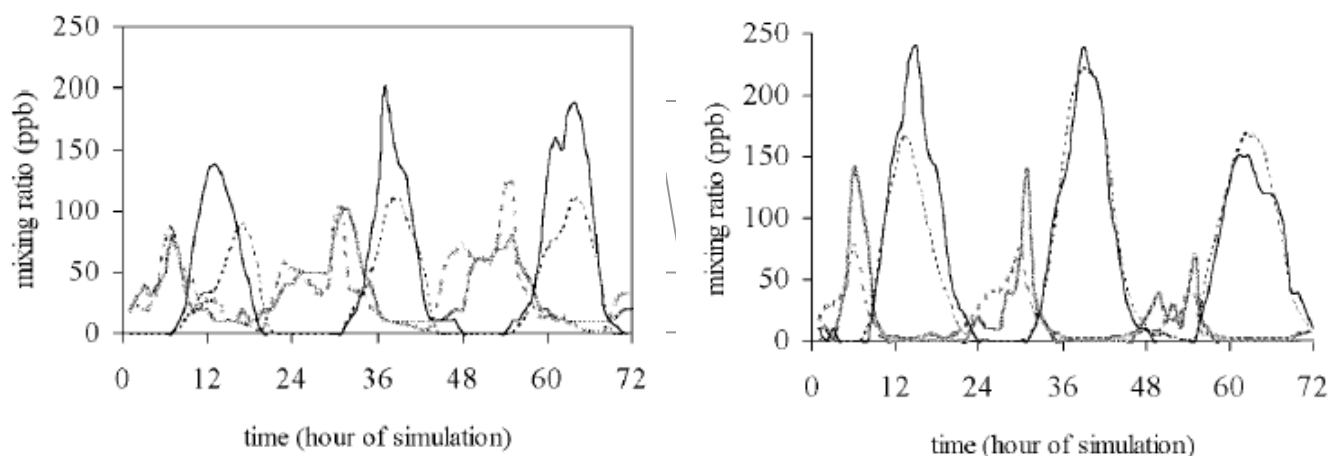
Figure 15. Comparison of simulated (dashed line) and measured (solid line) NO (shaded) and O₃ (black) mixing ratio in Pasadena (left) and Riverside (right) during August 27-29th, 1987 (from Griffin et al., 2002a).

Table 26. Statistical analysis of model performance versus observed data on 28th August, 1987, for O₃ and NO₂ (from Griffin et al. 2002a)

Statistical Measure	O_3	NO_2
Bias, ppb	15.9	-0.4
Normalized bias, %	21.7	12.6
σ of residuals, ppb	55.3	28.1
Gross error, ppb	39.5	21.4
Normalized gross error, %	41.1	51.6
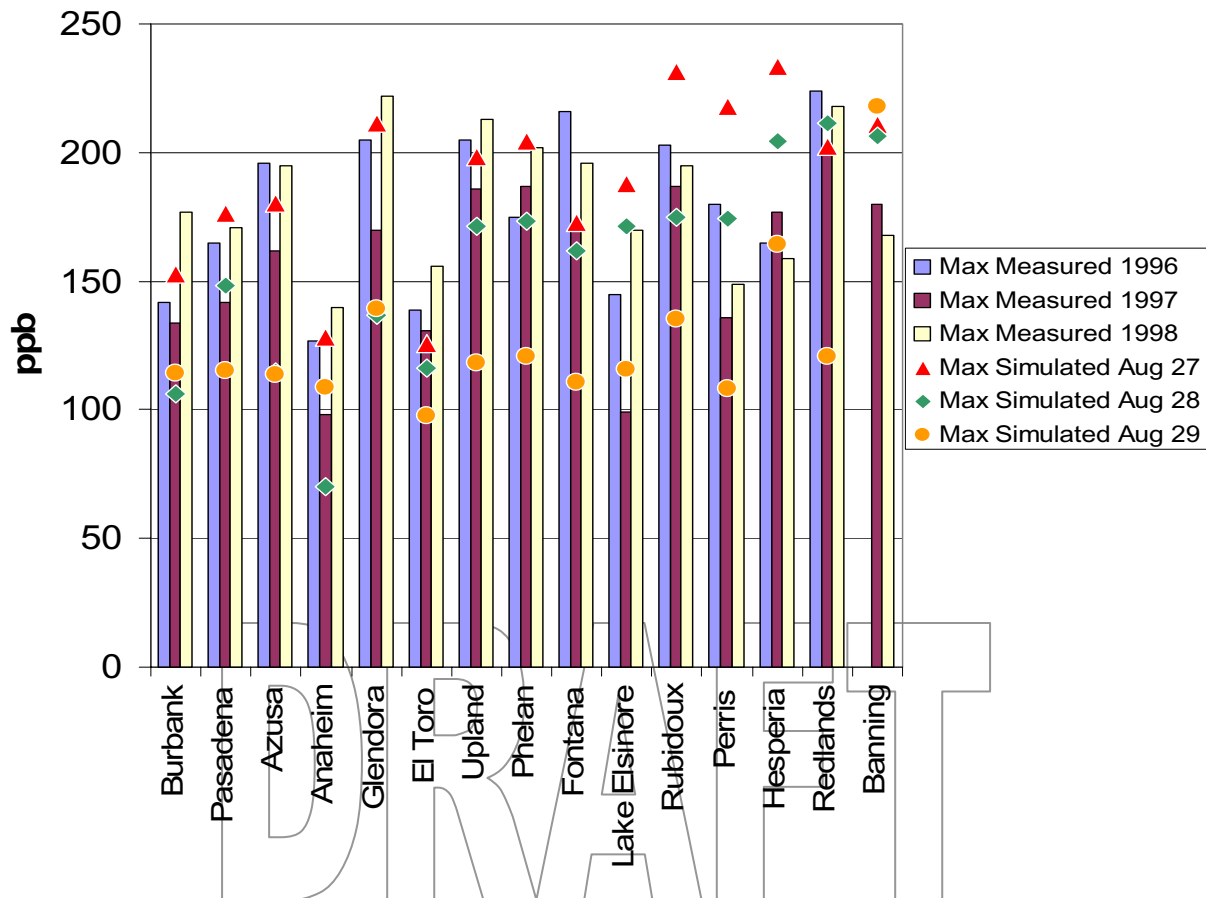
Figure 16. Comparison between measured maximum concentration of ozone in years 1996-1998, and concentration of ozone simulated using 1997 emission inventory and a high ozone-forming potential episode (SCAQS August 27-29th, 1987 meteorology)

Figure 16 shows a comparison between model predictions and observations of maximum ozone concentrations at different monitoring stations using August 27-29th meteorology and the emission inventory for year 1997. Measured maximum ozone concentrations reported in Figure 16 correspond to observations in the period from 1996 to1998 at the selected stations. Note that simulated data refers to a specific episode whereas measured data refers to maximum concentrations during the entire year. This comparison shows that simulation results fall within the range of measured ozone values at each station. Although not a strict validation, this kind of comparison establishes an additional sense of confidence in the simulation results, specially needed when different emission inventories will be used.

5.3   Uncertainty and Sensitivity Analysis

5.3.1   Importance and background

Air quality models (AQMs) are instrumental to assess the potential air quality impacts of DER within urban basins. Only through the use of a detailed AQM one can assess the effects of increased DG emissions on the complex, non-linear, and concurrent processes of transport, mixing, heterogeneous and homogeneous chemistry that lead to criteria pollutant concentrations of interest. However, numerical predictions from mathematical models are subjected to various sources of uncertainty. A quantitative analysis of AQMs responses to different input parameters is a prerequisite to characterize these sources of uncertainty. Additionally, such analysis also identifies those input parameters and simulation conditions responsible for most of the model output variation.

Emissions inventories represent the largest uncertainties associated with output concentrations in three-dimensional urban/regional air quality models (Griffin et al., 2002b). However, the gas-phase chemical mechanism could introduce significant uncertainties in model predictions. Sources of uncertainty in chemical mechanisms lie in the rate constants, the product yields, and the mechanisms of degradation of reaction products. Mathematical procedures to analyze uncertainty and sensitivity of complex photochemical mechanisms have been evaluated thoroughly. For instance, Dunker (1981, 1984), Milford et al. (1992), and Gao et al. (1995) used direct decoupled methods; Rabitz et al. (1983), and Rabitz and Hales (1995) employed the Green's Function or Adjoint Green's Function methods; whereas Carmichael et al. (1997) favored automatic differentiation techniques.

Monte Carlo methods that examine uncertainties in chemical parameters have been applied also to gas-phase chemistry and photochemical box models (Stolarski et al., 1978; Ehhalt et al., 1979; Thompson and Stewart, 1991; Gao et al., 1995; Yang et al., 1996). Monte Carlo methods are statistical simulation methods, where sequences of random numbers are used together with multiple trials (simulations in this case) and statistical analyses of variance to determine sensitivities. Monte Carlo methods are widely used because they can be applied to problems with a large number of input parameters. Furthermore, Monte Carlo methods have the advantage that estimates of the uncertainties in model outputs are calculated with systematic runs of the model with standard statistical tests that can be applied to output results.

This section presents the approach selected by the University of California, Irvine research team to conduct sensitivity analyses of the atmospheric chemical mechanism – CACM – and the full AQM – the CIT Airshed model – used to determine the air quality impacts of DG. This sections begins with a presentation of the results of the uncertainty and sensitivity analysis performed on CACM (Griffin et al., 2002a,b; Pun et al., 2002). CACM includes state-of-the-art treatment of ozone formation, but more importantly, is the first detailed atmospheric chemistry mechanism that includes explicit prediction of semivolatile products formation. These semivolatile products have the potential to be constituents of secondary organic aerosol (SOA) and are significant precursors to SOA formation in the south coast air basin (SoCAB).

A global sensitivity analysis of the chemical mechanism is performed and presented herein using Monte Carlo techniques combined with Latin hypercube sampling to vary simultaneously all

chemical parameters over their full ranges of uncertainty. Uncertainties in rate parameters are propagated through box model simulations with CACM for three summer cases. The cases cover a range of initial concentrations of reactive organic gases and nitrogen oxides that represents various episodes of high ozone levels in polluted urban areas.

This section describes the methodology used in the sensitivity analysis performed on the chemical mechanism (CACM) as an introduction to the methodology selected for the current project. The same methodology is applied to the complete air quality model and chemical mechanism used in this project. Different approaches and evaluations have been used to understand the sensitivity and uncertainty of air quality models (Yang et al., 1997; Hanna et al., 1998, 2001; Moore and Londergan, 2001; Hanna and Davis, 2002; Vardoulakis et al., 2002; Hakami et al., 2003; Sax and Isakov, 2003). However, the present analysis focuses on some specific aspects unique to this study. First, it examines the response of specific AQM predictions in order to separate the DG air quality impacts from the uncertainty of the model to various input parameters. Second, it provides a measure of the error bounds for model concentrations of ozone and particulate matter less than 2.5 micron ($PM_{2.5}$). Finally, this analysis explores the error spatial variation to determine those areas in the SoCAB of California where the model predictions display the largest uncertainties.

5.3.2   Chemical mechanism sensitivity

5.3.2.1   Methodology

Sensitivity and uncertainty analysis are accomplished using statistical methods to identify reaction parameters whose changes present the largest effect on both the concentration of selected key species and their associated errors. This section describes the statistical sampling used, the multiple regression approach to estimate sensitivity coefficients, and the corresponding uncertainty assessment under the simulation conditions established.

5.3.2.1.1   Latin Hypercube Sampling

A conventional approach to address uncertainty assessment is to apply Monte Carlo techniques. This particular methodology has been applied extensively in the study of regional-scale gas-phase mechanisms (Derwent and Hov, 1988; Gao et al., 1996; Phenix et al., 1998; Bergin et al., 1999; Grenfell et al., 1999; Hanna et al., 2001; Vuilleumier et al., 2001). Monte Carlo analysis investigates the response of model output (species mixing ratio) when the input variables (reaction rates) are changed by repeated sampling from some assumed joint probability distribution. The probability distribution of the species mixing ratio along with its mean, variance, and other characteristics are obtained from the evaluation of model output for each sample.

Monte Carlo analysis using random sampling yields reasonable estimates for the mixing ratio probability distribution if the sample size is large. However, acquiring a large number of samples (distinct randomly perturbed instances of running the full model in this case) is computationally expensive. An alternative approach, which yields more precise estimates, is to use a constrained Monte Carlo sampling scheme. One such scheme is Latin Hypercube Sampling

(LHS) (McCay et al., 1979), a stratified sampling technique that has been compared extensively with other techniques (Iman and Helton, 1983), and that is proven to be more efficient than simple random sampling.

Latin hypercube sampling selects n different values from each of the N_p total number of parameters treated as random variables in the following manner. The range of each variable is divided into m non-overlapping intervals on the basis of equal probability. One value from each interval is selected at random with respect to the probability density in the interval. This value is randomly paired with the n values of the other N_p variables. Thus, the m N_p-tuplets constructed in this manner form the Latin hypercube sample. It is convenient to think of this sample as an $n \times N_p$ input matrix where the lth row contains specific values of each of the N_p input variables used on the lth run of the computer model.

The proper size of an LHS sample is a compromise between the number of runs and the required accuracy. In this study, sample sizes ranging from 100 to 3,880 runs are used to test the convergence of the means and the corresponding standard deviations of selected species. Study of these sample sizes resulted in the selection of 1150 samples for the sensitivity analyses of the CACM box model. Results reported thereafter are obtained with a sample size of 1150 computational runs of the box model. Even though the random variables are sampled independently and paired randomly, the sample correlation coefficient of any of the m N_p-tuplets is not zero due to sampling fluctuations.

The input parameters in this study are treated as independent variables and the correlation coefficients determined by the sensitivity analyses for the samples used never exceeded a value of 0.015. As a result, the assumption of independence is a good one. Sensitivity of the model output to the input parameters is determined with multiple linear regression analysis techniques in a manner similar to Derwent and Hov (1988) and Gao et al. (1996).

5.3.2.1.2 Simulation Conditions

Computational runs performed in a box model with CACM as the chemical mechanism are the starting point for the proposed Monte Carlo analysis. The box model includes time varying photolysis rates at a latitude of 34° N, approximately that of the Los Angeles basin. A 12-hour period that spans from 6:00 to 18:00 LT is chosen to study an episode where photolysis plays a major role in the formation of important species such as ozone.

Initial conditions used represent those of an urban environment. Initial conditions for all species are obtained from typical data provided by the three-dimensional CIT model (Harley et al., 1993; Meng et al., 1998). The cell (box) in the CIT model that was selected represents Riverside because this location exhibits large ozone concentrations in the south coast air basin. Typical volatile organic compound (VOC) to nitrogen oxide (NO_x) ratios in this and similar urban regions vary from 6:1 to 50:1 (Baugues, 1986). Urban summer ground-level conditions for VOC/NOx ratio range from 6:1 to 24:1 with 1000 ppbC total VOC mixing ratio (Gao et al., 1995). The value of the initial VOC/NOx ratio in the chosen cell is 8.6 with 1534 ppbC total VOC. However, different cases for the VOC/NOx ratio are analyzed by changing the NOx mixing ratio.

Three cases are examined. First, the VOC/NOx ratio is set at 8:1 corresponding to a regime in which ozone increases as NOx gets reduced. Second, the optimal ratio for maximum ozone production is set at 17:1. Finally, a ratio of 32:1 corresponding to the regime where decreasing NOx results in O_3 reduction is applied.

All rate parameters are treated as random variables. Uncertainty estimates for the kinetic parameters of the chemical mechanism (CACM in this case) are compiled mostly from published reviews (DeMore et al., 1990; Gao et al., 1996), and from the Summary of Evaluated Kinetic and Photochemical Data for Atmospheric Chemistry (available from Atkinson et al. on the World Wide Web server for the IUPAC Subcomittee for Gas Kinetic Data Evaluation, http://www.iupackinetic.ch.cam.ac.uk/index.html).

5.3.3   Air quality model sensitivity

5.3.3.1   Description

The present study investigates the uncertainty and sensitivity of key species to variations in selected input parameters related to DG by use of a Monte Carlo methodology. Monte Carlo analysis has been applied to study the uncertainty of regional-scale gas-phase mechanisms (Derwent and Hov, 1988; Gao et al., 1996; Phenix et al., 1998; Bergin et al., 1999; Grenfell et al., 1999; Hanna et al., 2001; Vuilleumier et al., 2001). Also, previous work is based on calculations of the California Institute of Technology (CIT) three-dimensional air quality model over the SoCAB. Although responses of aerosol and gas-phase species to changes in nitrogen oxides (NO$_x$), volatile organic compounds (VOC), and ammonia (NH$_3$) emissions have been investigated by (Meng et al., 1997; Nguyen and Dabdub, 2002b), these studies focus on simulation scenarios for the Southern California Air Quality Study (SCAQS) on August 27, 28, and 29, 1987.

Sensitivity results presented use the 2010 baseline emissions inventory described in other parts of this report. This inventory helps to establish a baseline scenario, which accounts for the increase in population by the year 2010. Additionally, an improved model is used in the present work. For instance, the current CIT model incorporates the Caltech Atmospheric Chemistry Mechanism (CACM) (Griffin et al., 2002a,b; Pun et al., 2002), a detailed atmospheric chemical mechanism directed toward explicit prediction of semi-volatile products formation with the potential to be constituents of secondary organic aerosol (SOA). The potential air quality effects of DG implementation by the year 2010 motivate the current study. After performing various model evaluations, statistical analysis methods are used to identify the input parameters with the largest effect on both, concentrations of selected key species and their associated errors. This section describes the chosen statistical sampling, the multiple regression methodology used to estimate the sensitivity coefficients, and the corresponding uncertainty assessment for the simulation conditions established.

5.3.3.1.1   Latin Hypercube Sampling

Monte Carlo methods examine the changes in modeled output (species mixing ratio) when repeated sampling from an assumed joint probability distribution varies a pre-selected set of input variables. The probability distribution of species mixing ratio along with the mean and

other relevant statistics are evaluated from each sample of model output. LHS is proven to be more efficient than straight Monte Carlo sampling when the use of large samples is computationally costly. The LHS technique employed for the full air quality model is identical to that described in Section 5.3.2.1.1, used for the chemical mechanism sensitivity analysis.

5.3.3.1.2 Multiple Linear Regression

Model sensitivity to variation of selected input parameters is explored using multiple linear regression analysis (Derwent and Hov, 1988; Gao et al., 1996; Hanna et al., 2001). However, when many input variables are involved, the direct construction of a regression model containing all input variables may not be the most adequate approach. Moreover, only a small number of input variables typically have an impact on the output variable. Thus, stepwise regression (Helton, 1993) is used as an alternative to construct a regression model containing all the input variables. With this approach, a sequence of regression models is constructed. Namely, the first regression model contains the single input variable with the largest impact on the output uncertainty. The second regression model contains the two input variables with the largest impact, including the variable from the previous model. Additional models in the sequence are defined until a point is reached at which subsequent models are unable to increase meaningfully the amount of variation that can be accounted in the output variable. This study reports the results obtained in the last model of the sequence.

5.3.3.1.3 Simulation Conditions

Investigation of uncertainties in complex three-dimensional air quality models poses a major challenge in that a large number of computational simulations is required. Additionally, statistical tools are essential to derive a few useful conclusions from the numerous three-dimensional, time-dependent simulation results (modeled concentrations). An important step in the analysis is the selection of input variables that both, have the potential to affect the concentrations predicted by the model, and reflect changes due to the DG implementation. This selection typically includes parameters such as the meteorology, the chemical reaction rates, and initial conditions. The implementation of DG, however, will result in significantly different emissions profiles from those of central generation. Therefore, this study aims to understand whether changes in emission inventories similar to those caused by DG make a difference, and to what extent this difference is significant in the predictions of the air quality model. It is also important to characterize the temporal and spatial domain-wide differences in model uncertainties. This characterization will distinguish the numerical uncertainties of the model from the simulated air quality impacts of DG.

Table 27 presents the variables considered in this study and the values of their uncertainty ranges. The probability density function of the variables considered in the sensitivity analysis are assumed to follow a lognormal distribution. Values for the uncertainty ranges are compiled from published studies (Hanna et al., 1998, 2001). Table 27 reflects the careful selection of those quantities, such as boundary conditions and emissions, which drive spatial variation and affect the implementation of DG in the basin. The number of parameters is limited to less than 20 for three main reasons. First, this analysis focuses in the model sensitivity and uncertainty of ozone

and particulate matter, thus only input variables that affect these species are considered. Second, the number of input variables chosen is restricted in order to decrease the computational demands of the analysis, which requires large numbers of simulations when various input variables are considered. Third, not all chemical reaction rates need to be included since a comprehensive sensitivity and uncertainty analysis of CACM (Rodriguez and Dabdub, 2003) shows that only a subset of reactions is the most influential in the formation of ozone. Moreover, the reactions included in Table 27 are consistently the most important over different VOC:NOx ratios explored in the box model calculations (Rodriguez and Dabdub, 2003).

Computational runs, performed with the CIT model, are the starting point for the Monte Carlo analysis. Results reported in this study are obtained with a sample size of 50 computational model runs. The number of simulations is adequate, given the number of input variables (Hanna et al., 1998, 2001). Each model run represents a period of three simulation days (72 hours). However, this work only considers data results from the third day of simulations to lessen the influence of initial conditions. Lagrangian models confirm (Nguyen and Dabdub, 2002b) that more than 90% of the initial conditions leave the computational domain by the second day of simulation. Moreover, direct sensitivity analysis of multidimensional models (Yang et al., 1997) estimates that ozone peak sensitivity values to initial conditions are 12 times higher on the first day compared to values on the second and subsequent days. After simulations are performed, calculation of probability density functions for each output variable provides a way to characterize the uncertainty of predicted species concentrations. Sensitivity is based on the regression coefficients estimated with multiple linear regression as detailed in the previous section.

Table 27. Uncertainty ranges and associated sigmas for the Airshed input variables in the Monte Carlo runs.

Variable Type	Input Variable	Range of Uncertainty (σ_g log-normal)
Boundary Concentrations	1. Top Ozone	1.23
	2. Top NOx	1.73
	3. Top VOC	1.73
	4. Top NH$_3$	1.73
	5. Side Ozone	1.23
	6. Side NOx	1.73
	7. Side VOC	1.73
	8. Side NH$_3$	1.73
Emissions rates	9. Domain-wide NOx	1.41
	10. Domain-wide VOC	1.41
	11. Domain-wide NH$_3$	1.41
Chemical reactions	12. NO$_2$ + hν	1.30
	13. NO + O$_3$ $\rightarrow$ NO$_2$ + O$_2$	1.10
	14. NO$_2$ + OH + M $\rightarrow$ HNO$_3$	1.10
	15. HCHO + hν	1.40
	16. Alkenes + OH $\rightarrow$ RO2	1.13
	17. Aldehydes + hν	1.40

DRAFT

6   PROJECT OUTCOMES

6.1   Final DG scenarios

Through application of the criteria presented in this report and use of all of the data and information that is currently available to the APEP team, it was determined that only a very limited number of realistic scenarios can be developed and included in the current study. This is due to the fact that all available information and resources for well defining each of the parameters and factors is used to develop a "realistic" DG Scenario. APEP has sought and is including all possible information resources to ground these few "realistic" DG scenarios and is then including several parametric variations (excursions) on these scenarios that either complete or complement the overall analysis of air quality impacts of DG in SoCAB.

In addition, the APEP team is following the recommendation provided in the Industrial Stakeholder Workshops held on September 19, 2002 and May 21, 2003 to classify each of the DG scenarios in two categories according to the "likelihood" of the scenario. Some of the scenarios that are developed in this effort are therefore classified as "realistic" implementation scenarios for DG in the South Coast Air Basin. However, for scientific completeness, for sensitivity analyses, and for determination of potential impacts for unexpected outcomes we have developed a series of scenarios that "span the spectrum."   These scenarios are classified as "spanning" DG Scenarios.

These spanning scenarios should in no way be considered realistic or probable. The authors strongly caution readers to accept these spanning or "unrealistic" scenarios only in as much as they provide increased understanding or fundamental insight into DG air quality impacts. Under no circumstances do the authors suggest that the predicted impacts of a spanning scenario are realistic or expected due to the installation of DG in SoCAB. The spanning DG scenarios are not expected and are only used for purposes of garnering insights that may be useful.

The list of DG scenarios that is recommended includes: (1) three baseline scenarios without DG emissions, (2) five realistic DG scenarios, and (3) twenty one spanning DG scenarios. These recommended DG Scenarios are presented and described below.

6.1.1   Baseline Scenarios

Three baseline scenarios are included in the current study. Recall that these baseline scenarios are not perturbed by the addition emissions from the DG scenarios. DG scenario emissions are added to a baseline scenario to determine relative air quality impacts of the DG emissions. In each of the baseline scenarios, the emissions inventory for the South Coast Air Basin is not modified from that which was received by APEP from the California Air Resources Board. The 1987 Baseline Scenario is included as a reference case for checking the model and comparing results with real measured emissions and air quality measurements. Two Baseline Scenarios for the year 2010 are used in the current study. 2010 is the year that the current team is focused upon to evaluate the air quality impacts of DG in the South Coast Air Basin.

6.1.1.1   Scenario #B1: 1987 Baseline

No parameters or factors are changed from the 1987 Emissions Inventory obtained from the California Air Resources Board. This inventory has been tested against measured emissions and basin-wide air quality measurements by many research groups in hundreds of air quality studies.

6.1.1.2   Scenario #B2: 2010 Baseline

No parameters or factors are changed from 2010 Emissions Inventory obtained from the California Air Resources Board in May of 2003. Emissions in this scenario are assumed to be scaled for growth in population, industrial and commercial activity, and vehicle miles traveled, etc. with the expectation that NO ADDITIONAL REGULATORY REQUIREMENTS are instituted between now and 2010.

6.1.1.3   Scenario #B3: 2010 Attainment Baseline

No parameters or factors are changed from the 2010 Emissions Inventory obtained from the California Air Resources Board in 2004. Emissions in this scenario are those of the 2010 Attainment scenario used by the South Coast Air Quality Management District (SCAQMD) in their 2003 Air Quality Management Plan for demonstration of ozone NAAQS attainment (http://www.aqmd.gov/aqmp/AQMD03AQMP.htm).

6.1.2   Realistic Scenarios

As a result of applying the screening criteria described above, and using all the data that are currently available, the APEP team recommends a limited number of realistic DG Scenarios (5) that are included in the current study. The full characterization of these realistic scenarios uses all available reports, studies, measurements, APEP team insights, stakeholder comments, etc. that were available on DG characteristics, performance, market penetration, application compatibility, at the time of this report writing.

All of the realistic scenarios incorporate the recently acquired global information systems (GIS) land-use data of the SoCAB as a cornerstone to spatially distribute the DG throughout the basin. In addition, all of the latest studies regarding the potential application of various DG to certain applications, the degree of market penetration expected and the size, electrical performance, efficiency and emissions characteristics of each DG type are used in the realistic scenarios. A listing of these resources is presented in the References section.   In addition, a detailed description of the GIS data and a systematic approach of scenario development based on these and other DG data and resources can be found in the report entitled "Final DG Scenario Development Report", already available in the CEC website (www.energy.ca.gov/distgen_oii/documents/dgwg/R+D-7.pdf).

6.1.2.1   Scenario #R1

This realistic scenario #R1 is the basis for the other 4 realistic scenarios, which only incorporate a slight variation in one of the major factors that define Scenario #R1. Scenario #R1 makes use of all the resources available to justify DG overall penetration, DG power,

and DG mix in each of the discretized cells of the air quality model. For this particular scenario a medium early adoption for DG is assumed, which implies that the cumulative DG power implemented and operating in the SoCAB follows a linear trend from 2003 to 2010. Scenario #R1 also assumes a limited DG penetration (5% of the increased power requirements by 2010). This scenario contains a realistic duty cycle based on metered average electric hourly profiles for various energy sectors, a displacement of emissions due to the heat recovery mode of most of the units installed, and a low performance degradation of the DG units with time. Only in one of the spanning scenarios is an unrealistically high performance degradation considered (see section 6.1.4.20). The high rate of performance degradation is considered unrealistic since it will likely not be allowed by air quality regulations.

Table 28 presents the primary factors that contribute to the overall definition of the realistic scenario #R1. Note that the actual mix of technologies, detailed descriptions of the approach for use of GIS data, and other descriptions of the factors in Table 28 are presented in the report entitled "Final DG Scenario Development Report" produced and submitted to the California Energy Commission under this same contract.

Table 28. Factors that contribute to the definition of realistic scenario #R1.

Factor 1.1:	Limited DG penetration, 5% of increased power
Factor 2.1.6:	Different mix of Permitted and Certified DG in each cell based on the systematic approach to relate GIS data to DG mix
Factor 2.2.2.1:	High penetration of low emission technologies (strong regulation/policy drivers)
Factor 3.1.1:	Known emissions factors – literature, data, permitted/certified levels (upper bound)
Factor 4.4:	Different DG power in each cell based on the systematic approach to relate land use GIS data to spatial distribution of DG power
Factor 5.3:	Realistic Duty Cycle for every sector
Factor 6.3:	CHP Emissions Displaced
Factor 7.1.1:	PM and VOC speciation from ARB data
Factor 7.2:	Low performance degradation (3% increase of emissions per year)
Factor 7.3:	No geometrical features
Factor 7.4.3:	Medium Early Adoption of DG Power (linear trend)

6.1.2.2   Scenario #R2: Medium Penetration (10%) Version of #R1

Scenario #R2 is defined by all of the same factors and parameters as Scenario #R1 except for a variation in DG Penetration. The DG Penetration parameter is set to a higher, still realistic value of 10% of the increased power demand being met by DG in 2010.

6.1.2.3   Scenario #R3: High Penetration (20%) Version of #R1

The same parameters and factors that apply to Scenario #R1 are applied to #R3. In this case a DG Penetration parameter is set to an even higher value (20% of the increased power demand is met by DG in 2010) to account for the uncertainty associated with the future implementation of DG in the SoCAB. In addition, this high DG Penetration is consistent with the current rate of DG adoption and recommendations made by some of the stakeholders in the industry stakeholder workshop of May 21, 2003.

6.1.2.4   Scenario #R4: Low Early Adoption Version of #R1

The same parameters and factors that apply to Scenario #R1 are applied to #R4. The only variation is that a relatively low early adoption of DG is assumed, i.e., for #R4 most of the DG units operating in the SoCAB in 2010 will have been installed after the year 2007. Thus, the emissions signatures for the portion of the DG units that are smaller than 1 MW are set to be less or equal to the stricter CARB DG 2007 emissions standards.

6.1.2.5   Scenario #R5: No Emissions Displaced Version of #R1

The same parameters and factors that apply to Scenario #R1 apply also to #R5. However, in the case of #R5 emissions displacements that the implementation of DG in the SoCAB may produce are assumed to be zero.   That is, no current basin emissions are removed due to the installation of DG. This realistic case is included to account for the possibility that no net emission offsets occur because credits might be sold to other entities, or the market for credits could end up not being robust enough, or the demands for energy are so significant that they require additional in-basin emissions that cannot be offset by reductions elsewhere in the basin.

6.1.3   Resulting spatial distribution of DG power

The procedure described in Section 5.1.3 that relates DG implementation to power per sector and DG technology mix based on land-use GIS data was used to produce a spatial distribution of DG power in the SoCAB for the year 2010. Figure 17 presents a contour plot of the DG power (on a log scale) for a DG scenario with a 5% of the increased power in the basin being met by DG. This type of spatial distribution, called a land-use weighted spatial distribution, is typical of the realistic DG scenarios that have been developed in the current program.

Figure 18 presents a comparison of the land-use weighted spatial distribution of DG power and other spatial distributions used in this study; namely, population weighted, population growth weighted, and freeways density weighted spatial distributions. Except for the non-realistic freeway density spatial distribution of DG power, the other 3 distributions show relatively similar patterns with some differences that are worthy of note. Both the population weighted and the population growth weighted spatial distributions have higher DG power peaks localized in the central part of Los Angeles. On the other hand, the land-use based distribution spreads DG power to more locations (e.g., south of Riverside) and reduces the power peak in central Los Angeles. Note also that the locations of peak power production occur in slightly differing

regions of the SoCAB, representing zones permitted for industrial use and residential use for the land-use weighted and population and population growth weighted cases, respectively.

DG Power (kW), log scale
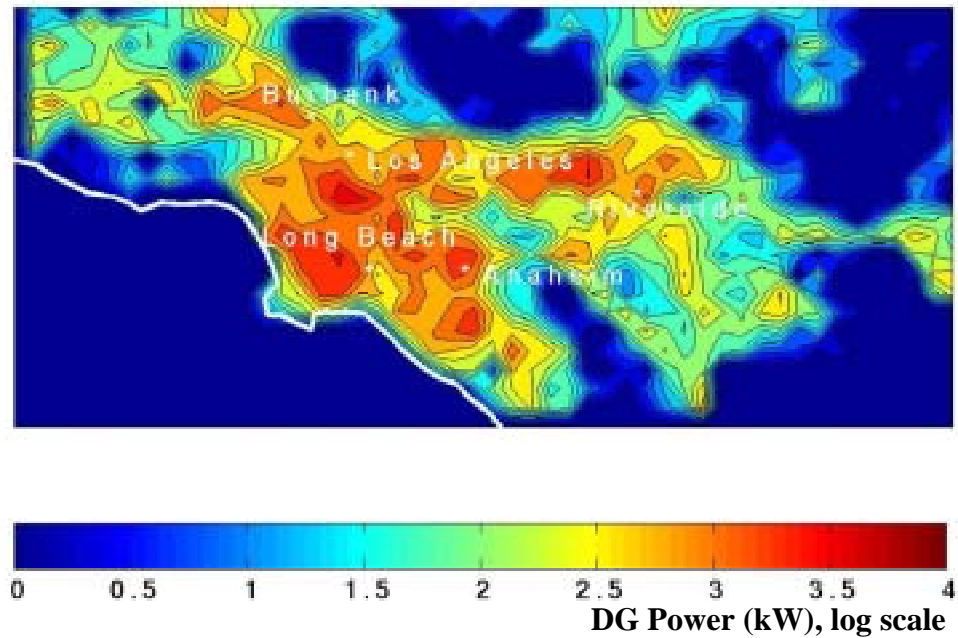
Figure 17: Spatial DG Power Distribution based on land-use GIS data

(a)

(b)

(c)

(d)
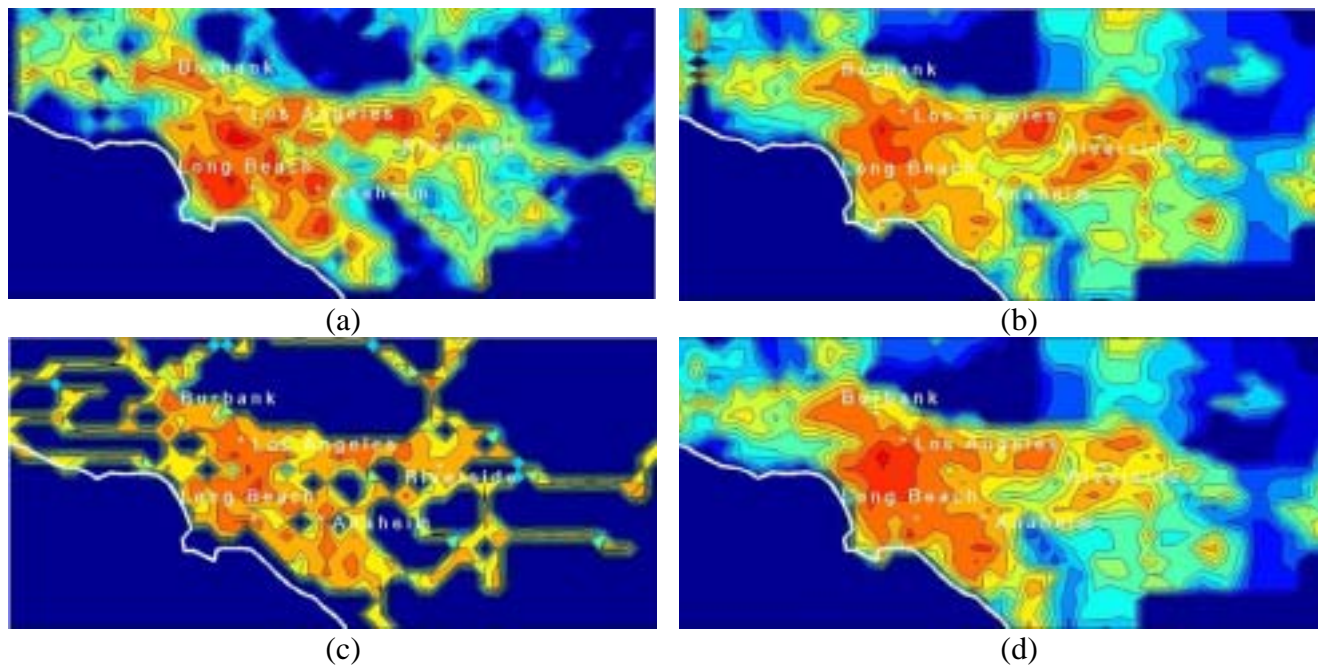
Figure 18: Comparison amongst 4 spatial distributions of DG power in the SoCAB: (a) land-use weighted; (b) population weighted; (c) freeway density weighted; (d) population growth weighted.

The application of the 10-step systematic approach for developing realistic DG implementation scenarios provides a reasonable distribution of DG power among sectors and among DG types in the SoCAB for 2010. Figure 19 presents the total DG power distribution amongst the various sectors considered in the current study. About 60% of total DG power is implemented in the industrial sector and more than 30% is going to the commercial-institutional sector (the sum of categories "commercial" and "other"). Only a small fraction of the DG power that is anticipated for installation in the SoCAB by 2010 is installed to meet power demands in the residential sectors.

Figure 20 presents the relative contribution of each type of DG technology considered in the current study for the systematic approach for developing a DG scenario outlined above. According to this approach, almost 50% of the DG market is being met by gas turbines, whereas ICEs, MTGs, PV, and FC account for 17%, 15%, 5%, and 10% of the total 2010 DG power market, respectively. These figures are presented on a total power contribution basis, and as a result do not accurately reflect the number of units installed, but, rather the contribution to total power demands that are met by each type of DG technology. For example, one large industrial gas turbine contributes much more to the power demand (and emissions) than does a host of small fuel cells installed in the residential sector.
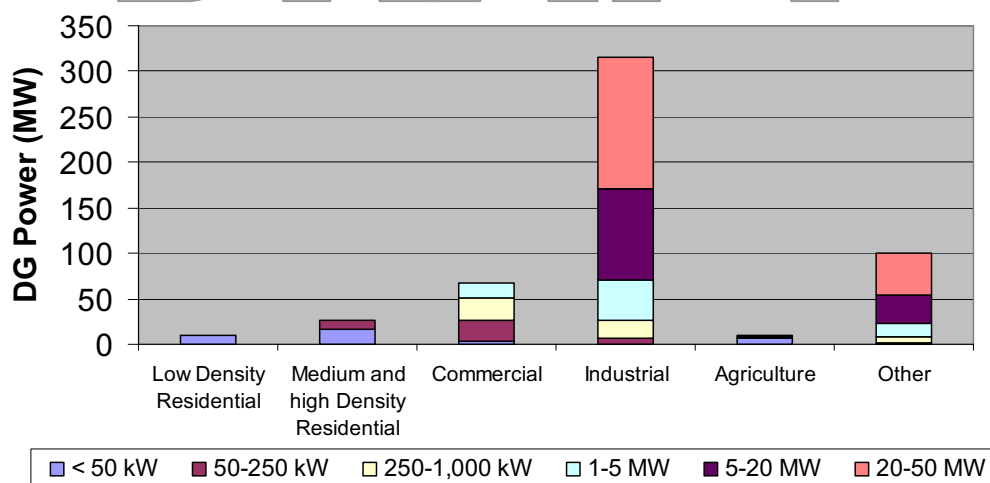
Figure 19: Total DG power distribution among sectors
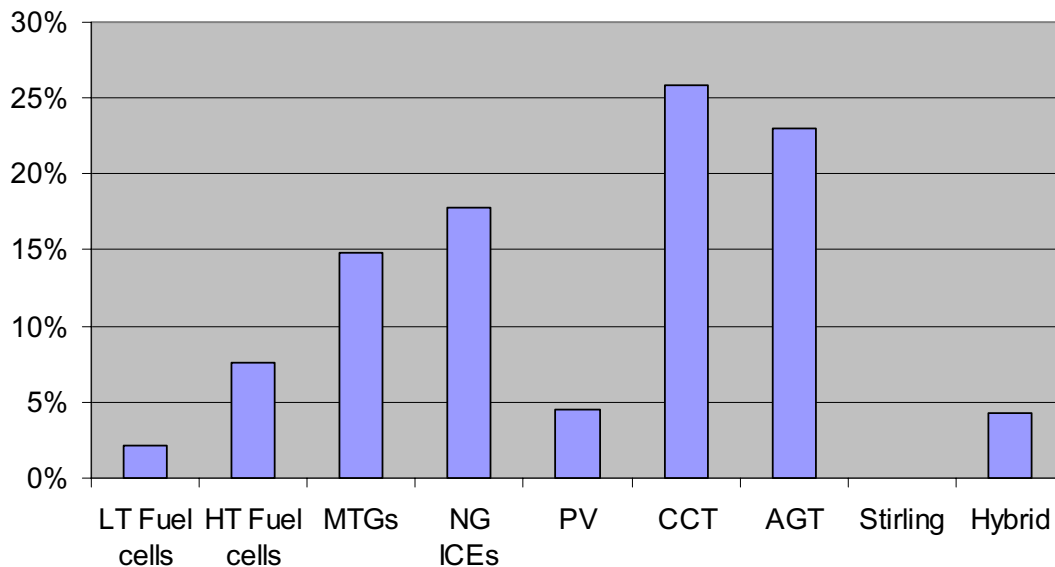
Figure 20: Total power distribution by DG type

6.1.4   Spanning DG Scenarios

In the spanning DG scenarios most of the complexity of a realistic, very detailed scenario is skipped to relatively quickly develop scenarios that can be insightful for scientific completeness, sensitivity analyses, and/or the determination of potential impacts for unexpected outcomes. In all, the screening process has led to the selection of 21 spanning cases that are included in the current study. The 21 spanning DG scenarios are listed below each with a simple one sentence description of the scenario purpose. For a more thorough description of these and all of the scenarios please see the report entitled "Final DG Scenario Report" produced under the same contract.

6.1.4.1   Scenario #S1: Population Weighted 2010 (PW2010)

Scenario #S1 contains a population weighted spatial distribution of emissions from an "aggregated mix" of DG technologies with an overall DG penetration of 20% of the increase in power demand between now and 2010.

6.1.4.2   Scenario #S2: ARB 2003 Emissions Standards (2003ES)

Scenario #S2 is identical to scenario #S1 except that all DG are assumed to emit pollutants at exactly the ARB 2003 Emissions Standard.

6.1.4.3   Scenario #S3: ARB 2007 Emissions Standards (2007ES)

Scenario #S3 is identical to scenario #S2 except that all DG are assumed to emit pollutants at exactly the ARB 2007 Emissions Standard.

6.1.4.4   Scenario #S4: Permitted levels for ICEs (PermICEPW20%)

Scenario #S4 contains a population weighted spatial distribution of emissions from DG technologies that are all assumed to emit pollutants at the current best available control technology (BACT) level approved by the SCAQMD in SoCAB.

6.1.4.5   Scenario #S5: High Early Adoption (HEAPW20%)

Scenario #S5 contains a population weighted spatial distribution of emissions from an "aggregated mix" of DG technologies with an overall DG penetration of 20% of the increase in power demand between now and 2010. The rate of DG adoption is such that 98% of DG are installed before 2007 and 2% are installed between 2007 and 2010.

6.1.4.6   Scenario #S6: Peaking Scenario (PeakPW)

Scenario #S6 assumes that all of the DG technologies ("aggregate mix" of various technologies) are operating as peaking units (operating only between noon and 6pm) with an installed capacity that equals 20% of the increase in power demand between now and 2010.

6.1.4.7   Scenario #S7: Large Gas Turbines w/o Ammonia Slip (LDG20%)

Scenario #S7 assumes that all DG are relatively large (50MW) gas turbines that have emissions consistent with a SCONOx approach to emissions reduction (i.e., no ammonia emissions).

6.1.4.8   Scenario #S8: Large Gas Turbines with Ammonia Slip (NH3_20%)

Scenario #S8 assumes that all DG are relatively large (50MW) gas turbines that have emissions consistent with a selective catalytic reduction (SCR) approach to emissions reduction (i.e., ammonia emissions are included).

6.1.4.9   Scenario #S9: Population Growth Weighted 2010 (PGW2010)

Scenario #S9 is similar to #S1, except that the spatial distribution of DG is determined by population growth between now and 2010, versus, population for 2010.

6.1.4.10   Scenario #S10: Land use Weighted 2010 (LU2010)

Scenario #S10 is similar to #S1, except that the spatial distribution of DG is determined by land use designations, versus, population for 2010.

6.1.4.11   Scenario #S11: Freeways (Free20%)

Scenario #S11 distributes all DG along the freeways in SoCAB.

6.1.4.12   Scenario #S12: All Fuel Cells (FCPW20%)

Scenario #S12 contains a population weighted spatial distribution of emissions from DG that are assumed to be all fuel cells (of various types).

6.1.4.13   Scenario #S13: All MTGs (MTGPW20%)

Scenario #S13 contains a population weighted spatial distribution of emissions from DG that are assumed to be all microturbine generators (of various types).

6.1.4.14 Scenario #S14: All CHP (DGCHP)

Scenario #S14 contains a population weighted spatial distribution of DG that are all assumed to use combined heating and power with appropriate emissions displacement for such technology being applied.

6.1.4.15 Scenario #S15: All Electricity emissions displaced (DGEED)

Scenario #S15 assumes that the operation of DG in SoCAB is one-for-one offset by a reduction in the electricity demanded from an in-basin power plant, reducing emissions from these power plants.

6.1.4.16 Scenario #S16: Technology distribution with 10% of the increased demand (TDPW10%)

Scenario #S16 contains a population weighted spatial distribution of emissions from a distribution of various DG technologies with an overall DG penetration of 10% of the increase in power demand between now and 2010.

6.1.4.17 Scenario #S17: Business as usual with linear trend (BAU)

Scenario #S17 assumes that the adoption rate of DG proceeds linearly throughout the SoCAB as it has been reported to occur in the years 2001 and 2002 by Southern California Edison and Los Angeles Department of Water and Power.

6.1.4.18 Scenario #S18: Business as usual with parabolic trend (BAU_par)

Scenario #S18 assumes that the adoption rate of DG proceeds exponentially throughout the SoCAB as it has been reported to occur in the years 2001 and 2002 by Southern California Edison and Los Angeles Department of Water and Power.

6.1.4.19 Scenario #S19: Extremely High Penetration (EHP)

Scenario #S19 assumes an extremely high DG penetration that accounts for meeting of 20% of the total power requirements in 2010.

6.1.4.20 Scenario #S20: High performance Degradation (HPD)

Scenario #S20 assumes a high rate of DG performance degradation just to the point of non-compliance for all DG technologies.

6.1.4.21 Scenario #S21: Peaking Total Power (PeakPW-2)

Scenario #S21 assumes that all of the DG technologies ("aggregate mix" of various technologies) are operating as peaking units (operating only between noon and 6pm) with a total power produced that equals 20% of the increase in power demand between now and 2010.

6.1.5 Summary of emissions from Spanning Scenarios

A brief description of DG scenarios is presented in Table 29, Table 30 and Table 31.

Table 29. Brief description of DG scenario parameters

DG Scenario	Parameters that describe each scenario
Realistic	
#R1	• 5% of increased power demand from 2002 to 2010 met by DG • Technology mix according to activity sector distribution • High penetration of low emission technologies • Spatial distribution according to GIS land use distribution • Realistic duty cycle per each sector • CHP emission displaced • Low performance degradation (3% increase of emissions per year) • Linear trend for DG power adoption (Medium early adoption of DG Power)
#R2	• 10% of increased power demand from 2002 to 2010 met by DG • Same assumptions as in #R1 for the rest of parameters
#R3	• 20% of increased power demand from 2002 to 2010 met by DG • Same assumptions as in #R1 for the rest of parameters
#R4	• Low early adoption of DG Power (98% of DG installed in 2007 or after) • Same assumptions as in #R1 for the rest of parameters
#R5	• No CHP emissions displaced • Same assumptions as in #R1 for the rest of parameters
Spanning **PW2010**	• 20% of increased power demand from 2002 to 2010 met by DG • Technology Mix – mix of permitted and certified DG: 28.9% large GT (>3 MW), 1.1% small GT (<3 MW), 30% ICE, 25% MTG, 8% PV, 4.9% HTFC, 2.1% LTFC • GT distributed in populated areas with high industrial activity, population weighted spatial distribution for rest of DG • Base-loaded duty cycle • No emission displacement • No performance degradation • Low early adoption of DG Power
2003ES	• Technology Mix - all DG are certified under ARB 2003 Emission Standards • Population weighted spatial distribution • Same assumptions as in PW2010 for the rest of parameters

Table 30. Brief description of DG scenario parameters (Continued)

DG Scenario	Parameters that describe each scenario
2007ES	• Technology Mix - all DG are certified under ARB 2007 Emission Standards • Same assumptions as in 2003ES for the rest of parameters
PermICEPW	• Technology Mix - all DG are ICE operating under BACT criteria • Same assumptions as in 2003ES for the rest of parameters
HEAPW20%	• High Early Adoption of DG Power: 95% of DG is installed before 2007 • Same assumptions as in PW2010 for the rest of parameters
PeakPW	• Peaking duty cycle (6 hours a day) • Peak power demand is equal to base load demand in PW2010 (20% of increased power demand from 2002 to 2010) • Total power delivered by DG during duty cycle • Technology Mix - mix of permitted and certified DG: 33.9 % large GT (>3 MW), 1.4% small GT (<3 MW), 35.3% ICE, 29.4% MTG • Same assumptions as in PW2010 for the rest of parameters
LDG20%	• Technology Mix – all DG are 49MW GT • No ammonia emissions from DG considered • GT distributed in populated areas with high industrial activity • Same assumptions as in PW2010 for the rest of parameters
NH3_20%	• Ammonia emissions from GT considered • Same assumptions as in LDG20% for the rest of parameters
PGW2010	• GT distributed in populated areas with high industrial activity, population growth weighted spatial distribution for rest of DG • Same assumptions as in PW2010 for the rest of parameters
LUW20%	• GT distributed in populated areas with high industrial activity, land use weighted spatial distribution for rest of DG • Same assumptions as in PW2010 for the rest of parameters
Free20%	• GT distributed in populated areas with high industrial activity, freeway weighted spatial distribution for rest of DG • Same assumptions as in PW2010 for the rest of parameters
FCPW20%	• Technology Mix – All DG are Fuel Cells • Population weighted spatial distribution • Same assumptions as in PW2010 for the rest of parameters
MTGPW20%	• Technology Mix – All DG are certified MTG • Population weighted spatial distribution • Same assumptions as in PW2010 for the rest of parameters

Table 31. Brief description of DG scenario parameters (Continued)

DG Scenario	Parameters that describe each scenario
DGCHP	• CHP emissions displaced • Same assumptions as in PW2010 for the rest of parameters
DGEED	• All Electricity Emissions Displaced from in-basin Electricity Generators • Same assumptions as in PW2010 for the rest of parameters
TDPW10%	• 10% of increased power demand from 2002 to 2010 met by DG • Technology Mix – 34% NG ICE, 46% MTG, 10% FC, 10% PV • Population weighted spatial distribution • Fuel Cells are base loaded, rest of DG operates in a 6-hour duty cycle (from 12 pm to 6 pm) • Same assumptions as in PW2010 for the rest of parameters
BAU	• Linear extrapolation from current data on 2001 and 2002 DG installations in the SoCAB to determine total DG power installed in 2010 • Technology Mix – Mix of permitted and Certified DG from current DG mix data • Medium early adoption of DG Power • Same assumptions as in PW2010 for the rest of parameters
EHP	• Extra high DG penetration: 20% of total power met by DG • Same assumptions as in PW2010 for the rest of parameters
BAU_par	• Parabolic extrapolation from current data to determine total DG power installed in 2010 • Same assumptions as in BAU for the rest of parameters
HPD	• High performance degradation: 10% increase of emissions per year • Same assumptions as in PW2010 for the rest of parameters
PeakPW-2	• Peaking duty cycle (6 hours a day) • Peak power demand is 4 times the base load demand in PW2010 so that Total cumulative electricity delivered by DG during duty cycle equals the DG electricity in the PW2010 • Technology Mix - mix of permitted and certified DG: 33.9 % large GT (>3 MW), 1.4% small GT (<3 MW), 35.3% ICE, 29.4% MTG • Same assumptions as in PW2010 for the rest of parameters

Figure 21 shows a comparison of criteria pollutant emissions rates resulting from the various DG spanning scenarios. As scenarios #S9 (PGW20%), #S10 (LUW20%), and #S11 (Free20) present exactly the same amount of total DG emissions as #S1 (PW2010) but with a different spatial distribution, they are not all presented in the bar chart of Figure 21. One of the realistic scenarios, #R3 is included for comparison purposes. Note that the emissions flux rates are presented on a log scale. Presented in this manner one should observe that the differences in overall, basin-wide DG emissions amongst the various DG implementation scenarios are not orders of magnitude different. Most of the DG scenarios contain DG emissions rates that are within an order of magnitude of the typical emissions fluxes. Exceptions to this are the EHP case with significantly higher CO_2 emissions and the DGEED case with significantly lower CO_2 emissions.

The same DG scenario emissions results that are presented in Figure 21 are presented in Figure 22. In Figure 22, however, the scale on which emissions fluxes are plotted is linear (vs. the logarithmic scale of Figure 21). Notice that there are significant differences amongst the DG scenarios that are more obvious when the data are plotted on a linear scale.
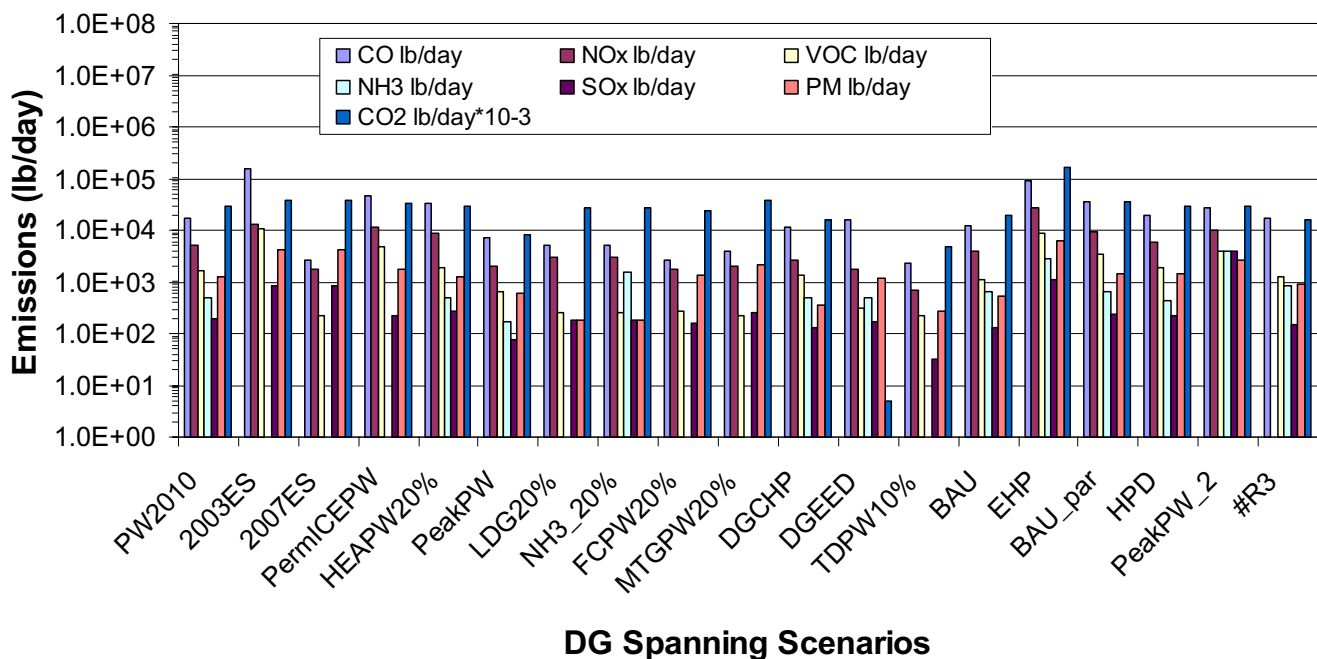
Figure 21: Comparison of criteria pollutant emissions among DG spanning scenarios (logarithmic scale).

DG Spanning Scenarios
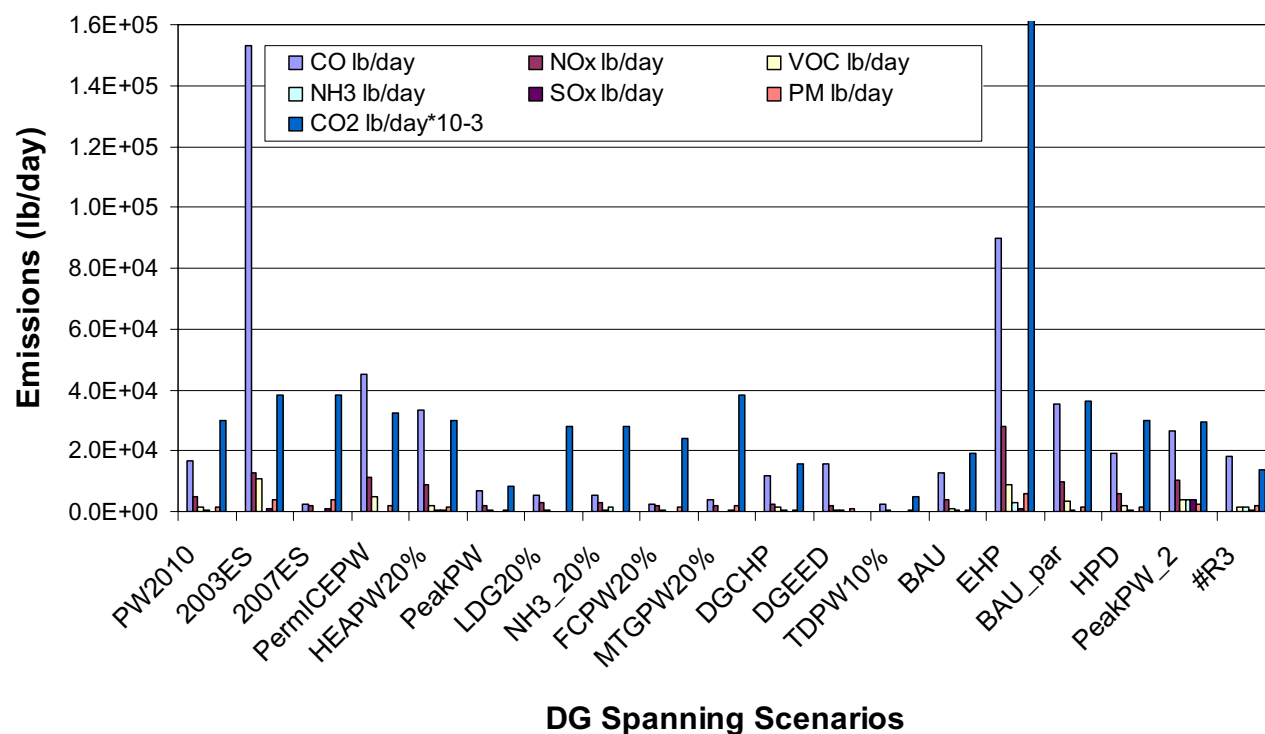
Figure 22. Comparison of criteria pollutant emissions among DG spanning scenarios (linear scale).

6.2 Simulation results: 2010 baseline scenario

This section presents simulation results using the baseline emission inventory for the year 2010 and the meteorological conditions of the August 27-29th, 1987 episode. Table 32 shows a summary of the basin-wide emissions used for the simulation. Also, Table 33 reports the maximum concentrations of some criteria pollutants.

Table 32. Summary of Basin-wide baseline emissions for 2010

Species	tons/day
Anthropogenic NMHC[*]	649
Biogenic NMHC	232
NO_X	407
CO	3,268
PM	580
SO_X	88
NH_3	168

[*]NMHC= Non-Methane Hydrocarbons

Table 33. Simulated concentration of some criteria pollutants: maximum hourly average concentration of O_3, NO_2 and CO and 24 hour-average concentration of $PM_{2.5}$ (2010 baseline scenario)

Species	Maximum	Location	Average	Time
O_3	238 ppb	San Bernardino	1 hr-average	13:00
NO_2	158 ppb	Ontario	1 hr-average	05:00
CO	3.0 ppm	Los Angeles	1 hr-average	08:00
$PM_{2.5}$	115 $\mu g/m^3$	Riverside	24 hr-average	N/A

Simulation results for the baseline case show that ozone, NO_2 and $PM_{2.5}$ concentrations peak at locations downwind from places, like Los Angeles, where maximum emission occur (Figure 23). On the other hand, CO concentrations peak in Central Los Angeles. This difference is due primarily to ozone, NO_2 and $PM_{2.5}$ being secondary pollutants, whereas CO is a primary pollutant and its concentrations depend mainly on direct emissions. Ozone and $PM_{2.5}$ concentrations exceed the established air quality standards (Table 34). The emissions inventory used in this simulation does not include prospective air pollution control measures to be implemented before the year 2010 but accounts for population growth and the corresponding increase in anthropogenic emissions. The introduction of new air pollution control strategies will lead to reductions in emissions of ozone precursors, and consequently, to reductions in ozone concentrations. The SoCAB must reach maximum ozone concentrations of 120 ppb or lower by November of 2010 to comply with ozone federal air quality standards.

(a)   (b)
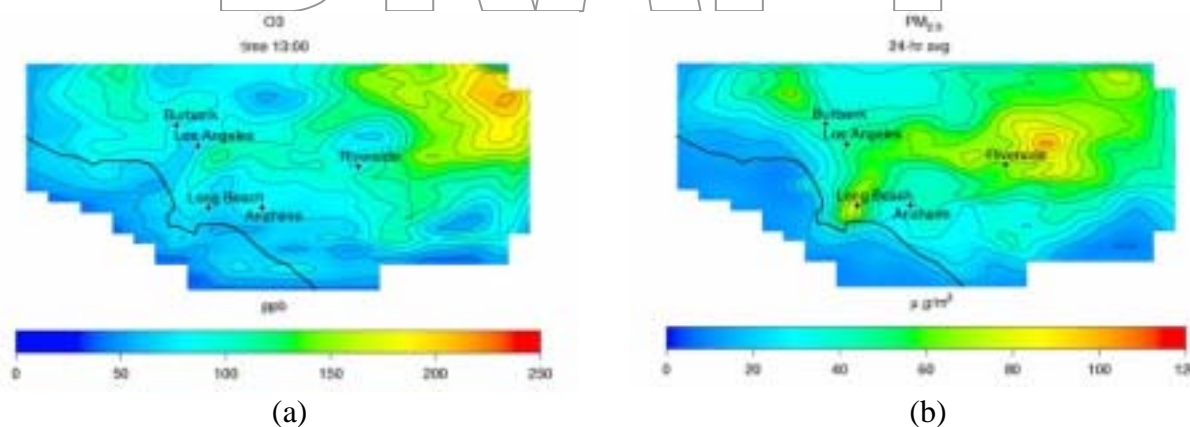
Figure 23. Concentration of criteria pollutants: a) Ozone concentration at hour 1300, b) 24-hour average concentration of $PM_{2.5}$

The South Coast Air Quality Management District's estimates of peak ozone concentration for 2010 are lower than the values reported in this work. – The AQMD predicts an ozone peak of 134 ppb, using the meteorological episode of August 27-29th, 1987, and baseline emissions inventory. Discrepancies among predictions arise from different chemical mechanisms used for the simulations. For instance, the AQMD uses the CB-IV chemical mechanism in their

simulations. However, Jimenez et al. (2003) showed that models that use CACM tend to exhibit significantly higher ozone formation than those that use CB-IV. Due to high solar radiation during the simulated episode, the tropospheric sinks of CO and NO_2 are enhanced. As a result, concentrations of CO and NO_2 are below air quality standard values.

Table 34. California and Federal Air Quality Standards for some criteria pollutants

Species	State standard	Federal standard	Averaging time
O_3	90 ppb	120 ppb	1 hr
NO_2	250 ppb	–	1 hr
CO	9 ppm / 20 ppm	9 ppm / 35 ppm	8 hr / 1 hr
$PM_{2.5}$	–	65 $\mu g/m^3$	24 hr

6.3 Air Quality Modeling: Evaluation

The California Institute of Technology (CIT) model has been used to analyze the air quality impacts produced by deployment of Distributed Generation (DG) in the South Coast Air Basin of California (Medrano et al. 2003, Carreras et al. 2004). Installation of DG introduces new emission sources throughout the basin. Changes in pollutant emissions affect the concentrations of both primary and secondary atmospheric contaminants. These effects need to be evaluated using a detailed air quality model that includes most of the chemical and physical processes that occur in the atmosphere, such as homogeneous and heterogeneous chemistry; advective and turbulent transport; spatial and temporal variability of emissions and meteorology. The performance of the California Institute of Technology (CIT) model has been partially analyzed in the past (Rodriguez et al. 2003, Griffin et al. 2002a) and features all the atmospheric processes mentioned above. The model is in continuous development at University of California, Irvine, in collaboration with researchers from the California Institute of Technology and other institutions.

Russell et al. presented a comprehensive review of the state of the art in air quality modeling (Russell et al. 2000). The review identified all the important pieces in an air quality model, and reported the relative importance of each element on air quality simulation results. The present work focuses on the CIT Airshed model, shows the sensitivity of baseline year 2010 simulations to input variables and to model components and identifies the parameters and elements that influence the most on air quality predictions. In addition, simulation results are compared with predictions shown in the 2003 Air Quality Management Plan using UAM and CALGRID air quality models. Furthermore, sensitivity of the CIT model to emissions changes due to weekday-weekend variation and to DG implementation is analyzed.

6.3.1 Elements for air quality modeling

Simulation of an air quality episode with an air quality model requires a series of inputs that are used to compute the numerical solution of the atmospheric diffusion/advection equation (Equation 20).

$$\frac{\partial Q_m^k}{\partial t} + \nabla \cdot \left(u Q_m^k \right) = \nabla \cdot \left(K \nabla Q_m^k \right) + \left(\frac{Q_m^k}{\partial t} \right)_{sources/sinks} + \left(\frac{Q_m^k}{\partial t} \right)_{aerosol} + \left(\frac{Q_m^k}{\partial t} \right)_{chemistry} \qquad \textbf{(20)}$$

Among the inputs needed for the simulation, there are meteorological conditions, and area and point emissions. Meteorological parameters include temperature, relative humidity, solar radiation, three-dimensional wind fields and inversion height. Chemical mechanisms and aerosol-phase formation mechanisms are required to account for gas-phase reactions and particulate matter formation in the atmosphere. Mechanisms of mixing and transport of pollutants are required to account for advective transport and diffusion of pollutants throughout the air shed considered.

6.3.1.1 Meteorological Conditions Input

A comprehensive campaign of atmospheric measurements was carried out in the California South Coast Air Basin (SoCAB), in August 27-29th 1987, in Southern California (Southern California Air Quality Study, SCAQS). The study collected a very extensive set of meteorological and air quality data that has been widely used to validate air quality models (Moya 2002 et al., Griffin et al. 2002a, Knipping et al. 2002, Meng et al. 1998). During SCAQS, vertical profiles of temperature, humidity and wind were obtained along with their temporal and spatial distribution. Posterior treatment of these measurements allowed obtaining a complete set of gridded meteorological data to be used in air quality simulations. Zeldin et al. conducted a study entitled "A Meteorological and Air Quality Assessment of the Representativeness of the 1987 SCAQS Intensive Days" (1990). Zeldin found August 28th, 1987 of 'reasonable central met-class tendency" which makes it suitable for modeling. In addition, August 27-28th 1987 episode was found statistically within the top 10% of severe ozone-forming meteorological conditions (SCAQMD 2003). Furthermore, this episode is also used by AQMD to show that air pollution control strategies proposed in the 2003 Air Quality Management Plan (AQMP 2003) will lead to ozone attainment by 2010. Hence, this episode will be used to evaluate the air quality impacts of DG during a reasonably severe smog episode.

The dominant winds in the SoCAB are from west to east during a typical day. The San Gabriel and San Bernardino Mountains form a natural barrier that enhances accumulation of air pollutants, especially over downwind locations, such as Riverside and San Bernardino. In addition, warm and sunny conditions and lack of natural scavenging processes, such as rain, favors the formation of photochemical smog and ozone.

The SCAQS episode in August 27-29th 1987 was characterized by weak onshore pressure gradient and warming temperature aloft. The wind flow was characterized by a sea breeze during the day and a weak land-mountain breeze at night. The presence of a well-defined diurnal inversion layer at the top of neutral and unstable layers near the surface, and a slightly stable nocturnal boundary layer facilitated the concentration of pollutants over the SoCAB and lead to an episode of high ozone concentration.

6.3.1.1.1 Temperature

This section presents the impact of temperature on ozone concentration. Previous studies have evaluated the effect of temperature on the concentration of atmospheric pollutants (Bärtsch-Ritter et al. 2003, Sillman et al. 1995). Ozone concentration is mainly affected due to strong temperature-dependence of PAN decomposition. High temperatures favor decomposition of PAN, and consequently NO_x concentrations increase, which tends to form more ozone. Sillman et al. suggest that increasing temperatures are correlated to higher biogenic VOC emissions and

higher UV radiation, which would contribute to enhance ozone formation. They also suggest that high temperatures could be correlated to higher anthropogenic emissions and stagnant circulation conditions. Bärtsch-Ritter et al. studied the effects of meteorological conditions on the air quality of Milan, Italy. Based on simulation results, the study shows that increasing temperatures leads to an increase of VOC-limited areas, mostly because of lower PAN formation. If VOC-limited areas increase, ozone concentrations are less sensitive to a change in NOx emissions. Therefore, temperature is potentially an important factor for the design of an air pollution control strategy.
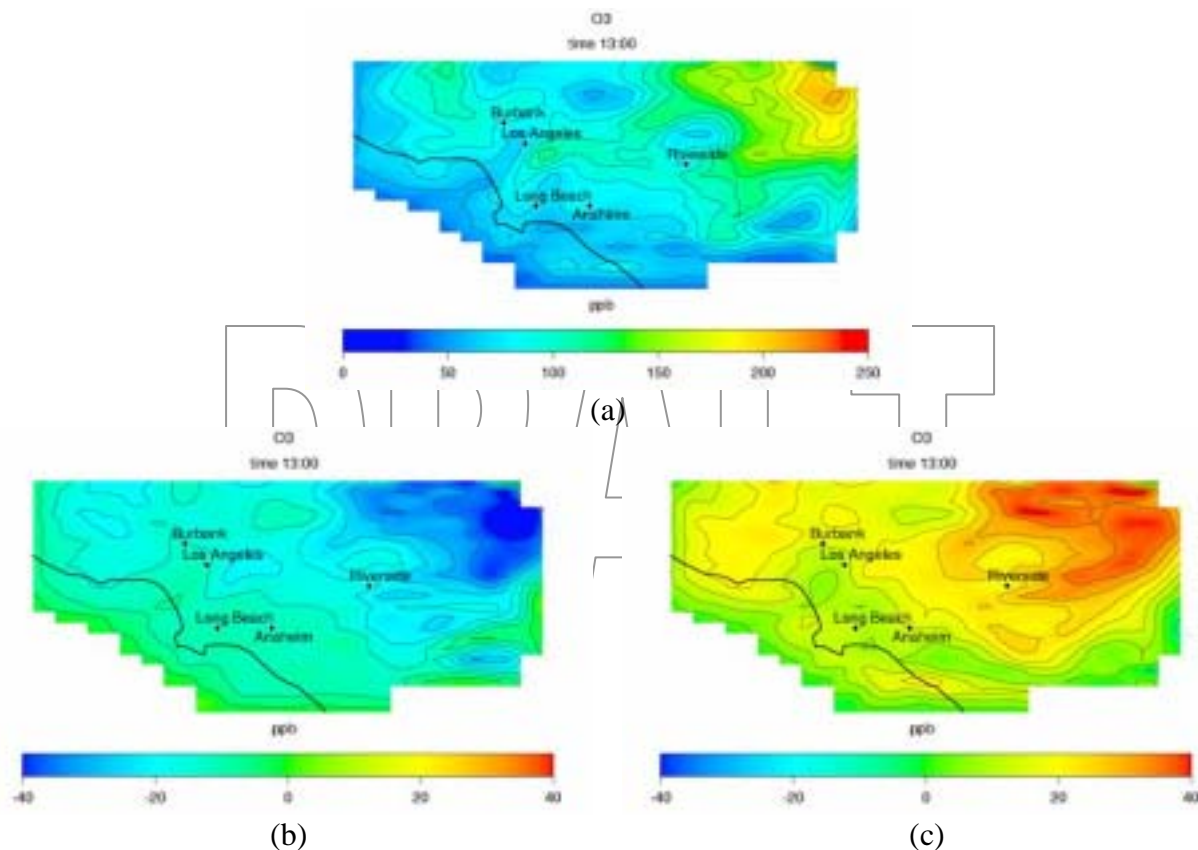
Figure 24. Effect of temperature in ozone concentration: (a) Ozone concentration in base case simulation, and difference in ozone concentration (in ppb) at hour 13 of the 3rd day of simulation between a study case and the base case for: (b) reduction of temperature by 5 K, (c) increase of temperature by 5 K

During August 27-29th, 1987, temperature ranged from moderate temperatures at night (around 15-20 ^{o}C) to high temperatures at downwind locations in the early afternoon (maximum temperature: 42 ^{o}C). Two scenarios are presented in this section to evaluate the effect of temperature on ozone concentration in the SoCAB: (a) temperature is decreased by 5 ^{o}C in each cell of the domain and at every hour and (b) temperature is raised by 5 ^{o}C in each cell and every hour. While scenario (a) could represent a warm episode during spring with temperatures ranging from 10 to 35 ^{o}C, scenario (b) presents temperatures extremely high in certain regions of the domain, reaching temperatures over 45 ^{o}C. However, these two cases are useful for clearly illustrating the effect of temperature on ozone concentration. Figure 24 presents the difference in

ozone concentration at hour 13:00 of the third day of simulation between scenarios (a) and (b), and the baseline case. A decrease of 5 $^{\circ}$C (scenario (a)) results in decreases over 40 ppb in ozone concentration, particularly in the northeast part of the domain.   In addition, peak ozone concentration decreases from 238 ppb to 188 ppb. An increase of 5 $^{\circ}$C (scenario (b)) results in increases over 40 ppb in ozone concentration, and the peak ozone reaches 277 ppb.

As suggested in previous studies, an increase in temperature could imply an increase in both biogenic and anthropogenic emissions, more stagnant conditions and more intense insolation. These parameters – not included in this section – could lead to even higher impacts.

6.3.1.1.2 *UV radiation*

Ozone formation is controlled by photolysis of NO_2 by UV radiation. As described in Harley et al. (1993), solar ultraviolet radiometers were operated at five locations in the SoCAB, for the August 27-29th 1987 episode.   Measurements of UV irradiance were used to obtain NO_2 photolysis rates. On the other hand, 'clear sky' photolysis rates can be obtained as a function of the solar actinic flux, which depends on the solar zenith angle, the elevation and the wavelength. For the baseline simulation, UV scaling factors are calculated as a ratio of actual photolysis rates to 'clear sky' values, for each monitoring station. These scaling factors are calculated for each hour, and then extrapolated for the rest of the domain. Typical UV scaling factors at midday for this episode are 1.0 at Central Los Angeles, 0.8 at Claremont, 0.65 at Rubidoux and 1.2 at Mount Wilson. Harley et al. (1993) evaluated the effect of UV scaling factors on ozone concentration by considering only 'clear sky' photolysis rates. In this scenario, in which scaling factors may be incremented by 50% with respect to the baseline in areas such as Rubidoux, ozone concentration increased by 10-30 ppb.

In this section, two scenarios in which the UV radiation is scaled by a constant factor are presented: (a) scaling factor of 0.8 is applied throughout the basin and during the three days of simulation, and (b) scaling factor of 1.2. Figure 25 shows the difference in ozone concentration at hour 13:00 of the third day of simulation between scenarios (a) and (b), and the baseline case. Reduction of UV radiation by 20% (scenario (a)) leads to reductions of over 20 ppb in ozone concentration at northeastern locations, and to a decrease in the absolute peak ozone of 20 ppb. Increase of UV radiation by a 20% (scenario (b)) leads to a maximum increase in ozone concentration of 20 ppb and to an increase in the peak ozone concentration of 17 ppb. Impacts from scenario (b) are comparable to the ones reported by Harley et al. (1993).
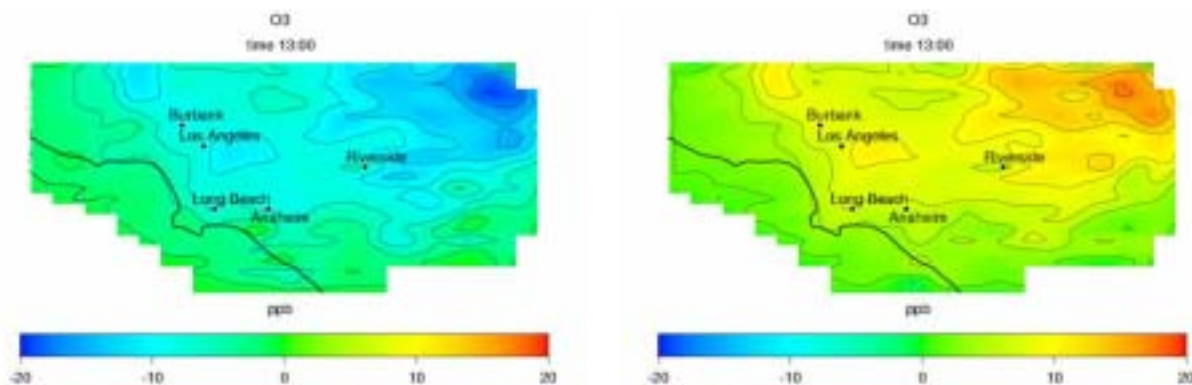
(a)   (b)

Figure 25. Effect of UV radiation on ozone concentration (in ppb). Difference in ozone concentration at hour 13 of the 3rd day of simulation between a study case and the base case for UV radiation scaling factor of (a) 0.8, (b) 1.2

Vuilleumier et al. (2001) studied the factors that contribute to UV optical depth in Los Angeles area. Results from the study suggested that light scattering and absorption contributed up to 90% in reducing actinic flux. A secondary factor was light absorption by ozone, which contributed up to 10% in the reduction of solar UV radiation. These results imply that changes in ozone and aerosol concentrations resulting from air pollution control strategies could have a feedback effect on UV scaling factor, and hence, on ozone formation.

6.3.1.1.3 Mixing height
The height of the mixing layer determines the vertical dispersion of pollutants. As described in Harley et al. (1993), during the SCAQS episode upper air soundings were performed in 8 sites that covered coastal and inland regions. Mixing heights were derived from potential temperature plots that were obtained from upper air sounding measurements. During the episode, a well-defined inversion layer was developed on the top of neutral/unstable layers close to the surface. Mixing heights ranged approximately from 50 m at night, to 1100 m in the afternoon.

Previous studies have evaluated the impact of mixing height on pollutant concentrations. Harley et al. simulated the 1987 SCAQS episode and doubled the mixing height. The result was small increments in the ozone concentration. Other works focused on the effect of mixing height on pollution control strategies. Sistla et al. (1996) compared results from control strategies in the area of New York City between scenarios with variable mixing height and with fixed mixing height. The study showed that reducing NOx emissions would be more effective than reducing VOC emissions in order to reduce ozone concentration if a uniform mixing height was used. The use of a variable mixing height showed the opposite trend. Li et al. (1998) studied the effect that mixing heights have on the efficiency of NOx emission control towards ozone reduction in the area of New York. The study showed that NOx emission controls were significantly more effective when the mixing height was reduced by 50% with respect to baseline values.

This section presents two scenarios: (a) mixing height is scaled by a factor of 0.8 and (b) mixing height is scaled by a factor of 1.2. Although these factors are applied evenly throughout the domain and during the three days of simulation, there are two limiting conditions that set minimum mixing height to 50 m and maximum height to 1100 m. Figure 26 presents the difference in ozone concentration at hour 13:00 of the third day of simulation between scenarios (a) and (b), and the baseline case. Reduction of the mixing height (scenario (a)) produces both positive and negative impacts on the ozone concentration, leading to differences of ±30 ppb. However, the peak ozone concentration only changes by –2 ppb. Increase of mixing height (scenario (b)) leads to increases in ozone concentration of the order of 10-35 ppb, over the north-central part of the domain. Reductions in ozone concentration produced by the increase in mixing height occur near the eastern boundary of the domain, and reach values of 30 ppb. In this scenario, the peak ozone concentration decreases by 5 ppb.

| (a) | (b) |
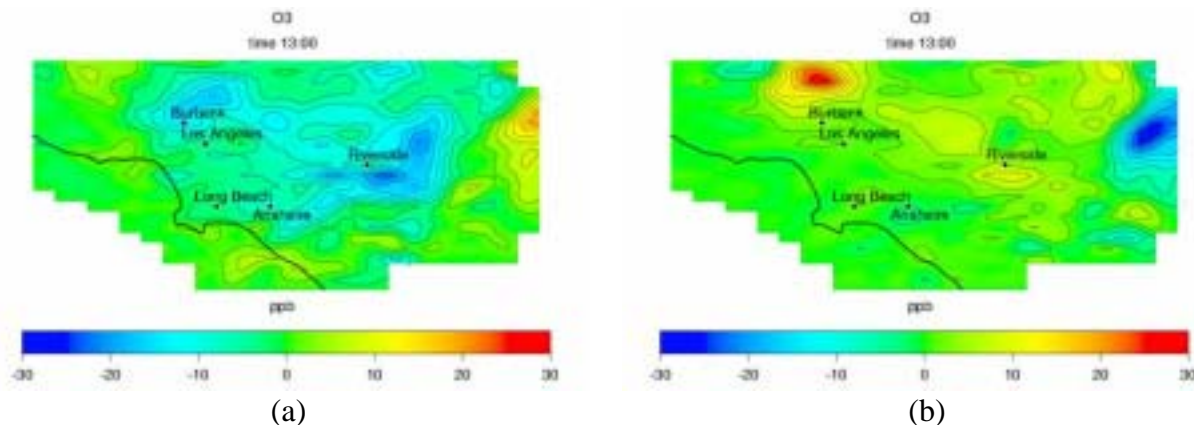
Figure 26. Effect of Mixing Height on ozone concentration.   Difference in ozone concentration (in ppb) at hour 13 of the 3rd day of simulation between a study case and the base case for: Mixing Height scaling factor of (a) 0.8, (b) 1.2

6.3.1.1.4 Wind fields

Previous studies have explored the effect of wind velocity on pollutant concentration (Harley et al. 1993, Dabdub et al. 1999, Bärtsch-Ritter et al. 2003). Results from these studies showed that an increase in wind velocity increases the effect of the upwind boundary conditions and tend to dilute pollutant concentration. On the other hand, decrease in wind velocity provides stagnant conditions that tend to accumulate air pollutants in the domain, increasing their concentration. This section presents how wind fields transport pollutants over the basin. In addition, two scenarios in which baseline wind velocity is modified by factor 0.5 and 2 are shown.

Baseline wind field was obtained by interpolation of measured data during the SCAQS episode in August 27-29th, 1987. As it is shown in the sequence of plots presented in Figure 27, pollutants are transported from west to northeast. Figure 27 shows the transport of two different shapes of 120-ppb ozone puffs over a background concentration of 20 ppb. Pollutant concentrations at the boundaries are zero, which tends to dilute the basin and ultimately removes any contaminant present in the basin. Both cases show that in this episode stagnant conditions prevailed until noon. After 1200 pm offshore winds started to blow in the northeast direction, transporting air pollutants towards the San Bernardino Mountains, which acted as a natural barrier and contained pollutants inside the basin. After 24 hours, the puffs have not fully disappeared, and pollutants remain in the basin during the early morning until winds start blowing faster again at around noon. This wind regime is characteristic of smog episodes that occur in the South Coast Air Basin, and that tend to accumulate ozone around the northeastern part of the basin.

hour 0100

hour 0100

hour 1200

hour 1200

hour 2400

hour 2400
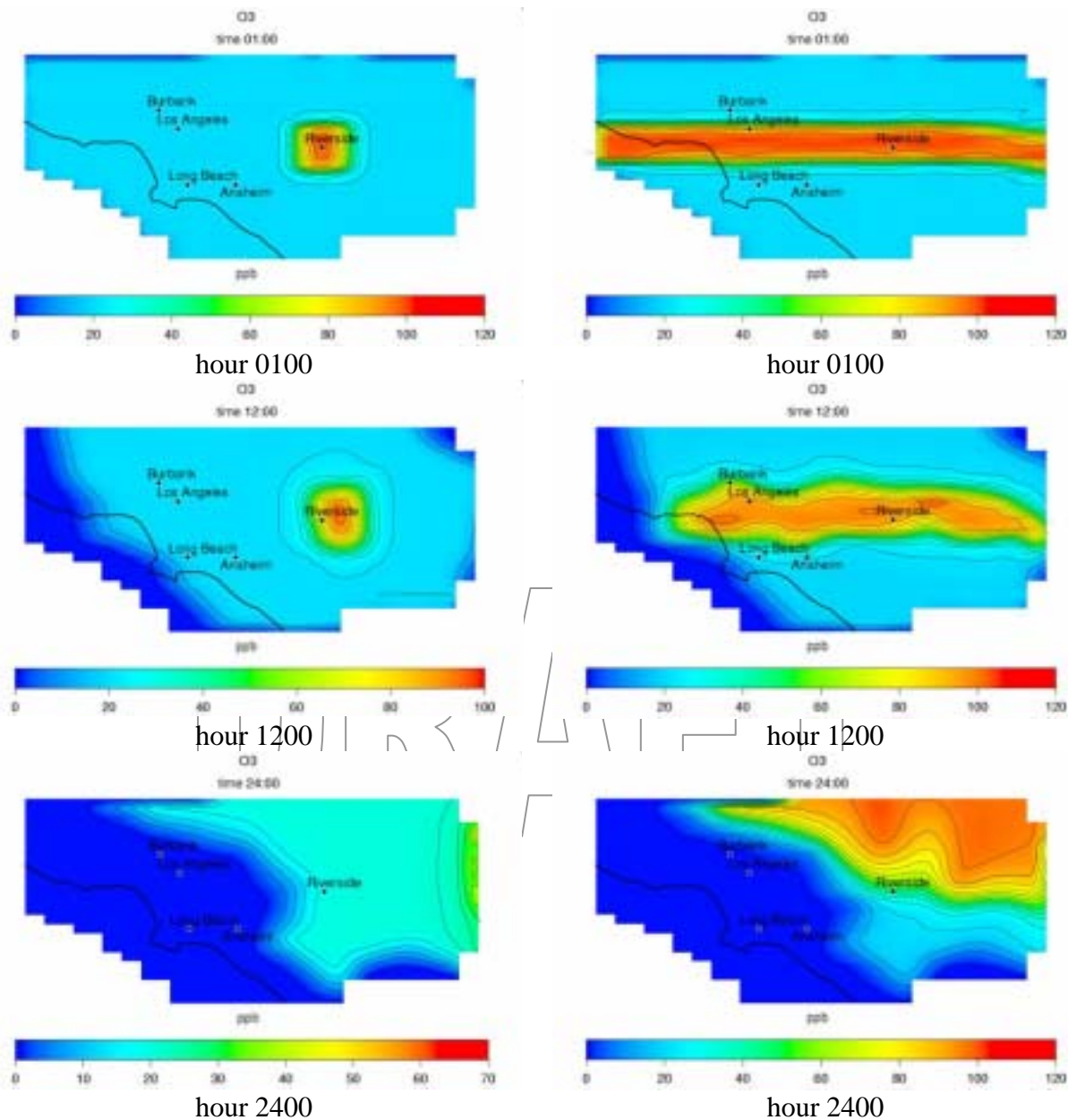
Figure 27. Transport of a 120-ppb ozone puff in a background of [O3]=20 ppb and zero ozone concentration at the boundaries: left – square puff; right – horizontal band puff

Harley et al. 1993 studied the effect of wind velocity using meteorological data and emissions for the August 27-29th, 1987 episode. They reported an increase of 50 ppb in ozone peak concentration by reducing wind velocity by a 50%. Figure 28 presents the results of two scenarios using the same meteorology used by Harley et al. and 2010 baseline emissions, and with: (a) wind velocity increased by a factor of two and (b) wind velocity scaled by a factor of 0.5. Peak ozone concentration in scenario (a) is 177 ppb, 61 ppb lower than in the base case. In addition, ozone concentration is reduced by up to 150 ppb in other areas. Scenario (b) predicts a peak ozone concentration of 311 ppb, 73 ppb higher than the baseline simulation. It is interesting to note that scenario (b), with slower winds, produces the ozone peak closer to the main source of emissions and later in time (at hour 18:00). On the other hand, higher wind

velocities, as in case (a), transport the ozone peak farther downwind. In addition, the peak ozone concentration is produced earlier.

(a) $[O_3]_{max}$= 177 ppb   (b) $[O_3]_{max}$= 311 ppb
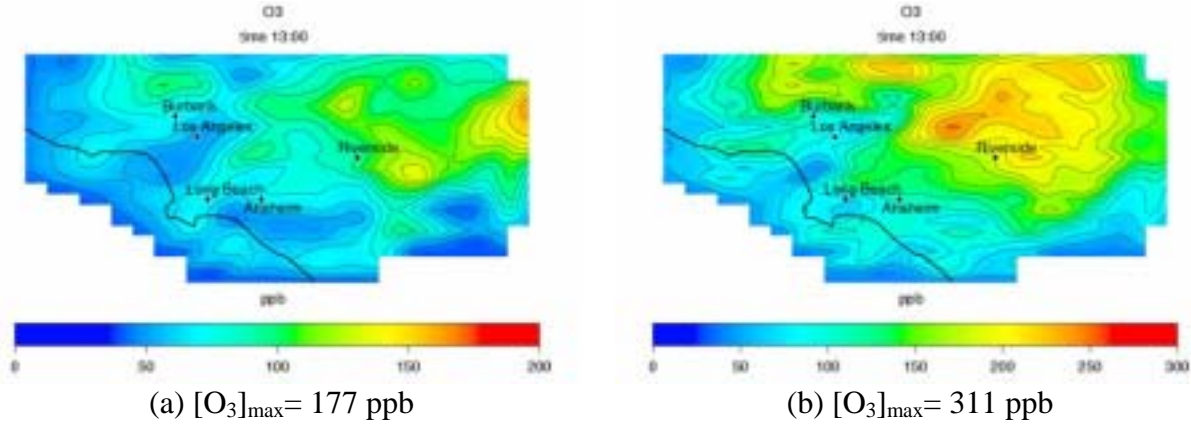
Figure 28. Ozone concentration (in ppb) using two different wind fields: (a) baseline wind velocity scaled by 2.0, (b) baseline wind velocity scaled by 0.5

6.3.1.2   Boundary Conditions

Typically, the region is defined by three general boundaries: (1) the ground surface, which is defined by specific topography $Z = h(X, Y)$, (2) the time-varying upper boundary $Z = H(X, Y, t)$, that is the base of the inversion layer, and (3) lateral boundary conditions at the horizontal extremes of the domain.

The boundary condition at the ground surface used in the simulations is:

$$K_{zz}\frac{\partial c_i}{\partial z} = \upsilon_{d,i}c_i \tag{21}$$

where K_{zz} is the eddy diffusivity in the vertical direction and $\upsilon_{d,i}$ is the deposition velocity of species i.

The boundary condition atop is:

$$K_{zz}\frac{\partial c_i}{\partial z} = 0 \tag{22}$$

The lateral boundary conditions are given by the following expressions:

$$\begin{aligned}[uc_i - K\nabla c_i]\cdot \vec{n} &= (uc_i^b)\cdot \vec{n}, & u\cdot \vec{n} \le 0 \\ -[\nabla c_i]\cdot \vec{n} &= 0, & u\cdot \vec{n} > 0 \end{aligned} \tag{23}$$

where c_i^b is the concentration of species i outside the modeling region, $\vec{n}$ is the unit outward normal to the time varying airshed domain. Note that for the latter boundary condition, specific values of pollutant concentration at the boundaries are required to solve Equation 20.

6.3.1.2.1 Lateral Boundary Conditions
The CIT Airshed model has been evaluated with the August 27-28, 1987 SCAQS episode. For 'backcasting' smog episodes, interpolated values from measurements are typically used as boundary conditions. For future year conditions, specific values of pollutant concentration have to be assumed. To minimize the impact of inadequate conditions for lateral boundaries on air quality predictions, boundaries should be located far away from the main area of study. However, the size of the domain is typically constrained by data availability and computational capacity.

Previous studies have tried to analyze the effect of boundary conditions on air quality simulation results. Winner et al. compared ozone isopleths produced by two different sets of boundary and initial conditions: the first case used interpolated values from data measured during the August 27-28th 1987 SCAQS episode for both boundary and initial conditions. The second case used 'clean air' values for both boundary and initial conditions. The study showed that using values based upon measurements it would be virtually impossible to reach peak ozone concentrations lower than the federal air quality standard (1-hour average concentration = 120 ppb). On the other hand, the study showed that if clean air values were used, the ozone federal air quality standard would be attained by reducing reactive organic gases (ROG) emissions by 50%. There are some indications based on previous studies that concentration of pollutants over the ocean to the west of the Los Angeles area (prevailingly upwind area) is affected by emissions from downwind onshore emissions (Benkovitz et al.). Hence, concentration at the boundaries will be affected by a significant reduction of emissions at downwind locations. Particularly, concentration at the boundaries would tend to reach 'clean air' conditions when continental anthropogenic emissions tend to zero.

Dabdub et al. showed the impact of boundary conditions on the air quality predictions in the San Joaquin Valley. Ozone formation in this area is not as strongly dominated by in-basin emissions as in the Los Angeles area, and hence boundary conditions affect more significantly air quality simulation results. Results showed that ozone concentration at locations near the inflow boundary (west boundary) was more sensitive to ozone boundary condition than to NO_X-VOC boundary condition. On the other hand, ozone concentration at downwind locations, far from the inflow boundary, was more sensitive to NO_X-VOC boundary condition.

The same approach used by Dabdub et al. and Winner et al. is pursued here in order to determine the sensitivity of ozone concentration in the Los Angeles area to boundary conditions. Six different scenarios are simulated: (1) baseline case, (2) zero all boundary conditions, (3) zero ozone boundary condition, (4) zero NO_X boundary condition, (5) zero VOC boundary condition and (6) 'clean air' boundary conditions as described in Winner et al. Table 35 presents the boundary conditions used in the simulation of case (1) and (6). Figure 29 shows the 1-hour average concentration of Ozone at hour 13:00 (time when ozone peaks in the baseline case) of the third day of simulation using the different sets of boundary conditions.

Table 35. Boundary conditions used for the simulation of the base case and the 'Clean air' case (in ppb)

		Baseline case					'Clean air' case				
		Vertical layer in model					Vertical layer in model				
Specie	Boundar	Surface	Lev 2	Lev 3	Lev 4	Lev 5	Surfac	Lev 2	Lev 3	Lev 4	Lev 5

s	y					e					
NO_2	N, S, W	1	1	1	1	1	1	1	1	1	1
NO_2	E	aq[a]	aq	1	1	1	1	1	1	1	1
NO	N, S, W	1	1	1	1	1	1	1	1	1	1
NO	E	aq	aq	1	1	1	1	1	1	1	1
O_3	N	aq	70	70	70	60	40	40	40	40	40
O_3	E	aq	aq	60	70	70	40	40	40	40	40
O_3	S, W	40	40	40	40	40	40	40	40	40	40
RHC	N	aq	100	100	100	100	10	10	10	10	10
RHC	E	aq	aq	100	100	100	10	10	10	10	10
RHC	S, W	100	100	100	100	100	10	10	10	10	10
HCHO	N, E	aq	aq	3	3	3	3	3	3	3	3
HCHO	S, W	3	3	3	3	3	3	3	3	3	3
ALD2	N, E	aq	aq	5	5	5	5	5	5	5	5
ALD2	S, W	5	5	5	5	5	5	5	5	5	5
MEK	N, E	aq	aq	4	4	4	4	4	4	4	4
MEK	S, W	4	4	4	4	4	4	4	4	4	4
CO	N, E	aq	200	200	200	200	120	120	120	120	120
CO	S, W	200	200	200	200	200	120	120	120	120	120

[a]aq refers to values based upon measurements obtained during Aug 27-29th 1987 SCAQS episode. These values are scaled down so that the maximum boundary value is 120 ppb of ozone.

(1) baseline, $[O_3]_{max}$= 238 ppb

(2) zero all boundary conditions, $[O_3]_{max}$= 244 ppb

(3) zero ozone boundary condition, $[O_3]_{max}$= 260 ppb

(4) zero NO_X boundary condition, $[O_3]_{max}$= 205 ppb

(5) zero VOC boundary condition, $[O_3]_{max}$= 238 ppb

(6) 'Clean air' boundary conditions, $[O_3]_{max}$= 269 ppb
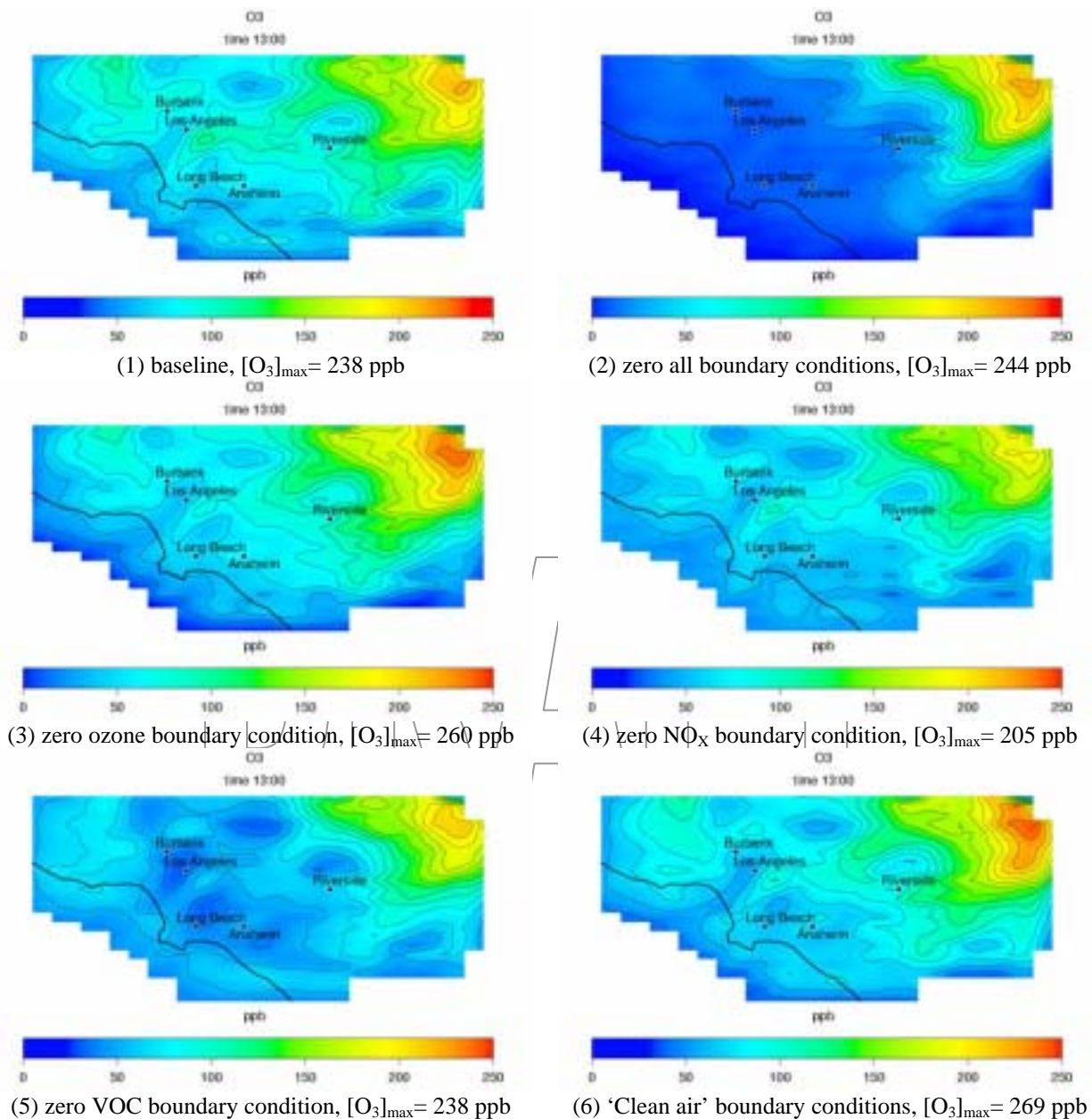
Figure 29. Ozone concentration (in ppb) in the South Coast Air Basin at time 13:00 of the third day of simulation (August 29th, 1987), using different sets of boundary conditions

Boundary conditions equal to zero are used purely diagnostically, since even in the cleanest air, concentrations of ozone, NO_X or VOC are not zero. Since the west boundary is predominantly an inflow boundary that transports air masses towards the eastern boundary, one would expect locations close to the western part of the domain to experience the largest impact in ozone concentration. Case (2) – zero all boundary conditions – shows a decreases of the order of 130 ppb in ozone concentration over the western and central part of the domain, due to dilution produced by an inflow boundary with zero pollutant concentration. However, peak ozone concentration increases by 6 ppb. Comparison of cases (3), (4) and (5) – zero O_3, NO_X and VOC

boundary conditions, respectively – shows that VOC boundary condition affects the most ozone concentration in the central part of the basin. These results confirm that formation of ozone near Los Angeles is VOC-limited. On the other hand, zeroing NO_X boundary condition leads to the largest decrease in 1-hour peak ozone concentration, of 33 ppb with respect to the baseline case. Zero ozone boundary conditions lead only to an increase of 22 ppb in the peak ozone concentration with respect to the base case, although in the central part of the domain, ozone concentration decreases by up to 80 ppb. As mentioned earlier, locations near the west boundary, which is predominantly an inflow boundary, are more affected by boundary conditions than downwind locations closer to the eastern boundary. Finally, case (6) – 'clean air' boundary conditions – presents an increase in the ozone peak of 30 ppb but overall ozone concentrations over the central area are comparable to the one achieved in the base case.

6.3.1.2.2 Height of the top boundary condition
Air quality models used by SCAQMD use vertical layers that extend up to 3000 m, whereas the CIT Airshed model considers a maximum height of 1100. Although the mixing height is typically below 1100 meters during the episode chosen for the simulations, ozone concentration predicted by the model is affected by the presence of extra layers atop the 1100 meters limit. The questions that may be answered then are: (1) how the increase in the top boundary height affects ozone concentration, and (2) how sensitivity of ozone to a change in emissions is affected by increasing the domain's height. A host of cases has been simulated to address these two questions: (a) the base case, in which the domain has 5 layers that add up to 1100 meters, (b) Case 2, in which one extra layer of 900 meters has been added to the base case domain and (c) Case 3, in which an extra layer of 1200 meters has been added to Case 2. Additionally, three other cases have been simulated using the three different domains mentioned above, and applying an emission reduction of 40% for NO_X and 25% for VOC.

Table 36 summarizes the effect of adding extra layers at the top of the computational domain of the CIT model. In the ground-level layer (layer 1), peak ozone concentration decreases by 17 ppb if a sixth layer is added and hourly ozone concentration in other areas is reduced by up to 27 ppb. Adding a 7th layer decreases peak ozone concentration 5 ppb more and maximum decreases of hourly ozone concentration are up to 3 ppb more. On the other hand, concentration of ozone decreases dramatically in the fifth layer if a sixth layer is added. The reason is that adding an extra layer facilitates dilution of the fifth layer due to air entrainment from the layer atop. Adding a seventh layer decreases ozone concentration only slightly further. This indicates that the height assumed by CIT model is not enough to disregard the effect of boundary conditions on top of the modeling domain. A low modeling height promotes pollutant accumulation and hence, model results tend to overestimate ozone concentration.

Table 36. Impact of adding extra layers on O3 concentration: 6 (case 2) and 7 layers (case 3) versus 5 layers (case 1); units in ppb:

	Layer 1				Layer 5			
	Peak O_3	Time	Max ΔO_3[a]	Time	Peak O_3	Time	Max ΔO_3	Time
Base case	238	13	-	-	312	16	-	-
Case 2	221	13	-27	17	222	16	-167	17
Case 3	216	13	-30	17	213	16	-170	17

[a]Change in O_3 is with respect to the base case

Table 37 compares different predictions of ozone concentration using 6 and 7 layers in the vertical direction. As already discussed above, ozone concentration predicted using 6 or 7 layers varies by less than 10 ppb. Thus, ozone concentration in layers one through five is not very sensitive to adding extra layers to the sixth one.

Table 37. Impact of adding extra layers on O3 concentration: 7 layers (case 3) versus 6 layers (case 2); units in ppb:

	Layer 1				Layer 5			
	Peak O_3	Time	Max ΔO_3[a]	Time	Peak O_3	Time	Max ΔO_3	Time
Case 2	221	13	-	-	222	16	-	-
Case 3	216	13	-7	16	213	16	-10	7

[a]Change in O_3 is with respect to the Case 2

Table 38 shows the impacts on ozone concentration of a certain emissions reduction using 5, 6 and 7 layers. Although, as seen before, absolute ozone concentration changes when extra layers are added atop the fifth layer, impacts of the same emission reduction are not very different in each case. Peak ozone concentration decreases by 25 ppb, 18 ppb and 17 ppb, if 5, 6 and 7 layers are used, respectively. In addition, maximum changes in hourly ozone concentration are 44 ppb, 42 ppb, and 41 ppb. Consequently, even though an extra layer added to the CIT model may affect moderately absolute ground-level ozone concentrations, it does not affect the impact on ozone concentration of changes in emissions. Specifically, impacts of DG on air quality will not change significantly if an extra sixth layer is added to the CIT model.

Table 38. Impact on ozone sensitivity to an emission change due to additional layers (units in ppb)

	Baseline emissions		Controlled emissions			
Case	Max O_3	Time	Max O_3	Time	Max ΔO_3	Min ΔO_3
Base case	238	13	213	13	44	-35
Case 2	221	13	203	13	42	-35
Case 3	216	13	199	13	41	-35

6.3.1.3   Initial Conditions

Previous works assumed that simulation of two-day episodes would be sufficient in order to minimize the effect of initial conditions on air quality modeling (Winner et al. 1995, AQMP 2003, Griffin et al. 2004). In addition, use of longer episodes is limited by data availability. This section presents the effect of initial conditions on air quality predictions. Two simulations are conducted: (1) 10-day episode with baseline initial conditions and (2) 10-day episode with zero initial conditions for all species. Since there is no data from an episode that long, meteorological conditions used from third day to tenth day are the ones corresponding to the second day. Since all parameters are equal for the third and subsequent days – meteorology, emissions, boundary conditions – one would expect that concentration of pollutants reached a stationary cycle after some days of simulation. In addition, one would expect that concentration of pollutants in the case of zero initial condition would tend to the levels reached in the base case when time advances.

Figure 30 presents the evolution of ozone concentration at six different locations, for the two cases studied: baseline case and zero initial conditions (IC) case. Figure 30 (a) and (b) show ozone concentration in Central Los Angeles and Long Beach. These two points represent upwind locations strongly dominated by direct emissions. As a result, concentration of ozone in the zero IC case recovers with respect to the baseline case by the second day of simulation. Figure 30 (c) and (d) show ozone concentration in Riverside and San Bernardino. These two cities are located at downwind locations, and although they have an important contribution of local emissions, the air quality in this region is dominated by transport of pollutants from the central area of Los Angeles. Since local emissions are not as important as in the previous upwind cities, ozone concentration in the zero IC case needs two days to recover with respect to the baseline case. This result is particularly important since maximum concentrations of ozone are usually found over these regions, and control strategies are mainly designed based on peak concentrations. Consequently, this work suggests that three days of simulation should be used, if possible, for air pollution control studies. Finally, Figure 30 (e) presents ozone in Hesperia, which is a location close to the North-eastern boundary, where the maximum ozone concentration is formed, and (f) presents ozone in Palm Springs, which is located far downwind from Los Angeles and from main anthropogenic emissions. For these two locations, recovering ozone concentration in the zero IC case with respect the baseline case takes three days. In conclusion, the farther a location is from the central area – where major emissions occur – the longer the effects of the initial conditions are. In addition, unlike what previous works assumed, this study suggests that control strategies should be based upon simulations of three days in order to minimize the impact of initial conditions over the areas where ozone concentration is typically the highest.
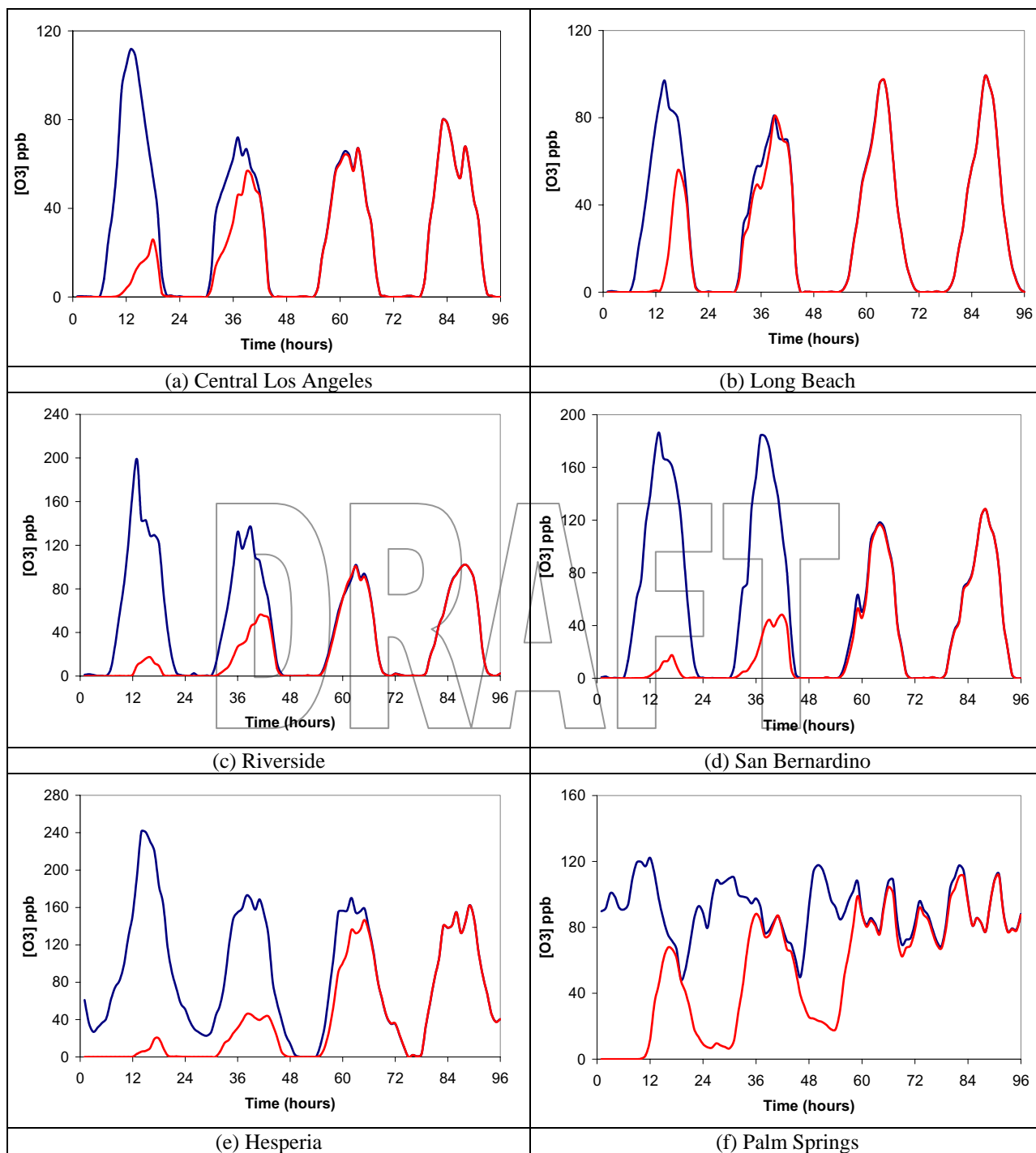
Figure 30. Evolution of ozone concentration (in ppb) at six different locations during 4 days of simulation: baseline case in blue, zero initial conditions case in red.

6.3.1.4   Advection Solver

The advection equation is one of the component operators in the solution of the atmospheric diffusion equation (Equation 20) by operator splitting schemes. Numerical solution of the advection equation by various solvers leads to numerical dispersions and oscillations. Previous studies have evaluated the effect of the advection solver on air quality modeling. Chock (1994) and Dabdub et al. (1994) reported that the Accurate Space Derivative scheme (ASD) is the best algorithm in terms of peak preservation properties, mass conservation and average absolute error. Dabdub et al. also reported that the finite-element Galerkin solver was the second-best advection scheme, and significantly less CPU-intensive than the ASD method. According to various studies (Dabdub et al. (1994), Chock et al. (1994)), the Smolarkiewicz method, which is used for ozone attainment demonstration with the UAM model (AQMP (2003b)), gives the least accurate results and consequently authors suggest using other methods for air quality modeling. Figure 31 show the numerical solution of the advection equation for a rotating wind field (as described in Dabdub et al. 1994) using the three different numerical schemes.

(a) Exact solution   (b) Galerkin

(c) Smolarkiewicz   (d) ASD

0   30   60   90
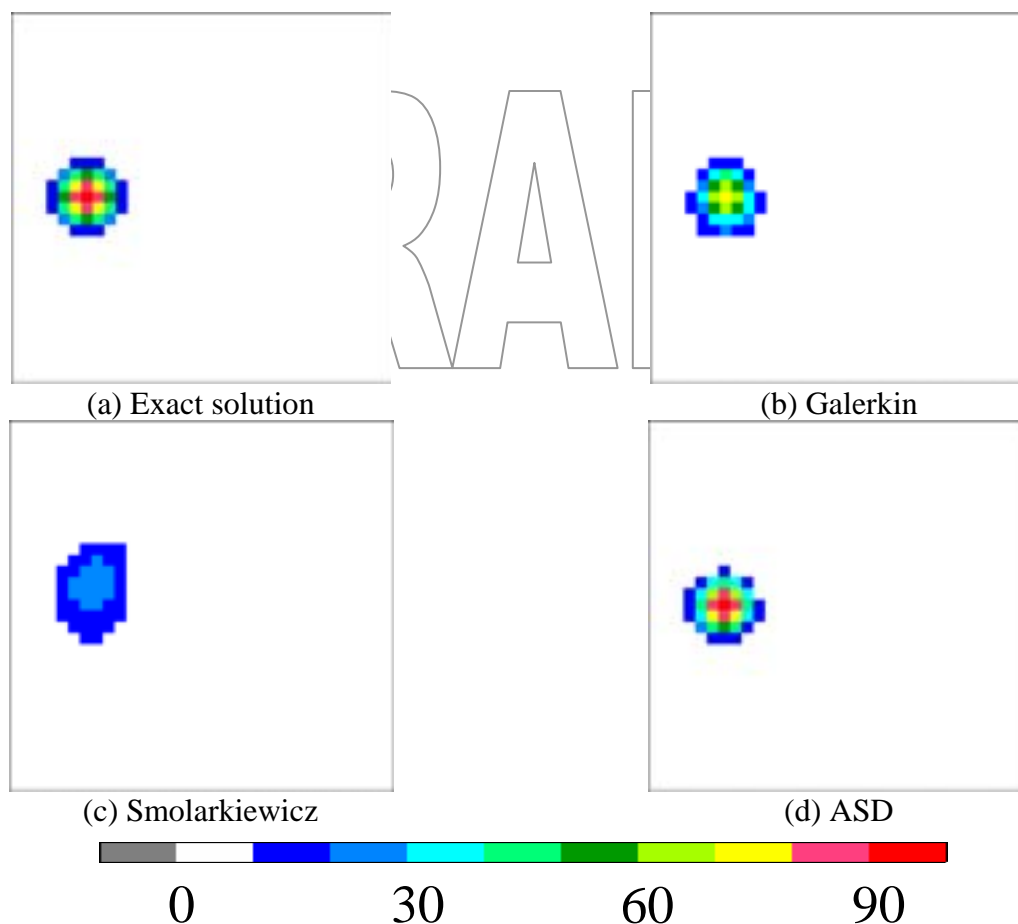
Figure 31. Solution of the advection equation for a rotating wind field using three different advection schemes. Plots show calculated concentration after one complete revolution

Nguyen et al. (2001) presented a new advection solver – Quintic Spline Taylor-series expansion, QSTSE – that is comparable with the Galerkin scheme in terms of CPU expenses, but it improves predicted peak ozone concentrations in a full model by 27.5%. QSTSE is significantly

faster than ASD although it produces similar peak retention, and maintains mass conservation and positive definiteness.

(a) baseline – using QSTSE   (b) Galerkin

Figure 32. Ozone concentration (in ppb) in the South Coast Air Basin at hour 13:00 of the 3rd day of simulation: (a) baseline case using QSTSE, (b) using Galerkin finite-element scheme

This section compares the simulation of the SCAQS episode using the QSTSE scheme (scenario (a)) and the Galerking scheme (scenario (b)). The Galerkin scheme is used with the CALGRID model for the SCAQMD's 2003 Air Quality Management Plan, to support ozone attainment demonstration by the UAM model. Figure 32 presents the ozone concentration at hour 13:00 of the third day of simulation for scenarios (a) and (b). Simulations with the Galerkin scheme produces lower ozone concentrations is over the central part of the domain and the ozone peak is transported towards the northeastern boundary. The maximum concentration of ozone in scenario (b) is 246 ppb, 8 ppb higher than in scenario (a). In addition, in scenario (b) ozone concentration over central areas is up to 90 ppb larger than in scenario (a). These differences are mainly due to the fact that Galerkin provides a smoother solution of the advection equation, compared to the QSTSE scheme, although QSTSE has a better peak retention than Galerkin. Having higher peak retention does not necessarily mean that predicted peak ozone concentration will be higher, since peak retention affects all species, including NO_X, that may enhance ozone destruction. As shown in Figure 33, Galerkin disperse NO_X concentration more than QSTSE, and since Los Angeles is typically under a VOC-limited regime, ozone concentrations predicted by Galerkin in this area are higher than the values predicted by QSTSE.

<center>(a)   (b)</center>
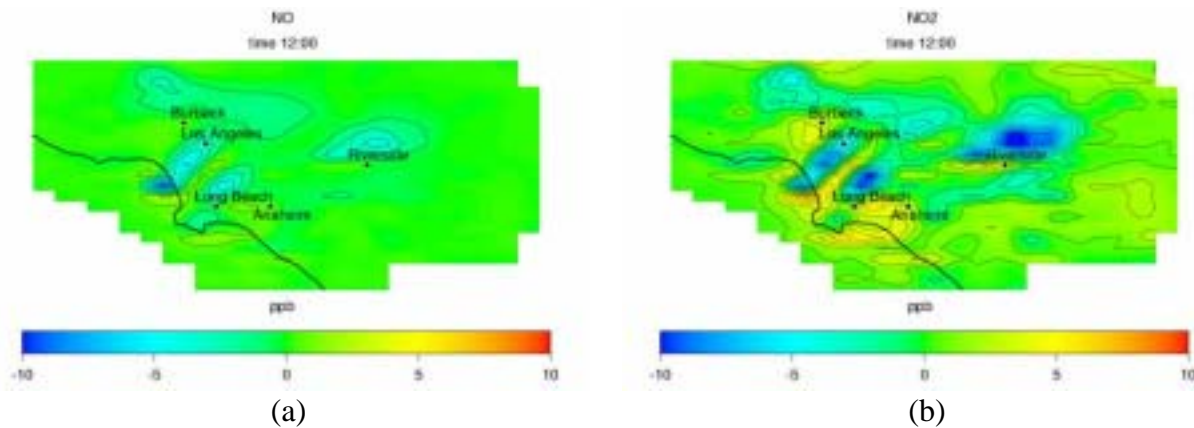
Figure 33. Difference in the predicted NO$_X$ concentration (in ppb) by the Galerkin and by QSTSE advection solvers (Galerkin – QSTSE) at hour 12:00 of the 3rd day of simulation: (a) difference in NO concentration, (b) difference in NO$_2$ concentration

6.3.1.4.1 Mass Conservation of Advection Solver

One important quality that determines the accuracy of an advection solver is the capacity to conserve mass. Previous studies (Chock (1994), Dabdub et al. (1994) and Nguyen et al. (2001)) have assessed mass conservation of the advection solvers mentioned above. According to Nguyen et al., QSTSE, ASD and Galerkin advection solvers achieve mass conservation in the simulation of a rotating cosine hill, after two revolutions. This test enables assessing mass conservation in a divergence-free field. Typically, urban air quality models assume that atmosphere has constant density. Consequently, these models require divergence-free wind fields so that mass conservation can be imposed from the continuity equation. However, obtaining wind fields with zero divergence from meteorological data is difficult. As a result, these wind fields include a residual divergence that has to be minimized. Nguyen et al. tested various advection schemes in a divergent field, and found that QSTSE conserve mass satisfactorily under such conditions. Galerkin and ASD advection solvers showed 6% and 36% mass loss, respectively, under the same conditions.

Application of any advection solver into an air quality model has to take into account the residual divergence that a wind field may have. From advection equation (Equation 24), the term $\nabla \vec{u}$ must be accounted for unless the wind field is completely divergence-free (Equation 25). Dismissing this term when the wind field is slightly divergent may impact dramatically mass conservation. Figure 34 shows the mass conservation with time of a puff being transported throughout the CIT Airshed domain, without leaving it. August 27th, 1987, is the meteorology used in this experiment. No losses or sources of any kind – such as chemical production or loss, deposition, emission – have been considered. Galerkin, QSTSE and QSTSE assuming $\nabla \vec{u} = 0$ are compared. As in the study by Nguyen et al., QSTSE proves to be the scheme with better mass conservation. The Galerkin scheme also performs well during the first hours, although at around hour 18 it starts adding extra mass in the system. This mass addition comes from the numerical filter, which has to compensate for negative concentrations generated by the numerical solution of the advection equation. Since QSTSE is positive definite, no extra mass is added since no filter is needed. The problem with divergent wind fields arises if the term $\nabla \vec{u}$ is assumed to be zero. As Figure 34 depicts, assuming divergence-free wind fields causes the total mass to decrease dramatically during the first hours, and later to increase suddenly, adding

artificially mass to the system. Consequently, divergence of a wind field has to be taken into account to maintain mass conservation.

$$-\frac{\partial c}{\partial t} = \nabla(uc) = u \cdot \nabla c + c \cdot \nabla u \qquad (24)$$

$$-\frac{\partial c}{\partial t} = \nabla(uc) = u \cdot \nabla c \qquad (25)$$
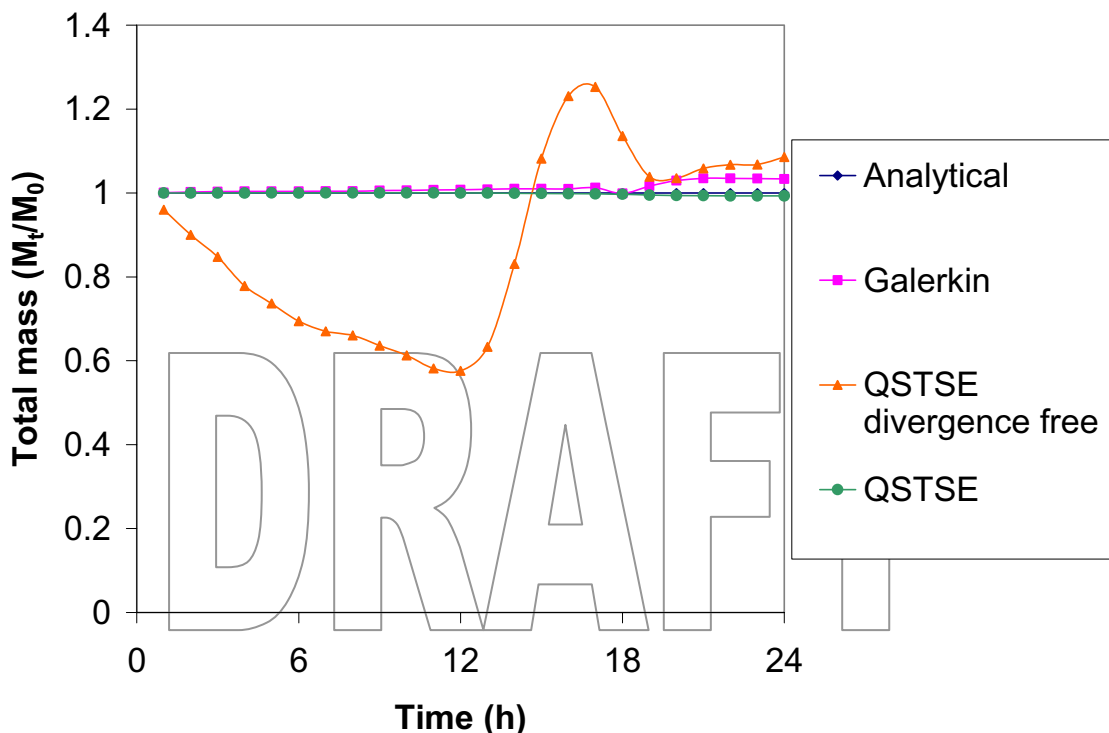
Figure 34. Mass conservation of different advection solvers applied to the CIT Airshed model. Values represent the mass conservation of a puff transported throughout the domain, with no chemistry, no deposition and no other loss. Meteorology of August 27th, 1987

6.3.1.5   Chemical Mechanism

The chemical mechanism is one of the major components of an air quality model. As discussed in Atkinson (2000), there is a large number of components in the atmosphere that can undergo innumerable reactions. A chemical mechanism is an approximate representation of all the chemical processes that take place, and is limited by the information available for each reaction, and the products that result from them. In addition, use of more complex chemical mechanisms may be limited by computational constraints. Russell et al. (2000) listed the Regional Acid Deposition Model (RADM), the Regional Atmospheric Chemistry Mechanism (RACM), the Carbon Bond IV (CB-IV) and the Statewide Air Pollution Research Center model (SAPRC-90), as the most commonly used chemical mechanisms in air quality modeling. The SAPRC model has been continuously updated to newer versions SAPRC-97 and SAPRC-99. Both SAPRC-99 and CB-IV are used in the SCAQMD's 2003 AQMP, for ozone attainment demonstration.

The chemical mechanism used in the present work for baseline simulations is the Caltech Atmospheric Chemical Mechanism (CACM, see Griffin et al. 2002a for an extensive description). The gas-phase mechanism is based on the RADM/RACM work of Stockwell et al. (1997), Jenkin et al. (1997), SAPRC-97 and SAPRC-99 (available from W.P.L. Carter at http://pah.cert.ucr.edu/~carter/) and includes O_3 chemistry as well as chemistry of secondary organic aerosol (SOA) precursors. The model consists of 361 chemical reactions and 191 gas-phase species – 120 fully integrated species, 67 pseudo-steady-state species and 4 species that have fixed concentration – and includes a comprehensively resolved treatment of VOC oxidation.

Jimenez et al. (2003) conducted a comparison between SAPRC-99, CB-IV and CACM, among other mechanisms (See Table 39 for main features of each mechanism). The comparison was based on box model simulations of remote atmosphere conditions. Neither emissions nor deposition were considered. As Jimenez et al. emphasized, it is impossible to know which mechanism is the 'correct' one. Measurements from smog chamber experiments could be used to complement their work but they also represent limited systems. On the contrary, Jimenez et al. based the comparison between mechanisms on the average value obtained using all the mechanisms. One limitation of this work is that comparisons are based on one set of initial conditions. Simulations in three-dimensional models usually start from a large set of initial conditions. Study of other initial conditions could reveal different results from the comparisons.

Jimenez et al. reported that CACM and LCC are the mechanisms that produce the highest ozone concentration. CACM produced a difference in ozone peak concentration of +41% with respect to the average, and LCC produced a difference of +18.2% (See Figure 35).

Table 39. Main features of three different photochemical mechanisms: CBM-IV, SAPRC-99 and CACM

	CBM-IV	SAPRC-99	CACM
# reactions	81	237	361
# species	33	72	191
# organics	11	39	129
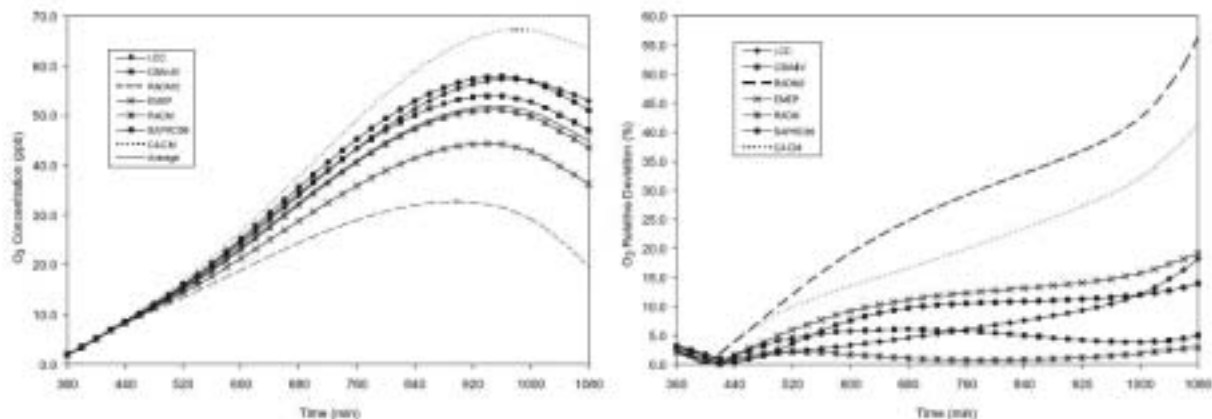
Figure 35. Comparison of ozone formation simulated by different photochemical mechanisms used in a box model (from Jimenez et al. 2003)

This section extends this comparison to the three-dimensional model and contrasts results from simulations of a 3-day episode using CACM and LCC mechanisms. Figure 36 presents the ozone concentration at hour 13:00 of the third day of simulation using (a) CACM mechanism and (b) LCC mechanism. As obtained by Jimenez et al., CACM mechanism produces a higher ozone peak than LCC. Maximum ozone concentration in case (a) is 238 ppb, whereas in case (b) is 150 ppb. In addition, distribution of ozone concentration in each case differs significantly, an effect that box model analyses cannot predict. CACM mechanism produces the peak ozone concentration over the northeastern region of the domain, at downwind locations, whereas LCC mechanism produces the peak ozone concentration over the east part of Riverside, much closer to main sources. The difference between cases may be mainly caused by faster ozone removal considered in the LCC mechanism. As reported in Jimenez et al., HNO_3 concentration produced by LCC is higher than CACM. In addition, formation of PAN is slower for CACM. As a result, PAN is transported farther downwind and therefore, peak ozone concentrations move towards the east.

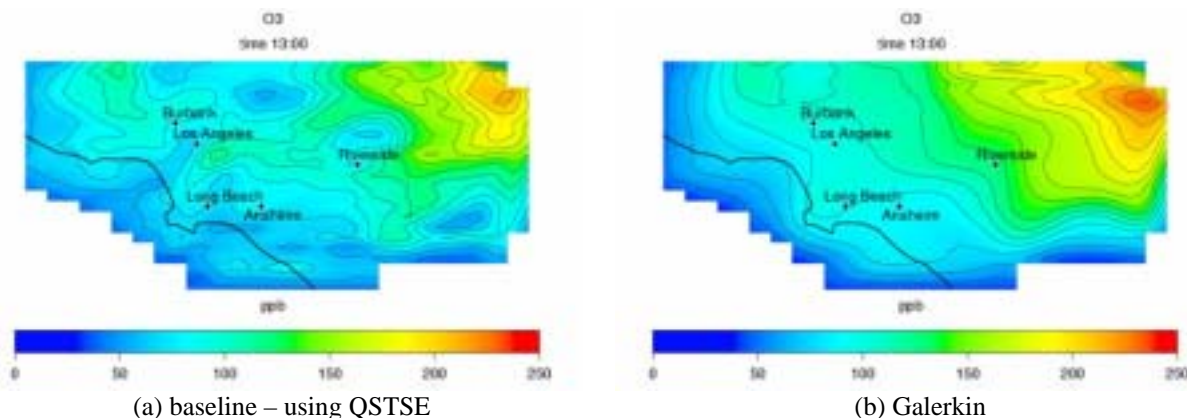(a) CACM chemical mechanism (baseline)   (b) LCC mechanism
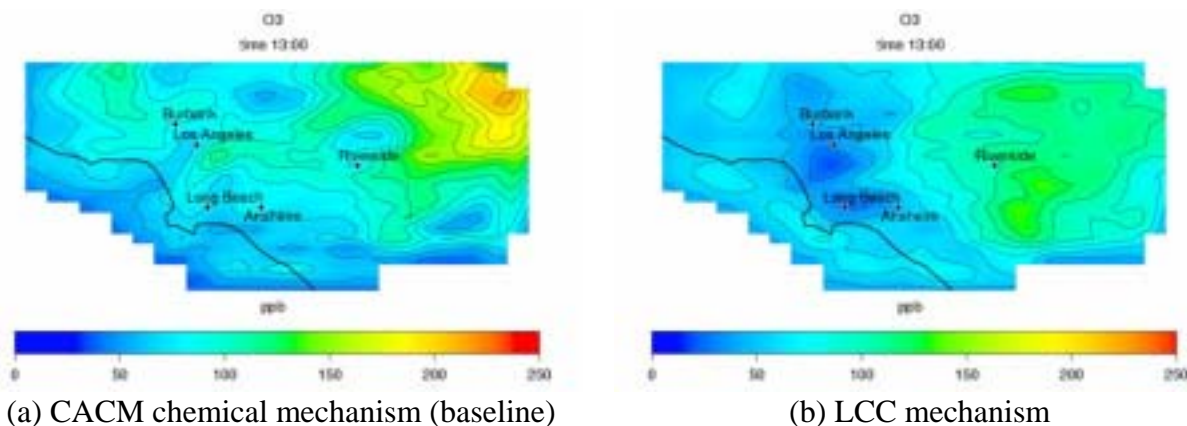
Figure 36. Ozone concentration (in ppb) in the South Coast Air Basin at hour 13:00 of the 3rd day of simulation: (a) baseline case and (b) using LCC mechanism

6.3.2   Comparison between CIT, CALGRID and UAM simulations

One of the major applications of an air quality modeling is to set bases for air pollution control strategies. The South Coast Air Quality Management District (SCAQMD) has been developing continuously plans to reduce emissions and hence comply with the National Ambient Air Quality Standards (NAAQS). To demonstrate that the measures proposed in the Air Quality Management Plan (AQMP) produce the desired pollutant reduction, SCAQMD uses two different air quality models: (1) UAM with CB-IV chemical mechanism and (2) CALGRID with SAPRC-99 chemical mechanism. This section compares results obtained with the models used by SCAQMD and the CIT Airshed model, used by the authors in previous works (Medrano et al. 2003, Carreras et al. 2004). Besides different chemical mechanism and other features listed in Table 40, the models encompass areas of different size. SCOS97 domain extends from 275 km to 595 km UTM Easting and from 3670 km to 3870 km UTM Northing. CIT domain has a smaller size and is not completely rectangular, but approximately extends from 300 km to 550 km UTM Easting and from 3700 km to 3810 km UTM Northing. Since CALGRID and UAM use a domain size different than the CIT model, different boundary conditions are needed. From conclusions in previous sections, different boundary conditions are a source of discrepancies between simulation results.

Resolution in the vertical direction is different in each model. UAM and CIT models consider five vertical layers with variable height, with finer resolution at ground level, and coarser resolution at the top layer. Although considering a larger number of vertical layers, CALGRID assumes a fixed vertical height. As a result, CALGRID provides coarser resolution than UAM and CIT at the ground level.

Two main aspects that are different in the three models are chemical mechanism and advection solver. Regarding the chemical mechanism, UAM uses CB-IV, CALGRID uses SAPRC-99 and CIT uses CACM mechanism. As mentioned above, CB-IV has the lowest ozone forming potential and CACM has the highest ozone forming potential. Regarding advection solver, UAM uses a Smolarkewicz scheme, which was found to be significantly less accurate than the Galerkin scheme and the QSTSE, used in CALGRID and in CIT, respectively.

Table 40. Comparison of CALGRID, UAM and CIT modeling systems

Parameter	CALGRID	UAM	CIT
Modeling system			
Domain size	SCOS97	SCOS97	CIT
Grid size	5-km	5-km	5-km
Vertical Layer Structure	Fixed 16 layers	Variable 5-Layers	Variable 5-Layers
Region Top	5000 meters	2000 meters	1100 meters
Boundary/top/initial conditions	Modified EPA Clean*	Modified EPA Clean*	Based on historical values
Modeling coordinate system	Lambert Conformal	UTM	UTM
Emissions			
Emissions inventory	2010 ARB/District	2010 ARB/District	2010 ARB/District
Chemistry			
Basic Module	SAPRC-99	CB-IV	CACM
Chemical Solver	Quasi Steady States analysis (QSSA) or Hybrid Solver	Quasi-steady state assumptions with Crank-Nicholson algorithm	Quasi Steady States analysis (QSSA) or Hybrid Solver
Photolysis rates	Radiation Extinction as height above sea level	One-dimensional based on Zenith angle	Radiation Extinction as height above sea level
Meteorology			
Meteorological data	1987 SCAQS	1987 SCAQS	1987 SCAQS
Wind model	MM5-4DDA	CALMET	
Advection	Chapeau function based scheme with Forester filter	Forward-upstream diffusive-corrected algorithm of Smolarkewicz	Quintic spline Taylor-series expansion
Vertical Diffusivity/ Diffusion	Horizontal diffusion-based on stability class with adjusted wind speed, (Smagorinsky method) Vertical diffusivity – Combination of various methods depending on stability and layer height	Vertical diffusivity coefficient is calculated internally	Horizontal diffusion-based on stability class with adjusted wind speed, (Smagorinsky method) Vertical diffusivity – Combination of various methods depending on stability and layer height
Dry Deposition	Surface Resistance model	Roughness length, stability, wind, speed, deposition factor	Surface Resistance model
Mixing Heights	CALMET	Holsworth	
Cloud cover	Yes	None	None
Mass continuity adjustment	NONR	O'Brien scheme	Included in QSTSE

Table 41 presents the maximum ozone concentration simulated by different air quality models. Among the models discussed above, CALGRID estimates the lowest peak ozone concentration, using meteorology of August 5-6, 1997. Although UAM uses a chemical mechanism that tends to produce less ozone and an advection solver that tends to diffuse more pollutant concentration than the scheme used in CALGRID, UAM estimates a higher peak ozone concentration than

CALGRID does, using the same meteorological episode. One reason for this difference could be attributable to different consideration of solar radiation and cloud cover. UAM does not consider cloud cover nor radiation extinction. As shown in section 6.3.1.1.2, stronger radiation tends to produce higher ozone concentration. Other factors such as difference in calculation of deposition or vertical transport not discussed in this work could also contribute to differences in the peak ozone predictions. CIT model estimates much higher peak ozone concentration than the other two models. Main causes of such difference are attributable to the chemical mechanism and the advection solver, as discussed in previous sections. An additional simulation using the CIT model with a similar chemical mechanism and advection solver used by CALGRID is summarized in Table 41. The peak ozone concentration obtained by this simulation is in concordance with the results obtained by CALGRID. Note that CIT is used with a different meteorological episode than the one used with CALGRID. As a result, peak ozone concentration estimated by CIT with LCC/Galerkin advection solver is a slightly lower than the one predicted by CALGRID.

Table 41. Comparison of peak ozone concentrations simulated using different air quality models

	(1) UAM[a]	(2) UAM[a]	(3) CALGRID[b]	(4) CIT	(5) CIT with LCC/Galerkin
Episode	August 5-6, 1997	August 27-28, 1987	August 5-6, 1997	August 27-28, 1987	August 27-28, 1987
Peak ozone	153 ppb	136 ppb	134 ppb	263 ppb	127 ppb

[a] from AQMP 2003
[b] from AQMP 2003, Appendix V

6.3.3 Weekend effect

The term 'weekend effect' refers to the consistent increase in ozone concentration during weekends with respect to weekdays. A variety of causes have been identified as possible reasons for its occurrence. Decrease in NO_X emissions in areas where NO_X concentrations are typically high is known to produce an increase in ozone concentration. In an area such as the SoCAB, where NO_X emissions are very high, lower NO_X emissions during weekends with respect to weekdays are thought to be a cause of higher ozone concentration during weekends. Qin et al. (2004a) reported weekly trends for ozone variation in the AQMD and showed that over the period from 1992 to 2001, the number of times that 1-hour and 8-hour O_3 air quality standards were exceeded during weekends was statistically larger than on weekends. Qin et al. (2004b) reported also weekly trends of ozone precursors concentrations, PM_{10} concentration and light scatter for the same period of time and region. In particular, they reported concentration values for NO_X, CO, NMHC and PM_{10}, and light scatter at morning rush hour (6:00 PST for NO_X and O3, and 5:00 PST for NMHC and CO) and at peak ozone time. Data consistently showed a decrease in ozone precursor concentrations and light scatter on weekends with respect to weekdays: 37%, 18%, 15%, 14% and 9% decrease in NO_X, CO, NMOC, PM_{10} and light scatter, respectively, at morning rush hour; 29%, 13%, 24%, 17% and 17% decrease in NO_X, CO, NMHC, PM_{10} and light scatter, respectively, at peak ozone time. On the other hand, peak ozone concentration and 8-hour average maximum concentration on weekends were on average 20%

and 22%, respectively, higher than during weekdays. Based on these observations Qin et al. concluded that lower NO_X emissions and light scattering on weekends with respect to weekdays are the main contributors to the 'weekend effect'.

As discussed in section 6.3.1.1.2, based upon model simulations, increase in UV radiation by 20% leads to maximum increases of 20 ppb in ozone concentration. This correlation corroborates one of the conclusions by Qin et al. that identifies less light scattering over the weekends as a cause for the 'weekend effect'. However, other factors must be considered since impacts from changing UV radiation cannot fully explain observations reported by Qin et al.: increasing UV radiation alone (which is a way of decreasing light scatter) increases ozone concentration in downwind locations more significantly than in central areas, whereas reported data show the opposite trend.

Modeling of the 'weekend effect' requires the use of an emissions inventory for weekends that takes into account emissions reductions due to the decrease of industrial activity and daily commute. However, such inventories are scarce. As an alternative, this section presents a scenario in which emission reductions are applied to a baseline weekday inventory. Reductions are applied following the weekday-weekend trends of ambient concentrations of ozone precursor reported by Qin et al (See Table 42). Although changes in pollutant ambient concentrations do not necessarily correlate to changes in pollutant direct emissions, this scenario is a first approximation to the conditions that define a weekend episode.

Table 42. Reductions applied to the baseline weekday emissions inventory and baseline light scatter to simulate a weekend episode

Pollutant	Reduction (%)
NO	45
NO_2	22
VOC	20
CO	15
PM	15
Light Scatter	15

Qin et al. show that differences in ozone concentration between weekdays and weekends, in percentage, are bigger at 6 am than at the ozone peak hour. Simulation results also show that in the early morning ozone concentration changes from weekdays to weekends by a greater percentage, since concentration at 6 am are already very low (see Figure 37). However, in absolute values, changes in ozone concentration in the early morning are comparable to the ones occurring at peak ozone time. In addition, measurements reported by Qin et al. show that at far downwind locations, such as Palm Springs, and at upstream locations, such Santa Clarita, there is no significant increases in ozone concentration due to the 'weekend effect'. As it appears in Figure 37, simulation results also show no significant increases in ozone concentration at far downwind locations and upstream locations on the west part of the domain.
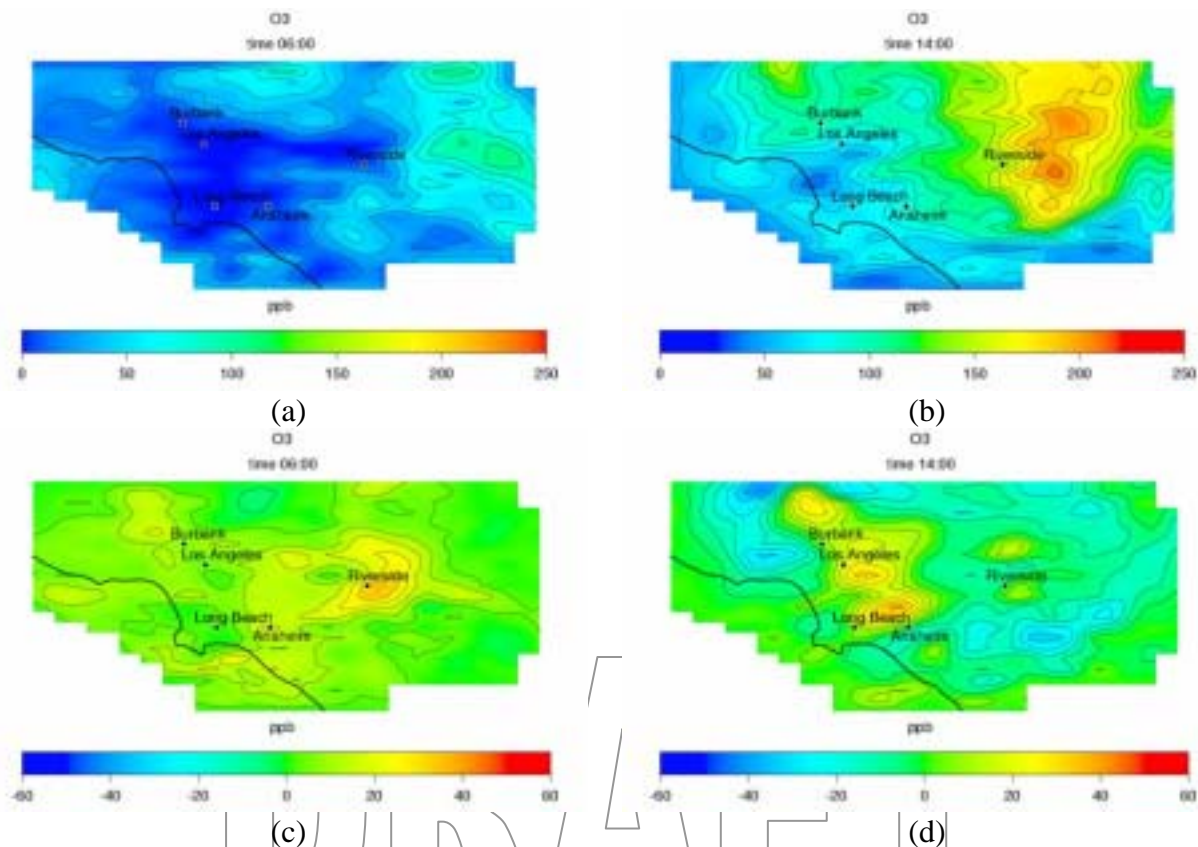
Figure 37. Weekend effect. Baseline weekday ozone concentration (in ppb) during the 2nd day of simulation (a) at 6 am, (b) at 2 pm; Difference in ozone concentration (in ppb) during 2nd day of simulation (weekend – weekday): (c) at 6 am, (d) at 2 pm

Increases in ozone concentration obtained from simulations due to the weekend effect range up to 60 ppb at peak ozone time. On the other hand, values reported by Qin et al. indicate more moderate increases due to the weekend effect, around 20 ppb, because these values are averages obtained for a period of 7 summers of data collection (June-October, 1995-2001). Nonetheless, simulation results show good agreement with measured data and suggest that the air quality model can predict satisfactorily air quality impacts resulting from emission changes. Consequently, CIT can also be used with confidence to determine air quality impacts of emissions increase due to DG.

6.3.4   Model improvements to capture DG impacts

A preliminary study of the air quality impacts of DG in the SoCAB was presented by Medrano et al. (2003). Simulations of air quality impacts were performed with the CIT model using LCC mechanism and a Galerkin scheme for the numerical solution of advection. In addition, a two-day episode was used to evaluate those impacts. In a posterior study, modifications are introduced to the CIT model based on the analyses presented above.

6.3.4.1   Improvements in initial conditions handling

Major air quality impacts potentially occur at downwind locations, on the eastern portion of the South Coast Air Basin. As shown in section 6.3.1.3, the effect of initial conditions on pollutant concentration at these locations is still important after two days of simulation. Consequently, a three-day episode is chosen to study air quality impacts of DG as opposed to using a two-day episode. In addition, previous simulations assumed same initial concentration at upper levels other than ground level for each day of simulation. In present simulations, initial concentrations for the second and third day of simulations are the concentrations at the last hour of the previous day, for all five vertical levels of the computational domain.

6.3.4.2   Improvements in the chemical mechanism

Preliminary results in Medrano et al. (2003) showed that DG deployment in the SoCAB would impact not only ozone concentration but also secondary aerosols. These preliminary results were obtained using the LCC mechanism. The CACM mechanism includes comprehensive treatment of oxidation paths that lead to ozone formation, based on RADM, SAPRC-97 and SAPRC-99 chemical mechanisms, which are more recent models than LCC. Hence, these three mechanisms and CACM use updated and more complete chemistry and chemical kinetics than LCC does. In addition, CACM includes chemistry of VOC oxidation that leads to formation of secondary organic aerosol precursors. Consequently, CACM chemical mechanism is chosen to determine air quality impacts of DG in the SoCAB, so that the impacts on ozone and aerosol formation are better captured.

6.3.4.3   Improvements in the advection solver

Previous versions of the CIT model used a Galerkin-type of numerical scheme for the solution of the advection equation. As reported in section 6.3.1.4, previous studies showed that the Accurate Space Derivative scheme (ASD) and the Quintic Spline Taylor-series expansion scheme (QSTSE) obtain better accuracy than the Galerkin method in the solution of sample advection problems. The ASD is the most accurate, although it is significantly more expensive than the QSTSE in terms of computational demand. Thus, the QSTSE scheme is used in the CIT model simulations of air quality impacts due to DG deployment.

6.3.5   Current understanding of model sensitivity to DG

Monte Carlo analyses help identify the uncertainty of the air quality model predictions to the variation of given input parameters. However, there are differences between Monte Carlo and spatial sensitivity analyses. For instance, the Monte Carlo methodology considers changes in the intensity of emissions through multiplicative factors, but their spatial distribution is not modified. This procedure, although important, does not explore the spatial sensitivities of emissions and their relevance to predictions. Moreover, the influence of DG installation in the SoCAB needs to be addressed more directly. In particular, the type of variations produced in simulation results when DG is placed in specific parts of the basin. To investigate spatial sensitivities, the current section presents a methodology in which only changes to DG emissions added to the baseline are systematically considered.

The development of a set of scenarios to investigate spatial sensitivities is based partly in the general methodology devised by Carreras et al. (2004). The total mass emissions selected for this sensitivity study correspond to the Extra High Penetration (EHP) scenario, for which Carreras et al. found one of the largest impacts on ozone concentrations due to DG implementation. The daily increases in emissions of NO_X, CO, VOC, NH_3, SO_X and PM in this scenario are 2.0%, 1.3%, 0.7%, 0.7%, 0.4% and 0.8%, respectively. Instead of using an arbitrary spatial distribution of emissions, five scenarios are developed to separate the adoption of DG by counties in the SoCAB using Geographic Information Systems (GIS) land-use data. For all scenarios, base-loaded emissions from the EHP scenario are added to the baseline for each county. Specifically, 50 cells of the computational domain are selected by using the non-vacant areas provided by the GIS land-use data. This ensures that the emissions variations are done equally in all scenarios and that the simulated effects are not due to more or less DG adoption in each county. Figure 38 shows the areas in each county where additional DG emissions are placed.
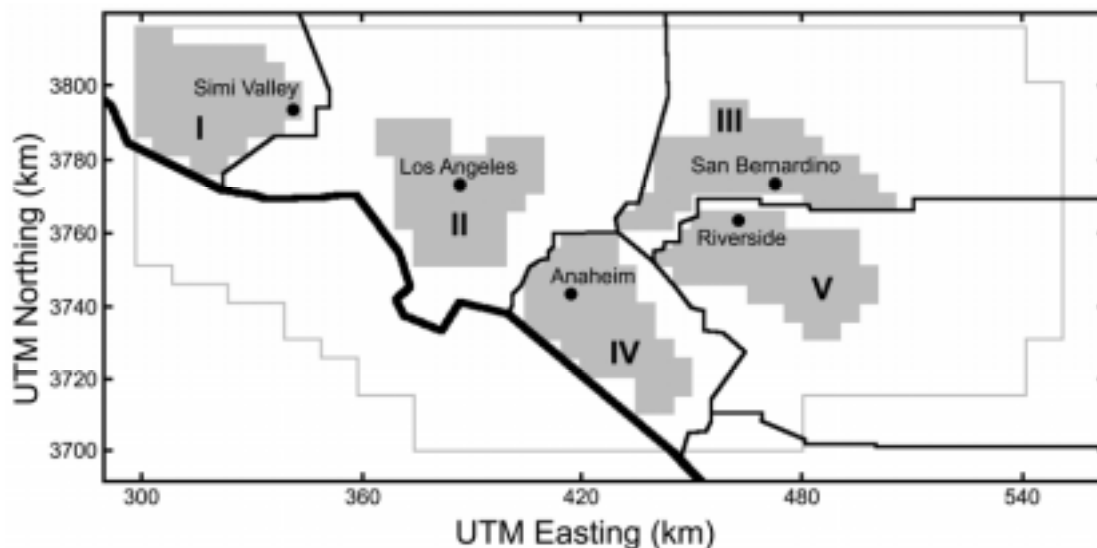
Figure 38. Regions where DG emissions for spatial sensitivity scenarios are placed in each county of the South Coast Air Basin of California.

Figure 39 presents the 1-hr average ozone concentrations difference between each scenario and the 2010 base-case at hour 13:00. This hour is selected to compare the impacts of the scenarios because it is when domain-wide ozone concentrations peak. Nonetheless, the largest differences may occur at different times. In general ozone impacts range from -36 to 39 ppb, which are significant differences, compared to the EHP scenario impacts ($\pm$ 8 ppb). Furthermore, this exhibits the importance of DG spatial accumulation since both the EHP and county scenarios input the same amount of emissions mass to the basin. Areas where emissions are typically low, such as Ventura present the largest impacts. Ozone increases with respect to the base-case can be as large as 39 ppb. In this region, increases in NOx emissions reduce ozone formation locally during the nighttime. However, as the sun rises at around 8:00 the differences start to become

positive indicating an increase in ozone concentrations. At night NO from DG emissions scavenges ozone. During the day the VOC to NOx ratios are such that Ventura is in a NOx-limited region where NO increases lead to higher ozone concentrations. Additionally, the meteorology of this episode shows that the ozone impacts elsewhere in the basin are not significant when DG is placed in Ventura. In Central LA the introduction of DG NOx emissions has the effect of decreasing ozone concentrations locally and downwind. Central LA is a VOC-limited region, therefore increases in NOx emissions decreases ozone concentrations. In fact, results show that the largest decreases in ozone occur during the peak of the daylight cycle. Another aspect this scenario exhibits is that with the given meteorology, the placement of DG in Los Angeles County does not directly impact the ozone concentration in the east side of the basin. For the scenario in which DG emissions are established in San Bernardino simulations predict that ozone concentrations decrease locally, but they increase downwind from the sources. Results show that the decrease is more pronounced during the nighttime – not presented in the figures – but during the peaks of the daylight hours, especially after 12:00, ozone increases up to 16 ppb. The mixing of pollutant downwind and the large VOC-to-NO_X ratios leads to more ozone at higher NO_X emissions. Placement of DG in Riverside produces a similar behavior in the ozone formation as in San Bernardino. Namely, local decreases during the night, downwind increases during the day. Although the decreases are similar in both counties, the increase in ozone concentration is more marked by placing DG in Riverside by almost 50%. However, one of the most prominent impacts is observed when DG is located near coastal areas such as Orange County. With the exception of the Ventura scenario, it represents the largest ozone increases from all scenarios explored. The positive and negative impacts have approximately the same magnitude, although they do not occur at the same time. As in the case of Riverside and San Bernardino, the largest decreases occur locally at nighttime, in particular just at before sunrise at 7:00 am. The largest increases, downwind from sources, occur at around 16:00. Finally, the effects of placing DG in Orange County can be felt as far as the east side of Riverside.

Figure 40 presents the 24-hr average $PM_{2.5}$ aerosol concentrations impacts for each county scenario. In general these impacts range from -2 to 14 µg/m^3. Also, the positive impacts on aerosol concentrations have larger magnitudes than the negative ones, which imply that the influence of DG on $PM_{2.5}$ is to increase aerosol concentrations. With the exception of Central LA, all the other scenarios produce impacts comparable to those observed in the EHP scenario. Impacts on aerosol concentrations for the Los Angeles scenario show increases of $PM_{2.5}$ concentrations north to the sources (±3 µg/m^3). The largest impacts occur for the Ventura scenario, since in the base-case no major emissions are associated with this region. These impacts, however, are seen locally and indicate that DG installation in this region does not have an effect in others in the SoCAB. The effect of placing DG in both Riverside and San Bernardino is very similar; those impacts do not exceed 7.5 µg/m^3. Typically, these regions have very high particulate matter concentrations, however, the contribution of additional DG places additional concentrations locally but not downwind. The Orange county scenario puts most of the $PM_{2.5}$ impacts far from the sources, suggesting that this aerosol is the product of gas to aerosol conversion from gas-phase precursors. Therefore, the placement of DG in coastal areas shows to be of utmost importance for impacts in regions that already have high aerosol concentrations.
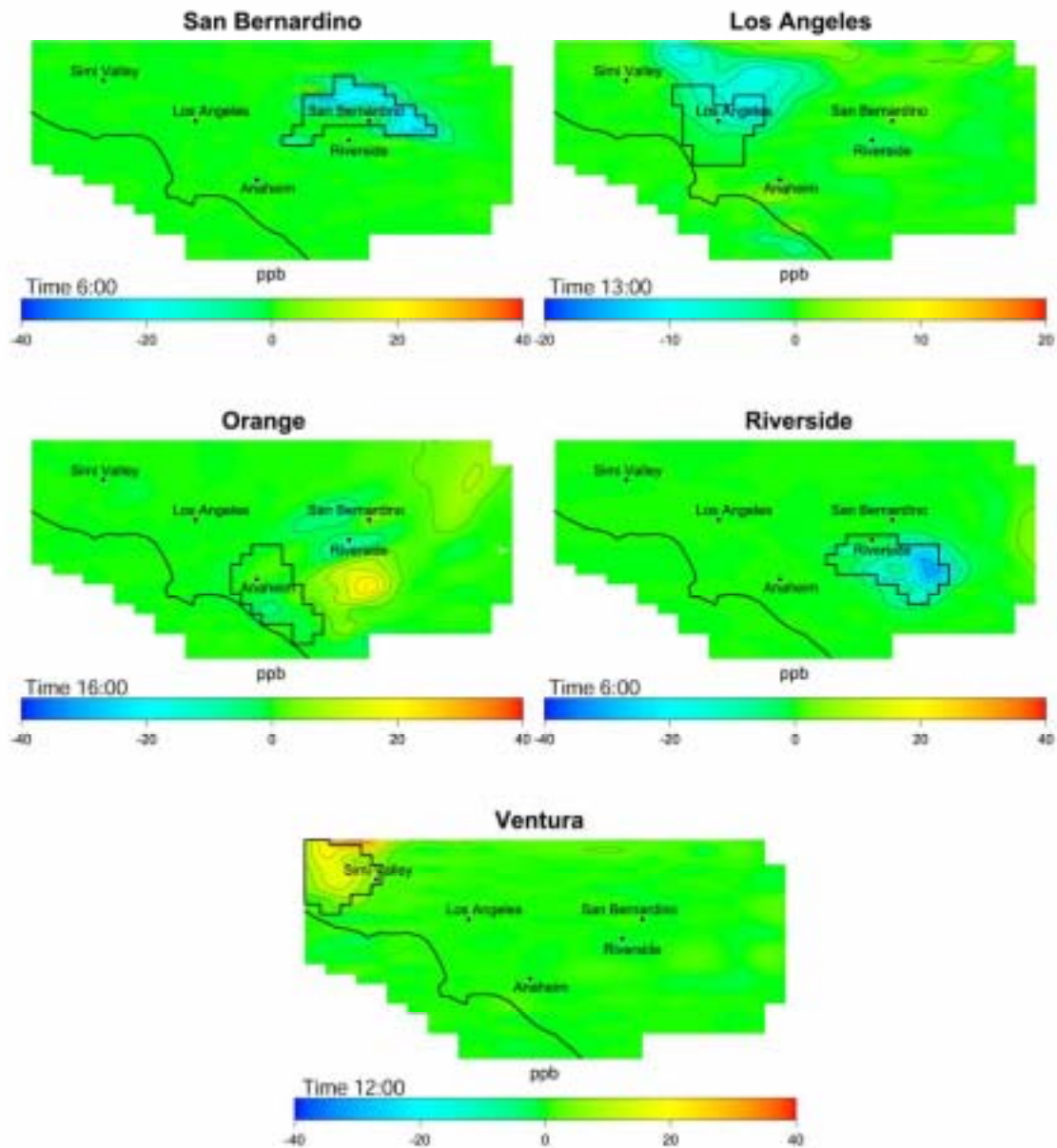
Figure 39. Difference between spatial sensitivity scenarios and baseline ozone concentrations at hours of maximum impact.
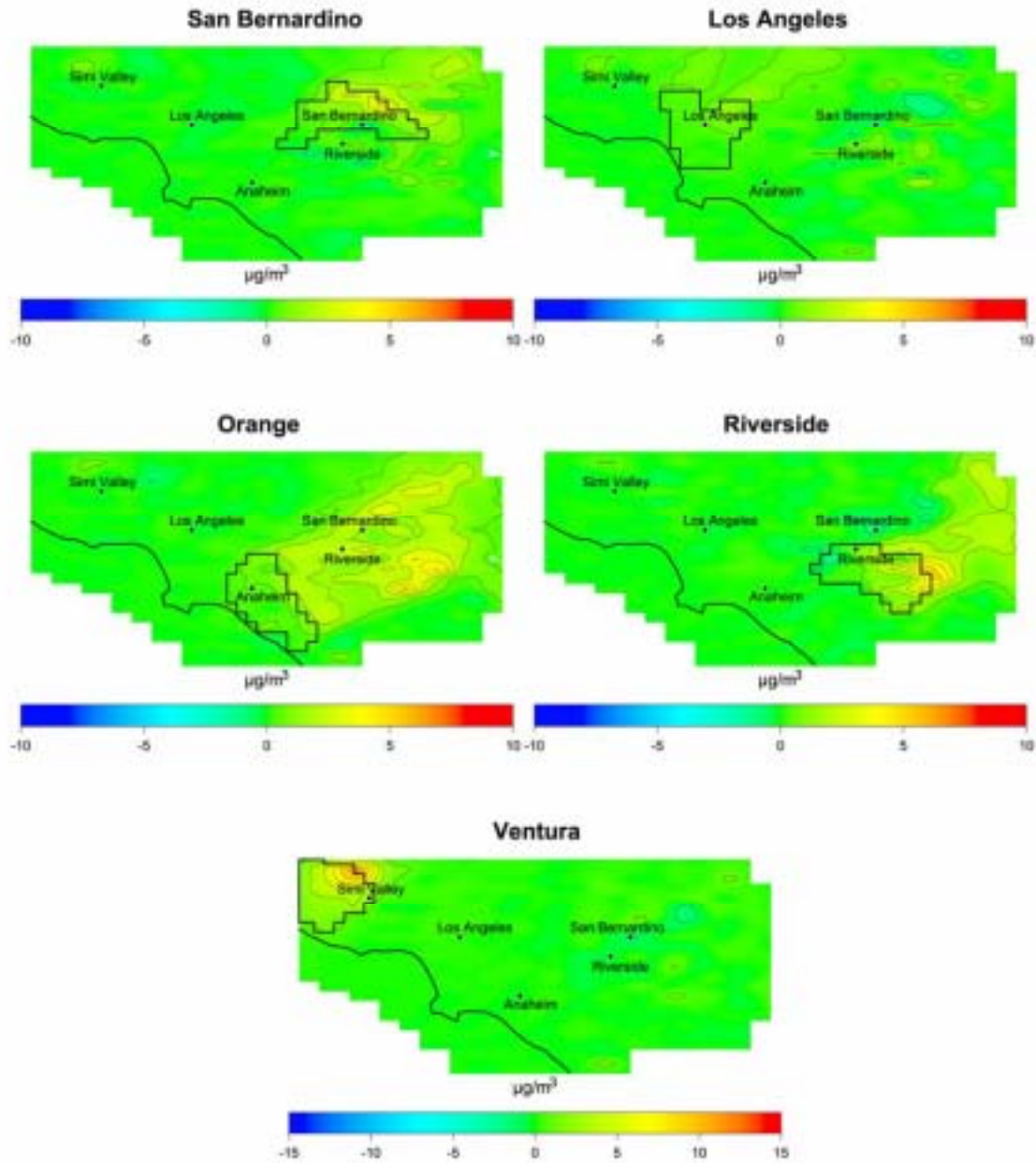
Figure 40. Difference between spatial sensitivity scenarios and baseline for 24-hr average PM$_{2.5}$ aerosol concentrations.

6.4   Air quality impacts of DG scenarios

This study presents an assessment of air quality impacts caused by the deployment of Distributed Generation systems throughout the SoCAB. Installation of such technologies by the year 2010 will depend upon market penetration for each DG type. Factors that will influence the degree of market penetration include the application for which DG is required, the cost of installation, and the ability of each technology to comply with pollutant emission standards. A set of 26 DG scenarios has been developed (Samuelsen et al., 2003) and divided into two categories: 1) realistic and 2) spanning scenarios. Realistic DG scenarios are developed to reflect an expected level of DG deployment in 2010.   Spanning DG scenarios are developed for scientific completeness, for sensitivity analyses, and for determination of potential impacts due to unexpected outcomes. Additionally, spanning scenarios help to set upper bounds for air quality impacts due to DG installation. A detailed description of the DG scenario development is presented in Section 5.1.

The process for developing DG implementation scenarios is a very significant advance of the current effort. This process, which is especially rigorous for the development of realistic DG implementation scenarios, resulted in the development of more than 100 DG implementation scenarios. After screening of these scenarios, 5 realistic and 21 spanning scenarios were studied in detail. A brief description of the parameters that define each of these scenarios is presented in . More detailed information on these scenarios can be found in Samuelsen et al., 2003.

Deployment of DG in most cases implies an increase of primary pollutants in-basin emissions. Some scenarios also account for emissions displacement, which leads to a decrease in the emission of certain pollutants. Table 43 shows the increase in criteria pollutant emissions for each DG scenario. Table 44 presents the increase due to DG implementation as a percentage of pollutant emissions relative to the total in-basin emissions. Scenarios 2 (2003ES) and 18 (EHP) present the highest increase in pollutant emissions whereas scenario 16 (TDPW10%) presents the lowest increase in emissions except for NO_X. Realistic scenario #R3 has the lowest NO_X emissions since #R3 assumes the highest net decrease in NO_X emissions due to combined heating and power (CHP) emissions displacement. In general, the increase of emissions with respect to the baseline in all DG implementation scenarios is less than 1%, for all species. Scenarios 22 through 25 consider a net in-basin decrease of NO_X emissions due to emissions displacement that result from the use of CHP.

Although the increase of basin-wide emissions in all cases is relatively small compared to total emissions, each scenario considers the implementation of a different DG technology mix and DG units are installed to operate according to different duty cycles. In addition, each DG technology has different emission factors and is implemented differently according to its use by activity sector. As a result, chemically resolved emissions vary widely in space and time. Furthermore, the effects of emissions fluxes on ambient concentrations depend upon a host of coupled processes including bulk transport, diffusion, chemical and photochemical reactions. Hence, localized air quality impacts can be determined only through use of the three-dimensional, air quality models. Detailed results, including variations in predicted criteria pollutants as a

function of space and time are presented in the following sections for both realistic and spanning DG implementation scenarios.

Table 43. Basin-wide absolute increase of primary criteria pollutant emissions per each DG scenario

Name DG Scenario	# DG Scenario	CO ton/day	NO$_X$ ton/day	VOC ton/day	NH$_3$ ton/day	SO$_X$ ton/day	PM ton/day
PW2010	1	8.19	2.54	0.80	0.25	0.10	0.61
2003ES	2	75.65	6.30	5.32	0.00	0.43	2.04
2007ES	3	1.26	0.88	0.11	0.00	0.43	2.04
PermICEPW	4	22.37	5.59	2.36	0.00	0.11	0.88
HEAPW20%	5	16.44	4.43	0.93	0.25	0.13	0.61
PeakPW	6	3.45	1.03	0.33	0.09	0.04	0.30
LDG20%	7	2.58	1.54	0.13	0.00	0.09	0.09
NH3_20%	8	2.58	1.54	0.13	0.78	0.09	0.09
PGW2010	9	8.19	2.54	0.80	0.25	0.10	0.61
LUPW20%	10	8.19	2.54	0.80	0.25	0.10	0.61
Free20%	11	8.09	2.52	0.78	0.26	0.10	0.81
FCPW20%	12	1.26	0.88	0.13	0.00	0.08	0.65
MTGPW20%	13	1.90	1.03	0.11	0.00	0.13	1.05
DGCHP	14	5.79	1.31	0.66	0.25	0.06	0.18
DGEED	15	7.67	0.86	0.16	0.25	0.09	0.60
TDPW10%	16	1.12	0.34	0.11	0.00	0.02	0.13
BAU	17	6.19	1.96	0.54	0.33	0.06	0.26
EHP	18	44.35	13.76	4.31	1.37	0.54	3.01
BAU_par	19	17.37	4.78	1.65	0.33	0.12	0.72
HPD	20	9.49	2.86	0.93	0.22	0.11	0.71
PeakPW-2	21	13.19	5.02	1.95	1.94	2.00	1.31
#R1	22	2.26	-0.09	0.16	0.20	0.03	0.24
#R2	23	4.53	-0.18	0.32	0.40	0.06	0.49
#R3	24	9.06	-0.35	0.64	0.80	0.12	0.97
#R4	25	1.22	-0.29	0.11	0.18	0.03	0.24
#R5	26	2.79	0.75	0.19	0.20	0.04	0.28

Table 44. Basin-wide relative (in %) increase of primary criteria pollutant emissions per each DG scenario

Name DG Scenario	# DG Scenario	CO %	NO$_X$ %	VOC %	NH$_3$ %	SO$_X$ %	PM %
PW2010	1	0.25	0.37	0.13	0.13	0.08	0.16
2003ES	2	2.30	0.93	0.84	0.00	0.34	0.55
2007ES	3	0.04	0.13	0.02	0.00	0.34	0.55
PermICEPW	4	0.68	0.82	0.37	0.00	0.09	0.24
HEAPW20%	5	0.50	0.65	0.15	0.13	0.11	0.16
PeakPW	6	0.10	0.15	0.05	0.05	0.03	0.08
LDG20%	7	0.08	0.23	0.02	0.00	0.07	0.02
NH3_20%	8	0.08	0.23	0.02	0.42	0.07	0.02
PGW2010	9	0.25	0.37	0.13	0.13	0.08	0.16
LUPW20%	10	0.25	0.37	0.13	0.13	0.08	0.16
Free20%	11	0.25	0.37	0.12	0.14	0.08	0.22
FCPW20%	12	0.04	0.13	0.02	0.00	0.06	0.17
MTGPW20%	13	0.06	0.15	0.02	0.00	0.10	0.28
DGCHP	14	0.18	0.19	0.10	0.13	0.05	0.05
DGEED	15	0.23	0.13	0.02	0.13	0.07	0.16
TDPW10%	16	0.03	0.05	0.02	0.00	0.01	0.04
BAU	17	0.19	0.29	0.09	0.18	0.05	0.07
EHP	18	1.35	2.02	0.68	0.74	0.43	0.81
BAU_par	19	0.53	0.70	0.26	0.18	0.10	0.19
HPD	20	0.29	0.42	0.15	0.12	0.09	0.19
PeakPW-2	21	0.40	0.74	0.31	1.05	1.60	0.35
#R1	22	0.07	-0.01	0.03	0.11	0.02	0.07
#R2	23	0.14	-0.03	0.05	0.22	0.05	0.13
#R3	24	0.27	-0.05	0.10	0.43	0.10	0.26
#R4	25	0.04	-0.04	0.02	0.10	0.02	0.07
#R5	26	0.08	0.11	0.03	0.11	0.03	0.08

6.4.1   Air quality impacts of Realistic DG scenarios

Scenarios that consider the realistic implementation of DG introduce small emission increments of 0.43% and less. Distribution of these new sources is based on land-use data, which concentrates DG technologies close to industrial zones, such as Long Beach, Los Angeles and Riverside. In contrast, population distribution places higher DG concentration in the central area of Los Angeles (see Figure 41). Although basin-wide emission increments are small, the additional emissions by DG are distributed throughout the basin and are especially installed in industrialized regions, where they have the potential to discernibly impact air quality.

<div align="center">(a)</div>
<div align="center">(b)</div>
<div align="center">(c)</div>
<div align="center">(d)</div>
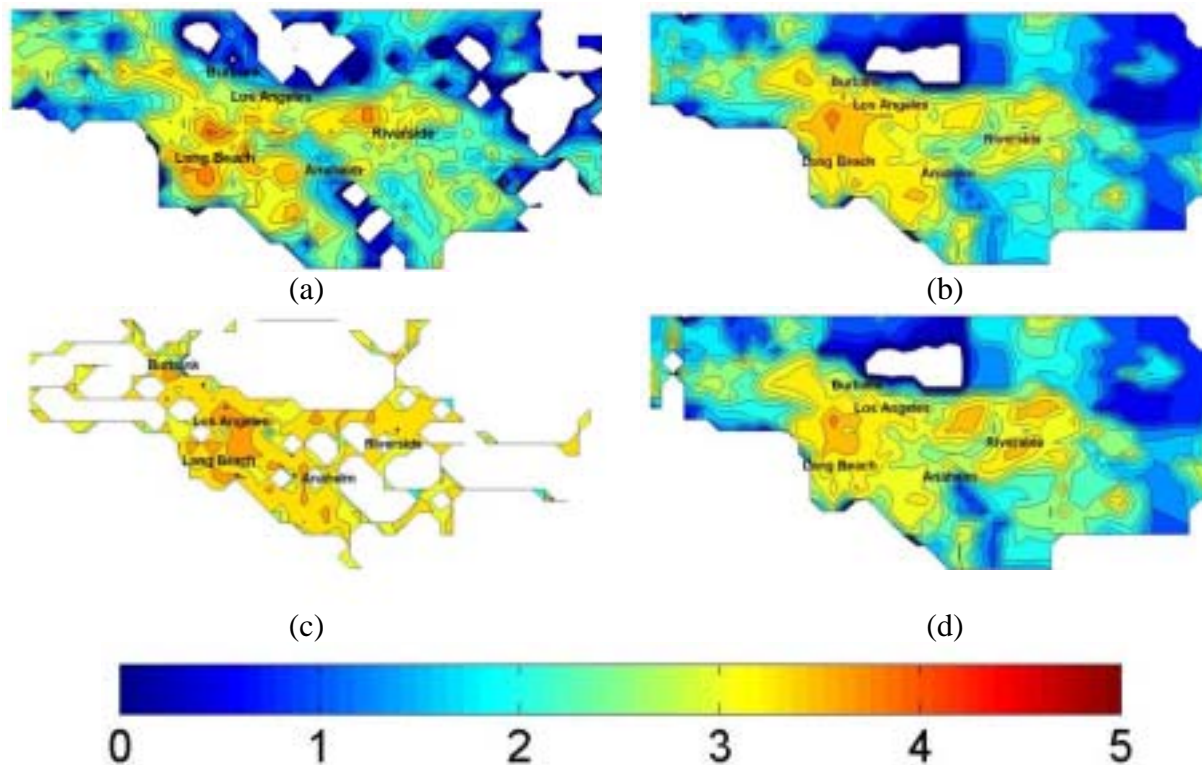
Figure 41. Comparison among 4 spatial distribution of DG power (in kW, Log scale) in the SoCAB in : (a) land-use based; (b) population based; (c) freeway density based; (d) population growth based

In the realistic scenario #R1, 5% of the increased power demand from 2002 to 2010 is met by DG. The distribution of DG throughout the basin is based on land-use data and DG operation follows realistic duty cycles corresponding to different activity sectors present in each cell of the computational domain. Thus the amount of emissions introduced by DG varies geographically and temporally. In addition, each DG technology is deployed differently depending on the activity area in which DG is installed. Therefore, the fraction of different pollutants introduced varies in each cell of the domain.

Realistic scenarios #R2 and #R3 have the same emissions spatial distribution as scenario #R1. However, #R2 and #R3 present DG penetration of 10% and 20% of the increased power demand during the years 2002 through 2010. Hence, increase in emissions of CO, VOC, PM, NH_3 and SO_X in scenario #R2 is twofold the increase in #R1, whereas the increase in #R3 is 4 times higher than that of #R1. On the other hand, NO_X emissions are reduced with the same ratios in #R2, #R3 and #R1, because the increase in emission displacement due to CHP applications is proportional to DG penetration.

Realistic scenario #R4 also presents the same DG distribution as #R1. However, the DG adoption rate for this scenario is assumed non-linear with time. This assumption means that DG technologies will be installed at a higher rate after the year 2007. As a result, a higher fraction of DG technologies installed by 2010 will produce lower emissions, in compliance with the

approved ARB emission standards for 2007. #R4 is the realistic scenario with the lowest CO and VOC emissions, and only #R3 has lower NO_X emissions since #R3 has higher NO_X emissions displacement than #R4.

Finally, realistic scenario #R5 presents the same DG distribution as #R1, but it neglects the emission displacement due to CHP. Therefore, #R5 is the realistic scenario with the highest NO_X emissions.

Table 45, Table 46 and Table 47 present the overall basin-wide impacts of realistic DG implementation scenarios on O_3, NO_2 and $PM_{2.5}$ concentrations, respectively. The domain-wide maximum ozone concentrations do not change among the different realistic scenarios (Table 45) and are equal to that of the baseline. This could suggest that compliance with ozone standards will not likely be affected by implementations of DG that are similar to the realistic scenarios of this study, since peak basin-wide 1-hour ozone concentration is the parameter upon which compliance with current federal standards is determined. However, increases in ozone concentration of the order of 2 ppb occur in areas where baseline concentrations exceed the air quality standards. Therefore, implementation of DG may contribute to the already poor air quality in certain downwind locations. The domain-wide maximum NO_2 concentration is also similarly not affected by any of the realistic DG scenarios (Table 46). However, the largest hourly changes in NO_2 concentrations range from –3 ppb to +3 ppb.

Table 45. Maximum O_3 concentration, and maximum decrease and increase in O_3 concentration for simulation of each realistic DG scenario (State Standard: 90 ppb, Federal Standard: 120 ppb)

Scenario	Basin-Wide Max (ppb)	Time	Max Increase (ppb)	Baseline reference (ppb)	Time, Max Increase	Max Decrease (ppb)	Baseline reference (ppb)	Time, Max Decrease
#R1	238	13	3	46	13	-2	60	12
#R2	238	13	5	45	14	-9	152	13
#R3	238	13	5	89	12	-4	178	13
#R4	238	13	3	70	11	-8	178	13
#R5	238	13	2	88	12	-8	178	13

Table 46. Maximum NO$_2$ concentration, and maximum decrease and increase in NO$_2$ concentration for simulation of each realistic DG scenario (State standard: 250 ppb)

Scenario	Basin-Wide Max (ppb)	Time	Max Increase (ppb)	Baseline reference (ppb)	Time, Max Increase	Max Decrease (ppb)	Baseline reference (ppb)	Time, Max Decrease
#R1	158	5	2	93	1	-1	60	1
#R2	158	5	2	83	1	-3	57	18
#R3	158	5	2	83	1	-3	49	21
#R4	158	5	3	49	6	-3	6	18
#R5	158	5	1	18	23	-1	60	1

The domain-wide hourly maximum PM$_{2.5}$ concentration obtained in all realistic scenarios is equal to the baseline PM$_{2.5}$ peak, except for scenario #R2, in which the maximum is 1 μg/m^3 higher. However, hourly PM$_{2.5}$ concentrations decrease 33 μg/m^3 in #R1 and increase 17 μg/m^3 in scenario #R5 with respect to the baseline. On the other hand, changes in 24-hour average PM$_{2.5}$ concentration fall within the range ± 3 μg/m^3. The 24-hour average PM$_{2.5}$ results from simulation of all of the realistic DG implementation scenarios are presented in Table 48. Since current regulations are based upon the 24-hour average of particulate matter (PM$_{10}$ in current regulations), the results of Table 48 suggest a potential slight improvement in compliance due to DG installation. This is the case because observed decreases in PM$_{2.5}$ occur in locations of high baseline 24-hour average PM$_{2.5}$ concentration.

Table 47. Maximum hourly PM$_{2.5}$ concentration, and maximum decrease and increase in hourly PM$_{2.5}$ concentration for simulation of each realistic DG scenario

Scenario	Basin-Wide Max (μg/m^3)	Time	Max Increase (μg/m^3)	Baseline reference (μg/m^3)	Time, Max Increase	Max Decrease (μg/m^3)	Baseline reference (μg/m^3)	Time, Max Decrease
#R1	248	3	15	17	6	-19	113	3
#R2	249	3	15	72	4	-14	96	4
#R3	248	3	13	59	6	-15	65	22
#R4	248	3	16	24	7	-15	88	4
#R5	248	3	17	54	7	-33	207	6

Table 48. Maximum 24-hour average PM$_{2.5}$ concentration, and maximum decrease and increase in 24-hour average PM$_{2.5}$ concentration in each realistic scenario (Federal Standard: 65 μg/m^3)

Scenario	Max (μg/m^3)	Max Increase (μg/m^3)	Baseline reference (μg/m^3)	Max Decrease (μg/m^3)	Baseline reference (μg/m^3)
#R1	115	3	45	-2	44
#R2	115	2	58	-2	81
#R3	114	2	39	-2	70
#R4	114	2	39	-2	69
#R5	112	3	39	-3	115

For scenario #R1, the maximum difference in ozone concentrations compared to the baseline case for any location at any time is on the order of 3 ppb (see Table 45). This occurs in areas where ozone concentrations are already lower than the peak concentration, so these changes will not affect compliance with ozone standards. However, the decreases in ozone concentration of Table 45 (for all realistic cases) occur in regions of relatively high baseline ozone concentration, whereas increases occur in regions of relatively low baseline ozone concentration. Thus, the simulation of realistic DG implementation scenarios suggests no impact of DG on basin compliance with air quality standards, but a potential to slightly decrease ozone in areas of relatively high ozone concentration.

Figure 42 presents the spatially resolved impacts on ozone concentration at 13:00, the hour when ozone concentrations reach their maximum for scenario #R1. Figure 42 shows the difference in ozone predictions between the realistic and the baseline cases. At this particular hour, increases and decreases in ozone concentration range from –2 to +2 ppb. Although this range is small, some of the increases occur downwind from Riverside, where ozone concentration is typically exceeding the air quality standards.

Impacts of scenario #R1 on NO$_2$ concentration range between –1 to +2 ppb, as shown in Table 46. The largest impacts occur at night and early morning, when NO$_2$ is not photolyzed yet and concentrations are still high. At night, NO$_2$ reacts with remaining ozone to form NO$_3$, which is the predominant atmospheric oxidant for unsaturated hydrocarbons and a precursor for particular matter. As a result, the maximum increase in particulate matter occurs in the early morning after NO$_2$ peaks. On the other hand, although wide ranges of change in hourly PM$_{2.5}$ concentrations occur in the basin, as shown in Table 47, there are no significant impacts on the PM$_{2.5}$ 24-hour average concentration.
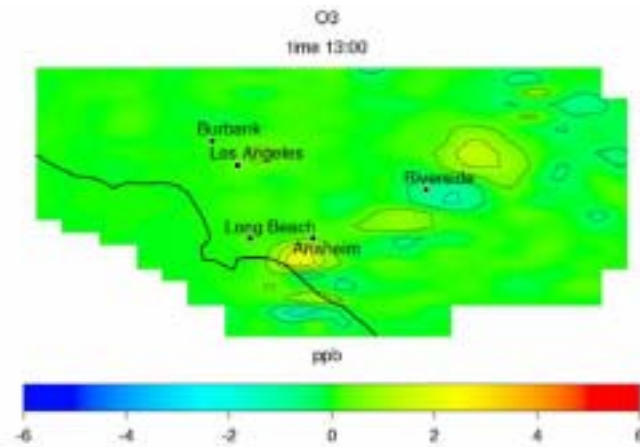
Figure 42. Difference in O₃ concentration (in ppb) between #R1 and Baseline at hour 13:00

Differences in the PM$_{2.5}$ 24-hr average concentrations between the realistic DG scenario #R1 and the baseline scenario range from −2 to +3 µg/m^3, as shown in Figure 43. The largest differences in PM2.5 24-hour concentration are located near San Bernardino and Riverside, where maximum concentrations of particulate matter are typically observed.
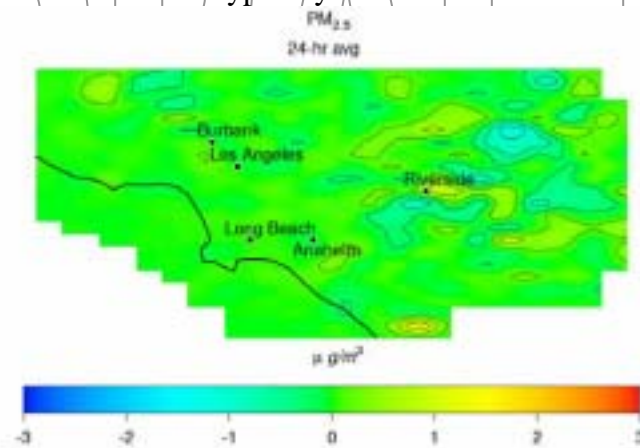
Figure 43. Difference in PM$_{2.5}$ 24-hour average concentration (in µg/m^3) between #R1 and Baseline

Impacts on ozone and PM$_{2.5}$ concentrations are also analyzed at two specific locations in the SoCAB: Riverside and Central Los Angeles. Riverside is characterized as one of the regions with the poorest air quality in the basin, with respect to both ozone and particulate matter. On the other hand, Central Los Angeles is typically in compliance with the ozone air quality standard, but it suffers from high particulate matter concentrations. Furthermore, air quality poses the most significant health risks in Central Los Angeles since it is the most populated region in the basin.

Figure 44 presents the entire two-day time evolution of ozone and PM$_{2.5}$ concentrations in Riverside and Los Angeles. In the realistic scenario #R1, ozone concentrations are not impacted

significantly at either location.   Impacts on PM$_{2.5}$ concentrations are more significant in Riverside than Central Los Angeles (Figure 44).   Differences in PM$_{2.5}$ concentrations in Riverside reach values of ± 5 μg/m^3. Major changes in PM$_{2.5}$ at Riverside are due to available nitric acid transported from central areas and local ammonia emissions. Both species combine and form secondary particulate matter.

(a)   (b)

(c)   (d)
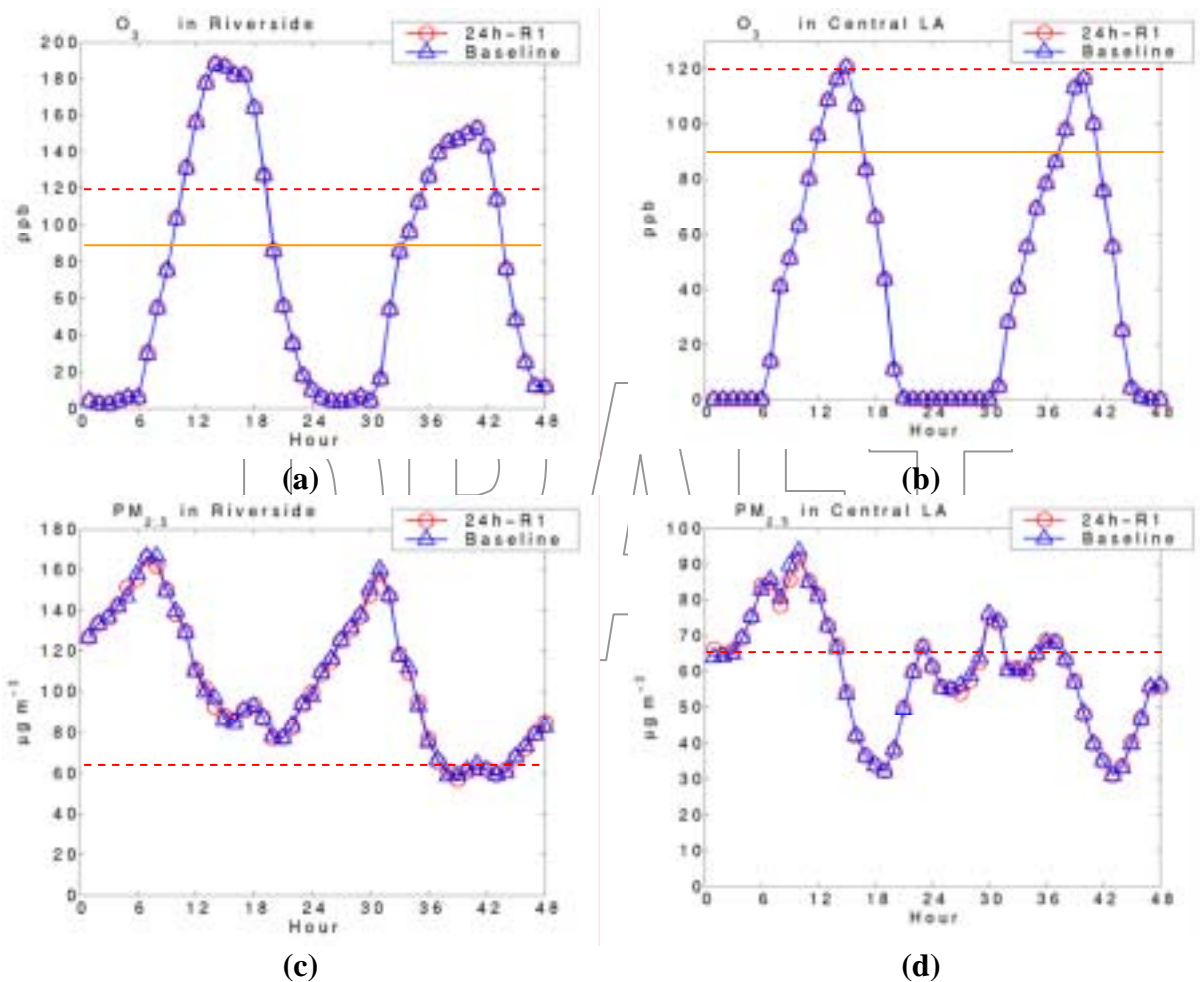
Figure 44. Impact on O$_3$ (in ppb) and PM$_{2.5}$ (in μg/m^3) concentrations at two different locations during the second and third day of simulation (Δ Base, ○ #R1, Federal standard: red discontinuous line, State standard: orange line): a) O$_3$ at Riverside, b) O$_3$ at Central LA, c) PM$_{2.5}$ at Riverside, d) PM$_{2.5}$ at Central LA

Figure 45 and Figure 46 show the effects of an increase in DG market penetration on ozone and PM$_{2.5}$ concentrations, respectively. Maximum changes in ozone concentration range from -9 to +5 μg/m^3 in all three scenarios #R1, #R2 and #R3 (Figure 45). In addition, increases of 2-3 ppb in ozone concentration occur at near Riverside, where ozone levels exceed air quality standards. However, due to progressively higher DG penetration in #R2 and #R3, the area in which ozone

concentrations are impacted becomes larger. The effects in PM$_{2.5}$ concentrations produced by increasing DG penetration are less evident than the effects in ozone concentrations (compare Figure 46 for PM$_{2.5}$ to Figure 45 for ozone).

(a)   **(b)**
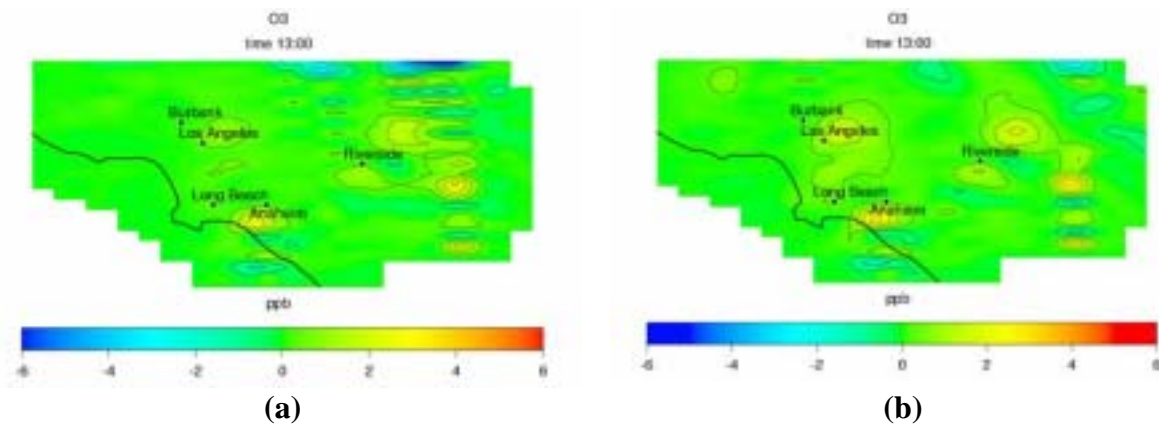
Figure 45. Effect of DG penetration on O$_3$ concentration (in ppb) at hour 1300 a) #R2, 10% of increased power demand met by DG, b) #R3, 20% of increased power demand met by DG

(a)   **(b)**
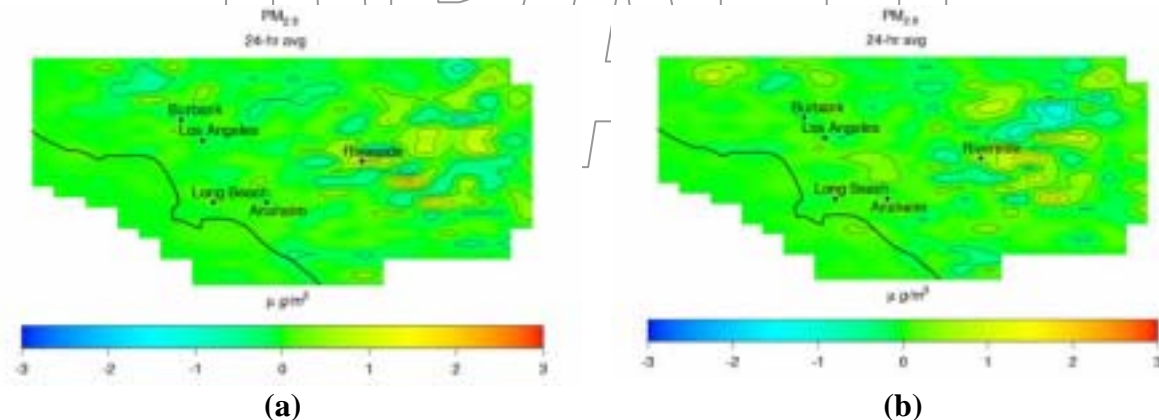
Figure 46. Effect of DG penetration on 24-hour average PM$_{2.5}$ concentration (in μg/m^3) a) #R2, 10% of increased power demand met by DG, b) #R3, 20% of increased power demand met by DG

Similar impacts on PM$_{2.5}$ concentration are observed for all five realistic scenarios. None of the changes amongst the realistic scenarios significantly changes the impact of DG on PM$_{2.5}$ concentrations in the SoCAB.

Realistic scenario #R4 introduces slightly lower emissions than #R1 (Figure 47a). As a result, impacts in both ozone and PM$_{2.5}$ concentrations are very similar. Realistic scenario #R5 does not account for emissions displacement, and therefore, NO$_X$ emissions increase. This increase in NO$_X$ emissions, which occur mainly in the central area of the basin, leads to slight reductions in ozone concentrations at hour 13:00 (Figure 47b). This decrease is due to the characteristic high

NO$_X$/VOC ratio in the Los Angeles area. In this region, ozone production is "VOC limited", thus, the increase in NO$_X$ emissions produced by DG leads to a reduction in ozone concentrations. Nevertheless, impacts on ozone concentration are small.

| (a) | (b) |
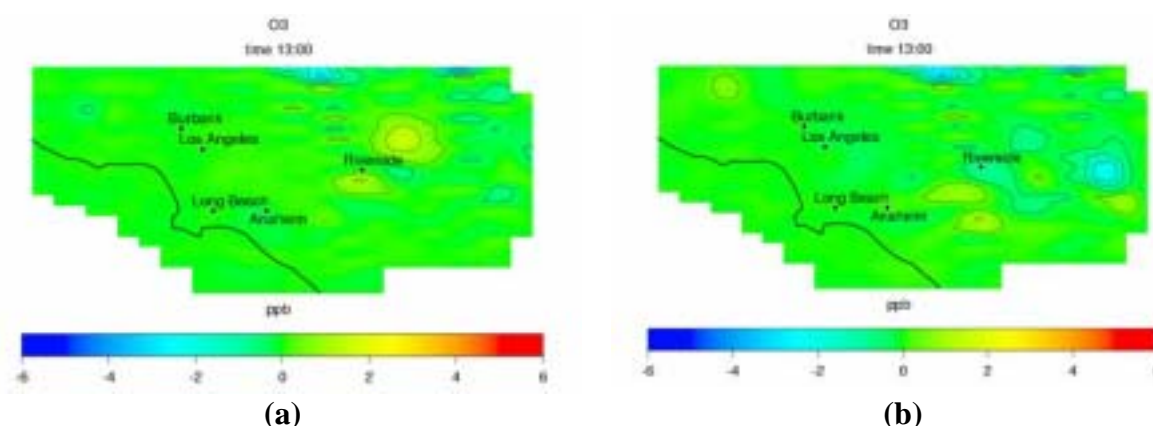
Figure 47. Impact on O$_3$ concentration (in ppb) at hour 1300: (a) #R4 - Base, (b) #R5 – Base

6.4.2   Air quality impacts of spanning DG scenarios

The aim of simulating spanning scenarios is to set bounds for the air quality impacts of DG. These scenarios are not meant to represent likely future installations of DG in the SoCAB. However, results from the investigation of spanning scenarios can provide insights into the sensitivity of the results to our assumptions for realistic scenarios, insights into scenarios that are unexpected, and/or estimates of air quality impacts produced in years beyond 2010.   A summary of the key features of each of the spanning DG implementation scenarios is presented in Table 49.

Most of the spanning DG implementation scenarios assume that distribution of DG throughout the SoCAB is proportional to population density. To determine the effects of DG allocation on air quality impacts, three scenarios have been developed to take into consideration other types of distribution: PGW2010 assumes DG distribution proportional to the population growth from 2000 to 2010; LUW20% assumes a distribution based on land-use data similar to #R3, but it does not estimate the DG mix in each cell based on land use, it does not account for emission displacement, nor for duty cycles; and Free20% considers a DG distribution proportional to freeway density.

All scenarios except for EHP, TDPW10, BAU and BAU_par, assume that a 20% of the increased demand from 2002 to 2010 will be met by DG. TDPW10% considers a DG penetration of 10% of the increased power demand (this scenario introduces the lowest emissions due to DG among spanning scenarios, except for NO$_X$, since no CHP was considered). EHP assumes that DG supply 20% of the total electricity demand. In BAU and BAU_par, linear and parabolic extrapolation of the market actual evolution during 2001 and 2002 is applied to calculate DG penetration and technology mix. Scenarios PeakPW, PeakPW-2 and TDPW10% are the only spanning scenarios that account for duty cycles. For the remaining spanning scenarios, DG units are set to operate constantly 24 hours a day. Finally, different technology mixes are considered,

including scenarios in which only fuel cells, MTG, gas turbines or ICE permitted under BACT criteria are operated exclusively (scenarios FCPW20%, MTGPW20%, LDG20% and PermICEPW, respectively).

Table 49. Summary of the key features of the spanning scenarios

#	DG Scenario	Penetration	Distribution	Technology Mix
1	**PW2010**	20% Inc.	PW[a]	30% GT, 30% ICE, 25% MTG, 7% FC, 8% PV
2	**2003ES**	20% Inc.	PW	100% 2003 ARB Standards
3	**2007ES**	20% Inc.	PW	100% 2007 ARB Standards
4	**PermICEPW**	20% Inc.	PW	100% Permitted ICE (BACT)
5	**HEAPW20%**	20% Inc.	PW	30% GT, 30% ICE, 25% MTG, 7% FC, 8% PV
6	**PeakPW**	20% Inc.	PW	35% GT, 35% ICE, 30% MTG
7	**LDG20%**	20% Inc.	HIA[b]	100% GT
8	**NH3_20%**	20% Inc.	HIA	100% GT
9	**PGW2010**	20% Inc.	PGW[c]	30% GT, 30% ICE, 25% MTG, 7% FC, 8% PV
10	**LUW20%**	20% Inc.	LUW[d]	30% GT, 30% ICE, 25% MTG, 7% FC, 8% PV
11	**Free20%**	20% Inc.	FreeW[e]	30% GT, 30% ICE, 25% MTG, 7% FC, 8% PV
12	**FCPW20%**	20% Inc.	PW	100% FC
13	**MTGPW20%**	20% Inc.	PW	100% MTG
14	**DGCHP**	20% Inc.	PW	30% GT, 30% ICE, 25% MTG, 7% FC, 8% PV
15	**DGEED**	20% Inc.	PW	35% GT, 35% ICE, 30% MTG
16	**TDPW10%**	10% Inc.	PW	34% ICE, 46% MTG, 10% FC, 10% PV
17	**BAU**	Linear	PW	28% ICE, 4% MTG, 1% FC, 15% PV, 52% GT
18	**EHP**	20% Total	PW	30% GT, 30% ICE, 25% MTG, 7% FC, 8% PV
19	**BAU_par**	Parabolic	PW	28% ICE, 4% MTG, 1% FC, 15% PV, 52% GT
20	**HPD**	20% Inc.	PW	30% GT, 30% ICE, 25% MTG, 7% FC
21	**PeakPW-2**	20% Inc.	PW	35% GT, 35% ICE, 30% MTG

[a] PW – Population-based distribution for all DG except for GT. GT are distributed in areas with high industrial activity

[b] HIA – Distribution following highly industrialized areas

[c] PGW – Population growth-based distribution for all DG except for GT. GT are distributed in areas with high industrial activity

[d] LUW – Land-use-based distribution

[e] FreeW – Freeways density-based distribution

Table 50, Table 51, Table 52, and Table 53 show the summary criteria pollutant results for the simulation of the spanning DG implementation scenarios. The domain-wide maximum concentration and the maximum change in the concentration of ozone, NO_2, and $PM_{2.5}$ are presented in Table 50, Table 51, and Table 52, respectively. Table 53 presents the domain-wide maximum 24-hour $PM_{2.5}$ concentration and the maximum change in such for each of the spanning scenarios. Table 50 shows that maximum basin-wide ozone concentration in scenarios 2003ES, HEAPW20, BAU_par, PeakPW2 and EHP increases by 1 ppb, suggesting an impact on compliance with ozone standards (even though the impact is small). On the other hand, simulation of scenario LDG20 results in a decrease in maximum basin-wide ozone concentration of 1 ppb. For the other spanning scenarios, maximum basin-wide ozone concentration remains unchanged. For the majority of DG scenarios, the largest differences between DG scenario and baseline ozone concentrations at any time and in any place throughout the basin range from –8 to +8 ppb. In half of the scenarios, maximum increases in ozone concentration occur in areas where baseline ozone concentrations are below the California Ambient Air Quality Standard (CAAQS, 90 ppb) whereas the rest of scenarios exhibit maximum increases where baseline ozone concentrations already exceed the CAAQS. On the other hand, maximum decreases in ozone concentration occur mainly in areas and hours where baseline ozone concentration is low. Maximum concentration of NO_2 remains unchanged in all spanning scenarios except for scenario PeakPW2, in which NO_2 peak concentration increases by 1 ppb. Changes in 1 hour-average maximum $PM_{2.5}$ concentrations range from –1 to +1 $\mu g/m^3$.

Table 50. Summary of impacts on O₃ concentration for all spanning DG scenarios: Maximum hourly average O₃ concentration, maximum increase and decrease in hourly average O₃ concentration, and baseline (reference) hourly average O₃ concentration where maximum differences occur

Scenario	Max (ppb)	time	Max Increase (ppb)	Baseline reference (ppb)	Time, Max Increase	Max Decrease (ppb)	Baseline reference (ppb)	Time, Max Decrease
PW2010	238	13	4	46	13	-3	5	5
2003ES	239	13	6	100	13	-4	12	6
2007ES	238	13	5	100	13	-7	66	11
PermICEPW20	238	13	7	100	13	-3	12	6
HEAPW20	239	13	6	100	13	-3	5	5
PeakPW	238	13	5	100	13	-13	24	5
LDG20	237	13	8	46	11	-7	66	11
NH3-20	238	13	3	73	12	-7	66	11
PGW20	238	13	6	108	14	-2	5	5
LUW20	238	13	5	134	13	-3	5	5
Free20	238	13	6	89	12	-3	54	22
FCPW20	238	13	3	53	12	-1	146	12
MTGPW20	238	13	5	89	12	-2	90	13
DGCHP	238	13	4	134	13	-2	60	12
DGEED	238	13	34	7	22	-14	73	14
TDPW10	238	13	5	89	12	-2	60	12
BAU	238	13	4	134	13	-4	146	12
EHP	239	13	8	46	14	-8	15	6
BAU_par	239	13	6	108	14	-7	66	11
HPD	238	13	6	100	13	-3	5	5
Peak_2	239	13	8	10	2	-26	29	2

For most scenarios, maximum hourly changes in NO₂ concentrations fall within the range of ±10 ppb (Table 51). Only scenarios PeakPW and PeakPW_2 produce larger increases, of up to 14 ppb and 30 ppb, respectively, and scenario DGEED produces larger decreases of up to –39 ppb. None of these changes imply an impact of DG installation on air quality that would affect SoCAB compliance with NOx air quality standards. Nonetheless some of these changes are very significant, especially when considering the small amount of emissions that DG introduces into the basin.

Maximum hourly changes in PM$_{2.5}$ concentration, presented in Table 52, range from –27 μg/m^3 to +23 μg/m^3. However, the maximum changes in 24-hour average PM$_{2.5}$ concentrations (Table 53) are on the order of -4 to +6 μg/m^3 for all of the spanning DG implementation scenarios. This is a significant change that could impact SoCAB compliance with air quality standards if a scenario would emerge that is well represented by these spanning scenarios (especially the EHP and Peak_2 spanning scenarios, which introduce the most concentrated DG emissions).

Table 51. Summary of impacts on NO$_2$ concentration for all spanning DG scenarios: Maximum hourly average NO$_2$ concentration, maximum increase and decrease in hourly average NO$_2$ concentration, and baseline (reference) hourly average NO$_2$ concentration where maximum differences occur

Scenario	Max (ppb)	time	Max Increase (ppb)	Baseline reference (ppb)	Time, Max Increase	Max Decrease (ppb)	Baseline reference (ppb)	Time, Max Decrease
PW2010	158	5	3	29	5	-3	6	18
2003ES	158	5	5	31	6	-3	6	18
2007ES	158	5	2	49	6	-3	6	18
PermICEPW20	158	5	4	31	6	-3	6	18
HEAPW20	158	5	4	29	5	-3	6	18
PeakPW	158	5	14	9	5	-3	24	2
LDG20	158	5	6	13	6	-3	6	18
NH3-20	158	5	6	13	6	-3	6	18
PGW20	158	5	3	29	5	-3	6	18
LUW20	158	5	3	29	5	-3	6	18
Free20	158	5	4	34	23	-3	6	18
FCPW20	158	5	2	61	5	-3	6	18
MTGPW20	158	5	2	49	6	-1	1	11
DGCHP	158	5	2	80	23	-3	6	18
DGEED	158	5	10	26	1	-39	45	23
TDPW10	158	5	2	80	23	-3	6	18
BAU	158	5	3	29	5	-4	46	1
EHP	158	5	9	2	5	-3	46	1
BAU_par	158	5	4	29	5	-3	6	18
HPD	158	5	3	29	5	-3	6	18
Peak_2	159	5	30	7	4	-8	24	2

Table 52. Summary of impacts on hourly PM$_{2.5}$ concentration for all spanning DG scenarios: Maximum hourly average PM$_{2.5}$ concentration, maximum increase and decrease in hourly average PM$_{2.5}$ concentration, and baseline (reference) hourly average PM$_{2.5}$ concentration where maximum differences occur

Scenario	Max ($\mu g\ m^{-3}$)	time	Max Increase ($\mu g\ m^{-3}$)	Baseline reference ($\mu g\ m^{-3}$)	Time, Max Increase	Max Decrease ($\mu g\ m^{-3}$)	Baseline reference ($\mu g\ m^{-3}$)	Time, Max Decrease
PW2010	248	3	18	54	7	-16	58	21
2003ES	248	3	17	54	7	-18	207	6
2007ES	249	3	16	100	8	-19	145	6
PermICEPW20	248	3	14	115	3	-16	68	18
HEAPW20	249	3	19	54	7	-15	112	6
PeakPW	248	3	17	54	7	-15	62	21
LDG20	247	3	17	54	7	-17	147	4
NH3-20	248	3	13	59	6	-27	137	3
PGW20	248	3	18	54	7	-22	108	5
LUW20	248	3	14	115	3	-21	106	8
Free20	249	3	14	56	4	-15	97	3
FCPW20	249	3	17	17	7	-18	122	1
MTGPW20	248	3	17	54	7	-16	105	5
DGCHP	248	3	17	54	7	-13	61	22
DGEED	249	3	14	104	3	-21	136	6
TDPW10	248	3	18	54	7	-22	207	6
BAU	248	3	17	17	7	-16	96	4
EHP	248	3	20	100	8	-14	34	7
BAU_par	248	3	14	104	3	-22	148	4
HPD	248	3	16	24	7	-20	132	7
Peak_2	249	5	23	100	8	-19	87	22

Table 53. Summary of impacts on 24-hour average PM$_{2.5}$ concentration for all spanning DG scenarios: Maximum 24-hour average PM$_{2.5}$ concentration, maximum increase and decrease in 24-hour average PM$_{2.5}$ concentration, and baseline (reference) 24-hour average PM$_{2.5}$ concentration where maximum differences occur

Scenario	Max (µg m^{-3})	Max Increase (µg m^{-3})	Baseline reference (µg m^{-3})	Max Decrease (µg m^{-3})	Baseline reference (µg m^{-3})
PW2010	114	3	78	-1	90
2003ES	113	3	45	-2	67
2007ES	114	3	45	-4	81
PermICEPW20	114	2	82	-2	69
HEAPW20	117	3	39	-2	69
PeakPW	114	3	45	-2	83
LDG20	115	3	39	-2	94
NH3-20	113	2	39	-2	82
PGW20	115	3	39	-1	62
LUW20	115	3	45	-2	17
Free20	114	3	39	-2	55
FCPW20	115	2	64	-2	87
MTGPW20	114	3	59	-2	104
DGCHP	114	3	39	-2	79
DGEED	113	2	59	-4	81
TDPW10	114	3	39	-2	46
BAU	115	3	45	-2	104
EHP	115	4	45	-2	17
BAU_par	115	2	78	-2	17
HPD	114	2	39	-2	69
Peak_2	116	6	75	-2	14

In the following sections, results from simulating all of the spanning scenarios are compared within different sub-categories that allow a parametric evaluation of air quality impacts. These sub-categories are chosen to permit comparisons between cases in which specific parameters that describe a DG scenario are changed one at a time. The comparisons are based on the impacts on ozone concentration at hour 13, when the maximum value occurs. In some other cases, differences in the formation of PM$_{2.5}$ are also highlighted.

6.4.2.1   Spatial Distribution

Ozone and PM$_{2.5}$ are secondary pollutants. Hence, their formation in the atmosphere not only depends upon precursor emissions, but also on other physical and chemical processes, governed by meteorological parameters. As a result, formation of ozone and PM$_{2.5}$ is influenced by the location of emissions sources.

This section presents four scenarios – PW2010, PGW2010, LUW20 and Free20 –, in which the same technology mix and DG penetration is assumed. These four scenarios introduce the same total basin-wide emissions. The only parameter that is varied amongst these scenarios is the geographic distribution of DG throughout the basin.

Figure 48 shows the difference in O$_3$ concentration between simulations of each scenario and the baseline case at hour 13. In general, there is an overall reduction in ozone concentration of less than 3 ppb in the central area of the basin (near Los Angeles), due to the already high NO$_X$/VOC ratio. On the other hand, ozone concentration increases by up to 6 ppb in some areas on the eastern part of the basin, downwind from the central area.

Figure 48. Difference in O$_3$ concentration (in ppb) at hour 13 between DG scenarios and the baseline for scenarios: a) PW2010, b) PGW2010, c) LUW20 and d) Free20%

Although there are differences between these four scenarios the results of Figure 48 show primarily that the level of emissions introduced by DG scenarios (0.37% of total NO_X, 0.13% of total VOC) consistently results in a similar and small ozone air quality impact. The different distributions of emission sources presented in Figure 48 show that scenario Free20% is the scenario with the highest impact. This scenario considers a distribution proportional to the freeway density. As shown in Figure 41, freeway density distribution is the one that concentrates DG emissions the most, leaving bigger areas in the basin free of DG. As a result, scenario Free20% produces higher increases in ozone concentration attributable to the spatial distribution.

The air quality impact of concentrating DG emissions in certain locations in the basin is a discernable feature revealed by the model in Figure 48 and in several other computational results. This is a significant result of the current effort, suggesting that attention should be paid to the spatial distribution of emissions in the basin. This result suggests that if DG is to be widely used in the basin then it should not be concentrated in a small area. DG scenarios with a higher penetration will likely show an even more pronounced dependence upon spatial distribution.

6.4.2.2   CARB and SCAQMD standards

Three scenarios are developed to evaluate DG emission standards by assuming that all DG in the scenario emit pollutants at exactly the level of the standard. Scenarios 2003ES and 2007ES introduce DG technologies that emit at the level of the emission standards approved by ARB for the years 2003 and 2007. Scenario 2003ES introduces 2.3%, 0.93% and 0.84% increases in CO, NO_X and VOC emissions, respectively. Emission standards for 2007 are far more stringent, resulting in emission increases of 0.04%, 0.13% and 0.02% for CO, NO_X and VOC. Scenario PermICEPW20% assumes that all DG are internal combustion engines permitted by SCAQMD under current best available control technology (BACT) regulations. These three scenarios are compared with PW2010 in Figure 49.

In general, simulations of Figure 49 show a decrease in ozone concentrations in the central area, and an increase at downwind locations at hour 13. As explained above, the primary difference between central areas and surrounding locations is with regard to VOC/NO_X ratios. Scenarios 2003ES and PermICEPW20 show increases in ozone concentrations up to 7 ppb at hour 13. These impacts are bigger than the ones produced by scenarios PW2010 and 2007ES, due to the difference in emissions introduced by DG. Emission standards for the year 2007 are more stringent than standards applied in other scenarios. Hence, scenario 2007ES shows the lowest impacts on ozone.

Both decreases and increases in ozone concentrations throughout the basin become larger as NO_X emissions from DG increase. Among the four cases, scenario 2003ES presents the largest decrease in ozone concentration, since it introduces the largest NO_X emissions. Decreases due to scenario PermICEPW20 are very similar to the ones obtained by scenario 2003ES because they introduce a similar percentage of NO_X emissions. Increases in downwind ozone, however, are the most significant for the PermICEPW20 case, which introduces the highest CO and VOC emissions levels in this comparison (see Figure 49).
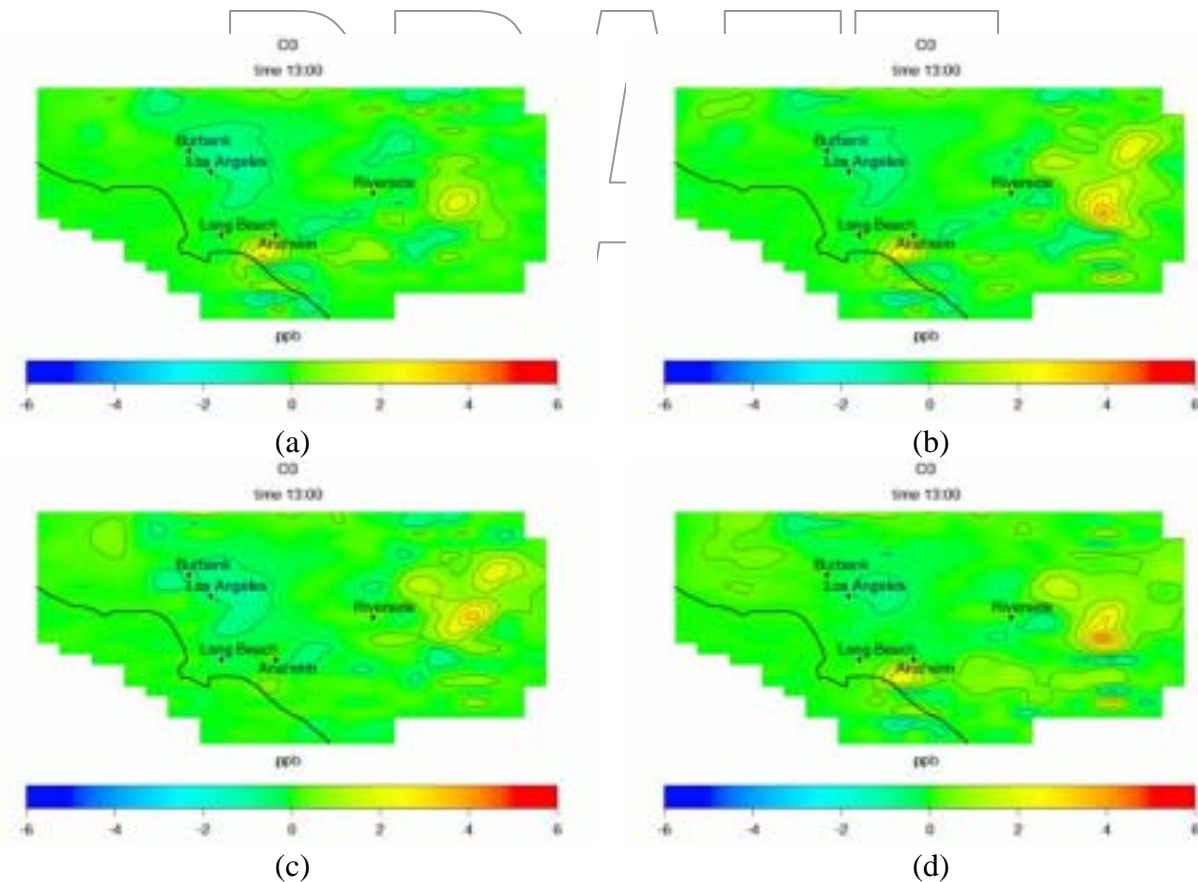
Figure 49. Difference in O$_3$ concentration (in ppb) at hour 13 between DG scenarios and baseline: a) PW2010, b) 2003ES, c) 2007ES and d) PermICEPW20%

6.4.2.3   Adoption Curve of DG Technologies

The adoption rate of DG technologies from 2002 to 2010 will affect the level of emissions by the end of this period. If DG is adopted with a high rate during the first years, they are not required to comply with more stringent emission standards in 2007. In addition, if a constant degradation rate of DG technologies is considered, emissions will increase as DG systems are adopted earlier. Scenario HEAPW20% assumes a high early adoption rate for DG deployment. Figure 50 presents the differences in air quality impacts between PW2010, a scenario with a low early adoption rate of DG (98% of DG installed in the period 2007-2010) and HEAPW20% (a case with higher early adoption of DG).

Scenario HEAPW20% introduces 75% more NO$_X$, 13% more VOC and 100% more CO emissions than scenario PW2010. As a result, impacts on ozone concentration in scenario HEAPW20% are more noticeable than the impacts observed for the PW2010 scenario. In particular, the decrease of ozone concentration near central Los Angeles is more widespread, and increases in ozone concentration are also bigger in the eastern part of the basin, in comparison to scenario PW2010. This is consistent with the previous finding and expectations that higher DG emissions rates lead to a larger ozone air quality impact. Whether this more significant impact

on ozone will likely have a negative affect on compliance with air quality standards is a more complicated question since both increases and decreases in ozone are more significant with the increased DG emissions.

Some insight into this can be garnered from Table 50. Note that for both the PW2010 and HEAPW20 scenarios, the increases in ozone occur at locations with already higher ozone concentration suggesting that the negative impact of emissions levels on ozone compliance is more likely. Note also, however, that the peak ozone concentrations are significantly higher than those in the regions where the maximum (positive and negative) impact is observed. Also, peak ozone concentration does not change significantly by the levels of DG emissions introduced in the current study. Finally, the authors caution that one should not draw general conclusions based only on the spanning DG scenario simulations of this effort.

(a)   (b)
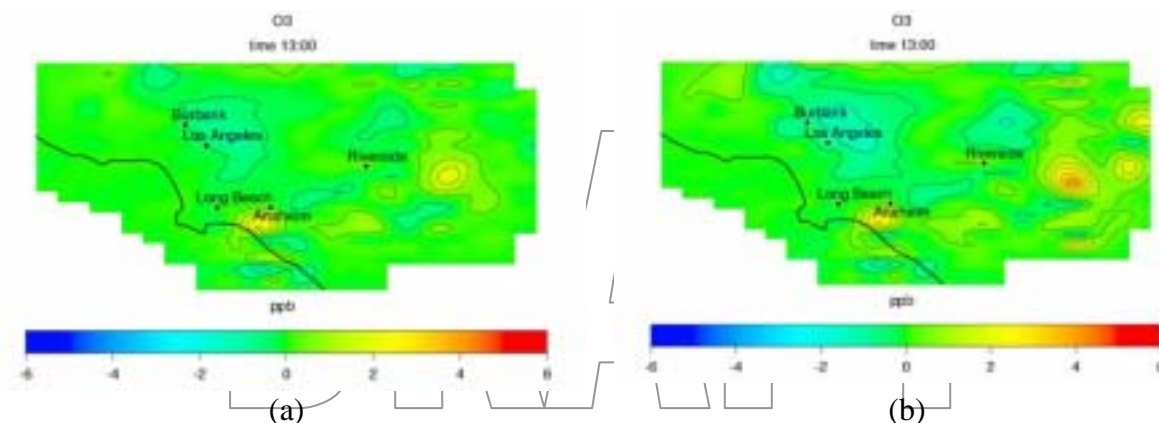
Figure 50. Difference in O_3 concentration (in ppb) at hour 13 between DG scenarios and baseline: a) PW2010, b) HEAPW20%

6.4.2.4   Duty Cycle

NO_X emissions in the SoCAB, peak at rush hours during the morning and evening, whereas VOC emissions are related to industrial activity. Nevertheless, NO_X and VOC emissions are high during the day and decrease dramatically at night. Scenarios PeakPW and PeakPW_2 assume that DG units operate for only six hours a day, from hour 12 to 18. Therefore, DG systems emit when baseline emissions are peaking. Scenario PeakPW considers that all DG installations have the capacity to supply 20% of the increased power demand from 2002 to 2010. Scenario PeakPW_2 assumes that DG supply, in 6 hours of operation, the same electric energy as the one supplied by DG in Scenario PW2010 during the 24 hours of base-load mode. Thus, DG power capacity in Scenario PeakPW_2 is 4 times higher than in PW2010. The energy supplied by DG in scenario PeakPW_2 is four times the electricity supplied by DG in scenario PeakPW. Both scenarios consider that emissions from DG at the first hour of operation are three times the normal emissions, due to the start-up process. Figure 51 presents a comparison between the impacts on ozone concentrations produced by a scenario in which all DG are base-loaded, and the two scenarios in which DG units are peaking 6 hours a day.

(a)

(b)

(c)
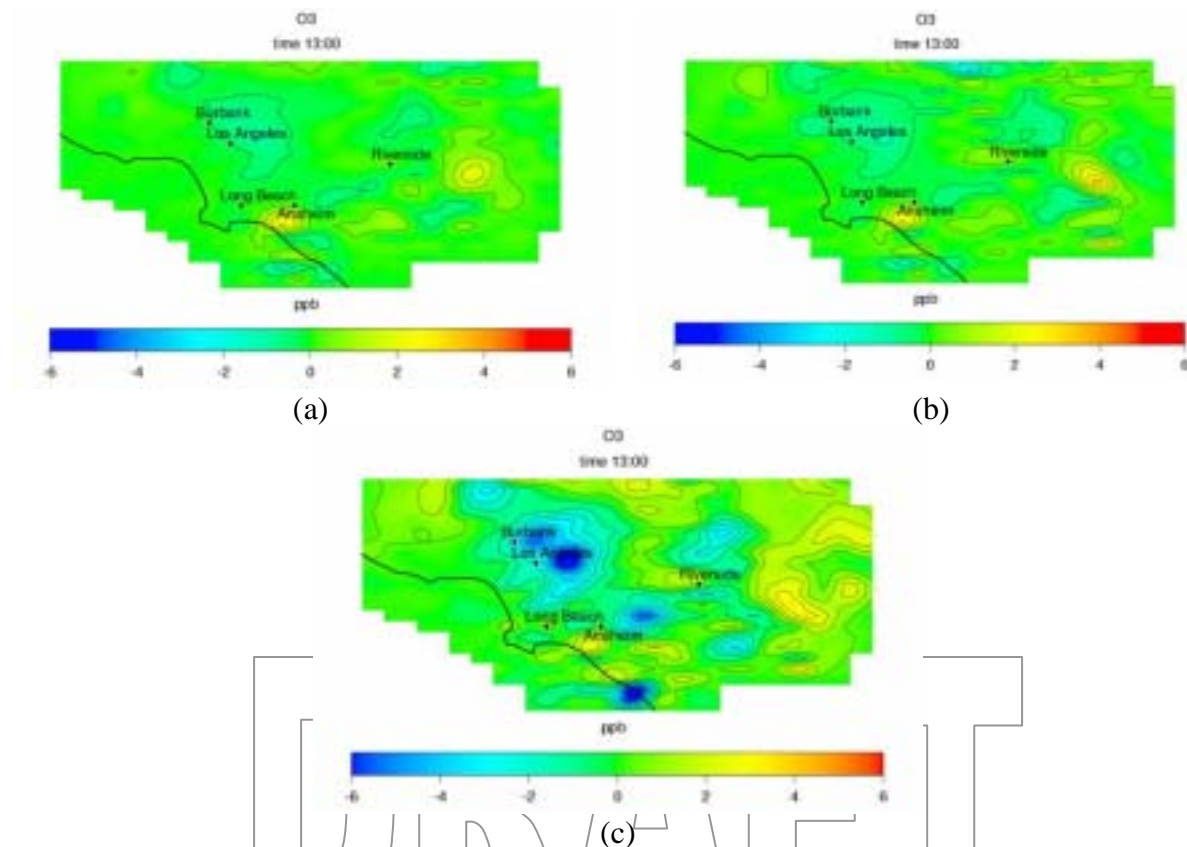
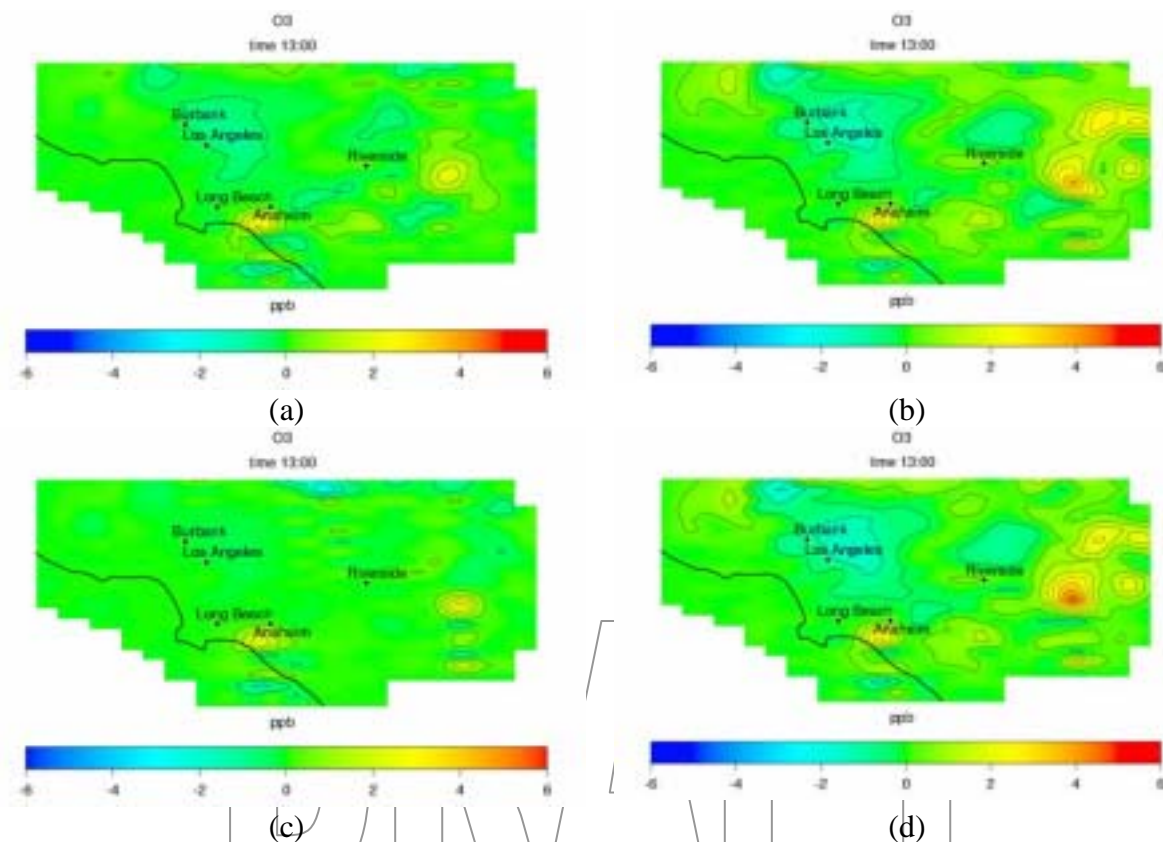**Figure 51. Difference in O₃ concentration (in ppb) at hour 14 between DG scenarios and baseline: a) PW2010, b) PeakPW and c) PeakPW_2**

Although Scenario PeakPW introduces lower emissions than PW2010, it produces similar changes on ozone concentration. Therefore, when the same amount of total emissions is considered, ozone concentrations are affected more significantly if emissions rates increase during the day (when ozone production is significantly higher), or are concentrated in time. Scenario PeakPW_2 introduces approximately four times the DG emissions of scenario PeakPW. It is observed that larger decreases in ozone concentration occur in the central area of the basin.

It should be noted that NO_X emissions in scenario PeakPW_2 are 20% lower than those of scenario 2003ES. However, impacts on ozone concentration – both increases and decreases – are more pronounced in scenario PeakPW_2 and ozone concentrations increase by up to 4 ppb over downwind locations in the eastern portion of the basin. In conclusion, if the same emissions are introduced, scenarios that concentrate emissions based on afternoon duty cycles have the potential to more significantly impact ozone concentrations compared to cases in which emissions are introduced constantly during 24 hours. Both reductions in the central part of the basin and increases in downwind locations are more significant when emissions are concentrated in time.

6.4.2.5   Large Scale DG/Ammonia Slip

Scenario LDG20% assumes that all DG units are large gas turbines. Since these units produce 49 MW of power, only 21 gas turbines are needed to supply the 20% of increased power demand from years 2002 to 2010. These 21 gas turbines are installed near industrialized regions.

NO_X emissions from gas turbines are typically controlled by selective catalytic reduction (SCR) of NO_X using ammonia introduced over a catalyst bed at a certain temperature.   One consequence of this process is ammonia emissions (often called "ammonia slip") that result from excess ammonia used in the catalytic reaction.   Ammonia is one of the gas-phase precursors involved in the formation of secondary particulate matter.   Thus, the current effort developed spanning scenario NH3_20%, which has the same assumptions as scenario LDG20%, but with the inclusion of ammonia emissions from the SCR process at each of the 21 large (50MW) plants installed in the SoCAB.

The locations of the 50MW power plants are shown as red dots in Figure 52, which presents the difference in ozone concentration between (a) the LDG20% scenario and the baseline, and (b) the NH3_20% scenario and the baseline.

(a)   (b)
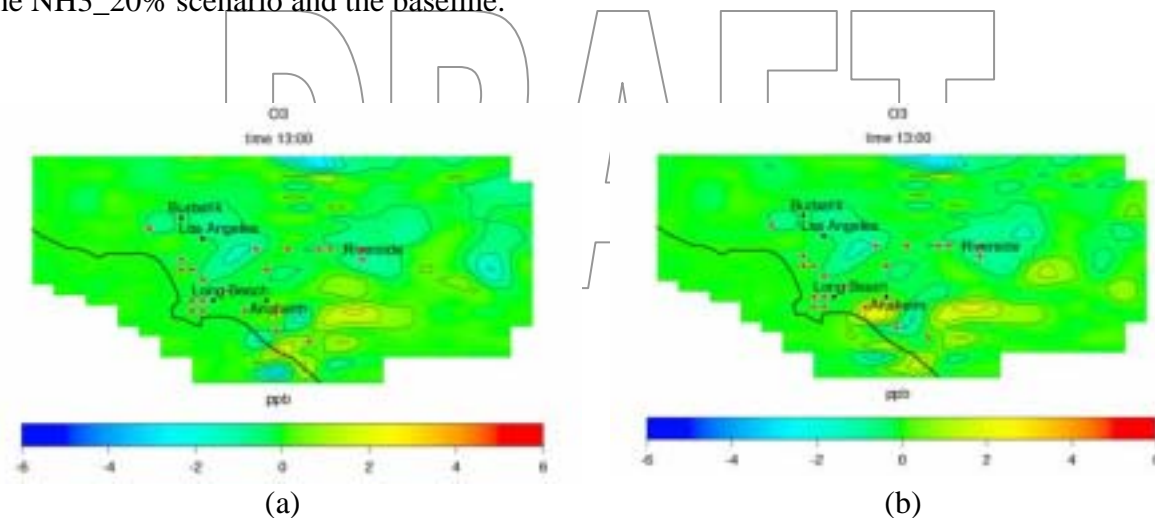
Figure 52. Difference in O_3 concentration (in ppb) at hour 13 between DG scenarios and baseline: a) LDG20%, b) NH3_20% (the red dots indicates the locations of large DG)

Figure 52 shows the impacts on ozone concentrations produced by both scenarios. Since emissions of ozone precursors (NO_X and VOC) are the same in both scenarios, ozone concentrations are affected similarly. Small differences are due to the reaction of nitric acid with the excess ammonia. This reaction consumes some nitric acid that would otherwise react with OH. This results in higher OH concentrations that are available to oxidize hydrocarbons present in the atmosphere to produce slightly more ozone in the NH3_20% case.

Figure 53 presents the difference in the 24-hour average concentration of $PM_{2.5}$ between the DG scenarios and the baseline. A priori, increase in ammonia emission would lead to an increase in

PM$_{2.5}$ concentration. However, at the level of the emissions introduced in these two scenarios, differences between LDG20% and NH3_20% are very small.

(a)   (b)
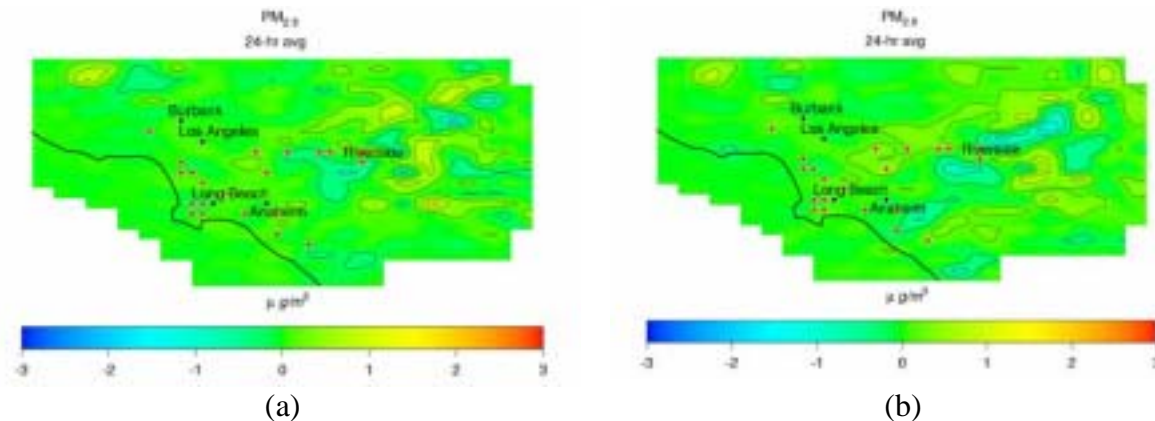
Figure 53. Difference in PM$_{2.5}$ 24-hour average concentration (in μg/m^3) between DG scenarios and baseline: a) LDG20%, b) NH3_20%

6.4.2.6   DG Technology Mix

Emissions levels from DG implementation depend upon the type of DG technology considered. Fuel cells typically have the lowest emissions compared to the other combustion-driven DG technologies. In this section the effects of DG technology type and mix of technology types are presented.

Scenario FCPW20% assumes that all the DG power is supplied by fuel cells whereas scenario MTGPW20% considers that all the DG units are MTGs. Scenario NH3_20% assumes that all DG are relatively large (50MW) gas turbine power plants (21 total power plants). Scenario TDPW10% considers a DG technology mix that includes natural gas internal combustion engines, fuel cells, microturbine generators, and larger gas turbine power plants. Scenario TDPW10% introduces the lowest emissions of all spanning scenarios primarily because the power supplied by DG in this scenario is 10% of the increased power demand from 2002 to 2010.

Figure 54 shows the difference in O$_3$ concentration at hour 13 between the DG scenarios (a) NH3_20%, (b) FCPW20%, (c) MTGPW20% and (d) TDPW10% and the baseline case. Since the level of emissions introduced in the four cases is low relative to total basin-wide emissions, only small differences are observed regarding the impact of DG technology type on O$_3$ concentrations throughout the basin. For all cases, the impact of DG on ozone concentration is relatively low (between -2 and +3 ppb). Clearly, however, the fuel cell only case (Figure 54b) has the least significant impact on ozone concentrations due to the very low emissions levels of these fuel cell systems. Note that the emissions from fuel cells in this case (FCPW20%) are based on natural gas operation and include total system emissions (i.e., all emissions from the fuel cell and natural gas reformation processes).

(a)   (b)

(c)   (d)
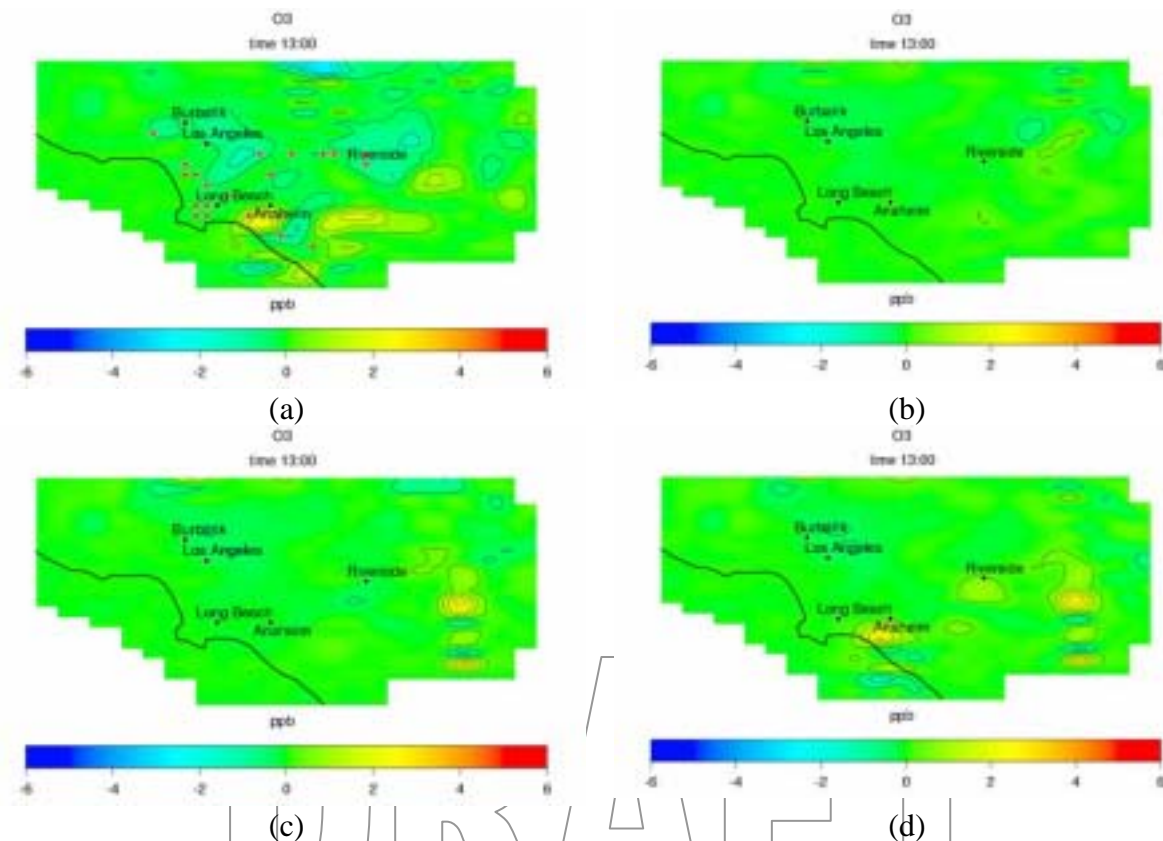
Figure 54. Difference in O$_3$ concentration (in ppb) at hour 13 between DG scenarios and baseline: a) NH3_20%, b) FCPW20%, c) MTGPW20%, d) TDPW10%

6.4.2.7 Emissions Displacement due to CHP

The use of CHP in combination with DG increases the overall efficiency of electricity production. In addition, CHP eliminates the need for a heat source, i.e. a boiler, for domestic water and heating, and therefore reduces emissions of pollutants. Scenario DGCHP examines the effects of CHP on air quality. This scenario makes the same assumptions as scenario PW2010, but it also accounts for emissions displacement due to CHP.

NO$_X$ emissions in scenario DGCHP are 50% lower than scenario PW2010, whereas VOC emissions are reduced by 25%. As in previous cases, a reduction in emissions leads to smaller decreases in ozone concentration in the central areas, and to smaller increases in ozone concentrations in the surrounding areas of the basin (Figure 55).

(a)   (b)

Figure 55. Difference in O₃ concentration (in ppb) at hour 13 between DG scenarios and baseline: a) PW2010, b) DGCHP

6.4.2.8   In-Basin Large Power Plants Displaced by DG

Implementation of DG power most likely will help meeting a part of the new power demand, and will not substitute any of the existing in-basin central power plants. Nevertheless, a scenario is presented to explore this possibility. Two power plants, one in Long Beach another in Huntington Beach, are turned off. As a result, NO_X emissions from DG are reduced by 65% and VOC emissions are reduced by 85%, with respect to scenario PW2010.


(a)   (b)

Figure 56. Difference in O₃ concentration (in ppb) at hour 13 between DG scenarios and baseline: a) PW2010, b) DGEED (red dots represent the two power plants; blue dots represent the large GT installed)

Figure 56 shows how the impact on ozone concentrations in scenario DGEED differs from PW2010. Although scenario DGEED has similar levels of NO_X and VOC emissions as scenario FCPW20%, impacts on ozone concentrations are different. This is a consequence of localized

reduction in emissions at two coastal cells. The power plant near Long Beach is upwind from an area in which NO_X emissions are very high (wind blows from southwest). Decreasing NO_X in this VOC-limited area increases ozone concentration slightly near Long Beach. The power plant located in Huntington Beach is close to areas with less intense NO_X emissions than central Los Angeles. Therefore, a decrease in NO_X emissions in this area produces a decrease in ozone concentrations at downwind locations from the power plant. In addition, offshore wind circulation produces localized decreases in ozone concentration along the southern part of the coast. Although large changes in ozone concentration occur in localized areas, peak ozone concentration in scenario DGEED is equal to the baseline peak.

On the other hand, the maximum increase in ozone concentration in scenario DGEED is 34 ppb. These large increases occur at night and next to the power plant located in Huntington Beach. This is due to a highly localized decrease in NO_X emissions in this location. NO_X at night acts as an important sink for ozone. Thus, a localized decrease in NO_X emissions leads to localized increases in ozone concentration. However, such increases do not occur during the day since baseline emissions are significantly larger.

6.4.2.9   Business-as-usual predictions

The specific mix of DG technologies that is likely to be installed in the SoCAB in 2010 is very difficult to forecast. This technology mix depends on the number and type of energy customers in the region, and a host of other economic and regulatory variables (e.g. electricity prices, gas prices, DG incentives, transmission constraints, emissions standards, etc.). Two scenarios have been developed to account for the current trends in DG technology adoption. Scenario BAU assumes a linear adoption of DG based on current data of DG penetration for each technology. Scenario BAU_par assumes a parabolic increased in the rate of adoption of DG technology. The emissions in scenario BAU end up being slightly lower than scenario PW2010, whereas emissions in scenario BAU_par are approximately twice as large as the emissions in PW2010.

As in previous cases, the detailed simulation of these three scenarios as applied to the south coast air basin in a state-of-the-art air quality model resulted in trends that are similar to those observed in most of the simulations. Figure 57 presents the difference in ozone concentrations between the DG scenarios (a) PW2010, (b) BAU, and (c) BAU_par, and the baseline case. Each of the three scenarios results in reduced ozone concentrations in the central areas and increased ozone concentrations over the eastern part of the basin. This trend has a larger and more widespread impact as emissions from DG increase (see Figure 57). Consistently observed trends such as these are perhaps the most certain results of the current effort, upon which the primary general conclusions of the study are based.

(a)   (b)

(c)
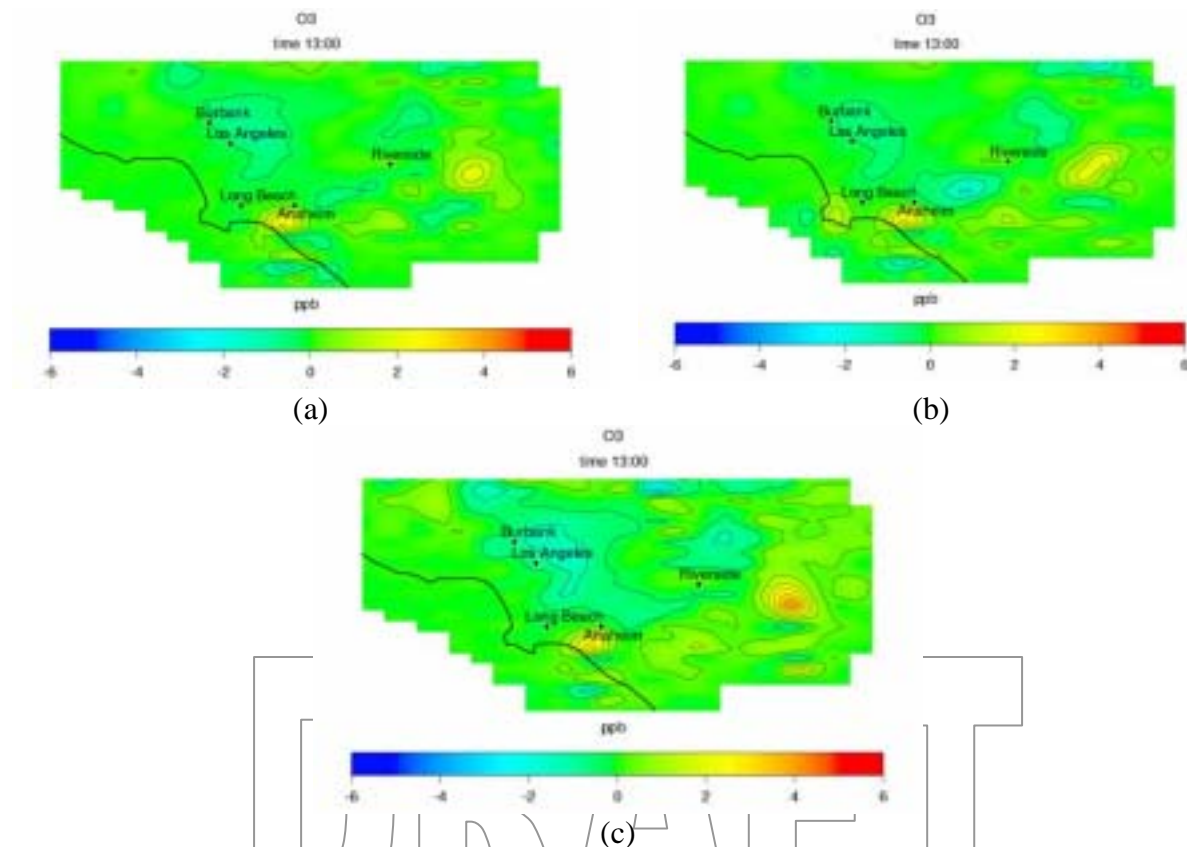
Figure 57. Difference in O₃ concentration (in ppb) at hour 13 between DG scenarios and baseline: a) PW2010, b) BAU, c) BAU_par

6.4.2.10 DG penetration

Forecasts of DG market penetration by 2010 suggest that 20% of the increased power demand may be met by DG with high market penetration. However, socio-economic factors might change the adoption of DG technologies in upcoming years. Scenario EHP assumes that 20% of the total energy demand will be supplied by DG, which is 5.5 times the DG power of scenario PW2010. EHP is the worst-case DG emissions scenario considered. Since scenario EHP uses the same DG technology mix as PW2010, emissions in EHP are 5.5 times larger than PW2010.

Figure 58 shows the difference in ozone concentrations at hour 13 between (a) the PW2010, and (b) the EHP spanning scenarios and the baseline case. Results show the tendency to reduce O₃ in the central areas of the basin and to increase O₃ downwind. Since scenario EHP introduces the highest NO$_X$ emissions, increases in ozone concentration at hour 13 are the largest for this case. Also, the decrease in ozone over the central area is more pronounced in scenario EHP than for any scenario (except for PeakPW_2). Although total NO$_X$ and VOC emissions of the EHP case are more than twice those of PeakPW_2, emissions of PeakPW_2 are concentrated in a six-hour time span.   As a result, air quality impacts caused by scenarios EHP and PeakPW_2 are comparable, indicating the importance of both duty cycle and overall emissions levels. Certainly

the high emissions of the EHP case (Figure 58b) lead to a more significant impact on ozone concentrations than the PW2010 case (Figure 58a).

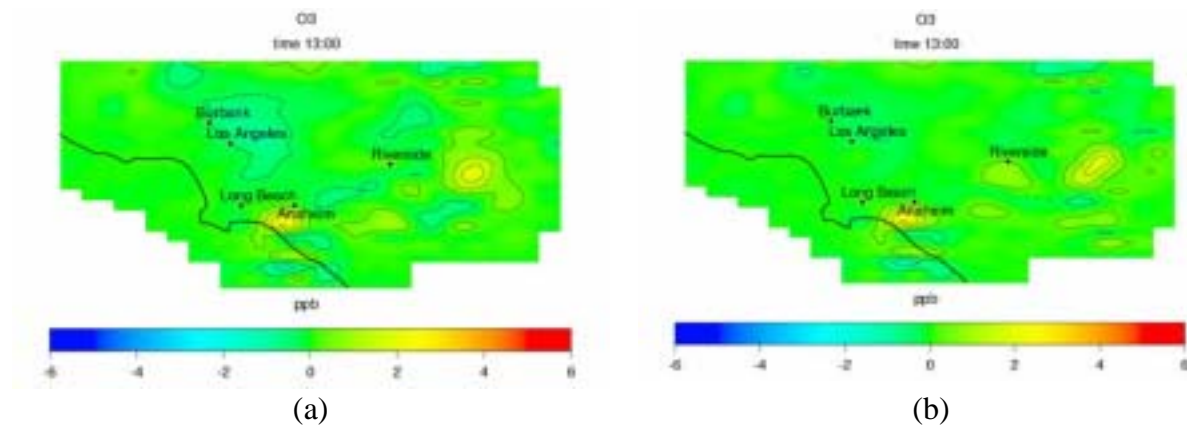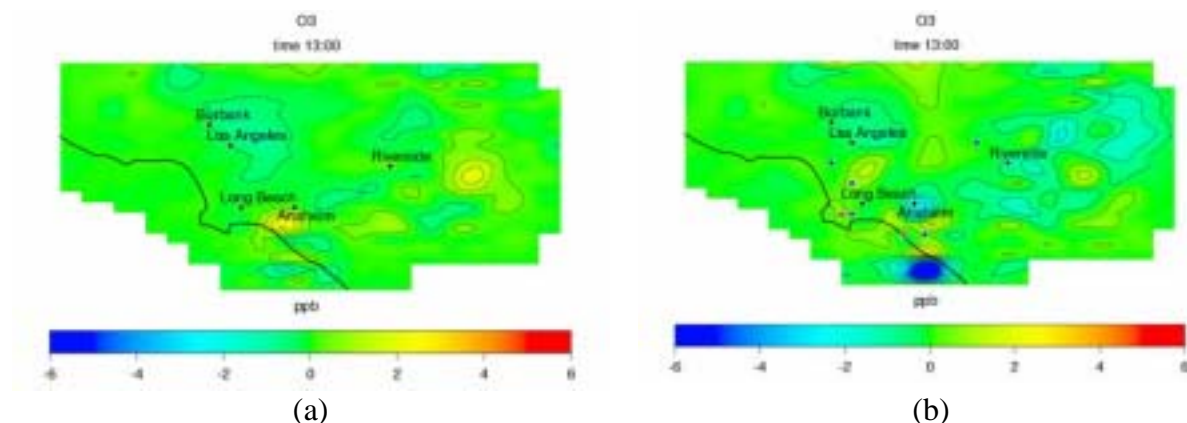(a)   (b)
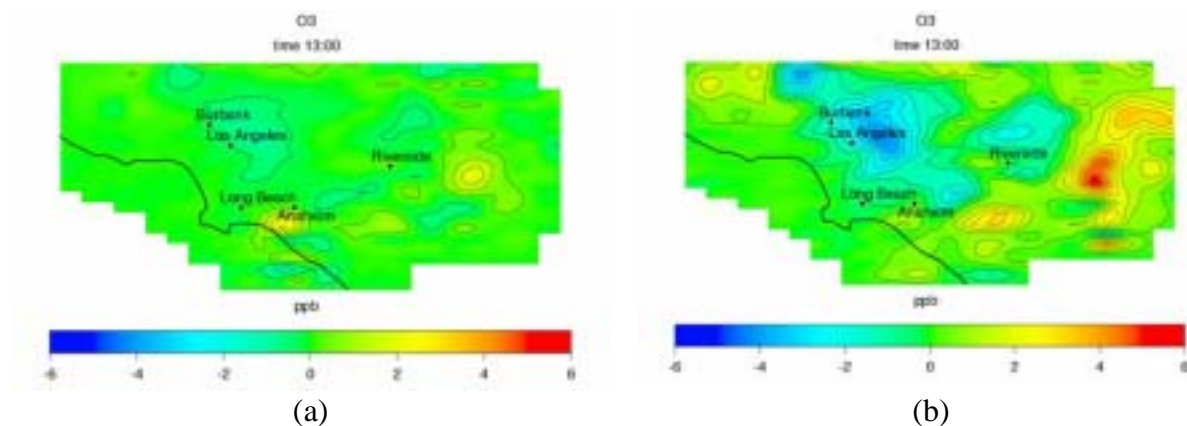
Figure 58. Difference in O$_3$ concentration (in ppb) at hour 13 between DG scenarios and baseline: a) PW2010, b) EHP

(a)   (b)

(c)
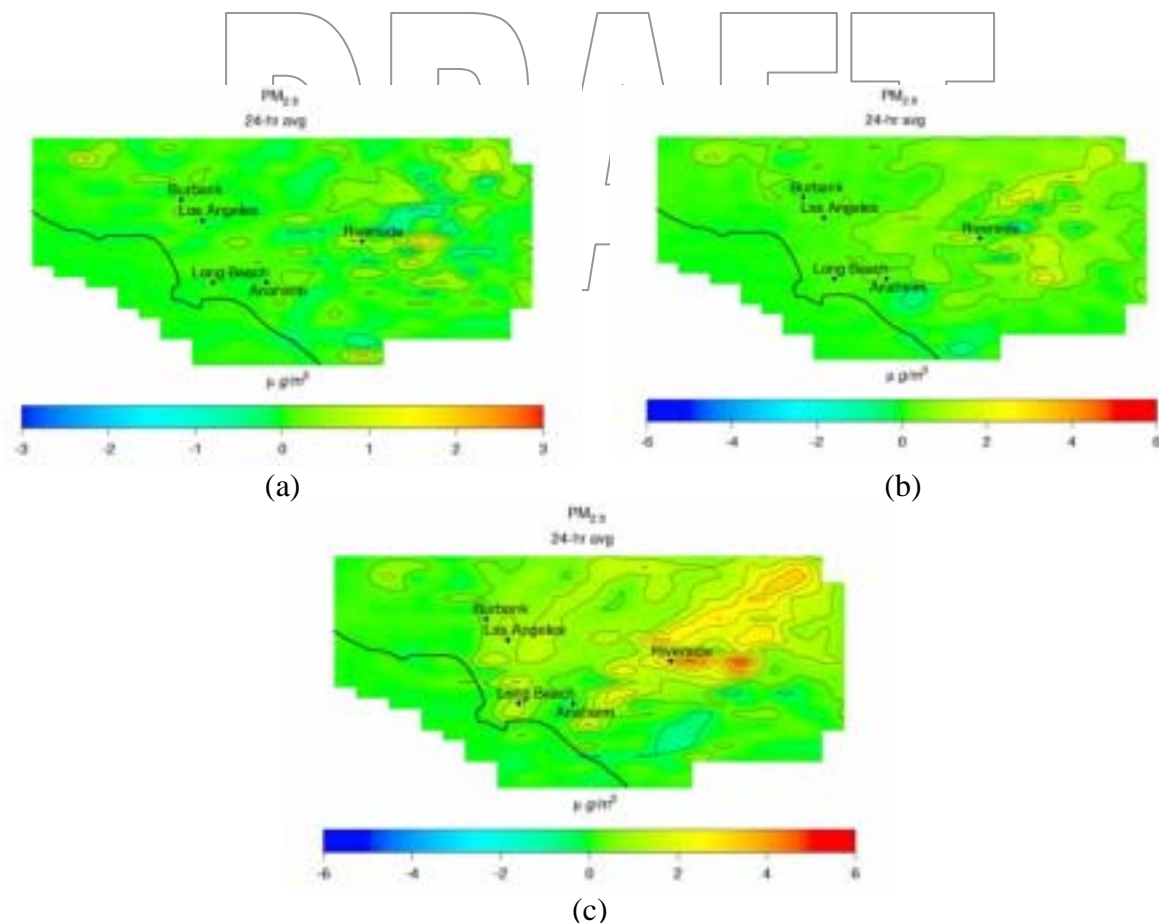
Figure 59. Difference in PM$_{2.5}$ 24-hour average concentration (in μg/m^3) between DG scenarios and baseline: a) PW2010, b) EHP, c) PeakPW_2

Differences in 24-hour average $PM_{2.5}$ concentration between the baseline case and three different scenarios are shown in Figure 59. Scenario PeakPW_2 (Figure 59b) produces a larger impact on $PM_{2.5}$ concentration than the EHP scenario (Figure 59a), even though the EHP scenario has the highest emissions of all scenarios.

In both scenarios (EHP and PeakPW_2) there is a net increase in $PM_{2.5}$ concentration over the eastern side of the basin, where nitric acid transported to from Los Angeles and ammonia emitted from cattle react to form secondary particulate matter. Scenario PeakPW_2 leads to a maximum increase in 24-hour average $PM_{2.5}$ concentration of 6 $\mu g/m^3$, being the largest increase among all the scenarios. Scenario EHP leads to a maximum increase in 24-hour average $PM_{2.5}$ concentration of 4 $\mu g/m^3$, the second largest increase among all the scenarios. As was the case for ozone concentration, operation of DG in a peaking duty cycle could impact secondary particulate matter formation much more significantly than if DG were operated constantly (base-loaded).

6.4.2.11 Performance Degradation

Degradation of DG units with time produces an increase in emissions. Baseline degradation rate assumed for most of the scenarios is such that produces an annual 3% increase in emissions due to equipment degradation. Scenario HPD assumes a higher degradation rate which causes an annual increase in emissions of 10%. The difference in the performance degradation implies that emissions introduced by scenario HPD are 13% higher than DG emissions assumed in scenario PW2010. Simulations show that small changes occur between scenarios regarding the impact on both ozone (Figure 60) and $PM_{2.5}$ concentration.

(a)   (b)
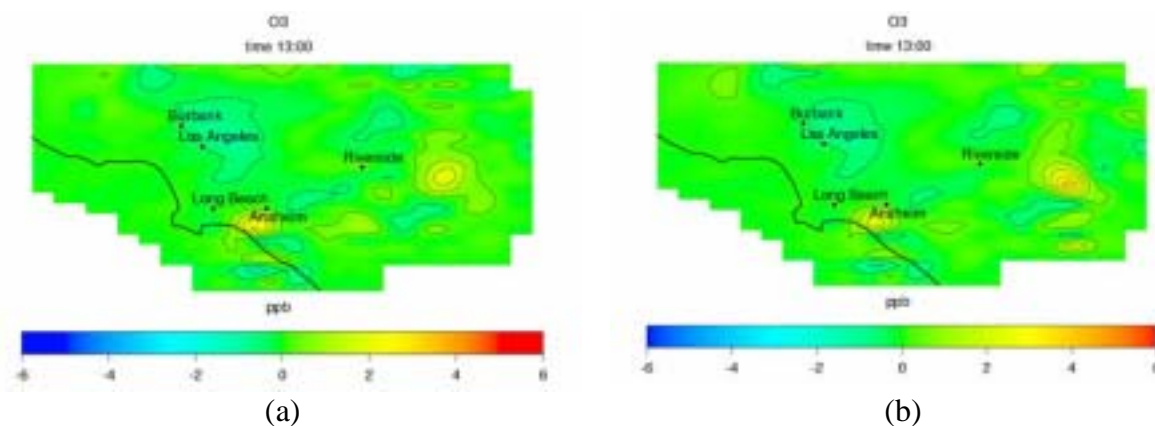
Figure 60. Difference in O_3 concentration (in ppb) at hour 13 between DG scenarios and baseline: a) PW2010, b) HPD

6.4.3   Air quality impacts of DG with 'attainment' inventory

The AQMD has been developing a baseline scenario for year 2010 in which ozone NAAQS is attained. This 'attainment' emission inventory has been continuously modified to include all different emission controls considered in the 2003 Air Quality Management Plan, and it has not been available for this work until recently. Therefore, most of DG air quality impacts have been evaluated with the 'non-attainment' emission inventory. Representative DG scenarios have been used with the 'attainment' scenario to discuss the effect of baseline emissions to the overall air quality impacts of DG. Difference in emissions between 'attainment' and 'non-attainment' scenarios are presented in Table 54.

Table 54.   Difference in emissions between 'attainment' and 'non-attainment' emission inventories

Species	Non-attainment ton/day	Attainment Ton/day	Change %
VOC	981	583	- 40.6
NO$_X$	407	296	- 27.3
CO	3,268	3,368	3.1
PM	580	580	0.0
SO$_X$	88	48	- 45.5
NH$_3$	168	168	0.0

In the attainment inventory, emissions of ozone precursors, VOC and NO$_X$, are reduced by 40% and 27%, respectively. These emission reductions lead to a decrease in peak ozone concentration of 20 ppb. In addition, the maximum 1-hour average concentration of NO$_2$ and the maximum 24-hour average concentration of PM$_{2.5}$ decrease by 48 ppb and 20 $\mu g/m^3$, respectively. Despite the emission reductions applied in the attainment inventory, ozone and PM$_{2.5}$ levels obtained in the simulations still exceed the NAAQS values (Table 55).

Table 55. Simulated concentration of some criteria pollutants: maximum hourly average concentration of O$_3$, NO$_2$ and CO and 24 hour-average concentration of PM$_{2.5}$ (2010 'attainment' scenario)

Species	Maximum	Location	Average	Time
O$_3$	218 ppb	San Bernardino	1 hr-average	13:00
NO$_2$	110 ppb	Ontario	1 hr-average	01:00
CO	3.0 ppm	Los Angeles	1 hr-average	08:00
PM$_{2.5}$	95 $\mu g/m^3$	Riverside	24 hr-average	N/A

With the use of the attainment inventory one would expect the air quality impacts of DG to be more intense, since the net increase in emissions due to DG relative total emissions is higher. Table 56 shows the relative increase of emissions due to DG with respect to the baseline and the attainment emission inventories, for selected DG scenarios. Even though the attainment emission inventory considers significantly lower emissions than the baseline inventory,

emissions from DG are still a small fraction of the total emissions. In particular, increase of VOC and NO_X emissions due to DG represent 1.01%, or less, with respect to total emissions.

Table 56. Basin-wide (in %) increase of primary criteria pollutant emissions relative to baseline and attainment emission inventories, for selected DG scenarios

Name DG Scenario	# DG Scenario	CO %	NO$_X$ %	VOC %	NH$_3$ %	SO$_X$ %	PM %
With respect to baseline emission inventory							
PW2010	**1**	0.25	0.37	0.13	0.13	0.08	0.16
PeakPW_2	**21**	0.40	0.74	0.31	1.05	1.60	0.35
#R1	**22**	0.07	-0.01	0.03	0.11	0.02	0.07
With respect to attainment emission inventory							
PW2010	**1**	0.26	0.51	0.22	0.13	0.15	0.16
PeakPW_2	**21**	0.41	1.01	0.52	1.05	2.93	0.35
#R1	**22**	0.07	-0.01	0.05	0.11	0.04	0.07

Impacts of DG on O_3 obtained by using the two different inventories differ slightly but increasingly as the emissions from DG increase. As shown in Table 57 and in Table 58, maximum increases in O_3 concentration due to DG are slightly larger if the attainment inventory is used. In increasing order of DG emissions, maximum increases in O_3 concentration due to DG scenarios #R1, PW2010 and PeakPW-2 are 3, 6, and 11 ppb when the attainment inventory is used. The same values obtained with the baseline inventory are 3, 4, and 8 ppb, respectively. Similar trends are observed for maximum decreases in O3 concentration. Nevertheless, maximum differences in ozone concentration occur in areas where the baseline O3 concentration is below the O3 NAAQS, regardless the emission inventory used.

Changes in the peak ozone concentration due to DG implementation are not affected significantly by the inventory used. As shown in Table 57 and in Table 58, peak ozone concentration increases by less than 2 ppb due to DG implementation regardless the emission inventory used.

Table 57. Maximum O_3 concentration, and maximum decrease and increase in O_3 concentration in each scenario

Scenario	Max (ppb)	Time	Max Increase (ppb)	Baseline reference (ppb)	Time	Max Decrease (ppb)	Baseline reference (ppb)	Time
dg_24h_R1_att	219	13	3	41	6	-11	96	16
dg_PW2010_att	218	13	6	72	15	-11	93	15
DgPeakPW2_att	220	13	11	61	18	-28	32	1

Table 58.   Maximum O₃ concentration, and maximun decrease and increase in O₃ concentration in each scenario

Scenario	Max (ppb)	Time	Max Increase (ppb)	Baseline reference (ppb)	Time	Max Decrease (ppb)	Baseline reference (ppb)	Time
dg_24h_R1	238	13	3	46	13	-2	60	12
dg_PW2010	238	13	4	46	13	-3	5	5
DgPeakPW2	239	13	8	10	2	-26	29	2

Impacts of DG scenarios on $PM_{2.5}$ using the attainment inventory are similar to the ones obtained when the baseline inventory is used. As shown in Table 59 and in Table 60, maximum increases in 24-hour average $PM_{2.5}$ concentration due to DG scenarios using the attainment inventory are the same as the ones obtained by using the baseline inventory. On the other hand, increases in the maximum 24-hour average are slightly larger if the attainment inventory is used.   In particular, maximum 24-hour average $PM_{2.5}$ concentration increases by 6 $\mu g/m^3$ (from 95 to 101 $\mu g/m^3$) in the DG scenario PeakPW-2, when the attainment inventory is used. In contrast, the same value only changes by 1 $\mu g/m^3$ (from 115 to 116 $\mu g/m^3$) if the baseline inventory is used. For the other two scenarios, differences due to the use of the two inventories are less important.

Table 59. Maximum 24-hour average $PM_{2.5}$ concentration, and maximun decrease and increase in 24-hour average $PM_{2.5}$ concentration in selected scenarios, ussing the attainment inventory

Scenario	Max ($\mu g/m^3$)	Max Increase ($\mu g/m^3$)	Baseline reference ($\mu g/m^3$)	Max Decrease ($\mu g/m^3$)	Baseline reference ($\mu g/m^3$)
#R1_att	95	3	72	-2	61
PW2010_att	96	3	53	-2	41
PeakPW-2_att	101	6	95	-3	41

Table 60. Maximum 24-hour average $PM_{2.5}$ concentration, and maximun decrease and increase in 24-hour average $PM_{2.5}$ concentration in selected scenarios, using the baseline inventory

Scenario	Max ($\mu g/m^3$)	Max Increase ($\mu g/m^3$)	Baseline reference ($\mu g/m^3$)	Max Decrease ($\mu g/m^3$)	Baseline reference ($\mu g/m^3$)
#R1	115	3	45	-2	44
PW2010	114	3	78	-1	90
PeakPW-2	116	6	75	-2	14

In general, DG scenarios add a relatively small mass of pollutants to the total emissions. Hence, even if baseline emissions are reduced significantly – as in the attainment scenario – emissions introduced by DG still add a small portion relative to total emissions. Therefore, air quality

impacts of scenarios with low and moderate DG penetration do not vary significantly with changes in the baseline emissions inventory. Conversely, air quality impacts of scenarios with high DG penetration are more sensitive to changes in the baseline emissions.

6.5 Uncertainty and Sensitivity Analysis

6.5.1 Chemical mechanism

This section presents a portion of the overall sensitivity analysis methodology described above to the chemical mechanism itself. The results presented herein focus upon the examination of those chemical mechanism features that most significantly affect the prediction of ozone formation, destruction, and resulting atmospheric concentration.

Figure 61 presents mean ozone concentrations and their corresponding 1σ (standard deviation) uncertainty bounds as a function of time for each simulated case. The standard deviation provides a measure of how spread out the distribution of results is when perturbed in the manner described above. The standard deviation at each hour (σ_j) is defined as

$$\sigma_j = \sqrt{\frac{\sum_{i=1}^{N}(X_{ij} - \mu_j)^2}{N-1}} \tag{26}$$

where X_{ij} is the value of the parameter for the ith sample, μ_j is the mean at each simulated hour, and N is the number of samples. Final ozone concentrations range from 186 ± 75 ppb at a VOC/NO$_x$ ratio of 8:1 to 420 ± 77 ppb at a VOC/NO$_x$ ratio of 17:1. At VOC/NO$_x$ ratios higher than 17:1, O$_3$ concentrations using nominal CACM parameters are closer to the mean values from the Monte Carlo simulations. A measure of the statistical deviation is the root mean square (*RMS*) deviation between nominal (c_n) and mean (μ) value concentrations defined as

$$RMS = \sqrt{\frac{\sum_{i=1}^{N}(c_n - \mu)^2}{N}} \tag{27}$$

For the higher VOC/NOx ratios, the *RMS* = 0.007 at a 17:1 ratio, and *RMS* = 0.006 at a 32:1 ratio. At the 8:1 ratio, the nominal parameters (parameters used in the baseline CACM model) lead to ozone concentrations that are consistently under-predicted compared to the best estimates (*RMS* = 0.01) of the sensitivity analyses. However, the predictions still lie within one standard deviation of the best estimates.

Figure 62 shows the time variation for ozone relative uncertainties, presented as parts per million difference over the mean parts per million predicted. This figure illustrates that CACM exhibits the largest relative errors for ozone concentrations at a VOC/NO$_x$ ratio of 8:1 where the maximum error is 44%, these uncertainties then decrease at the 17:1 ratio (28%), and are the smallest at 32:1 (down to 26%).
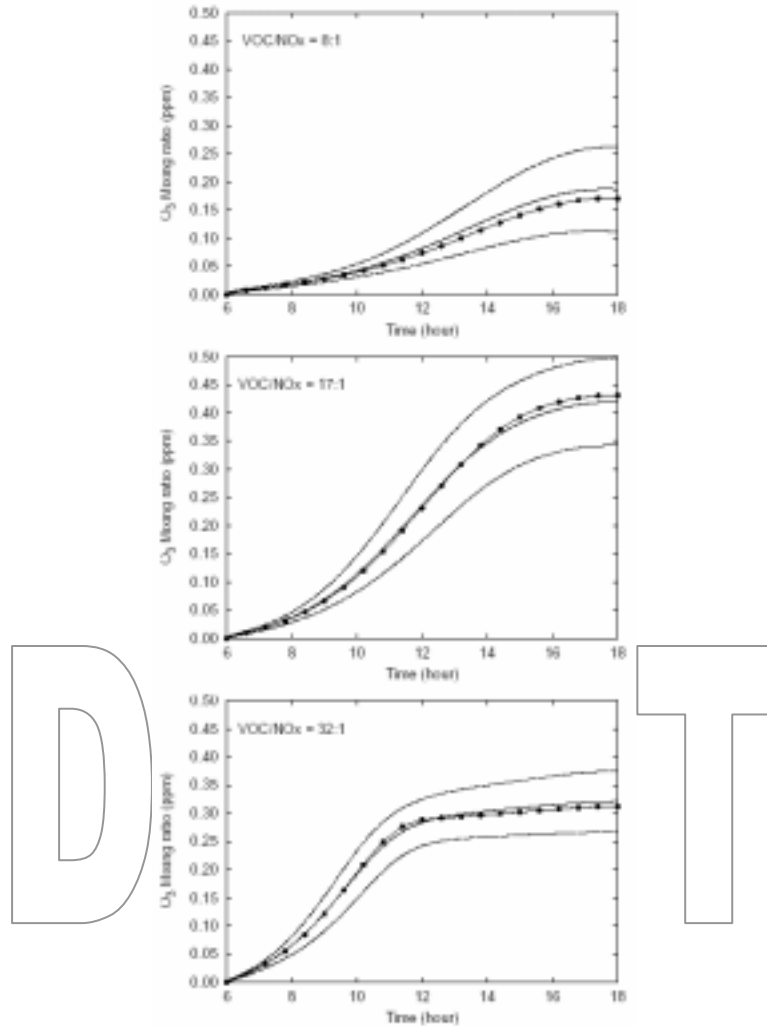
Figure 61. Mean concentrations and 1σ uncertainty ranges for ozone at different VOC/NOx ratios. Solid line, mean from all results; line with circles, concentrations with nominal parameters; dashed curves, 1σ uncertainty bounds for results.
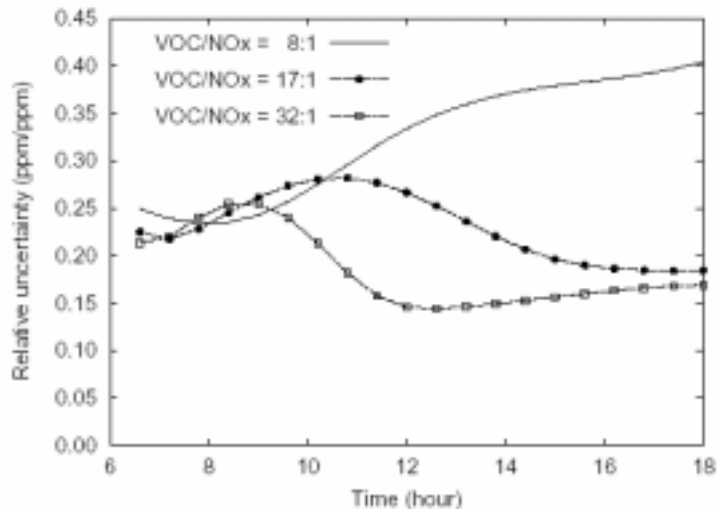
Figure 62. Relative uncertainty for ozone as a function of time for indicated VOC/NO$_x$ ratios. Uncertainty is defined as the estimated σ divided by the mean from all results.

Table 61 shows the most important reactions ordered in terms of their contribution to ozone relative uncertainty from most to least significant. The regression analysis shows that at VOC/NO$_x$ ratios less than 17:1 the NO$_2$ photolysis rate and HCHO + hv → CO + 2 HO$_2$ are the reactions that most significantly contribute to ozone uncertainty. However, ozone itself is more sensitive to changes in the reaction rate of O$_3$ with NO to regenerate NO$_2$ and the reaction of OH with NO$_2$ to produce nitric acid. Reactions that also contribute to the total uncertainty of ozone are the photolysis reactions of methyl glyoxal (MGLY) and the lumped higher aldehydes. This is consistent with the original formulation of CACM, since MGLY is modeled to behave as an aldehyde.

Results at VOC/NO$_x$ ratios of 32:1 differ from those at lower ratios. Although NO$_2$ photolysis remains the major contributor to ozone uncertainty, the second most uncertain rate parameter is that of the reaction of the acyl radical (RO26) from aldehydic H abstraction of the lumped aldehydes with NO. However, in terms of sensitivity, ozone loss with NO is more important than that of RO26. The fact that reactions that involve the acyl radical RO26, the acyl peroxy radical RO28, and peroxy alkyl nitrates (PAN1 and PAN2) become relevant at these ratios is a consequence of the low NO$_x$ concentrations. As a result, peroxy radical reactions begin to become important at high VOC/NOx ratios. At sufficiently low NO$_x$ concentrations or high VOC/NO$_x$ ratios, a further decrease in NO$_x$ favors peroxy-peroxy reactions that in effect retards O$_3$ formation by removing free radicals from the system.

Table 61. Most Important Parameters Based on the Contributions to Uncertainty on the Time-Averaged O_3 Concentrations

Reaction : Product	Regression Coefficient	Uncertainty Contribution %
VOC/NO$_x$ = 8:1		
$HCHO + h\upsilon \rightarrow CO + 2\ HO_2$	0.413	25
$NO_2 + h\upsilon$	0.470	19
$ALD2 + h\upsilon$	0.240	8
$NO_2 + OH + M$	-0.699	5
$MGLY + h\upsilon$	0.127	5
$NO + O_3$	-0.591	4
$RO_234 + NO$	-0.088	3
$ALKL + OH$	0.181	3
RO_234	0.080	2
$HCHO + h\upsilon$	-0.125	2
VOC/NO$_x$ = 17:1		
$NO_2 + h\upsilon$	0.341	21
$HCHO + h\upsilon \rightarrow CO + 2\ HO_2$	0.220	15
$MGLY + h\upsilon$	0.142	12
$RO_26 + NO$	0.085	6
$RO_26 + NO_2 + M$	-0.106	3
$RO_234 + NO$	-0.064	3
$NO + O_3$	-0.364	3
$ALD2 + h\upsilon$	0.097	3
RO_234	0.055	2
$NO_2 + OH + M$	-0.319	2
VOC/NO$_x$ = 32:1		
$NO_2 + h\upsilon$	0.342	35
$RO_26 + NO$	0.091	11
$MGLY + h\upsilon$	0.085	7
$RO_26 + NO_2 + M$	-0.110	6
$PAN1$	0.094	4
$RO_28 + NO$	0.057	4
$HCHO + h\upsilon \rightarrow CO + 2\ HO_2$	0.088	4
$NO + O_3$	-0.306	4
$PAN2$	0.082	3
$RO_28 + NO_2 + M$	-0.080	3

6.5.2   Air quality model

6.5.2.1   Model Uncertainty

This section examines the uncertainty ranges exhibited by simulated ozone and particulate matter concentrations as the result of changes in selected input values. Both, spatial and temporal variations of model uncertainties are investigated for the SoCAB. Given the large amount of output data produced by the model evaluation, detailed study of the time variation of

uncertainties is performed only for six stations (Simi Valley, Burbank, Central Los Angeles, Long Beach, Riverside, and San Bernardino). However, modeling results for these sites represent the general aerosol dynamics and trends for ozone throughout the basin. For example, the location at Central Los Angeles experiences particularly intense emissions from automobiles as a hub of the region's freeway system and also exhibits great secondary photochemistry, whereas Riverside represents those areas downwind of major emissions, where higher concentrations of both ozone and secondary species are typically present.

6.5.2.1.1 Time

In order to investigate the uncertainty of modeled species as time progresses, concentrations time series are summarized as box plots. These box plots provide an alternative, more efficient display of the multiple distributions that result from the statistical analyses. Figure 63 shows ozone mixing ratios as a function of time at selected sites in the form of box plots, using the output of all Monte Carlo simulations. In this figure, the endpoints (hinges) of the gray boxes are formed by the lower and upper quartiles of the data, i.e., where the 25th and 75th percentiles lie. The horizontal line within the box represents the median. The bars above and below the box (whiskers) are drawn from each hinge to the most extreme measurement inside the inner fence. The inner fence is a distance equivalent to 1.5 the difference between upper and lower quartiles (inter-quartile range, IQR). Box plots contain the same information as a distribution function, but in a reduced form allowing the time dependence of the distributions to be presented in the regions of interest. The selection of a norm is necessary to investigate the error bounds of species considered. A value of interest is the 1-hr maximum concentration during the last day of simulation, since this norm is of most concern to those interested in complying with regional and national air quality standards (Gipson et al., 1981; Meyer, 1986).

Figure 63 presents box plots for the six stations, each showing the photochemical nature of ozone formation. However, the particular hour at which the maximum ozone mixing ratio occurs differs in each site analyzed. It is apparent from Figure 63 that sites at Riverside and San Bernardino are located in areas with large domain-wide ozone mixing ratios. Ozone maxima occur at 15:00 in Riverside (median = 96 ppb) and at 16:00 in San Bernardino (median = 111 ppb). Model uncertainty at these peaks is similar as indicated by the IQR value of 15 ppb in both places.

Close examination of the box plots at the peaks shows that the length of the whiskers is approximately the same, an indication that the distribution is symmetrical. This observation suggests that a Gaussian distribution function fits the output data variation adequately and may better characterize the uncertainty of these predictions. Figure 64a compares the cumulative distribution function (CDF) as estimated by the model simulations and the best fit to a normal distribution curve. The comparison is made at Riverside and Central Los Angeles for a 12-hr average that comprises most of the daylight time, when ozone concentrations are significant, starting at 8:00. Similar results (not shown) have been plotted also for the remaining stations. Two parameters are required to determine completely a normal CDF, namely the mean (μ) and the standard deviation (σ). Figure 64 shows that calculated normal distributions fit the data adequately. Furthermore, RMS of the difference between fitted and simulated values when the distributions are assumed normal is always smaller than when the distributions are assumed log-

normal. Therefore, a normal probability density distribution is adopted to describe the variance of predicted concentrations.

Figure 63. Box plots for simulated ozone mixing ratios from Monte Carlo runs at different sites in the SoCAB. Median, upper and lower quartiles are shown inside the gray box.
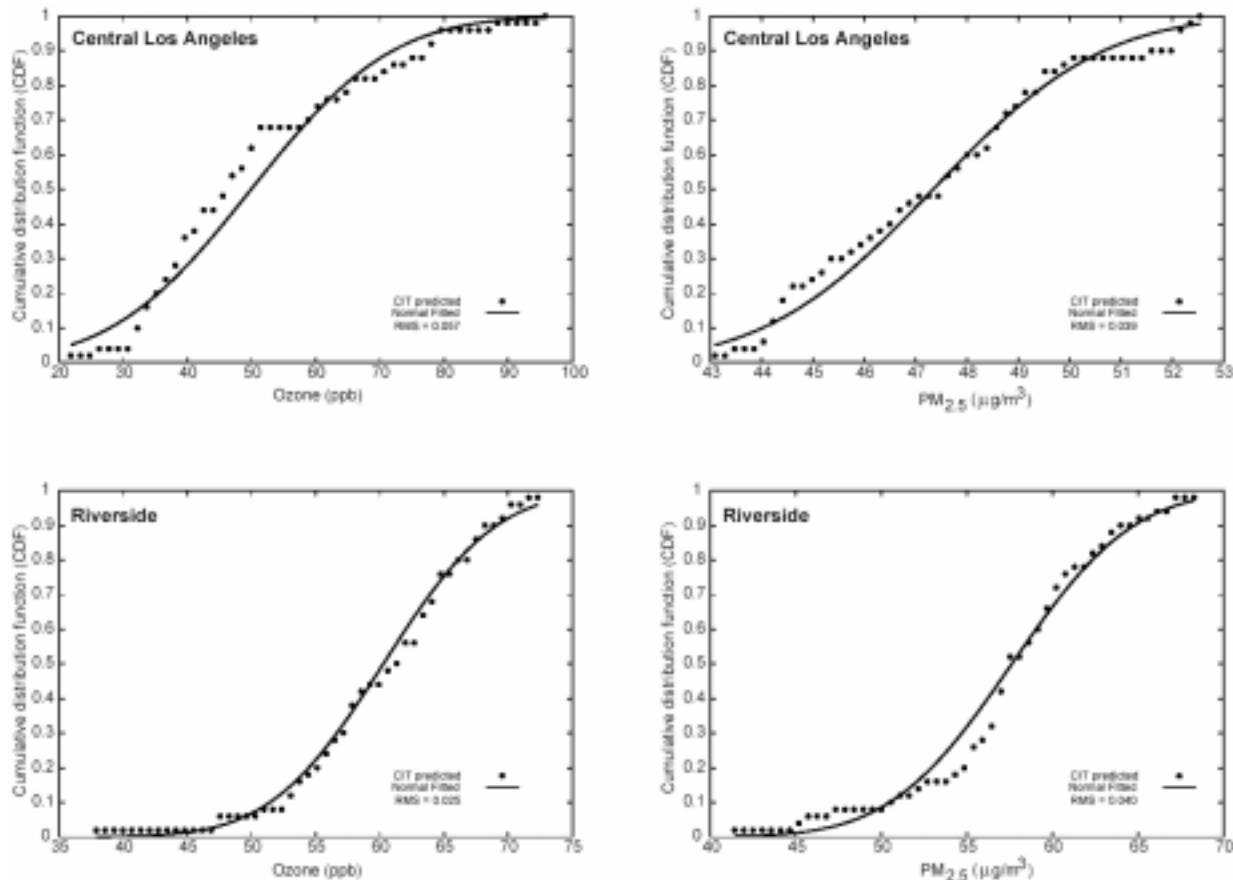
Figure 64. Comparison between the cumulative distribution function (CDF) estimated from 50 Monte Carlo runs (shown as bullets) and the best-fit normal distribution (solid line). Ozone and PM$_{2.5}$ concentrations shown for Riverside and Central LA.

Figure 65 shows the time evolution of PM$_{2.5}$ aerosol at selected sites in the form of box plots. Sites in Riverside and San Bernardino show the largest basin-wide aerosol concentrations, consistent with the formation of secondary particulate matter observed in measurements and previous studies (Meng et al., 1998; Nguyen and Dabdub, 2002b). Predicted PM$_{2.5}$ maxima occur at 6:00 and 7:00 respectively in Riverside (mean = 114 μg m^{-3}) and San Bernardino (mean = 146 μg m^{-3}). Model uncertainty in these two locations is within the same order of magnitude given the IQR values of 10 and 21 μg m^{-3} respectively. Figure 64b compares simulation results with the fit to a normal CDF. The comparison is made for 24-hr average PM$_{2.5}$ aerosol in Riverside and Central LA. As with ozone, variance of PM$_{2.5}$ data can also be characterized with a normal probability distribution. Calculated distributions show that the estimated variance is comparable in Riverside (σ = 11 μg m^{-3}) and San Bernardino (σ = 16 μg m^{-3}). As in the case of ozone, the hours in which the uncertainty of PM$_{2.5}$ predictions is the greatest do not coincide with the time when predicted concentrations reach their maximum.
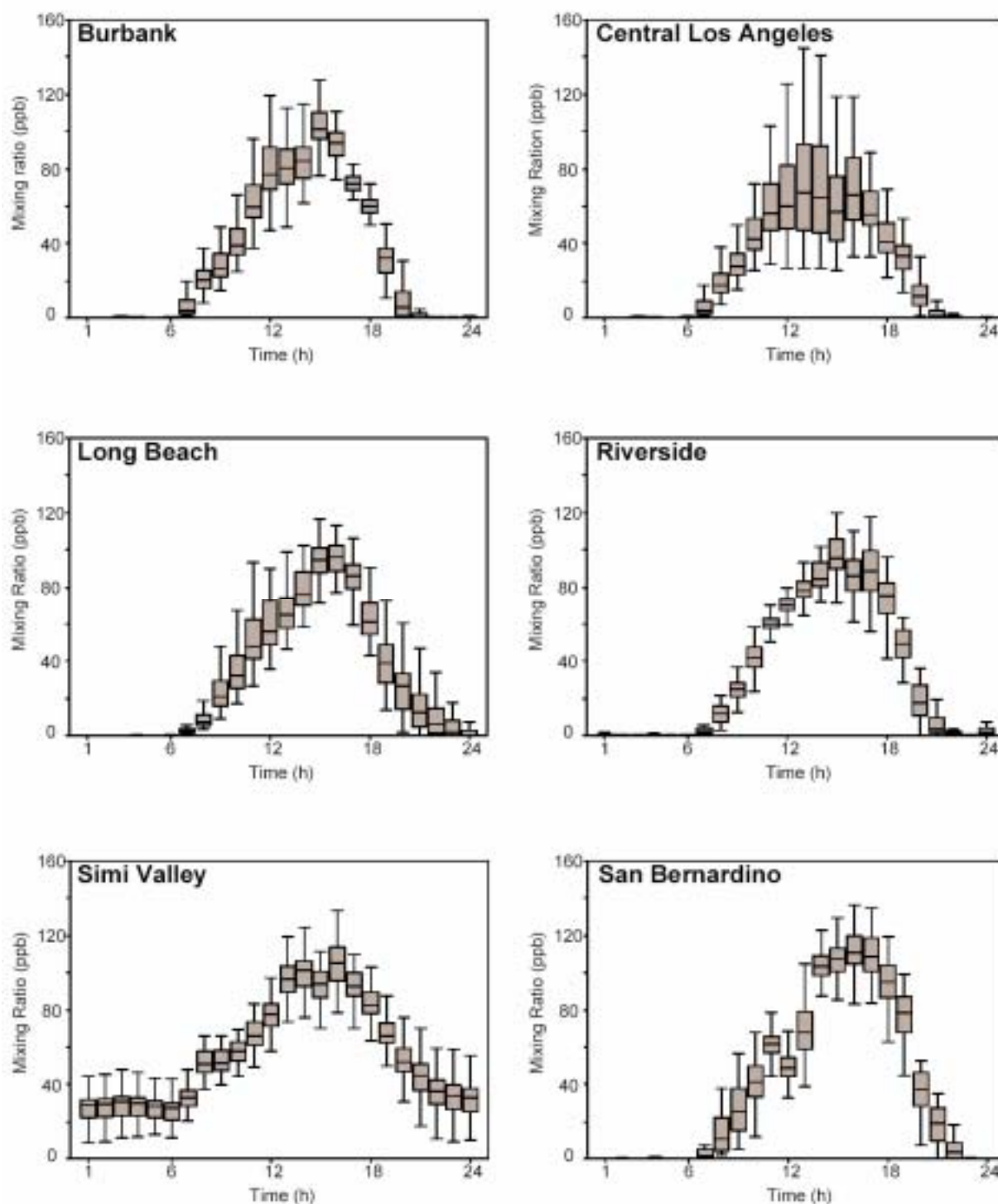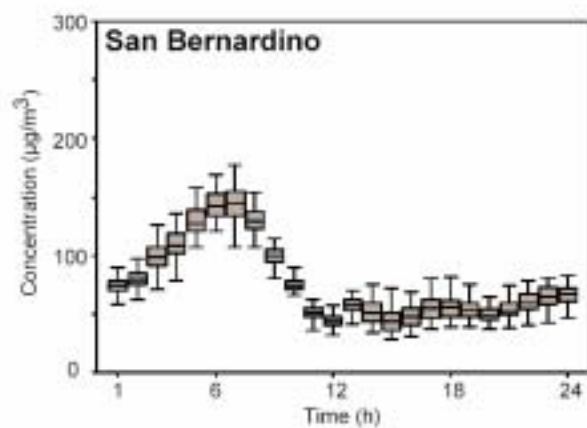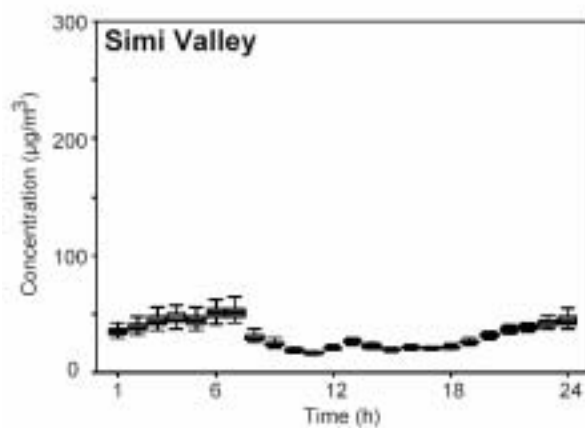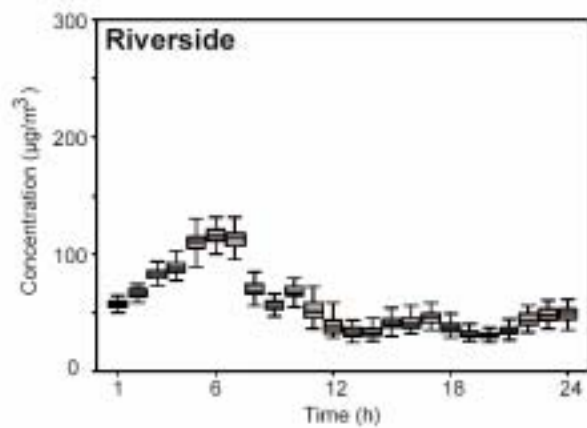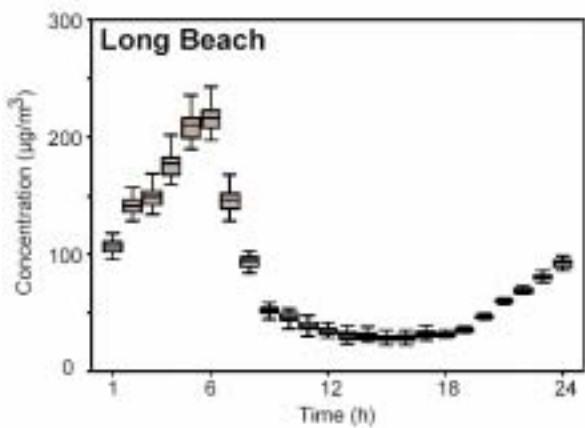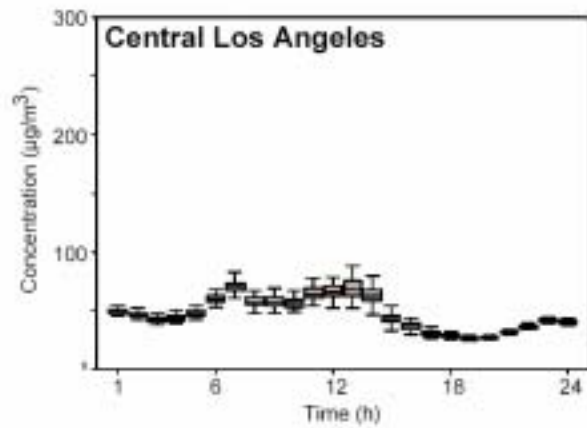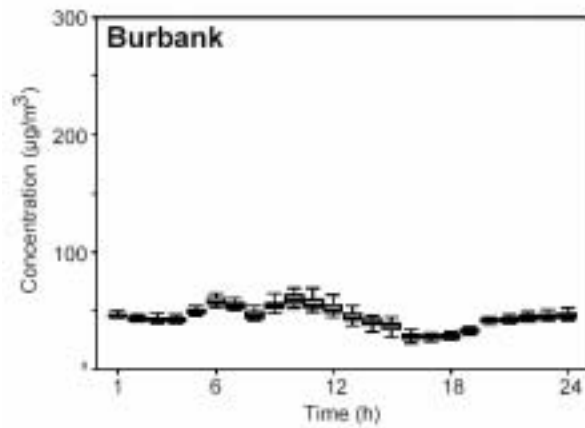
Figure 65. Box plots for simulated PM2.5 concentrations from Monte Carlo runs at different sites in the SoCAB. Median, upper and lower quartiles are shown inside the gray box.
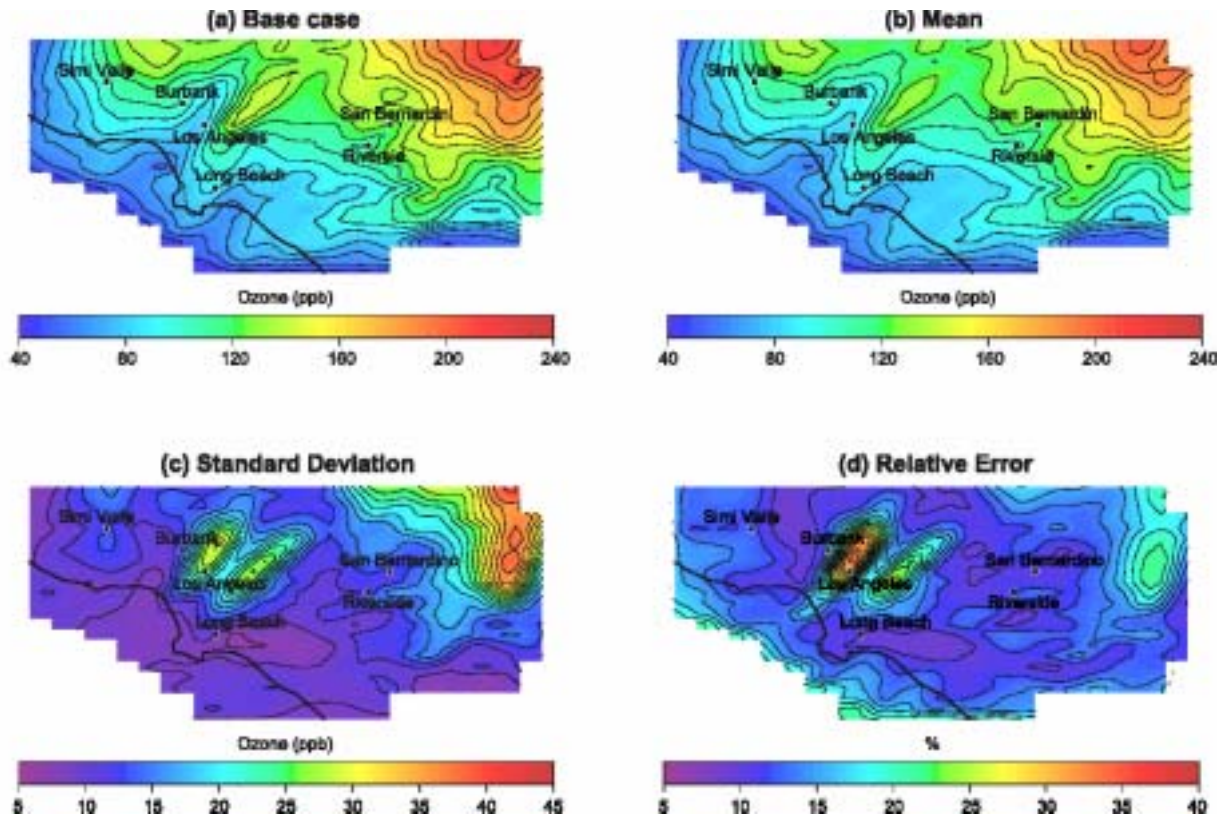
Figure 66. Plots of ozone a) base case, b) mean mixing ratios, c) standard deviation and d) estimated relative error for the 1-hr maxima of the third day of simulation.

6.5.2.1.2 Space

The spatial variation of model uncertainties is determined with probability density distributions that best describe the variance of predicted concentrations in the SoCAB. For ozone, 1-hr maximum concentrations are stored and subsequently plotted for each location in the basin during the 24 hours that correspond to the third day of simulation. This procedure offers a general portrait of maximum values everywhere in the domain, regardless of the specific hour in which they occurred. For $PM_{2.5}$, a similar process is followed with the exception that concentrations stored represent 24-hr averages. Uncertainties associated with these concentrations are important since compliance with air quality standards is required for domain-wide peak concentrations.

Figure 6 compares the basin-wide mean, estimated from Monte Carlo simulations, with the ozone base case throughout the SoCAB. The corresponding comparison for aerosol $PM_{2.5}$ is

shown in Figure 7. Base case results in both figures characterize the concentrations calculated using nominal values for the input parameters. These figures show that the location and numerical values of maxima are equivalent for both, the base case and the mean. Further comparison with calculated median concentrations (not shown) demonstrate that normal probability density distributions adequately describe the variance of predicted concentrations.
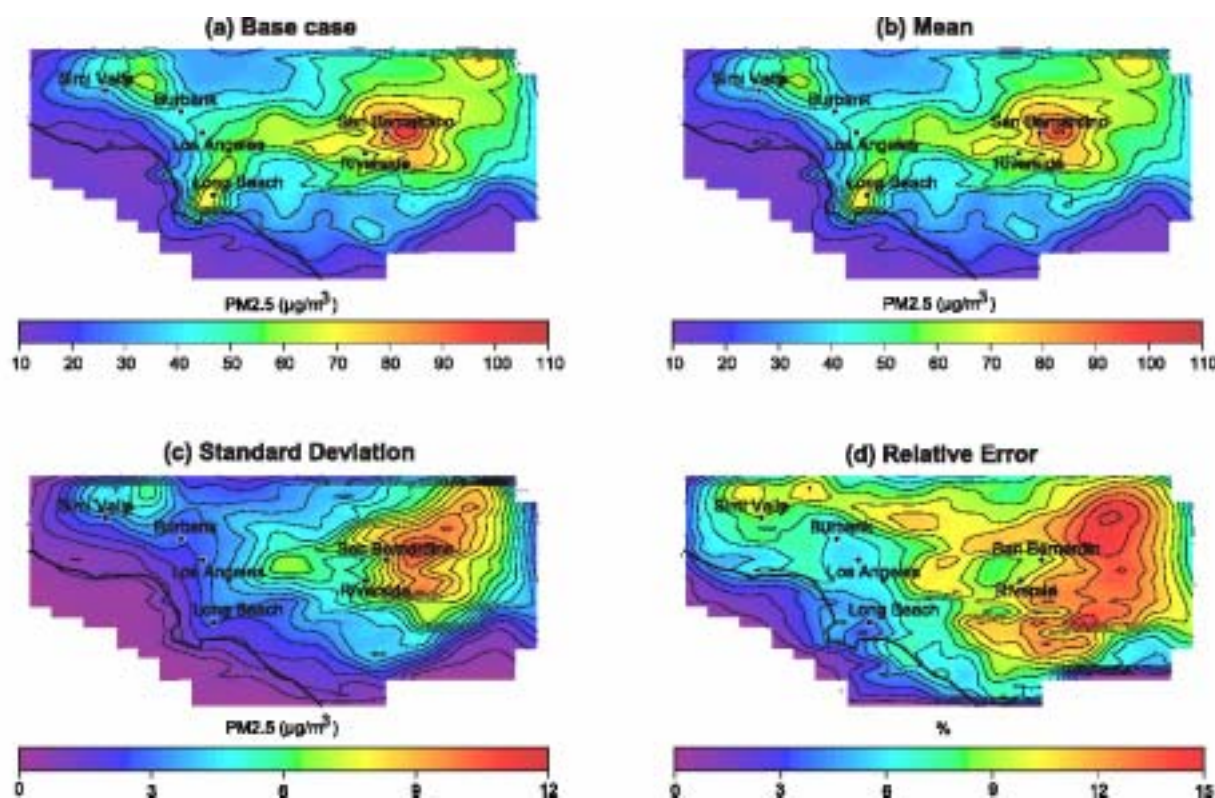
Figure 67. Plots of aerosol PM$_{2.5}$ a) base case, b) mean concentrations,   c) standard deviation and d) estimated relative error for the 1-hr maxima of the third day of simulation.

Figures 6 and 7 present the estimated basin-wide standard deviation and mean for ozone and PM$_{2.5}$ concentrations, and not only the statistics of a limited number of sites. The largest ozone mixing ratios arise on the eastern side of the basin, consistent with previous studies (Meng et al., 1998; Nguyen and Dabdub, 2002b) and observations (CARB, 2002, 2003). Moreover, calculated σ reveals that the variation of modeled ozone mixing ratios is not the largest in this area of the basin. For instance, the location with the largest mixing ratio (221 ppb) shows a σ of 37 ppb, which is equivalent to a relative error of 17%. In contrast, a location with one of the largest basin-wide relative errors (42%) is Central Los Angeles that exhibits concentrations in the range of 76 ± 32 ppb.

For PM$_{2.5}$ aerosol, Figure 7 illustrates that the highest concentrations are observed near Riverside and San Bernardino, consistent with previous predictions and observations. East of San

Bernardino the largest domain-wide concentrations (108 ± 11 µg m^{-3}) present a relative error of 10%. However, the location with the largest relative error (17%) is found southeast of Riverside with concentrations of 48 ± 8 µg m^{-3}. Although modeled output variations are not the smallest in the regions where PM$_{2.5}$ aerosol reaches its maximum it is bounded to less than 15% relative error.

6.5.2.2   Sensitivity analysis

Sensitivity of ozone and PM$_{2.5}$ aerosol concentrations to selected input variables is explored following the methodology described in Section 5.3.3.1.2. Instead of using stepwise regression analysis at each time step, regression coefficients are calculated using 12-hr averaged concentrations for ozone and 24-hr averages are for PM$_{2.5}$ aerosol. This approach lessens the computational demands in the present analysis and also provides information of the sensitivity values that are of interest for compliance with air quality standards. Table 62 presents a list of the input variables with significant influence in the prediction of ozone mixing ratios at selected sites throughout the domain. Table 62 shows, for each parameter, the calculated standardized regression coefficients (SRC) and the corresponding contribution to the total uncertainty (UC) expressed as a percentage. The regression coefficients values are a measure of the sensitivity of ozone and PM$_{2.5}$ to changes in the input parameters.

Table 62. Most Important Parameters Based on the Contributions to Uncertainty of Ozone at Selected Cases.

Riverside			San Bernardino			Los Angeles		
Parameter	SRC	UC	Parameter	SRC	UC	Parameter	SRC	UC
$R^2 = 0.69$			$R^2 = 0.93$			$R^2 = 0.98$		
NO$_x$ emissions	-0.549	29.2	NO$_x$ emissions	-0.755	56.2	NO$_x$ emissions	-0.683	48.3
side VOC	0.478	23.7	side VOC	0.494	24.8	side VOC	0.531	32.9
NO + O$_3$	0.282	80.0	VOC emissions	0.250	6.4	side O$_3$	0.345	11.7
			NO + O$_3$	0.146	1.9	side NO$_x$	0.199	4.1
			alkenes + OH	0.120	1.4	VOC emissions	0.059	0.3

Burbank			Long Beach			Simi Valley		
Parameter	SRC	UC	Parameter	SRC	UC	Parameter	SRC	UC
$R^2 = 0.94$			$R^2 = 0.96$			$R^2 = 0.98$		
NO$_x$ emissions	-0.767	60.7	NO$_x$ emissions	-0.674	46.8	side O$_3$	0.702	45.1
side O$_3$	0.417	18.6	side O$_3$	0.518	29.4	side NO$_x$	0.572	28.2
side NO$_x$	0.259	7.7	side VOC	0.361	14.3	side VOC	-0.369	13.7
side VOC	0.234	5.4	side NO$_x$	0.217	4.6	NOx emissions	0.305	9.4
						VOC emissions	0.062	0.4
						NH$_3$ emissions	-0.056	0.3

In general the regression model explains 69 to 98% of the ozone uncertainty as reflected by the R^2 values, with the smallest value (69%) reported for Riverside. Variation in basin-wide NO$_x$

emissions and side boundary conditions imposed on VOC are the most significant contributors to uncertainty and sensitivity of ozone predictions. Ozone boundary conditions have contributions to uncertainty that range from 18.6 to 45.1% in the west side of the SoCAB. The largest contribution (45.1%) is located in Simi Valley, a site close to the boundaries of the computational domain. The SRC sign indicates that increasing NO_x emissions leads to reductions in ozone mixing ratios. In contrast, increasing the values of ozone and VOC's side boundary conditions results in higher ozone mixing ratios.

Results in Table 62 suggest the regions analyzed are VOC-limited or have low VOC-to-NO_x ratios. This is typical of city centers and plumes immediately downwind of NO_x sources. The results are consistent with the basin residing in an overall NO_x-rich state, and with findings in previous studies (Meng et al., 1997). However, most sites also show that VOC and ozone boundary conditions have an important effect on ozone concentrations. Some of these results reflect the proximity to the computational boundaries, like Simi Valley, and the lesser amount of NO_x emissions in that region (higher VOC-to-NO_x ratios).

Table 63. Most Important Input Parameters Based on the Contributions to the Uncertainty of $PM_{2.5}$ aerosol concentrations at Selected Cases.

Riverside			San Bernardino			Los Angeles		
Parameter	SRC	UC	Parameter	SRC	UC	Parameter	SRC	UC
$R^2 = 0.90$			$R^2 = 0.93$			$R^2 = 0.93$		
NO_x emissions	0.792	61.1	NOx emissions	0.773	56.6	NH_3 emissions	0.723	45.6
NH_3 emissions	0.436	18.9	NH_3 emissions	0.531	28.3	NOx emissions	0.476	21.9
side VOC	-0.146	2.6	$NO + O_3$	0.174	3.1	side NOx	0.316	10.8
$NO + O_3$	0.131	1.8	side O_3	-0.137	1.6	side O_3	0.258	7.2
side O_3	-0.131	1.5	VOC emissions	0.104	1.0	$NO + O_3$	0.157	2.5
side NOx	-0.122	1.4	$NO_2 + h\nu$	0.096	0.9	$NO_2 + h\nu$	0.141	1.9
alkenes + OH	0.112	1.2				Side VOC	0.121	1.4

Burbank			Long Beach			Simi Valley		
Parameter	SRC	UC	Parameter	SRC	UC	Parameter	SRC	UC
$R^2 = 0.94$			$R^2 = 0.94$			$R^2 = 0.95$		
NO_x emissions	0.667	38.9	NH_3 emissions	0.685	39.1	NO_x emissions	0.701	43.7
NH_3 emissions	0.631	36.0	NO_x emissions	0.518	25.4	side NOx	0.539	24.9
side NOx	0.303	8.2	side NOx	0.404	16.4	side VOC	-0.425	16.2
side VOC	-0.250	5.6	side O_3	0.300	9.1	NH_3 emissions	0.258	6.1
side O_3	0.126	1.6	$NO_2 + h\nu$	0.136	1.8	side O_3	0.128	1.7
$NO_2 + h\nu$	0.123	1.4	$NO + O_3$	0.098	0.9	$NO_2 + h\nu$	0.087	0.8
$NO + O_3$	0.111	1.3						

A similar analysis is applied to $PM_{2.5}$ for the selected sites in the SoCAB (Table 63). The regression model explains 90 to 95% of the variation that the computational model exhibits for

$PM_{2.5}$ aerosol concentrations. In most selected sites, $PM_{2.5}$ aerosol concentrations are most sensitive to changes in NH_3 and NO_x emissions. The positive sign of the SRC values indicates that any increase in NO_x or NH_3 emissions results in higher $PM_{2.5}$ aerosol concentrations, consistent with the finding that a mayor component of this aerosol in the basin is ammonium nitrate (Nguyen and Dabdub, 2002b).

7   SUMMARY AND CONCLUSIONS

7.1   Summary

The present study investigates the air quality impacts of DG in the SoCAB for the year 2010. The scenarios presented here are developed with a systematic process, which includes the use of detailed data from geographic information systems databases. The scenarios are simulated in a state-of-the-art air quality model to assess environmental impacts of potential DG installation throughout the SoCAB. Results in this work lead to the following findings and conclusions:

- CHP emissions displacements associated with most of the realistic scenarios lead to significant reductions in some criteria pollutant emissions and CO_2 emissions. For NO_X, displaced boiler emissions are higher than NO_X emissions directly produced by DG, resulting in net negative values for realistic scenarios with CHP.
- Realistic DG implementation scenarios introduce small basin-wide mass increments no larger than 0.43% with respect to baseline emissions. Mass increments for spanning DG scenarios are no larger than 1.35%.
- The spatial distribution of DG power based on GIS land-use data results in DG scenarios that concentrate large capacity DG technologies nearby industrial zones due to the relatively high adoption rate intensity factor estimated for the industrial sector.
- The calculation of basin-wide DG power distribution amongst the various sectors showed that 60% of total DG power is implemented in the industrial sector and nearly 32% is going to the commercial-institutional sector.
- Results of basin-wide relative contribution of each type of DG technology showed that 49% of the DG market is being met by gas turbines, whereas ICEs, MTGs, PV, FC, and GT-FC hybrids account for 17%, 15%, 5%, 10% and 4% of the total 2010 DG power market, respectively.
- In general, increases in NO_X emissions produced by DG scenarios reduce ozone concentrations in the central area of Los Angeles – typically VOC-limited – and increase ozone concentrations at downwind locations – typically NO_X-limited. Increases in NO_X emissions also lead to an increase in 24-hour average $PM_{2.5}$ concentrations over downwind locations near Riverside. Scenarios in which there is a net reduction of NO_X due to emissions displacement by CHP produce small increments in ozone over the central area of Los Angeles and no significant changes elsewhere
- With representative characterizations of DG use in SoCAB for the year 2010 the air quality impacts of DG scenarios are:

  Realistic DG scenarios:
  o Maximum basin-wide ozone concentrations do not change. Changes in maximum 24-hour average $PM_{2.5}$ range from 0 to –3 $\mu g/m^3$
  o Maximum changes in ozone concentrations at any point throughout the basin range from +5 ppb to –9 ppb. Increases of up to 3 ppb in ozone concentration occur in areas where baseline values already exceed air quality standards.
  o Maximum changes in 24-hour average $PM_{2.5}$ concentrations range within $\pm 3 \mu g/m^3$

Spanning DG scenarios:
o Changes in basin-wide maximum ozone concentration ranges within ± 1 ppb. Maximum 24-hour average $PM_{2.5}$ changes from –2 µg/m^3 to +2 µg/m^3
o Typically, maximum changes in ozone concentrations at any point throughout the basin are within ±10 ppb, although there are specific cases in which changes in ozone concentration range from –26 ppb to +34 ppb. Maximum changes in 24-hour average $PM_{2.5}$ concentrations range from -4 µg/m^3 to +6 µg/m^3

- Various cases with different DG spatial distributions are explored. The level of emissions introduced by these spanning DG scenarios produce similar air quality impacts. However, additional scenarios that place a considerably higher concentration of DG show that air quality impacts due to DG are affected by the geographical location of DG units. In particular, results suggest that if DG is to be widely used in the basin, then it should not be concentrated in a small area
- Different temporal distributions of DG emissions are explored. Results show that an amount of DG emissions concentrated during a 6-hours period (peak duty cycle) produce a larger impact in air quality than the same amount emitted during 24 hours (base load duty cycle)

Also, this study investigates the uncertainty and sensitivity of ozone and $PM_{2.5}$ aerosol to variations in selected input parameters using a Monte Carlo methodology. The selection of input parameters is based in their potential to affect the concentrations predicted by the model and also to reflect changes in emissions due to DG implementation in the SoCAB. Numerical simulations are performed with the CIT three-dimensional air quality model. Multiple model evaluations are completed, and statistical methods applied to identify those parameters with the largest effect on both the predicted concentrations of selected species and the uncertainty associated with their prediction. This analysis leads to the following findings:

- Comparison between basin-wide distributions of base case and calculated mean values demonstrate that normal probability density distributions are the most adequate to characterize the uncertainty of modeled spatial maxima throughout the basin. Therefore domain-wide error bounds for species considered here are reported in terms of standard deviation values, consistent with the normal distributions
- The largest relative error for ozone is approximately 42% (76 ± 32 ppb), whereas maximum concentrations show an error of approximately 17% (221 ± 37 ppb). For $PM_{2.5}$, the largest error is ~17% (48 ± 8 µg m^{-3}), but the largest domain-wide concentration (108 ± 11 µg m^{-3}) has a relative error of 10%
- Results show that changes no greater than 70 to 80% in nominal values of input variables results in 18 to 40% variability of ozone mixing and $PM_{2.5}$ aerosol concentrations.
- Sensitivity analyses performed in this work demonstrate that the variation in side boundary conditions imposed on VOC and NO_X emissions are the major contributors to uncertainty and sensitivity of ozone predictions in most regions throughout the SoCAB
- Ozone boundary conditions have a marginal contribution to uncertainty in most locations, except for sites located near the boundaries of the computational domain. An increase in

NO$_X$ emissions leads to reductions in ozone mixing ratios. In contrast, increasing the values of VOC's side boundary conditions results in higher ozone mixing ratios. This is due to ozone formation being VOC-limited over most of the SoCAB

- Sensitivity analyses also show that PM$_{2.5}$ aerosol is sensitive to changes in NH$_3$ and NO$_X$ emissions. Furthermore, increasing these emissions results in higher PM$_{2.5}$ aerosol concentrations throughout the basin.

7.2   Conclusions

- Simulation of realistic* DG implementation scenarios for the year 2010 shows that peak basin-wide ozone concentration[†] does not increase due to DG installation
- The CIT Airshed model is sensitive enough to predict trends in ozone and PM$_{2.5}$ concentrations in the basin due to DG emissions
- There are discernable increases and decreases in local concentrations of ozone and PM$_{2.5}$ that can be attributed to DG installation in SoCAB in 2010
- Observed maximum local changes in air quality due Realistic DG Scenarios are:
    - < 3 ppb O$_3$
    - < 2 μg/m^3 PM$_{2.5}$
- Observed maximum local changes in air quality due Spanning DG Scenarios are:
    - < 10 ppb O$_3$
    - < 6 μg/m^3 for PM$_{2.5}$
- Simulation of DG scenarios shows consistently observable changes/trends in ambient concentrations of ozone and PM$_{2.5}$ due to DG installation
    - Maximum increases in pollutant concentrations occur in areas with typically poor air quality (San Bernardino, Riverside)
    - Maximum decreases occur in locations already in attainment
- Concentration of DG units in a small area leads to higher air quality impacts than spreading DG units over large areas
- Operation of DG in a duty cycle with a high peak of electricity production leads to higher air quality impacts than DG operation in a base-loaded mode that introduces the same total daily emissions
- DG air quality impacts in out-years or with higher DG penetration may have significant air quality impacts that affect both attainment and local air quality

---

* Realistic DG implementation scenarios include consideration of the current regulatory framework (i.e., current CARB 2003 and 2007 standards and AQMD BACT requirements) and detailed DG market, DG use, and geographic information systems (GIS) data.

[†] Peak basin-wide 1-hour ozone concentration is the parameter upon which compliance with current federal standards is determined.

8   RECOMMENDATIONS AND FUTURE WORK

8.1   Recommendations

The current work has produced the following recommendations regarding the impacts of DG on air quality:

- The impact of DG installation on air quality should be studied through use of a detailed understanding and development of DG implementation scenarios
- Air quality assessments should not be made without the application of DG emissions to a detailed atmospheric chemistry and transport model that includes all the major chemical and physical processes and geographic and meteorological features of the region of interest.
- Substantial DG emissions should not be released in concentrated spatial locations.
- Substantial DG emissions should not be concentrated in their temporal release into urban air sheds.
- If possible, DG should be installed and operated in as disperse a manner as possible in space and time to reduce potential air quality impacts.
- Clean DG, such as fuel cells and photovoltaics, have the least air quality impact and should be preferred to other DG that have higher emissions levels.

8.2   Future Work

Based on the conclusions of the present study listed above, the authors recommend that the Energy Commission investigate and consider several research and policy initiatives as follows:

- This study is the first effort to design DG implementation scenarios at a urban level following a systematic procedure that ultimately generate gridded emissions to be used in a three-dimensional air quality model. The authors recommend using the capability for development of DG implementation scenarios advanced in the present study to develop DG implementation scenarios for other polluted local areas/regions in California.
- Air quality models and their input requirements are tools that are updated continuously. Hence, the authors recommend supporting advancement of air quality models and air quality models input data in other regions for consideration of DG implementation.
- DG has the potential of being implemented throughout the state of California. However, as in Los Angeles area, there are other areas with air pollution problems. The authors recommend applying air quality modeling tools to study the impacts of DG on local air quality in other regions of interest such as:
  - San Joaquin Valley (CA)
  - Bay Area (CA)
- This study is based on air quality impacts at 5 km x 5 km grid resolution. However, emissions from DG may impact exposure to contaminants at more local scale. Hence, it is recommended to support air quality studies for DG impacts at a localized scale using high-resolution local models.

- The use of DG may reduce emissions of CO_2 and other green house gases due to higher fuel utilization. The authors recommend the CEC support studies of DG impacts on emissions of green house gases on the California scale. These studies should be done using a life cycle analysis approach which can address not only emissions during operation, but, overall emissions associated with fuel production, technology manufacture, technology disposal or recycle. In addition, authors recommend analyses to consider and evaluate a carbon reduction policy that includes the benefits of fuel cells and other DG for GHG reductions.
- There is not sufficient data available on DG performance degradation to study increase of emissions caused by installation aging. For this study, performance degradation has been estimated, but authors recommend the CEC study performance degradation of DG and its effects on increase of DG emissions
- Speciation of DG emissions is limited to generic groups of contaminants. To better capture the air quality impacts of DG the authors recommend to develop more comprehensive speciation profiles for DG emissions

9 REFERENCES

Air Quality Management Plan (AQMP). Air Quality Management District (AQMD). Available at: http://www.aqmd.gov/aqmp/AQMD03AQMP.htm, 2003.

Allen, P. SoCAB emissions inventory, The California Air Resources Board.

Allison, J. E. and Lents, J. (2002). Encouraging distributed generation of power that improves air quality: can we have our cake and eat it too? Energy Policy 30(9): 737-752, 2002.

ARB 2000. Emission information for facilities, http://www.arb.ca.gov/app/emsinv/facinfo, 2000.

Atkinson R. Atmospheric chemistry of VOCs and NOx. Atmos. Environ. 34, 2063-2101, 2000.

Attachment to the Air Quality Management Plan (AQMP). Air Quality Management District (AQMD). Available at: http://www.aqmd.gov/aqmp/AQMD03AQMP.htm Attachment available at: http://www.aqmd.gov/aqmp/docs/2003aqmd_appv_calgrid.pdf, 2003.

Bärtsch-Ritter N., Keller J., Dommen J. And Prévôt S. H. Effects of various meteorological conditions and spatial emission resolutions on the ozone concentration & ROG/Nox limitation in the Milan area (I), Atmos. Chem Phys. Discuss., 3, 733-768, 2003.

Baugues, K., A review of NMOC, NO_x ratios measured in 1984 and 1985, Rep. EPA/450/4-86-015, U.S. Environ. Prot. Agency, Research Triangle Park, N. C., 1986.

Benkovitz C. M., Berkowitz C. M., Easter R. C., Nemesure S., Wagener R. and Schwarz S. E. Sulfate over the North Atlantic and adjacent continental regions: evaluation for October and November 1986 using a three-dimensional model driven by observation-derived meteorology. J. geophys. Res. 99(D10), 20,725-20,756, 1994.

Bergin, M. S., G. S. Noblet, K. Petrini, J. R. Dhieux, J. B. Milford, and R. A. Harley, Formal uncertainty analysis of a Lagrangian photochemical air pollution model, Environ. Sci. Technol., 33, 1116-1126, 1999.

Boedecker, E., Cymbalsky, J. and Wade, S. Modeling Distributed Generation in the NEMS building models, Energy Information Administration, 2000.

CARB, 2002. The 2002 California Almanac of Emissions and Air Quality of the California Air Resources Board. http://www.arb.ca.gov/aqd/almanac/almanac.htm, 2002.

CARB, 2003. Monitoring Sites in the South Coast Air Basin. California Air Resources Board web site. http://www.arb.ca.gov/adam/mapfiles/scozone.html, 2003.

Carmichael, G. R., A. Sandu, and F. A. Potra, Sensitivity analysis for atmospheric chemistry models via automatic differentiation, Atmos. Environ., 31, 475-489, 1997.

Carreras M., Medrano M., Samuelsen G. S., Brouwer J., Rodriguez, M. A., Dabdub D. Urban air quality impacts of distributed generation. Proceedings of ASME Turbo Expo 2004, Power for Land, Sea, and Air. June 14-17, 2003, Vienna, Austria

Chin, G., Dixon, H., Kato, J. and Komorniczack, A. Guidance for the Permitting of Electrical Generation Technologies, Air Resources Board, 2001.

Chock D. P. A comparison of numerical methods for solving the advection equation – III. Atmos. Environ. 19, 571-586, 1991.

Chock D. P., Winkler S. L. A comparison of advective algorithms coupled with chemistry. Atmos. Environ. 28, 2659-2676, 1994.

CPUC 2003. California Self-Generation Incentive Program. Second Year Impacts Evaluation Report, Tirón Inc., prepared for Southern California Edison, 2003.

Dabdub D., DeHaan L. L. and Seinfeld J. H. Analysis of ozone in the San Joaquin Valley of California. Atmos. Environ. 33, 2501-2514, 1999.

Dabdub D., Seinfeld J. H. Numerical advective schemes used in air quality models – sequential and parallel implementation. Atmos. Environ. 28, 3369-3385, 1994.

DeMore, W. B., S. P. Sander, D. M. Golden, M. J. Molina, R. F. Hampson, M. J. Kurlyo, C. J. Howard, and A. R. Ravishankara, Chemical Kinetics and Photochemical Data for Use in Stratospheric Modeling, Evaluation Number 9, JPL Publ., 90-1, 1990.

Derwent, R., and Ø. Hov, Application of sensitivity and uncertainty analysis techniques to a photochemical ozone model, J. Geophys. Res., 93, 5185-5199, 1988.

Dunker, A. M., Efficient calculation of sensitivity coefficients for complex atmospheric models, Atm. Environ., 15, 1155-1161, 1981.

Dunker, A. M., The decoupled direct method for calculating sensitivity coefficients in chemical kinetics, J. Chem. Phy., 81, 2385-2393, 1984.

Ehhalt, D. H., J. S. Chang, and D. M. Butler, The probability distribution of the predicted CFM-induced ozone depletion, J. Geophys. Res., 84, 7889-7894, 1979.

EIA 1999. 1998 Manufacturing Energy Consumption Survey (MECS), Energy Information Agency, 1999.

EIA 1999. A Look at Residential Energy Consumption in 1997, Energy Information Agency, 1999.

EIA 2000. A Look at Building Activities in the 1999 Commercial Buildings Energy Consumption Survey (CBECS), Energy Information Agency, 2000.

ENERGY COMMISSION 1999. Market Assessment of CHP in the State of California, Onsite Sycom Energy Corporation, prepared for California Energy Commission, 1999.

ENERGY COMMISSION 2001. California Power Plants Database, California Energy Commission, http://www.energy.ca.gov/database/index.html#powerplants, 2001.

ENERGY COMMISSION 2003. Current, Expected and Approved Peaker Power Plants, California Energy Commission, http://www.energy.ca.gov/maps/PEAKER_MAP.PDF, 2003.

Gao, D., W. R. Stockwell, and J. B. Milford, First-order sensitivity and uncertainty analysis for a regional-scale gas-phase chemical mechanism, J. Geophys. Res., 100, 23,153-23,166, 1995.

Gao, D., W. R. Stockwell, and J. B. Milford, Global uncertainty analysis of a regional-scale gas-phase chemical mechanism, J. Geophys. Res., 101, 9107-9119, 1996.

Gipson, G. L., Freas, W., Kelly, R., Meyer, E. Guideline for use of city-specific EKMA in preparing ozone SIPs. EPA-450/4-80-027, U.S. Environmental Protection Agency, Research Triangle Park, N.C., 1981.

Grenfell, J. L., N. H. Savage, R. M. Harrison, S. A. Penkett, O. Forberich, F. J. Comes, K. C. Clemitshaw, R. A. Burgess, L. M. Cardenas, B. Davison, G. G. McFadyen, Tropospheric box-modeling and analytical studies of the hydroxyl (OH) radical and related species: Comparison with observations, J. Atmos. Chem., 33, 183-214, 1999.

Griffin R. J., Nguyen K., Dabdub D., Seinfeld J.H. A coupled hydrophobic-hydrophilic model for predicting secondary organic aerosol formation. Journal of Atmospheric Chemistry 44: 171-190, 2003.

Griffin RJ. Dabdub D. Seinfeld JH. Secondary organic aerosol - 1. Atmospheric chemical mechanism for production of molecular constituents - art. no. 4332. *Journal of Geophysical Research-Atmospheres. 107(D17):4332*, 2002a.

Griffin RJ. Dabdub D. Kleeman MJ. Fraser MP. Cass GR. Seinfeld JH. Secondary organic aerosol - 3. Urban/regional scale model of size- and composition-resolved aerosols - art. no. 4334. [Article] *Journal of Geophysical Research-Atmospheres. 107(D17):4334*, 2002b.

Hakami, A., Odman, M. T., Russell, A.G. High-order, direct sensitivity analysis of multidimensional air quality models. Environmental Science and Technology 37, 2442-2452, 2003.

Hanna, S. R, Chang, J. C., Fernau, M. Monte Carlo estimates of uncertainties in predictions by a photochemical grid model (UAM-IV) due to uncertainties in input variables. Atmospheric Environment 32, 3619-3628, 1998.

Hanna, S. R, Davis, J. M. Evaluation of a photochemical grid model using estimates of concentration probability density functions. Atmospheric Environment 36, 1793-1798, 2002.

Hanna, S. R, Z. G. Lu, H. C. Frey, N. Wheeler, J. Vukovich, S. Arunachalam, M. Fernau, and D. A. Hansen, Uncertainties in predicted ozone concentrations due to input uncertainties for the UAM-V photochemical grid model applied to the July 1995 OTAG domain, Atmos. Environ., 35, 891-903, 2001.

Harley R. A., Russell A. G., McRae G. J., Cass G. R. and Seinfeld J. H. Photochemical Modeling of the Southern California Air Quality Study. Environ. Sci. Technol. 27, 378-388, 1993.

Helton, J. C. Uncertainty and sensitivity analysis techniques for use in performance assessment for radioactive waste disposal. Reliability Engineering and System Safety 42, 327-367, 1993.

Ianucci, J., Horgan, S., Eyer, J. and Cibulka, L. Air Pollution Emissions Impacts Associated with the Economic Market Potential of Distributed Generation in California, Distributed Utility Associates, prepared for The California Air Resources Board, 2000.

Iman, R. L., and J.C. Helton., A comparison of uncertainty and sensitivity techniques for computer models, Rep. SAND83-2365, U.S. Dep. of Energy, Sandia Natl. Lab., Albuquerque, N. M., 1984.

Iman, R. L., Conover.,W. J. Small sample sensitivity analysis techniques for computer models with an application to risk assessment. Communications in Statistics A9, 1749–1842, 1980.

Knipping E. M. and Dabdub, D. Impact of chlorine emissions from sea-salt aerosol on coastal urban ozone. *Environ. Sci. Technol.* 37, (2003) 275-284

Jenkin ME. Saunders SM. Pilling MJ. The tropospheric degradation of volatile organic compounds - a protocol for mechanism development. [Article] *Atmospheric Environment. 31(1):81-104, 1997 Jan.*

Jenkin ME. Saunders SM. Pilling MJ. The tropospheric degradation of volatile organic compounds - a protocol for mechanism development. [Article] *Atmospheric Environment. 31(1):81-104, 1997 Jan.*

Jimenez P., Baldasano J. M., Dabdub D. Comparison of photochemical mechanisms for air quality modeling. Atmos. Environ. 37, 4179-4194, 2003

Kay, M. (2003). Personal communication, SCAQMD.

Knipping EM. Dabdub D. Modeling surface-mediated renoxification of the atmosphere via reaction of gaseous nitric oxide with deposited nitric acid. [Article] *Atmospheric Environment. 36(36-37):5741-5748, 2002 Dec.*

Lenssen, N.. The California Power Crisis. The Role of Distributed Generation. Cogeneration and On-Site Power Generation 2(3), 2001.

Lents, J., Allison, J. E. Can We Have Our Cake and Eat It, Too? Creating Distributed Generation Technology to Improve Air Quality, University of California Riverside, CA, prepared for the Energy Foundation, 2000.

Li Y., Dennis R. L., Tonnesen G. S., Pleim J. E. Effects of uncertainty in meteorological inputs on O3 concentration, O3 production efficiency, and O3 sensitivity to emissions reductions in the Regional Acid Deposition Modeling. In: Preprints of the 10th Joint Conference on the Applications of Air Pollution Meteorology with Air and Waste Management Association, January 11-16, 1998, Phoenix, Arizona, Paper no. 9A.14, American Meteorological Society, Boston, MA, pp. 529-533

Little, A. Opportunities for Micropower and Fuel Cell Gas Turbine Hybrid Systems in Industrial Applications, Arthur D Little, prepared for Lockheed Martin Energy Research Corporation and the DOE Office of Industrial Technologies, 2000.

Marnay, C., Chard, J. S., Hamachi, K. S., Lipman, T., Moezzi, M. M., et al. Modeling of Customer Adoption of Distributed Energy Resources, Consortium for Electric Reliability Technology Solutions, Ernest Orlando Lawrence Berkeley National Laboratory, prepared for California Energy Commission, 2001.

McCay, M. D., W. J. Conover, and R. J. Beckman, A comparison of three methods for selecting values of input variables in the analysis of output from a computer code, Technometrics, 221, 239-245, 1979.

Medrano M., Brouwer J., Samuelsen G. S., Carreras M., Dabdub D. Urban air quality impacts of distributed generation. Proceedings of ASME Turbo Expo 2003, Power for Land, Sea, and Air. June 16-19, 2003, Atlanta, GA, USA

Meng, Z., D. Dabdub, and J. H. Seinfeld, Size–resolved and chemically resolved model of atmospheric aerosol dynamics, J. Geophys. Res., 103, 3419-3435, 1998.

Meng, Z., Dabdub, D., Seinfeld, J. H. Chemical coupling between atmospheric ozone and particulate matter. Science 277, 116-119, 1997.

Meng, Z., J. H. Seinfeld, P. Saxena, and Y. P. Kim, Atmospheric gas-aerosol equilibrium, IV, Thermodynamics of carbonates, Aerosol Sci. Technol., 23, 131– 154, 1995.

Meyer, E. L. Review of control strategies for ozone and their effects on other environmental issues. EPA-450/4-85-0011, U.S. Environmental Protection Agency, Research Triangle Park, N.C, 1986.

Milford, J. D., D. Gao, A. G. Russell, and G. J. McRae, Use of sensitivity analysis to compare chemical mechanisms for air-quality modeling, Environ. Sci. Technol., 26, 1179-1189, 1992.

Moore, G. E., Londergan, R. J. Sampled Monte Carlo uncertainty analysis for photochemical grid models. Atmospheric Environment 35, 4863–4876, 2001.

Moya M. Pandis SN. Jacobson MZ. Is the size distribution of urban aerosols determined by thermodynamic equilibrium? An application to Southern California. *Atmospheric Environment. 36(14):2349-2365, 2002 May.*

Nexus 2002. Performance and Cost Trajectories of Clean Distributed Generation Technologies, Energy Nexus Group, prepared for the Energy Foundation, 2002.

Nguyen K., Dabdub D. Two-level time-marching scheme using splines for solving the advection equation. Atmos. Environ., 35, 1627-1637, 2001

Nguyen, K., Dabdub, D. NOx and VOC control and its effects on the formation of aerosols. Aerosol Science and Technology 36, 560–572, 2002b.

Nguyen, K., Dabdub, D. Semi-Lagrangian flux scheme for the solution of the aerosol condensation/evaporation equation. Aerosol Science and Technology 36, 407–418, 2002a.

NREL 2003. Gas Fired Distributed Generation Technology Characterization: Microturbines, Energy and Environmental Analysis, Inc, prepared for National Renewable Energy Laboratory, 2003.

Owen, A. B. A central limit theorem for Latin hypercube sampling. Journal of the Royal Statistical Society Series B 54, 541–551, 1992.

Phenix, B. D., J. L. Dinaro, M. A. Tatang, J. W. Tester, J. B. Howard, and G. J. McRae, Incorporation of parametric uncertainty into complex kinetic mechanisms: Application to hydrogen oxidation in supercritical water, Combust. Flame, 112, 132-146, 1998.

Preview of the proposed 2003 Air Quality Management Plan for the South Coast Air Basin. South Coast Air Quality Management District, January 2003.

Pun, B. K., R. J. Griffin, C. Seigneur and J. H. Seinfeld, Secondary organic aerosol 2. Thermodynamic model for gas/particle partitioning of molecular constituents, J. Geophys. Res., 107(D17), 4333, doi:10.1029/2001JD000542, 2002.

Qin Y. Tonnesen GS. Wang Z. One-hour and eight-hour average ozone in the California South Coast air quality management district: trends in peak values and sensitivity to precursors. Atmospheric Environment. 38(14):2197-2207, 2004 May.

Qin Y. Tonnesen GS. Wang Z. Weekend/weekday differences of ozone, NOx, Co, VOCs, PM10 and the light scatter during ozone season in southern California. Atmospheric Environment. 38(19):3069-3087, 2004.

Rabitz, H. and J. Hales, An ACP Primer on Sensitivity Analysis, Monthly Update, DOE Atmospheric Chemistry Program, 6(11), K9-30, BPNL, POB 999, Richland, Washington, 1-7, 1995.

Rabitz, H., M. Kramer, and D. Docol, Sensitivity analysis in chemical kinetics, Ann. Rev. Phys. Chem., 34, 419-461, 1983.

RAP 2001. DG Emissions, National Renewable Energy Laboratory, on-going study for Regulatory Assistance Project, http://www.rapmaine.org/workgroup.html, 2001.

Rodriguez, M. A., Dabdub, D. Monte Carlo uncertainty and sensitivity analysis of the CACM chemical mechanism. Journal of Geophysical Research 108 (D15), 4443 (DOI:10.1029/2002JD003281), 2003.

Russell A. G., Dennis R. NARSTO critical review of photochemical models and modeling. Atmos. Environ. 34, 2283-2324, 2000.

Samuelsen, G.S., J. Brouwer, and M. Medrano, Air Quality Impacts of Distributed Generation, Final DG Scenario Development Report, Prepared for the California Energy Commission. 500-00-033, 2003.

Sax, T., Isakov, V. A case study for assessing uncertainty in local-scale regulatory air quality modeling applications. Atmospheric Environment 37, 3481–3489, 2003.

SCAQMD 2000. Best Available Control Technology Guidelines, SCAQMD, 2000.

SCAQMD 2003. Addendum to the proposed modification to the draft 2003 air quality management plan and additional comments and responses, South Coast Air Quality Management District, 2003.

Sillman S. and Samson P. J. Impact of temperature on oxidant photochemistry in urban, polluted rural and remote environments. J. Geophys. Res. 100, D6, 11,497-11,508, 1995.

Sistla G., Zhou N., Hao W., Ku J.-Y., Rao S. T., Bornstein R., Freedman F., Thunis P. Effects of uncertainties in meteorological inputs on urban airshed model predictions and ozone control strategies. Atmos. Environ. 30, 2011-2055, 1996.

Stein, M. Large sample properties of simulations using Latin hypercube sampling. Technometrics 29, 143–151, 1987.

Stockwell W.R., F. Kirchner, M. Kuhn, and S. Seefeld, A new mechanism for regional atmospheric chemistry modeling, J. Geophys. Res., 102, 25,847 – 25,879, 1997.

Stolarski, R. S., D. M. Butler, and R. D. Rundel, Uncertainty propagation in a stratospheric model, 2, Monte Carlo analysis of imprecisions due to reaction rates, J. Geophys. Res., 83, 3074-3078, 1978.

Thompson, A. M., and R. W. Stewart, Effect of chemical kinetic uncertainties on calculated constituents in a tropospheric photochemical model, J. Geophys. Res., 96, 13,089-13,108, 1991.

Tomashefsky, S. and Marks, M. Distributed Generation Strategic Plan, California Energy Commission, 2002.

Vardoulakis, S., Fisher, B. E. A., Gonzalez-Flesca, N., Pericleous, K. Model sensitivity and uncertainty analysis using roadside air quality measurements. Atmospheric Environment 36, 2121–2134, 2002.

Vuilleumier L., Harley R. A., Brown N. J., Slusser J. R., Kolinski D., Bigelow D. S. Variability in ultraviolet total optical depth during the Southern California Ozone Study (SCOS97). Atmos. Environ. 35, 1111-1122, 2001

Vuilleumier, L., J. T.Bamer, R. A. Harley RA, and N. J. Brown, Evaluation of nitrogen dioxide photolysis rates in an urban area using data from the 1997 Southern California Ozone Study, Atmos. Environ., 35, 6525-6537, 2001.

Winner A. D., Cass G.R. and Harley R.A. Effect of alternative boundary conditions on predicted ozone control strategy performance: a case study in the Los Angeles area. Atmos. Environ. 29, 3451-3464, 1995.

Yang, Y. J., Wilkinson, J. G., Russell, A. G. Fast, direct sensitivity analysis of multidimensional models. Environmental Science and Technology 31, 2859-2868, 1997.

Yang, Y., W. R. Stockwell, and J. B.Milford, Effect of chemical product yield uncertainties on reactivities of VOCs and emissions from reformulated gasolines and methanol fuels, Environ. Sci. Tech., 29, 1336-1345, 1995.

Zeldin, M. D., L. D. Bregman, and Y. Horie. A Meteorological and Air Quality Assessment of the Representativeness of the 1987 SCAQS Intensive Days. Final report to the South Coast Air Quality Management District, 1990.

10 GLOSSARY

Nomenclature

C_i: Concentration of species i
K: Eddy diffusivity tensor
Q_i: Source term that accounts for the elevated point sources of species i
R_i: Rate of generation of species i by chemical reaction
u: Mean wind velocity
t: Time

List of Acronyms

AGT   Advanced Gas Turbine
AQMP   Air Quality Management Plan
CARB   California Air Resources Board
CACM   Caltech Atmospheric Chemistry Mechanism
CB-IV   Carbon Bond version IV chemical mechanism
CGT   Conventional Gas Turbine
CHP   Combined Cooling, Heating and Power
CIT   California Institute of Technology
CO   Carbon Monoxide
CO_2 Carbon Dioxide
DER   Distributed Energy Resources
DG   Distributed Generation
FC   Fuel Cell(s)
GT   Gas Turbines(s)
HHV   Higher Heating Value
HT   High temperature
HTFC   High Temperature Fuel Cell
ICE   Internal Combustion Engine
LADWP   Los Angeles Department of Water and Power
LT   Low temperature
LTFC   Low Temperature Fuel Cell
MCFC   Molten Carbonate Fuel Cell(s)
MTG   Microturbine Generator(s)
MPMPO   Model to Predict the Multiphase Partitioning of Organics
NH_3 Ammonia
NOx   Nitrogen Oxides
NG   Natural Gas
PEMFC   Proton Exchange Membrane Fuel Cell(s)
PM2.5   Particulate Matter (less than 2.5 microns)
PM10   Particulate Matter (less than 10 microns)
PV   Photovoltaics
SCAG   Southern California Association of Governments
SCAPE2   Simulating Composition of Atmospheric Particles at Equilibrium 2 model

SCAQMD   South Coast Air Quality Management District
SCAQS   Southern California Air Quality Study
SCE   Southern California Edison
SCR   Selective Catalytic Reduction
SoCAB   South Coast Air Basin
SOFC   Solid Oxide Fuel Cell(s)
SOx   Sulfur Oxides
VOC   Volatile Organic Compounds

11 APPENDIX A: RESULTS FROM THE FIRST INDUSTRY STAKEHOLDER WORKSHOP (19 SEPTEMBER, 2002)

11.1 Stakeholder Workshop Description

A workshop was organized and hosted by the Advanced Power and Energy Program at UCI to garner help from industrial stakeholders to develop accurate DG implementation scenarios and to adequately consider technologies of interest to the stakeholders. The workshop was characterized as:

Workshop Title: ***"Distributed Generation Implementation Scenarios for Air Quality Impacts in the South Coast Air Basin"***
Workshop Date/Time: Thursday, September 19, 9:00am to 4:30pm
Workshop Location: Advanced Power and Energy Program, University of California, Irvine

The purpose of this workshop was to: (1) provide the stakeholders a brief overview of the current air quality impacts of DG project, (2) receive important feedback and guidance from the DG community, (3) accept critique and modify program direction and approach appropriately, and (4) better ground the research effort to garner insight into real potential air quality impacts of DG.

The discussion topics of this workshop included:
- (1) Program overview and approach
- (2) Types of DG considered
- (3) Characteristics of DG considered
- (4) DG Scenarios Development
- (5) DG Scenario Screening
- (6) Examples of Air Quality Impacts

The agenda for the workshop was (discussion/presentation leader in parentheses):

9:00am Introductions/Agenda Review (Prof. Scott Samuelsen)
9:15am Program Overview and Approach (Dr. Jack Brouwer)
9:45am Discussion of DG Types and Characteristics
10:15am Break
10:30am Distributed Generation Scenarios Development and Screening (Dr. Marc Medrano, Dr. Jack Brouwer)
11:00am Discussion of Scenario Development and Screening
11:30am Air Quality Modeling Approach and Sample Results (Prof. Donald Dabdub, Mr. Marc Carreras)
12:00pm Lunch (Establish Breakout Groups)
1:00pm Breakout Sessions (Prof. Scott Samuelsen – red; Dr. Jack Brouwer – green; Dr. Marc Medrano – yellow)
Types of DG considered (20 minutes)
Characteristics of DG considered (20 minutes)
Scenario Development Strategy (20 minutes)
Scenarios themselves (20 minutes)

> Scenario Screening (20 minutes)
>
> Air Quality Issues (20 minutes)

3:00pm   Break

3:30pm   Summary of Breakout Sessions (Reports from red, green, & yellow breakout groups)

4:15pm   Summary Discussion

4:30pm   Adjourn

Attendees of the Stakeholder workshop are presented in Table 64.

Table 64.   List of attendees and corresponding organizations for the DG industry stakeholder workshop held at UCI on 19 September, 2002.

ORGANIZATION:
SCAQMD
SCAQMD
Alliance Power
Alliance Power
Bowman Power Systems
CARB
CEC
CEC
Capstone Turbines
Capstone Turbines
Coalition for Clean Air
Coalition for Clean Air
Elliot Turbines
EPRI
EPRI
FuelCell Energy
LADWP
Millenium Cell
Pacific Gas & Electric
Planergy
U.C. Berkeley
O'Conner Consultants
Southern California Gas
Southern California Gas
SCAQMD
SCAQMD
Southern California Edison
Southern California Edison
Clean Air Now
UCI
UCI
UCI
UCI
UCI
UCI

11.2 APEP Compilation and Assessment of Stakeholder Recommendations

The Advanced Power and Energy Program (APEP) of UCI recorded the input from stakeholders at this workshop and compiled the notes that were gathered as a result of the questions raised during the formal presentations, issues discussed and recommendations made during the full discussion periods and in each of the three breakout sessions, held in the afternoon. From all of this input from Stakeholders, APEP researchers compiled and assessed the stakeholder recommendations as follows in this section.

11.2.1 Recommendations to Definitely Include

- For DG spatial distribution:
  - Base distribution on population and population growth. (Population - reflects installed base--power, and peak power demand, whereas Population Growth reflects emerging opportunities.)
  - Consider zoning/permitting in scenario development.
  - Use economic "models" that are realistic for market penetration (e.g., CHP) – limited per discussion below.
  - Use utility interconnect data and other applicable statistics – if data are available/provided (need cooperation of LADWP, SCE).
  - Use highway miles scenario for model "sensitivity" only

- For DG temporal distribution:
  - Account for the likelihood that the majority of DG will NOT be base-loaded

- For DG technology mix:
  - Remove windmills from consideration in the South Coast Air Basin (SoCAB).
  - Natural gas-fired ICEs should be included in the scenarios (check PM emissions rate).
  - For 2010 DG Scenarios, incorporate a population of DG that reflects emissions performance at the date of installation. (Include likely performance degradation)
  - Account for significant adoption of CHP systems (between 40 and 60% - FuelCell Energy, 65% - Capstone) in this timeframe.

- For DG penetration:
  - 20% of increase is most likely "worst case" penetration scenario (not a consensus opinion with many supporting 20%).

- For DG Scenarios in general:
  - Adopt the following DG classifications:
    - Residential: 1kW to 5kW (FC, PV)
    - Commercial/Small Industrial: 25kW to 500kW (PV, MTG, FC)
    - Large Commercial/Institutional: 500kW to 2MW (reciprocating engines)

- Large Institutional: 2MW to 50MW (GT)
  - o Account for CHP emission offsets (e.g., boiler replacement).
  - o Develop baseline scenarios for both the "uncontrolled" and "controlled" 2010 base case emissions inventory (use the latest "release" relative to the project schedule).
  - o Strongly differentiate cases that are "forecasts" (i.e., likely or realistic) from those that are "excursions" (i.e., used for engineering insight or brainstorming).
  - o Do a few excursions to bracket the problem and capture uncertainty ("you never know").
- For DG Emissions Characterization:
  - o For larger systems (>5MW?) emissions offsets must be purchased and should be included in the scenario.
  - o Use the CARB, or AQMD standards that apply to the technology, size, and application.
  - o Report emissions of CO_2 as a result, but don't use possible CO_2 impacts or regulatory action in development of scenarios (perform a separate DG scenario calculation that accounts for non-regional sources as well).
  - o Carefully include an analysis of displaced emissions (especially for CHP, opportunity fuels, etc.).
  - o Apply the 2003 and 2007 ARB standards scenarios to the moderate penetration case.

11.2.2 Recommendations to Consider

- For DG Spatial Distribution:
  - Focus on consumption growth to locate power generators.
  - Use current transmission grid constrained locations as a weighting consideration.

- For DG Technology Mix:
  - o Solar is not expected to contribute a high percentage of DG, rather, consider solar-thermal combined with heat and power (e.g., Nevada and North Carolina).
  - o PV is only residential (But, penetration could be increased in commercial applications due to future policy decisions (e.g., AB970 incentives, San Francisco Bond)
  - o Add solar-thermal and external combustion engines (e.g., Stirling external combustion engine).
  - o Focus on natural gas DG.
  - o Categorize and organize as existing technologies and emerging technologies.
  - o Consider digester gas installations in the Chino Valley.

- o Consider the use of DG at oil and gas recovery locations.
- o Assume that large plants (3-50 MW) are more likely to use gas turbine. 1-3 MW gas turbines and ICE. Below 1 MW plants are more likely to incorporate small DG technology (MTGs, FCs).
- o Diesel fuel related technology will not be used in the basin in the future.
- o Hydrogen ICEs should be considered as another potential source – with H_2 generated "in the basin."
- o Consider larger combined cycle plants – could affect DG adoption in vicinity.
- o Gas turbine fuel cell hybrid systems will not be widely available by 2010.
- o Consider fuel cells vehicles – only as linked to hydrogen production and refueling.

- ▪ For DG temporal distribution:
  - o Characterize DG based on operational hours, and applications in various market segments (particularly important considering temporal aspects of the simulation)
  - o Since majority of DG will NOT be base-loaded (60% not base-loaded), need to define by application and consider TOU pricing.

- ▪ For DG Emissions Characterization:
  - o "Worst Case" must include diesel-fueled internal combustion engines (ICE).

- ▪ For DG Scenarios in general:
  - o Consider applications and market segments when determining both penetration and DG characterization (e.g., chiller, hot water, steam, residential, industrial, commercial).
  - o Include economic (value driven) and policy factors in scenario development including (1) current economic incentives, (2) renewable portfolio standard, (3) departing load charges, (4) CHP benefits, (5) fuel availability, (6) cost of fuel, (7) applicable CC & R's, (8) zoning / permitting, (9) applicable tariff, in the DG scenario development. (NOTE: this is quite challenging, and could comprise a completely new DG penetration study project – we suggest a limited economic analysis)
  - o Up to 15% of the existing load on a substation does not require an upgrade. Above that, there are additional costs, which should be considered as an economic constraint for DG deployment.
  - o Limit the cases to a top 10 list, and add sub-cases.
  - o Use hydrogen more widely in a brainstorming scenario including hydrogen infrastructure development. While low penetration may be true for 2010, H_2 may be prominent in 2050.

o Include consideration of UPS, premium power increased demands for DG.
o Consider a "worst case" scenario that allows diesel gen-sets to operate more than 200 hours.
o Divide DG into "clean but polluting" and "non-polluting" categories
o Correlate results to DG size, type, application:
  - Residential: 1kW to 5kW (FC, PV)
  - Commercial/Small Industrial: 25kW to 500kW (PV, MTG, FC)
  - Large Commercial/Institutional: 500kW to 2MW (reciprocating engines)
  - Large Institutional: 2MW to 50MW (GT)

11.2.3 Recommendations to Reject

- Consider multimedia environmental impacts (e.g., noise, EMF, water, soil, etc…)
- Consider retiring plants, possible large demand due to lack of merchant plant installations as an opportunity (if not replaced) or discouragement for DG (if replaced).
- Consider fuel cell vehicle emissions in the scenarios.
- Be careful to not analyze two (or more) DGs with same emissions profiles (and end uses).
- Do an emergency generator operating case. (potential overlap with UCR study)
- Consider diesel-fueled DG can operate continuously in basin.
- Consider doing only emission modeling instead of air quality modeling.

11.2.4 APEP Actions

- Differentiate between regional and local impacts. Local impacts need to be studied closer. Identify where impacts are expected to be stronger.
- Demonstrate early on that DG does have an impact (e.g., model sensitivity to incremental emissions associated with DG)
- Determine if NG reciprocating engines are the same, better than, or worse than MTG.
- Define bounds on the problem. DG might not have an impact even in the worst case.
- Have another meeting to report back to this group of stakeholders.
- Revise natural gas ICE emission factors. They appear to be too high for PM especially.
- VOC emissions for a PEMFC seem too high.
- Need to know how the AQMD, ARB or EPRI (E2I) will use results, to narrow the span.
- Do 2007 ARB standards include CHP credit?

- How does definition of DG differ from ARB definition? (SB1298)
- Gain access to the "controlled" emission inventory for 2010
  - Get unprocessed emissions inventory
  - Get controlled emissions inventory
- Discuss the better way to approach CHP for the emissions accounting
- Compile more emissions rates from other sources and also partial performance emissions factors.
- Find out which land parcel classification (zoning) information for SoCAB is available in GIS or other formats.
- Try to get information on hourly electricity profiles for industrial, commercial and residential sub-segments from SoCAB utilities.

12 APPENDIX B: RESULTS FROM THE SECOND INDUSTRY STAKEHOLDER'S WORKSHOP (21 MAY, 2003)

12.1 Stakeholder Workshop Description

A workshop was organized and hosted by the Advanced Power and Energy Program at UCI to garner help from industrial stakeholders to develop accurate DG implementation scenarios and to adequately consider technologies of interest to the stakeholders. The workshop was characterized as:

Workshop Title: ***"Distributed Generation Implementation Scenarios for Air Quality Impacts in the South Coast Air Basin – Part II"***
Workshop Date/Time: Wednesday, May 21, 2003, 9:00am to 4:30pm
Workshop Location: Advanced Power and Energy Program, University of California, Irvine

The purpose of this workshop was to: (1) provide you with an update on this air quality impacts of DG project, (2) receive final feedback and guidance from the DG community on the DG implementation scenarios, and (3) accept critique from the community and modify program direction, approach, and DG implementation scenarios appropriately.

The discussion topics of this workshop included:
(1)   Update on DG implementation scenario development approach,
(2)   Description of DG implementation scenarios developed to-date,
(3)   Examples of Air Quality Impacts,
(4)   Feedback and Critique on scenario development approach, and
(5)   Feedback and Critique of actual scenarios developed.

The agenda for the workshop was (discussion/presentation leader in parentheses):

9:00am   Introductions/Agenda Review (Prof. Scott Samuelsen)
9:15am   Program Overview and Update (Dr. Jack Brouwer)
9:30am   DG Implementation Scenarios Development Approach (Dr. Marc Medrano, Dr. Jack Brouwer)
9:45am   Discussion of DG Implementation Scenarios Development Approach
10:15am   Break
10:30am   DG Scenarios Developed to-date (Dr. Marc Medrano, Dr. Jack Brouwer)
11:30am   Discussion of DG Implementation scenarios developed to-date
12:00pm   Lunch
1:00pm   Sample Air Quality Modeling Results (Prof. Donald Dabdub, Mr. Marc Carreras)
1:45pm   Discussion of Air Quality modeling results
2:00pm   Breakout Sessions (Prof. Scott Samuelsen – red; Dr. Jack Brouwer – green; Dr. Marc Medrano – yellow)
                Scenario Development Strategy (30 minutes)
                Scenarios themselves (30 minutes)
                Air Quality Issues (30 minutes)
3:30pm   Break
3:45pm   Summary of Breakout Sessions

Reports from red, green, and yellow breakout sessions (15 minutes each)
4:30pm   Adjourn

List of organizations participant in the second Stakeholder workshop are presented in Table 65.

Table 65. List of organizations that attended the DG industry stakeholder workshop held at UCI on 21 May, 2003.

Organization
City of Santa Monica
SCAQMD
Flex Energy
US EPA
Southern California Edison
Southern California Edison
Blue Scape Environmental
LADWP
STM / GTI
ARB
CEC
PG & E
FuelCell Energy
Caterpillar, Inc
DE Solutions
UCI
UCI
Capstone Turbine Corp
SCAQMD
EPRI
PROBE
Coaliiton for Clean Air
SCAQMD
APEP
APEP
APEP
UCI
GE Global Resreach Center
Sempra Utilities
Combined Energy Systems
T&D Planning, Communication, and CPUC Regulation
UC Berkeley
Xenergy
Alliance Power
EPRI
GE Power Systems

12.2 Recommendations to Definitely Include

- Obtain SCE data, LADWP data, and SCPPA data on current installed DG and trends to both benchmark and check our estimates for DG adoption rates and technology mix.
- Construct a Business as Usual scenario based on the above data
- Make sure ammonia emission factors are consistent with AQMD's regulations
- Check CEC "requirement" for percentage of renewable energy in mix of electricity production and include this level in the scenarios
- Divide the DG into those that are permitted (under SCAQMD rules) and those that are certified (under ARB rules)
- For permitted sources, consider the type of engine technology (different emissions profiles):
  - Lean burn: for large projects, can afford SCR, usually gas turbines, higher efficiency (~39%)
  - Rich burn: smaller projects, three way catalyst, lower efficiency (~34%)   (Note: AQMD standard same for both, kg/kw-hr; few lean projects)
- Look to the source test data of AQMD for emissions levels
- Spanning scenarios should include a mix of technologies (vs. heavily MTG weighted)
- The "realistic" technology mix should definitely include more internal combustion engines (ICE) and gas turbines (GT) and less fuel cells (FC) and hybrids in technology mix
- Consider that use of averages in the generation of power per cell may reflect an unrealistic specification of DG. As a result, specific cells may need to accommodate instances of specific DG sizes.
- Consider a spanning scenario that is almost 100% ICE and MTG

12.3 Recommendations to Consider

- Should consider increased adoption of opportunity fueled DG
- Should consider more displaced emissions – we include for CHP, opportunity fuels, port, but not for any displaced electricity currently – we will consider a spanning case that includes electricity displacement – significant caveat: studies to-date have not shown an actual proven in-basin displacement
- Add start-up emissions for peak power spanning scenarios. This in challenging since we do not have a data source, but, we will consider a spanning case where these are estimated.
- Recognize that some gas turbine NOx control may be SCONOX (non-ammonia) versus SCR (potential ammonia slip) and will not contribute to the ammonia slip emissions
- Penetration may be too low – check current permitting records from AQMD (use SCE, LADWP, Muni interconnect data to check)
- Think about the DG duty cycle – most current DG projects are operating base loaded and using the grid for peaking (this is especially the case when not exporting power, when using CHP)
- Consider utility rates, demand charges, etc. in analyses of duty cycle

- The 2007 standards may drive more FC adoption, but, ICEs and GTs will still dominate (in terms of MW capacity) without any violation of standards (most of these will be permitted by SCAQMD vs. certified by ARB)
- Consider demand reduction, energy efficiency and energy saving methods that can be coupled with DG - introduce these into the scenarios to see what impact taking credit for energy savings methodologies may have – spanning scenario or uncertainty analysis
- Think about a hydrogen economy scenario
- Think about a high spark-spread scenario
- Consider the additional benefit of installed DG that lowers the peak demand. Is there a large emissions benefit associated with easing the load during peak time in existing plants (e.g., peaking plants in the basin)?
- In the spanning scenarios, develop a database that could provide a capability to estimate the impacts of a specific set of DG installation conditions
- Land use, and sector spatial distributions are more appropriate than population growth

12.4 Recommendations to Reject

- Develop an overall statistical index for air quality
- Suggest expanding the project to consider other sources beyond DG. AQMD is about to put a plan for 2003, using similar tools to forecast air quality concentrations.

12.5 APEP Actions

1. Work on effective presentation formats for both reports and presentations.
2. Obtain SCE data, LADWP data on DG installations and check our numbers versus the observed current trends
3. Contact Southern California Public Power Authority (SCPPA) to obtain data on DG
4. Make sure ammonia emission factors are consistent with AQMDs regulations
5. Check CEC "requirement" for percentage of renewable energy in mix of electricity production
6. Divide the DG into those that are permitted (under SCAQMD rules) versus those that are certified (under ARB rules)
   a. Obtain and use current BACT standards for appropriate permitted equipment
   b. Use ARB certified emissions rates for 2003, 2007 or measured emissions (if lower than ARB standards) for the certified equipment.
7. Use technology mixes in the spanning scenarios
8. Consider a "spanning" case that includes more displaced emissions
9. Include more ICE, GT and less FC and hybrid in the technology mix
10. Add start-up emissions for peak power spanning scenario.
11. Think about actual size of DG units and how this affects the spatial distribution (distinct sizes should be included for some, especially larger, DG)

12.6 Raw Workshop and Discussion Notes

12.6.1 Previous Workshop Review
- Edan Prabhu: Opportunity Fuels: Are they included.

12.6.2 Scenarios

- Tod O'Conner: SCAPA: Pasadena, Glendale, DWP
- Keith Davidson: Did you consider "displacement of emissions" from existing sources as a result of DG; Jack: NO! Should look at this on at least a sensitivity basis
- Tod O'Conner. Renewable Portfolio policy allows utilities are required to make 20% of new power to come from renewables by 2017 with 1 % per year. Jack: we have spanning cases that will capture.
- SCE: Spanning, should consider concentrated emissions in east part of basin? Jack; have done uniform, and population growth based – effectively concentrates emissions
- Keith Davidson: Is characterization information available? Jack: yes. Will present subsequently. Nexus (Keith), NREL, APEP data, and others all used in the compilations.
- Tod O'Conner: Scenario 16. Will you consider MTG-CHP to DG-CHP? Jack: yes
- Edan Prabhu: Wants basis that most opportunity fuels are spoken for. Between now and 2010 could be opportunity fuels, and throwing them out may miss a huge opportunity. Jack: We most definitely do no throw out. Most likely early adopters. Edan: Use of opportunity fuels could have a significant improvement on air quality. Jack: most true. That is way we consider offsets. Chino is one example that will benefit (although not on our list).

12.6.3 Scenarios Presentation

- What about emissions of CO – they are included, but not presented here.
- What about O_3 (produced in the basin as a result of NOx, VOC emissions and leads to additional PM (secondary organic aerosols).
- Land-Use Data Extraction:
  - Do you have the definitions of low density versus medium to high density residential, yes.
- Approach for Realistic Scenarios:
  - How many i,j,k are you considering (i = 1 to 6 sectors, j = 1 to 5 size classes, k = 1 to 994 cells)
  - How are the $e_{l,k}$ defined (use of literature sources, APEP data, and degradation rate, date of installation, etc.) – we need to do some more work here, especially w.r.t. degradation, date of installation.
- Edison provides interconnect data to CPUC – very useful for benchmarking data, this is reported on a sector basis – data is available for sector type, size type, building type, etc. (Stephanie Hamilton)
- Rich-burn, lean-burn division may be required for the ICEs (Mills, AQMD)
- Looks like ICE technology estimate may be low (Stephanie Hamilton)
- Can we use APEP results to determine the optimal scenario for DG installations – perhaps not "optimal," but certainly identify trends that will improve or reduce air quality.
- Current estimates are low for ICE technology penetration, too high for MTGs

- Where do estimates come from (the market studies presented earlier)
- Given the widely accepted belief that high temperature fuel cells are more applicable to stationary power the estimates for HT fuel cells seem too low compared to LT fuel cells. (Steve Torres)
- Very impressed, very intelligent, thoughtful and well laid out process (Edan Prabhu)
- Are the emissions profiles related to the DG types available? – Yes.
- Need to determine where to install actual units of particular size (cannot just use average data) – Keith Davidson
- Should have a much larger fraction of DG power represented by larger gas turbine and ICEs (since a couple of larger units will have much more significant impacts) – Mosen Nazemi
- Are units that do not meet 2003 or 2007 standards going to be allowed to be installed (ARB standards, or SCAQMD permit is required)
  - Are we comparing apples to apples?
  - BACT applies for larger units – jurisdiction of AQMD
  - Non-permit size – ARB regulations apply
  - District has jurisdiction over permitted units and ICEs need only BACT or LAER
- Since current law requires 2003 and 2007 for DG, why consider anything else? (Steve Torres)
- Matter of jurisdiction – permitted sources fall under BACT (AQMD jurisdiction), non-permitted under ARB (Certification)
- Maybe we should divide technologies as those that are permited versus those that fall under ARB certification law – have a separate estimate for growth/adoption rate of permitted versus certified sources – although moving together, definitely NOT the same (VERY IMPORTANT suggestion – Mosen Nazemi – many in audience agree with this approach)
- Hybrid numbers seem way too high for next ten years, ICEs are under represented. (Keith Davidson)
- Try to use census data for 2001 – just released this week.
- DG mix is controversial – seems inconsistent with intuition – but it resulted from studies – we need your feedback to justify a better mix of technologies – base this on your experience and available trends today.
- Edan Prabhu mentioned having some interconnect data, working with SCE on a project with Mark Rawson, Joe Simpson,

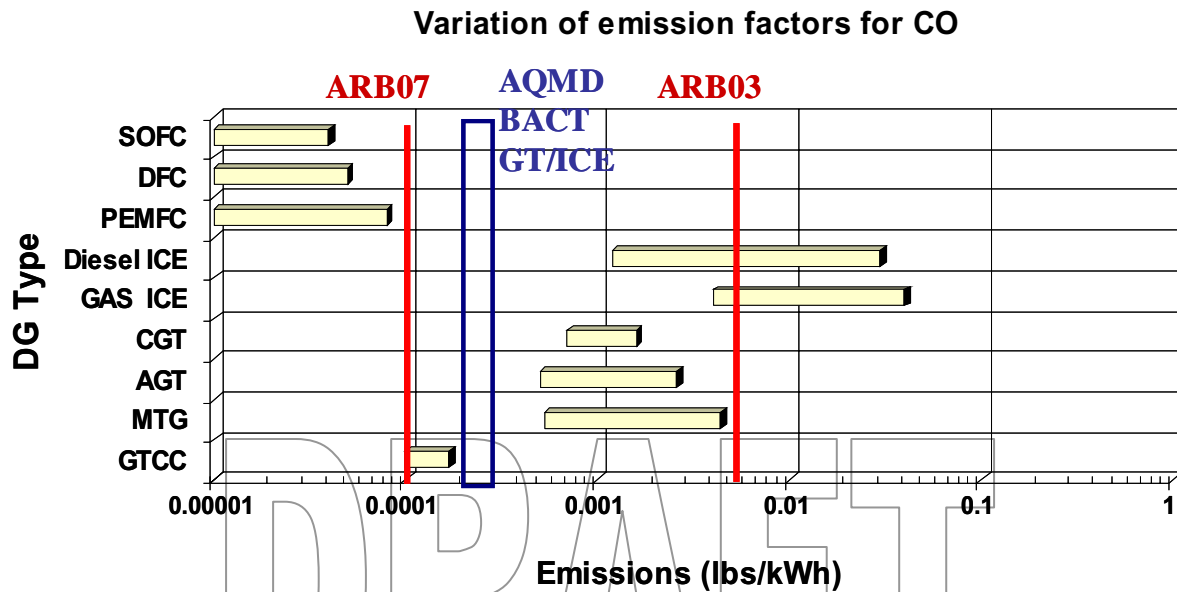# 13 APPENDIX C: PLOTS OF DG EMISSIONS FACTORS FROM DIFFERENT SOURCES

Variation of emission factors for CO

Figure 68: CO emissions factors and ARB and AQMD CO emissions standards.

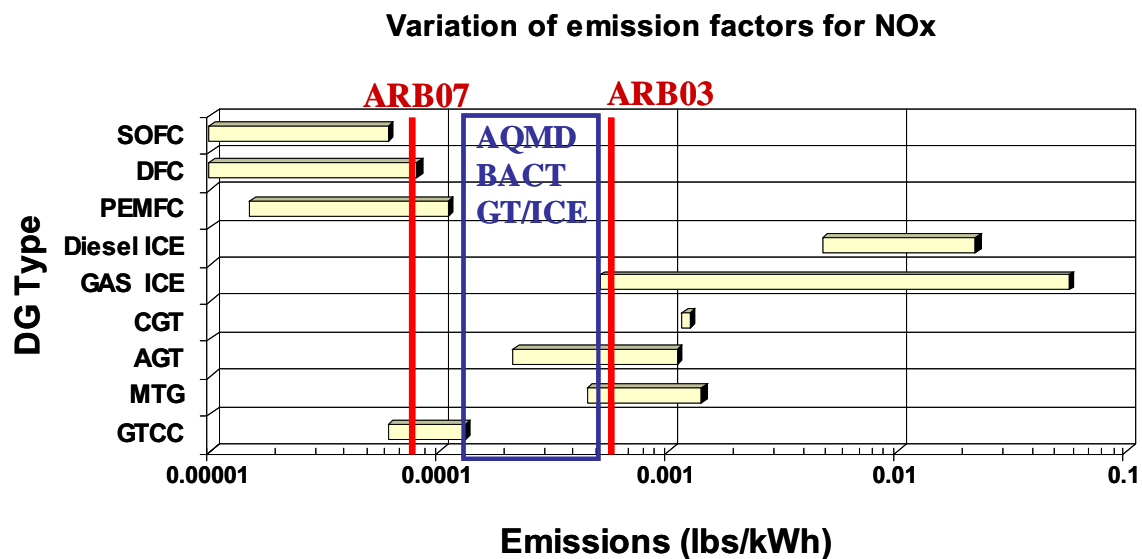**Variation of emission factors for NOx**

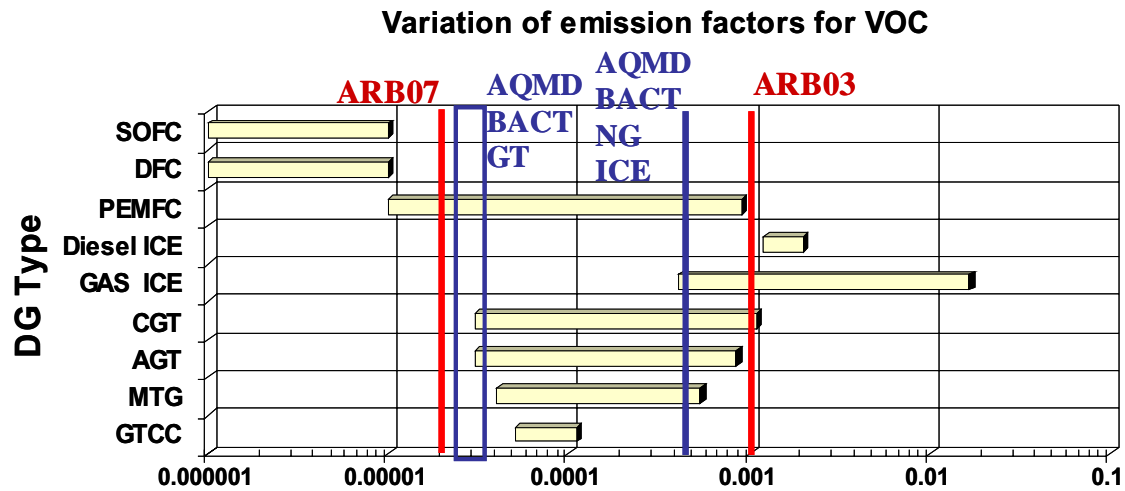**Figure 69: NO_x emissions factors and ARB and AQMD NO_x emissions standards.**
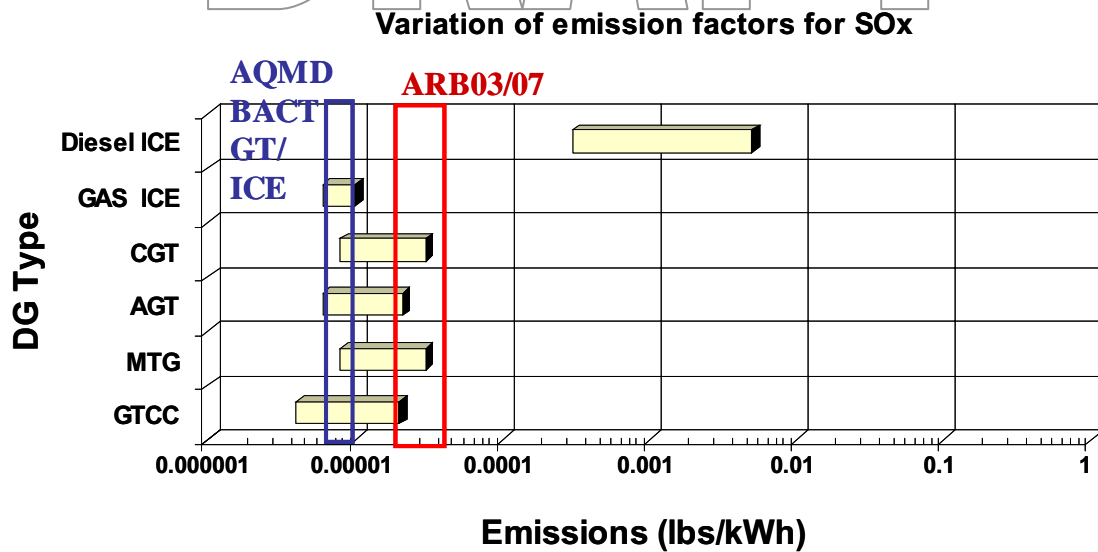
22222

222

Figure 70: VOC emissions factors and ARB and AQMD VOC emissions standards.

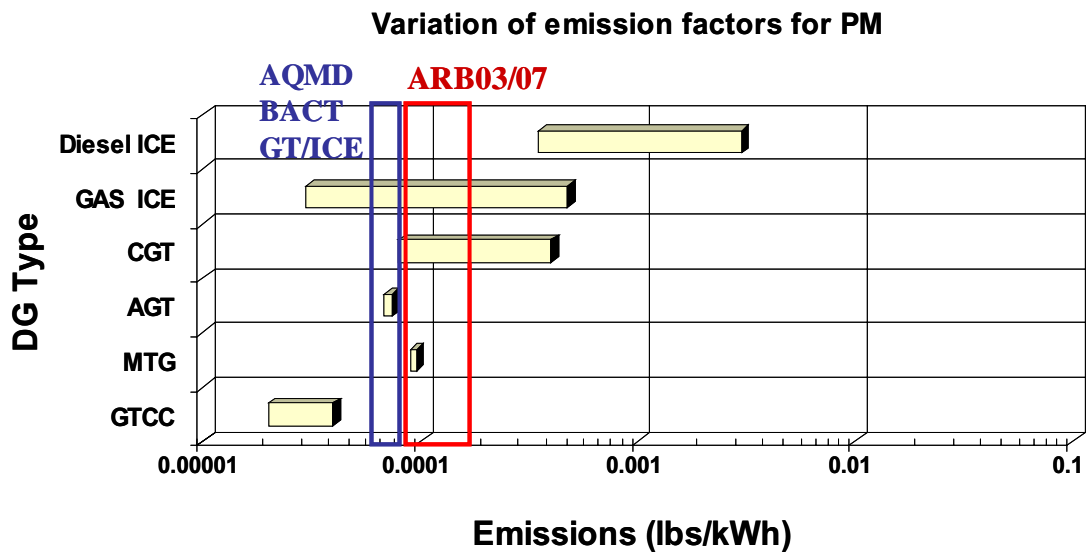Figure 71: SOx emissions factors and ARB and AQMD SOx emission standards.

Variation of emission factors for PM

Figure 72: PM emissions factors and ARB and AQMD PM emissions standards.

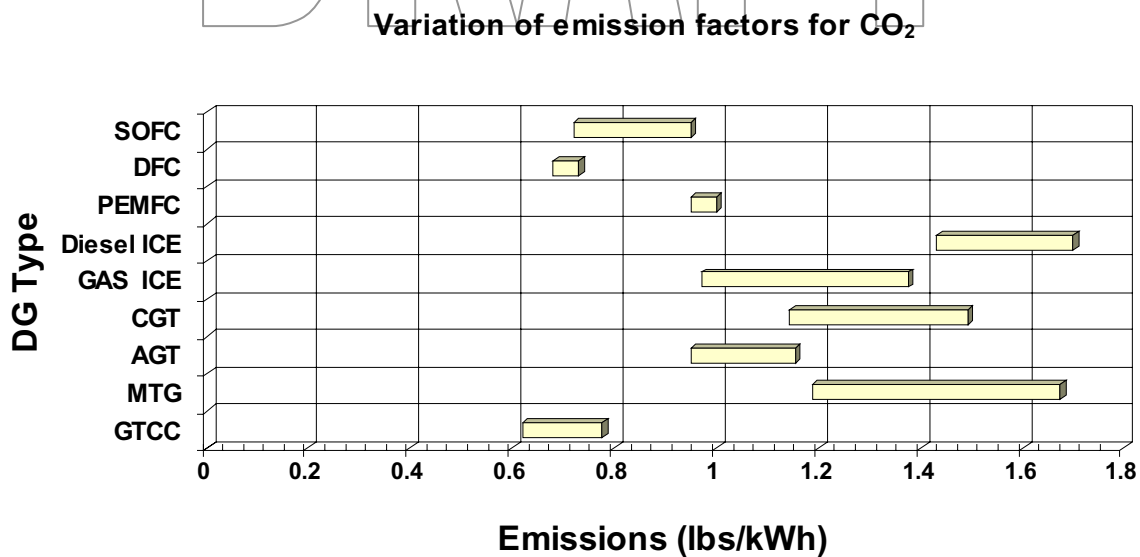**Variation of emission factors for CO$_2$**

Figure 73: CO$_2$ emissions factors.

14 APPENDIX D: CONVERSION TOOLS

14.1 Coordinates Web converter

In the first months after the kick off of the current effort we found useful to develop an interactive map of the SoCAB region that could easily and visually translate the pixel coordinates of the map picture into geographical projections coordinates in the Universal Traverse Mercator system, Zone 11 (UTM), as well as the model internal coordinates.
The relationship the X and Y grid coordinates in the air quality model and the UTM Zone 11 system can be written as:

X model coordinates (range 1-80 units) to X UTM coordinates (range: 215-610 km):
$$X_{UTM} = X_M \cdot 5 + 210$$
Y model coordinates (range 1-30 units) to Y UTM coordinates (range: 3685-3830 km):
$$Y_{UTM} = T_M \cdot 5 + 3680$$

The above mentioned conversion tool was successfully developed and posted in Internet for public access in the following URL:

http://albeniz.eng.uci.edu/map/

As an illustrative example, Figure B.1 below shows the UTM and model coordinates when the city of Victorville is clicked.
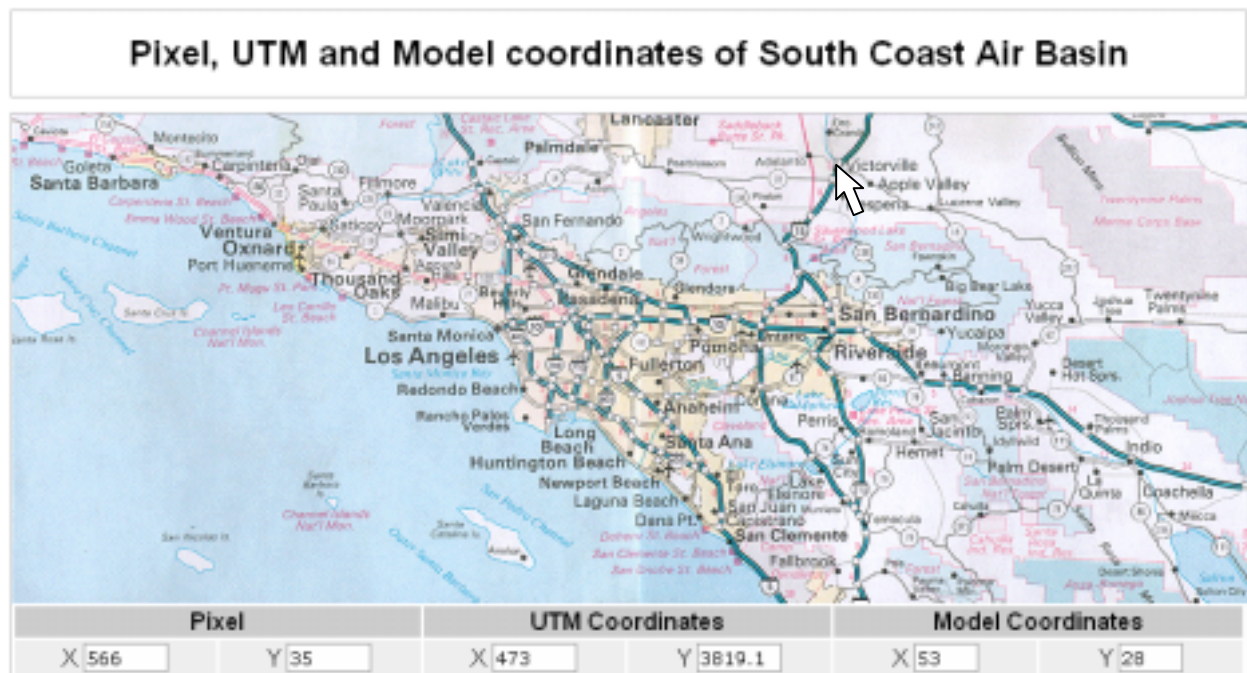

Figure 74: UTM-Model coordinates web converter

14.2 Emission rates converter

We noticed at the early stages of the project that the emission flux units understood by the air quality model (parts per millions x meter / min) were completely different to the typical emission rates units found for distributed generator systems (pounds or kg / hour or pounds or kg/ kWh).

An emission rates converter was successfully developed in Excel to easily relate the two different emission units. The conversion factors used to ascertain how many (ppmv-m/min) of generic pollutant A correspond to x pounds of A/kWh of electricity generated are presented as follows:

$$x\frac{\text{lb A}}{\text{kW} \cdot \text{h}} \times y\frac{\text{GW}}{\text{cell}} \times \frac{10^6 \text{ kW}}{1\,\text{GW}} \times \frac{1\,\text{h}}{60\,\text{min}} \times \frac{1\,\text{kg A}}{2.205\,\text{lb A}} \times \frac{1\,\text{mol A}}{\text{MW A kg}} \times \frac{1\,\text{cell}}{25 \cdot 10^6 \text{ m}^2} \times \frac{8.314\dfrac{\text{Pa} \cdot \text{m}^3}{\text{mol air} \cdot \text{K}} \cdot 288\,\text{K}}{1.01325 \cdot 10^5 \text{ Pa}} \times \frac{10^6 \text{ ppmv A}}{\text{mol A/mol air}}$$

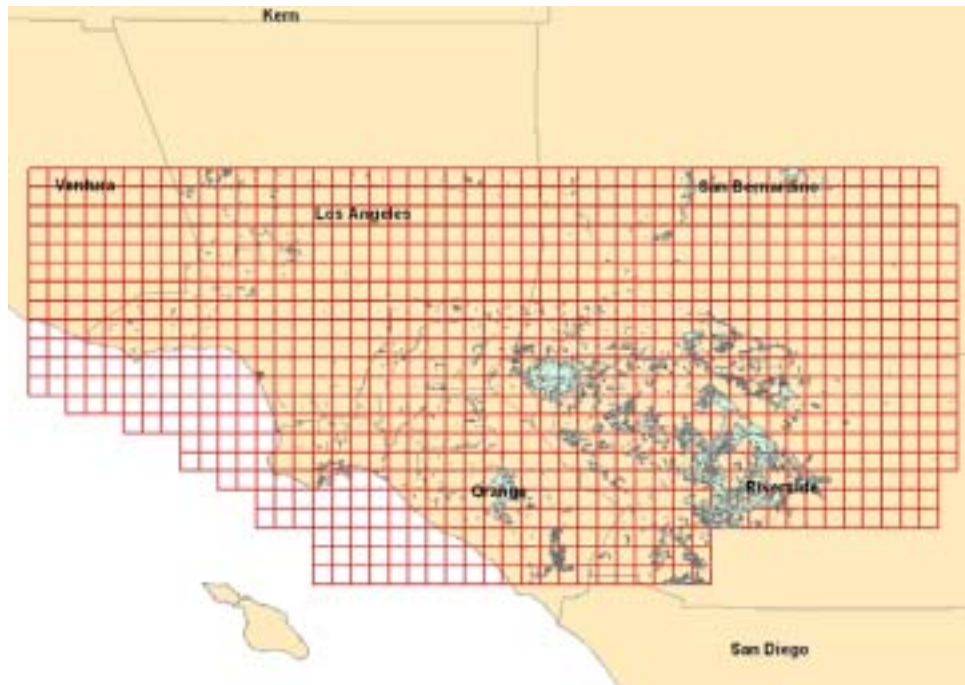## 15 APPENDIX E: LOCATION OF LAND-USE PARCELS FOR THE 13 GENERIC LAND-USE CATEGORIES

Figure 75: Location of land-use parcels pertaining to the Agriculture category
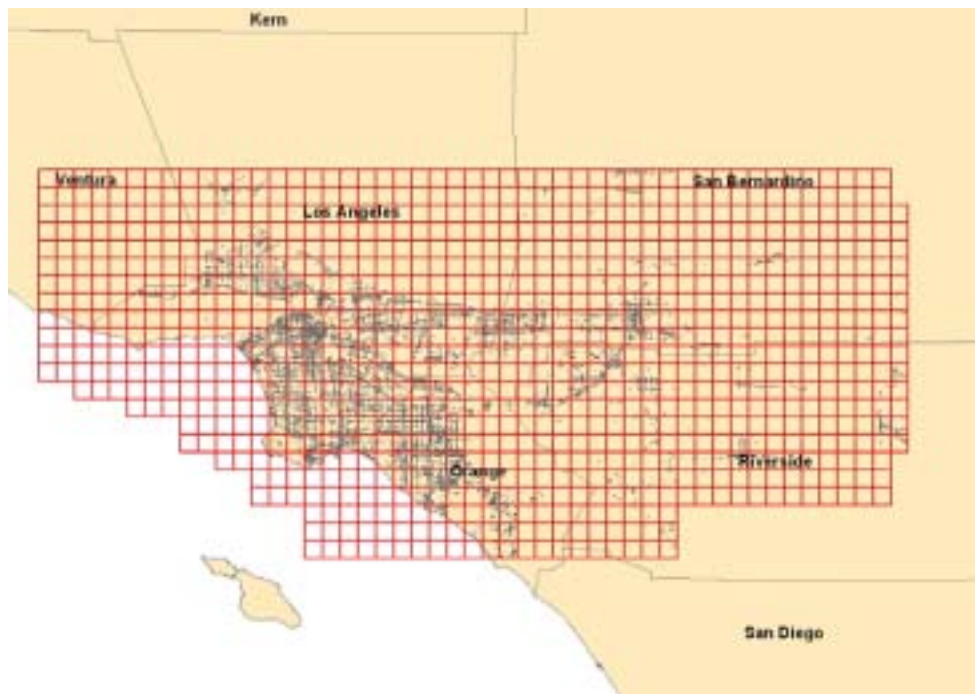

Figure 76: Location of land-use parcels pertaining to the Commercial category

Figure 77: Location of land-use parcels pertaining to the Extraction category

Figure 78: Location of land-use parcels pertaining to the Industrial category

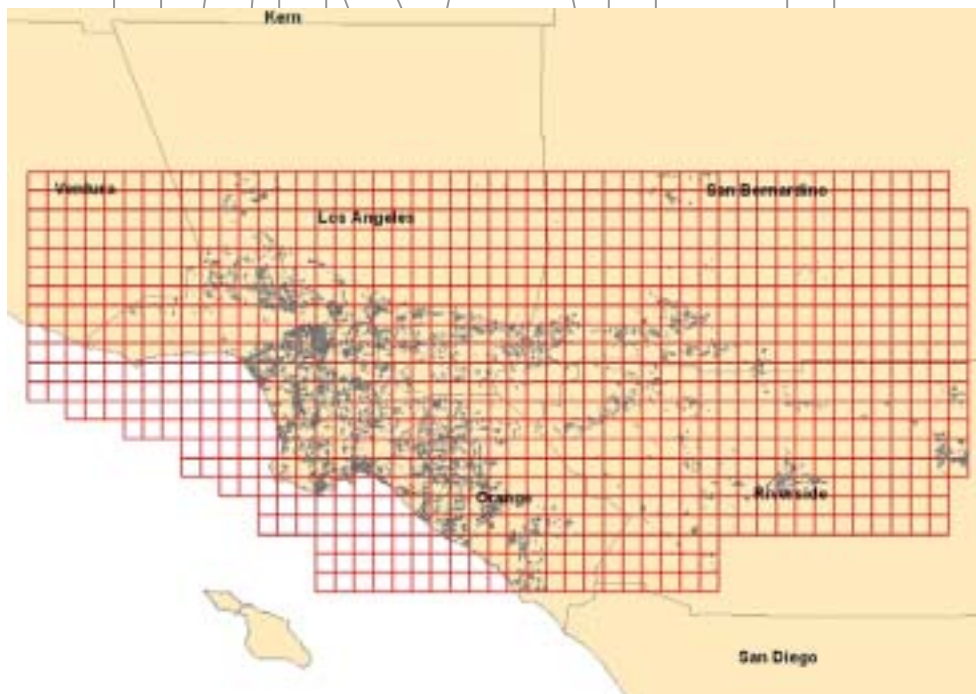**Figure 79: Location of land-use parcels pertaining to the Low Density Residential category**

Figure 80: Location of land-use parcels pertaining to the Medium to High Density Residential category

Figure 81: Location of land-use parcels pertaining to the Open Space and Recreation category

Figure 82: Location of land-use parcels pertaining to the Public Facilities and Institutions category

Figure 83: Location of land-use parcels pertaining to the Rural Density Residential category

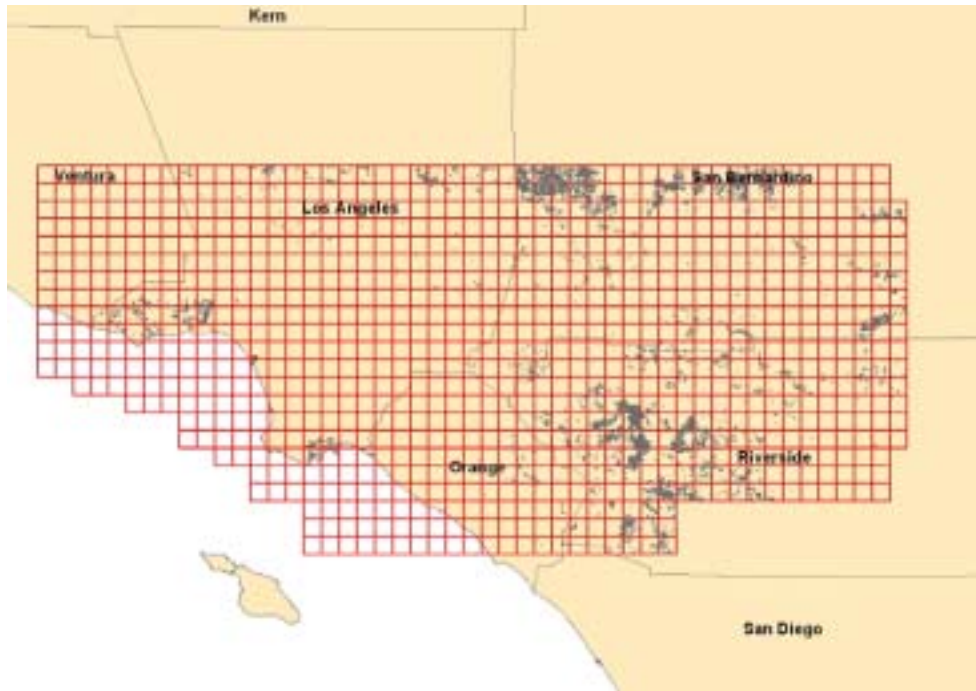**Figure 84: Location of land-use parcels pertaining to the Transportation and Utilities category**
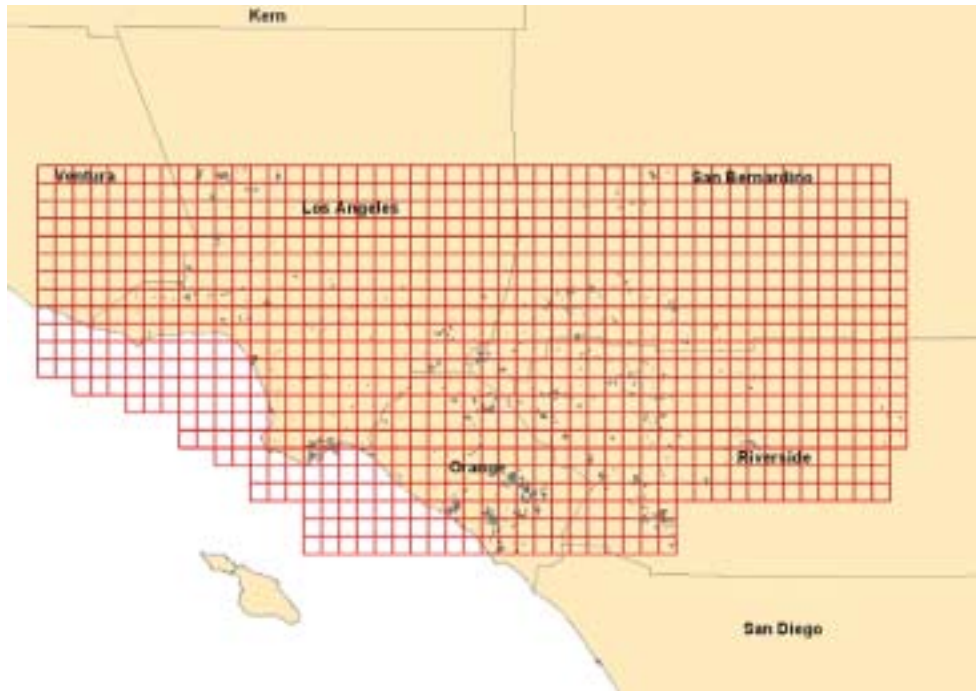
Figure 85: Location of land-use parcels pertaining to the Under Construction category
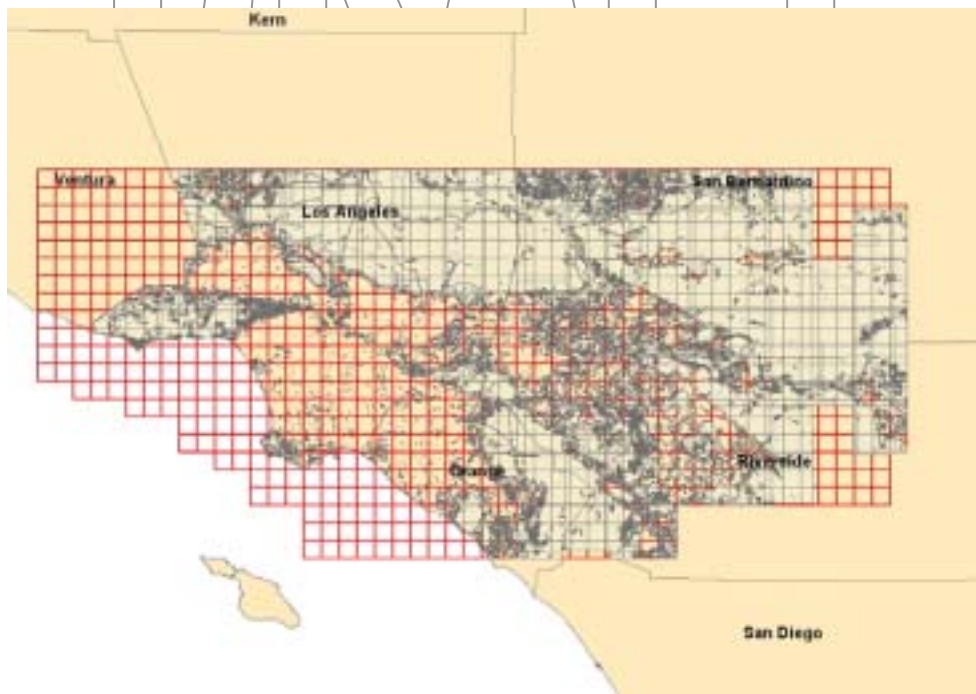

Figure 86: Location of land-use parcels pertaining to the Vacant category

Figure 87: Location of land-use parcels pertaining to the Water and Floodways category

16 APPENDIX F: DUTY CYCLE APPROACH

Hourly electric load average profiles for the residential, commercial, agriculture and water pumping, and industrial sectors were downloaded from the Southern California Edison (SCE) web page. In the cases in which more than one load profile was available due to the different current rates, an aggregate load profile weighted by power demand was determined and applied in that sector. The "Other" sector category was assumed to have the same profile as the commercial aggregated electric load profile. Those profiles were normalized and applied in the systematic approach to develop realistic DG scenarios, as explained in the main text. Figure 88 through Figure 91 show the average profiles provided by SCE. The application of these profiles in the realistic DG scenarios will produce variable DG emission inventories for each hour of the day.
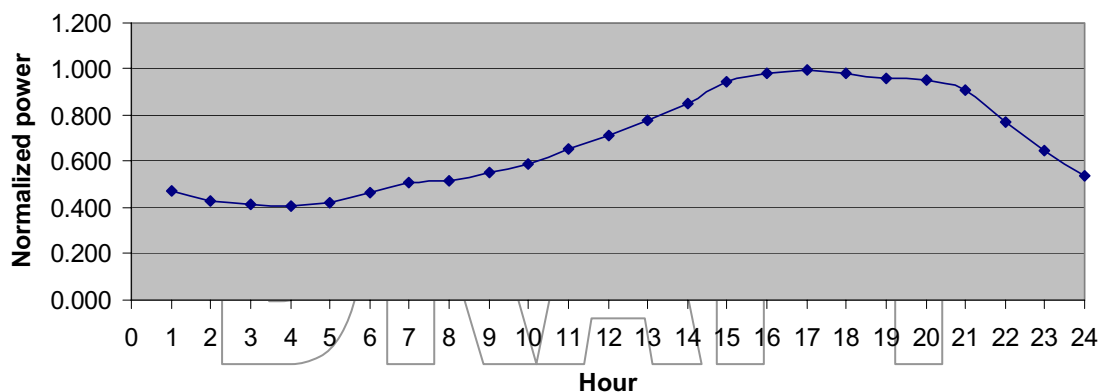

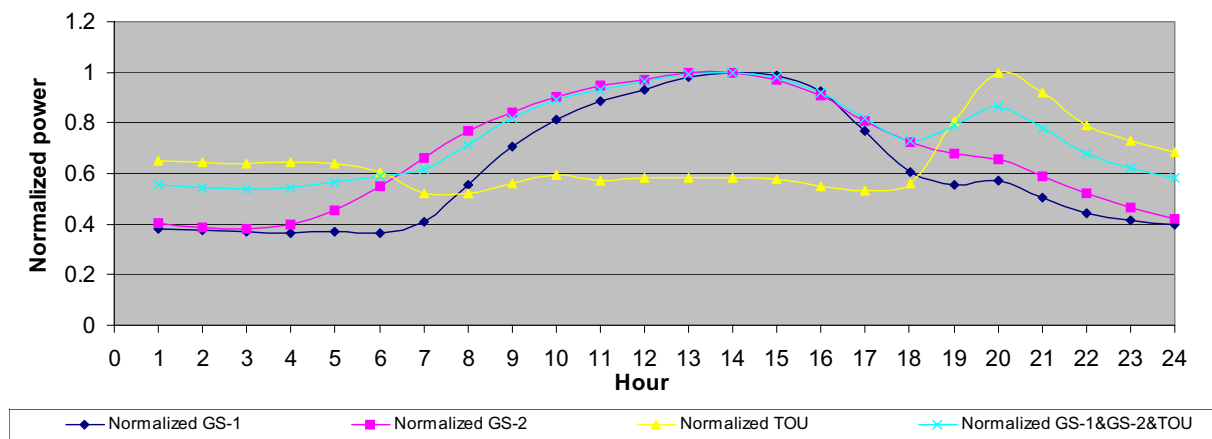**Figure 88: Normalized hourly electric profiles for SCE residential sector**

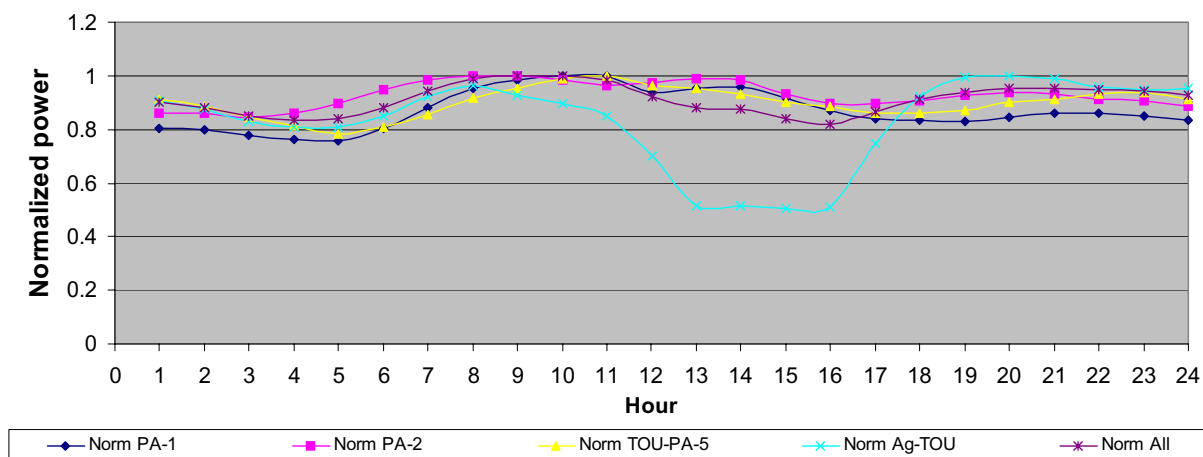**Figure 89: Normalized hourly electric profiles for SCE commercial sector**

Figure 90: Normalized hourly electric profiles for SCE Agriculture and water pumping sector
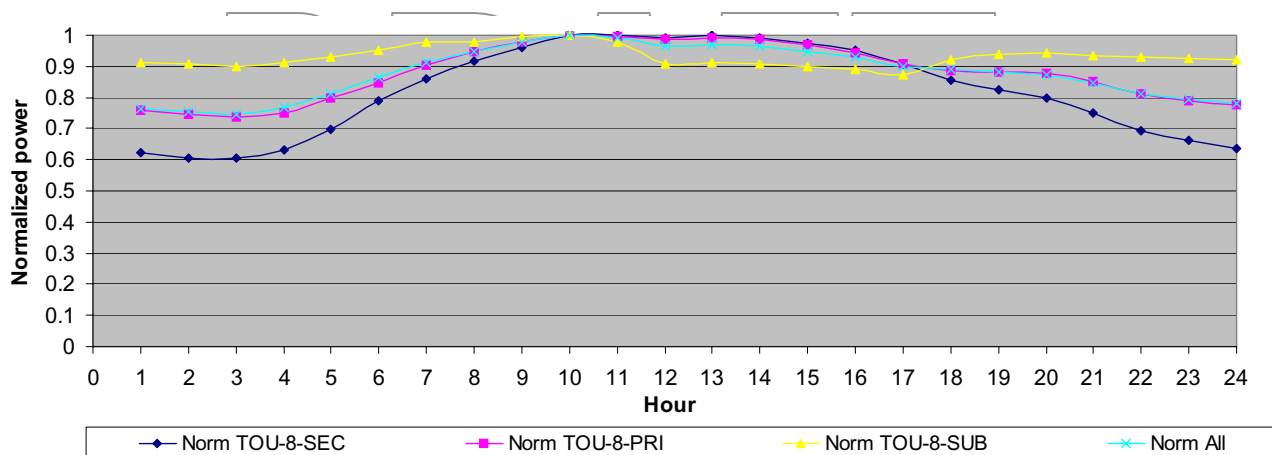

Figure 91: Normalized hourly electric profiles for SCE industrial sector

17 APPENDIX G: TABLES OF ESTIMATED CONTRIBUTIONS OF DG TECHNOLOGY TYPES FOR EACH SECTOR

Table 66. Estimated relative contributions of DG technology types ($W_{i,l,j}$) in the Industrial sector as a function of size class.

Size categories	% LT Fuel cells	% HT Fuel cells	% MTGs	% NG ICEs	% PV	% CCT	% AGT	Stirling	Hybrid
< 50 kW	0.0%	0.5%	4.3%	0.0%	0.0%	0.0%	0.0%	0.0%	0.0%
50-250 kW	0.0%	2.1%	10.0%	0.0%	0.0%	0.0%	0.0%	0.0%	0.0%
250-1,000 kW	0.0%	2.6%	0.0%	10.1%	0.0%	9.7%	0.0%	0.0%	2.5%
1-5 MW	0.0%	0.0%	0.0%	10.1%	0.0%	9.7%	0.0%	0.0%	2.5%
5-20 MW	0.0%	0.0%	0.0%	0.0%	0.0%	9.7%	13.0%	0.0%	0.0%
20-50 MW	0.0%	0.0%	0.0%	0.0%	0.0%	0.0%	13.0%	0.0%	0.0%
Total	0.0%	5.2%	14.4%	20.1%	0.0%	29.2%	26.0%	0.0%	5.0%

Table 67. Estimated relative contributions of DG technology types ($W_{i,l,j}$) in the Low-density residential sector as a function of size class.

Size categories	% LT Fuel cells	% HT Fuel cells	% MTGs	% NG ICEs	% PV	% CCT	% AGT	Stirling	Hybrid
< 50 kW	40.5%	2.5%	0.0%	0.0%	50.0%	0.0%	0.0%	0.0%	0.0%
50-250 kW	4.5%	2.5%	0.0%	0.0%	0.0%	0.0%	0.0%	0.0%	0.0%
250-1,000 kW	0.0%	0.0%	0.0%	0.0%	0.0%	0.0%	0.0%	0.0%	0.0%
1-5 MW	0.0%	0.0%	0.0%	0.0%	0.0%	0.0%	0.0%	0.0%	0.0%
5-20 MW	0.0%	0.0%	0.0%	0.0%	0.0%	0.0%	0.0%	0.0%	0.0%
20-50 MW	0.0%	0.0%	0.0%	0.0%	0.0%	0.0%	0.0%	0.0%	0.0%
Total	45.0%	5.0%	0.0%	0.0%	50.0%	0.0%	0.0%	0.0%	0.0%

Table 68. Estimated relative contributions of DG technology types ($W_{i,l,j}$) in the medium- and high-density residential sector as a function of size class.

Size categories	% LT Fuel cells	% HT Fuel cells	% MTGs	% NG ICEs	% PV	% CCT	% AGT	Stirling	Hybrid
< 50 kW	4.8%	2.8%	3.0%	0.0%	17.5%	0.0%	0.0%	0.0%	0.0%
50-250 kW	7.2%	11.2%	7.0%	5.0%	10.5%	0.0%	0.0%	0.0%	0.0%
250-1,000 kW	0.0%	14.0%	0.0%	5.0%	7.0%	0.0%	0.0%	0.0%	2.5%
1-5 MW	0.0%	0.0%	0.0%	0.0%	0.0%	0.0%	0.0%	0.0%	2.5%
5-20 MW	0.0%	0.0%	0.0%	0.0%	0.0%	0.0%	0.0%	0.0%	0.0%
20-50 MW	0.0%	0.0%	0.0%	0.0%	0.0%	0.0%	0.0%	0.0%	0.0%
Total	12.0%	28.0%	10.0%	10.0%	35.0%	0.0%	0.0%	0.0%	5.0%

Table 69. Estimated relative contributions of DG technology types ($W_{i,l,j}$) in the comercial sector as a function of size class.

Size categories	% LT Fuel cells	% HT Fuel cells	% MTGs	% NG ICEs	% PV	% CCT	% AGT	Stirling	Hybrid
< 50 kW	0.2%	0.9%	1.1%	0.0%	4.5%	0.0%	0.0%	0.0%	0.0%
50-250 kW	2.0%	6.3%	10.1%	7.3%	4.5%	0.0%	0.0%	0.0%	0.0%
250-1,000 kW	0.0%	1.8%	0.0%	7.3%	2.2%	9.1%	0.0%	0.0%	0.0%
1-5 MW	0.0%	0.0%	0.0%	0.0%	0.0%	9.1%	0.0%	0.0%	0.0%
5-20 MW	0.0%	0.0%	0.0%	0.0%	0.0%	9.1%	12.2%	0.0%	0.0%
20-50 MW	0.0%	0.0%	0.0%	0.0%	0.0%	0.0%	12.2%	0.0%	0.0%
Total	2.2%	9.0%	11.2%	14.6%	11.2%	27.3%	24.3%	0.0%	0.0%

Table 70. Estimated relative contributions of DG technology types ($W_{i,l,j}$) in the agricultural and water pumping sector as a function of size class.

Size categories	% LT Fuel cells	% HT Fuel cells	% MTGs	% NG ICEs	% PV	% CCT	% AGT	Stirling	Hybrid
< 50 kW	0.1%	1.0%	1.1%	0.0%	4.5%	0.0%	0.0%	0.0%	0.0%
50-250 kW	1.0%	7.1%	10.1%	7.3%	4.5%	0.0%	0.0%	0.0%	0.0%
250-1,000 kW	0.0%	2.0%	0.0%	7.3%	2.2%	9.1%	0.0%	0.0%	0.0%
1-5 MW	0.0%	0.0%	0.0%	0.0%	0.0%	9.1%	0.0%	0.0%	0.0%
5-20 MW	0.0%	0.0%	0.0%	0.0%	0.0%	9.1%	12.2%	0.0%	0.0%
20-50 MW	0.0%	0.0%	0.0%	0.0%	0.0%	0.0%	12.2%	0.0%	0.0%
Total	1.1%	10.1%	11.2%	14.6%	11.2%	27.3%	24.3%	0.0%	0.0%

Table 71. Estimated relative contributions of DG technology types ($W_{i,l,j}$) in the "others" sector as a function of size class.

Size categories	% LT Fuel cells	% HT Fuel cells	% MTGs	% NG ICEs	% PV	% CCT	% AGT	Stirling	Hybrid
< 50 kW	0.1%	0.4%	1.0%	0.0%	0.0%	0.0%	0.0%	0.0%	0.0%
50-250 kW	1.9%	3.2%	19.2%	0.0%	0.0%	0.0%	0.0%	0.0%	0.0%
250-1,000 kW	0.0%	4.4%	0.0%	7.3%	0.0%	7.1%	0.0%	0.0%	2.5%
1-5 MW	0.0%	0.0%	0.0%	7.3%	0.0%	7.1%	0.0%	0.0%	2.5%
5-20 MW	0.0%	0.0%	0.0%	0.0%	0.0%	7.1%	9.4%	0.0%	0.0%
20-50 MW	0.0%	0.0%	0.0%	0.0%	0.0%	0.0%	9.4%	0.0%	0.0%
Total	2.0%	8.0%	20.2%	14.6%	0.0%	21.2%	18.9%	0.0%	5.0%

18 ATTACHMENTS

DRAFT